



## City Research Online

### City, University of London Institutional Repository

---

**Citation:** Wolf, J. E. (1996). Identification of defects in specific parallel "channels" of the human visual system. (Unpublished Doctoral thesis, City, University of London)

This is the accepted version of the paper.

This version of the publication may differ from the final published version.

---

**Permanent repository link:** <https://openaccess.city.ac.uk/id/eprint/30997/>

**Link to published version:**

**Copyright:** City Research Online aims to make research outputs of City, University of London available to a wider audience. Copyright and Moral Rights remain with the author(s) and/or copyright holders. URLs from City Research Online may be freely distributed and linked to.

**Reuse:** Copies of full items can be used for personal research or study, educational, or not-for-profit purposes without prior permission or charge. Provided that the authors, title and full bibliographic details are credited, a hyperlink and/or URL is given for the original metadata page and the content is not changed in any way.

585.

**IDENTIFICATION OF DEFECTS IN SPECIFIC PARALLEL  
"CHANNELS" OF THE HUMAN VISUAL SYSTEM**

**by**

**JANET ELIZABETH WOLF**

**Thesis submitted for the degree of**

**Doctor of Philosophy**

**to**

**CITY UNIVERSITY**

**Department of Optometry and Visual Science**

**February, 1996**

## CONTENTS

<b>LIST OF FIGURES</b>	<b>5</b>
<b>ACKNOWLEDGEMENT</b>	<b>7</b>
<b>DECLARATION</b>	<b>8</b>
<b>ABSTRACT</b>	<b>9</b>
<b>CHAPTER 1. INTRODUCTION</b>	
1.1 General introduction	10
1.2 The anatomy and physiology of the primate visual system	13
1.2.1 The gross structures of the human eye	13
1.2.2 The anatomy of the retina	15
1.2.3 Contrast, contrast sensitivity and contrast gain	21
1.2.4 The physiology of the retina	24
1.2.5 Primate foveal ganglion cells	32
1.2.6 A brief description of the retinogeniculocortical pathways	34
1.3 Introduction to psychophysics	38
1.3.1 Spatial, temporal and chromatic psychophysical channels	42
1.3.2 Neural mechanisms underlying psychophysical channels	46
<b>CHAPTER 2. THE 'ROTATING STRIPES EFFECT'</b>	
2.1 Introduction	51
2.2 Preliminary experiments to investigate the 'band characteristics' for normals	53
2.2.1 Equipment	53
2.2.2 Effect of angular speed on width of band	54
2.2.3 Temporal frequency 'cut-off' for the 'inner' and 'outer' bands seen by normals: The effect of (1) luminance and (2) eccentricity	55
2.2.4 Orientation 'lag' associated with 'inner' and 'outer' bands	58

2.3	Theoretical analysis of the 'band effect' for uniform illumination:	60
2.3.1	Introduction to Paper 1: <i>Rotating stripes and the impulse response of the eye: Uniform illumination</i>	60
2.3.2	Paper 1:	After page 62
2.4	Theoretical analysis of the effect seen under stroboscopic illumination:	63
2.4.2	Introduction to Paper 2: <i>Rotating stripes and the impulse response of the eye: Stroboscopic illumination</i>	63
2.4.3	Paper 2	After page 63

### CHAPTER 3. THE COMPLEX BAND

3.1	Introduction	64
3.2	Computer simulation of the complex band:	67
3.2.1	Introduction to Paper 3: <i>Rotating stripes provide a simultaneous display of sustained and transient channels</i>	67
3.2.2	Paper 3	After page 67

### CHAPTER 4. CLINICAL APPLICATION OF THE 'ROTATING STRIPES EFFECT'

4.1	Optic Neuritis and Multiple Sclerosis	68
4.2	Melanoma Associated Retinopathy (MAR)	73

### CHAPTER 5. FURTHER PSYCHOPHYSICAL TESTS TO IDENTIFY SPECIFIC PATHWAY LOSSES: MAGNOCELLULAR AND PARVOCELLULAR DAMAGE

5.1	Introduction	74
5.2	What is Melanoma-Associated Retinopathy?	75
5.2.1	The tests	76
5.2.2	Equipment and procedure	77
5.2.3	Results and conclusions in MAR	78
5.3	Congenital Stationary Night Blindness (CSNB)	80
5.3.1	Results and conclusions for CSNB	80
5.3.4	Paper 4: <i>Selective Magnocellular damage in Melanoma -Associated Retinopathy: Comparison with Congenital Stationary Night Blindness</i>	After page 80

5.4	The 'Epidemic Neuropathy' of Cuba, 1992-1993	96
5.4.1	Methods	97
5.4.2	Results and conclusions	99
<b>CHAPTER 6. DISCUSSION</b>		<b>102</b>
<b>REFERENCES</b>		<b>105</b>

## LIST OF FIGURES

		Following page
1.1	A parallel 'band' is seen when a grating rotates slowly	9
1.2	Horizontal section of the right human eye	13
1.3	Neurons of the primate retina and their synaptic relations	15
1.4	Vertical section of the central fovea of the human retina.	15
1.5	Distribution of rods, cones and visual acuity along a horizontal meridian	17
1.6	The six most common types of bipolar cell of the primate retina	17
1.7	Drawings of Golgi-stained amacrine cells in vertical view in the monkey retina	19
1.8	Drawings of the most common Golgi-stained ganglion cell types in the monkey retina	19
1.9	Optic nerve fibres and blood vessels circumnavigate the fovea	21
1.10	Photopic threshold-versus-intensity function	23
1.11	Scotopic threshold-versus-intensity function	23
1.12	Excitation of a rod by the absorption of light	25
1.13	Hyperpolarisation of a rod and cone for different flash intensities	27
1.14	Centre-surround organisation of the receptive field of bipolar cells	29
1.15	Firing of an 'on-centre' ganglion cell to different stimuli	31
1.16	Summary of the properties of ganglion cells of the cat retina	31
1.17	Main neural pathways involved in vision	33
1.18	Cross-sectional representation of the LGN	35
1.19	The parallel channels of the geniculostriate pathway of the primate visual system	35
1.20	Response-contrast functions of P- and M- ganglion cells	35
1.21	Temporal frequency response of the human visual system	43
1.22	Spatial contrast sensitivity of the human visual system, for different retinal illuminations	43
1.23	Spatial and temporal contrast sensitivity functions for the human visual system	43
1.24	Chromatic and achromatic channels in the human visual system	45
1.25	Sensitivity of ganglion cells to luminance modulation	47
1.26	Sensitivity of ganglion cells to chromatic modulation	47
1.27	Temporal frequency response curves for the human visual system	47
2.1	Predicted appearance of the 'rapidly' rotating grating	51
2.2	Distribution of velocities across a 'slowly' rotating grating	51

2.3	Photograph of slowly rotating grating	51
2.4	The effect of angular velocity on the width of band	53
2.5	Cut-off frequency as a function of luminance and eccentricity for 'outer' band	55
2.6	Cut-off frequency as a function of luminance and eccentricity for 'inner' band	55
2.7	Cut-off frequency as a function of luminance for combined 'outer' and 'inner' bands: a single width of band	55
2.8	Relation between critical frequency, retinal illumination and eccentricity	55
2.9	Cut-off frequency as a function of eccentricity for different retinal illuminations	55
2.10	Orientations of 'inner' and 'outer' bands	58
2.11	Multiple bands: the diffraction analogy	63
3.1	Temporal cut-off frequency as a function of luminance for P- and M-cells	65
3.2	Temporal luminance profile associated with the rotation of the grating	67
3.3	Computer simulation of the band for a rectangular temporal impulse response	67
4.1	Cut-off frequency as a function of luminance; patients with optic neuritis and multiple sclerosis	71
4.2	Cut-off frequency on red/green isoluminant grating: comparison of MAR patient and a normal	73
5.1	MAR: achromatic contrast thresholds for increments and decrements in luminance	89
5.2	MAR and CSNB: achromatic contrast sensitivity function	89
5.3	MAR and CSNB: achromatic temporal contrast sensitivity	91
5.4	MAR: velocity displacement thresholds	91
5.5	MAR and CSNB: red/green temporal contrast sensitivity	91
5.6	MAR and CSNB: blue/yellow temporal contrast sensitivity	91
5.7	MAR: colour discrimination thresholds	93
5.8	Cuban amblyopia: achromatic contrast sensitivity function	99
5.9	Cuban amblyopia: chromatic and achromatic contrast thresholds	99

## ACKNOWLEDGEMENTS

I owe a great deal to many people. I shall always be grateful to Professor John Barbur for his decisive guidance in the early days of my research and also to Professor Geoffrey Arden, not only for giving me the unique opportunity to work with him, but also for his subsequent encouragement and help as my supervisor.

At different stages of my research, I have had crucial help from several people. In developing my diffraction analogy, I had many enjoyable discussions with Professor Edward Steward. His enthusiasm was a tonic, and I particularly appreciate his including my diffraction analogy as an appendix in his book, 'Fourier Optics'. Professor Marion Marré led me to consider the clinical potential of the 'rotating stripes effect' and, together with Professor David Foster, gave me the opportunity to pursue this. I was also very fortunate in having Mr Nicholas Lusty as an undergraduate project student and thereafter, very briefly, as a Research Assistant, during which time he produced elegant simulations of given channel responses. He is co-author of Paper 3.

Much help has been given me over the years by Professor Keith Ruddock, particularly through his refereeing and editing of the three papers included in this thesis.

In the later work, involving patients with specific functional losses, I enjoyed many critical discussions with Professor Janusz Kulikowski.

None of this would have been possible without the endless encouragement of my husband, Peter, who has specifically asked me not to mention him!

## DECLARATION

I grant powers of discretion to the University Librarian to allow this thesis to be copied in whole or in part without reference to me. This covers only single copies made for study purposes, subject to normal conditions of acknowledgement.

## ABSTRACT

Chapter 1 is a general introduction to the work of the thesis. The anatomy and physiology of the visual system is described, especially in relationship to the primate eye and visual pathway. The description concentrates on the distinction between of primate ganglion cells types, M and P, and their projections to the lateral geniculate nucleus, and the visual cortex. An account is given of psychophysical methods, and how quantities defined by such experiments, such as sensitivity, incremental sensitivity, contrast sensitivity, etc. may be related to activity of single cells, determined by physiologists. The evidence for separate channels for spatial, temporal, achromatic and chromatic channels in the visual system is reviewed, and theories of possible neural correlates are critically discussed.

Chapter 2 introduces some preliminary experiments, on the visual effect seen on viewing a slowly rotating striped pattern. The subsequent analysis demonstrates that the effect displays the temporal frequency response of the eye ( illustrated by papers 1 and 2 ).

Chapter 3, illustrated by Paper 3, discusses the complex appearance of the 'rotating stripes', and how it provides a direct display of the underlying channels. It is illustrated with a computer simulation of the component channel images.

Chapter 4 shows the abnormalities in perception of rotating stripes found in cases of optic neuritis, and relates them to the loss of the 'transient' channel.

Chapter 5 ( paper 4) deals with the psychophysics of two diseases, Melanoma-Associated Retinopathy, in which it is found that there is a highly selective loss of the achromatic M- pathway, and another condition which is its converse, a nutritional amblyopia in which the P-cell pathway is selectively affected.

The results are reviewed and discussed in the final chapter.

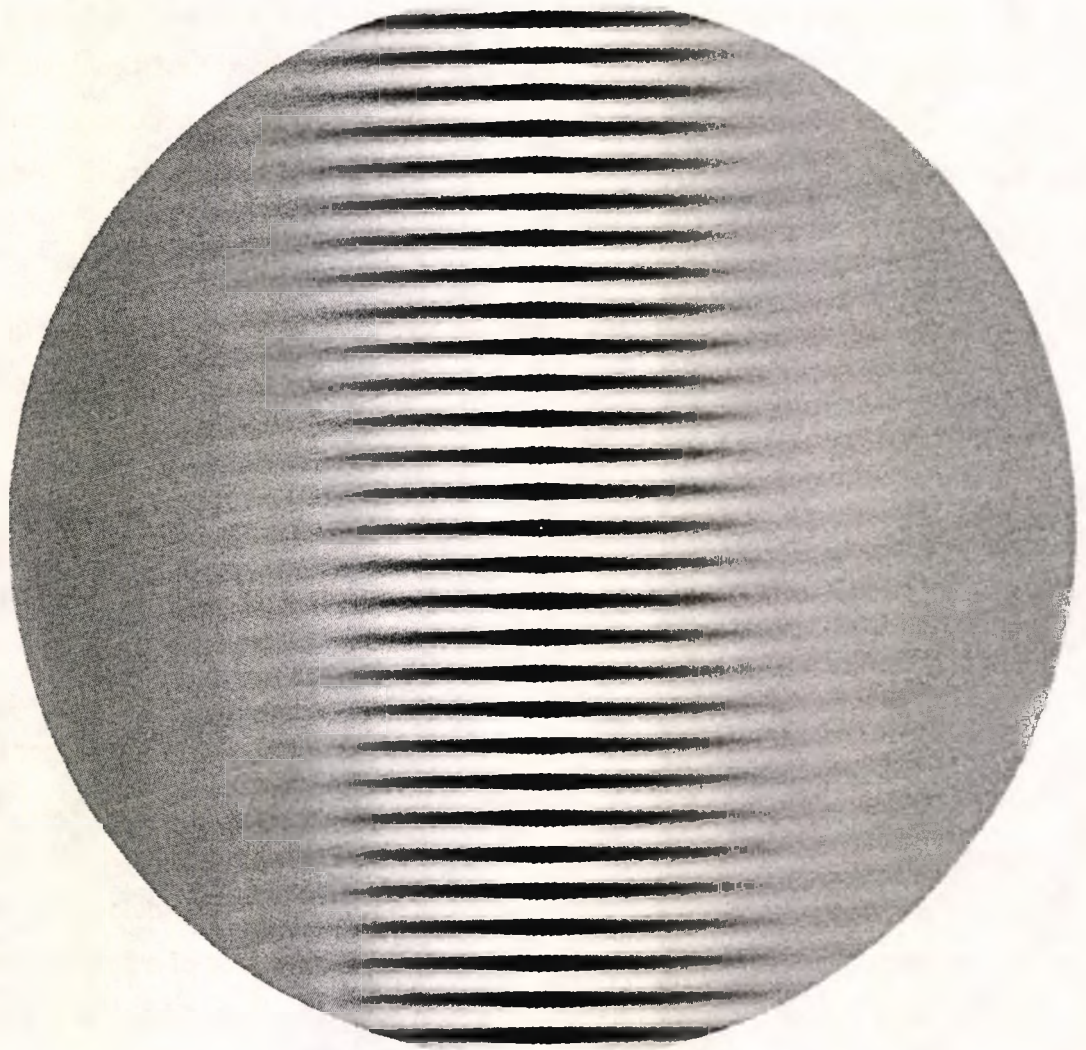


Figure 1.1: A slowly rotating grating (e.g.  $\pi \text{ rad.s}^{-1}$ ) is seen as a clearly resolved parallel sided 'band' similar to the simulation shown here.

## CHAPTER 1: INTRODUCTION

### 1.1 GENERAL INTRODUCTION

In a well ordered world, a topic for a Ph.D. thesis is agreed upon and a student is set on to it, rather in the manner of a hound after a quarry. The value of the outcome depends to some extent on the calibre of the animal but also on the intrinsic worth of the quarry. In this case there was no quarry: the thesis did not start out as a thesis. It evolved from one small puzzle. I shall describe this and the sequence of questions that arose from the first answer that ultimately led to this entire sequence of investigation.

As my training is in physics and visual perception, not surprisingly the puzzle was one of psychophysics and concerned the visual effect one experiences on looking at a slowly rotating striped pattern. Part of the pattern is blurred, leaving a central parallel-sided column or band of resolved stripes (rather like Figure 1.1) moving around with the pattern as a whole with the band getting narrower as the speed increases. The puzzle was "what is going on?". It turns out (Chapter 2) that there is a very simple relationship between the general appearance of the band and the temporal characteristics of the visual system. The perceived contrast distribution along the stripes provides an instantaneous display of the temporal frequency response of the observer, the width of the band indicating the temporal cut-off frequency. The anti-symmetric shape of the stripes in the band provides a graphical display of the temporal phase response, and the orientation of the band can provide information on 'transport delay'. This means that the temporal characteristics of a single channel are contained in the width, contrast and orientation of a single two-dimensional shape.

However, the band is complex in the sense that there is a substructure within it. If there is more than one channel involved in detecting the image, each with its own spatio-temporal characteristics, we might expect to see some kind of substructure corresponding to a superposition of the separate bands, each with a distinct width and orientation. Indeed, we find that an inner band is apparently superimposed on and lagging slightly behind a wider band, suggesting that we are seeing the action of at least two independent mechanisms or channels. Whilst any moving object has an appearance that reflects the contributions of the underlying spatio-temporal channels, the separate contributions are generally not distinguishable, whereas with this simple stimulus, the rotation of the image of one component with respect to another enables

them to be separately visualised. This raises the exciting possibility that the effect can be used to study channel characteristics. Chapters 2 and 3 analyse the phenomena in detail and demonstrates that the components one actually sees correspond well to the temporal characteristics of the two, well established, parallel and largely independent psychophysical channels, namely the sustained and transient channel, the transient channel having a particular responsibility for signalling motion. This is all firmly in the territory of psychophysics! However, there are some striking characteristics of these two components that inevitably introduces the question "what are the physiological substrates of these bands?".

At a later date I was given the opportunity of showing the 'stripes' to a patient with optic neuritis who had specifically complained of problems in seeing moving targets. It transpired that the transient component of the band was largely absent. The same was true for a person with multiple sclerosis. This finding had the double effect of (i) reinforcing the conclusion that the visibly distinct bands correspond to the separate spatio-temporal channels with specific roles, and (ii) that there is some diagnostic potential in having some simple way of exposing channel loss.

The last 30 years has produced a mass of psychophysical evidence of there being two parallel and largely independent visual channels. Depending on the method of isolation, they are described variously as sustained and transient, low-pass and band-pass, chromatic and achromatic or even pattern and movement channels. More recently there has been an upsurge of interest in the parvocellular and magnocellular pathways of the primate which also appear to process, in parallel and again largely independently, the chromatic and achromatic aspects of the image. The separation is substantially maintained even beyond the visual cortex. There is some evidence that the parvocellular and magnocellular systems are the physiological substrates for the chromatic and achromatic psychophysical channels, although the correlation is not complete and there is some conflicting evidence. In particular, the sustained and transient components seen with the rotating stripes have chromatic and achromatic characteristics which correspond well to those of the parvocellular and magnocellular pathways suggesting that this simple device is providing a window into the activity of these two neural pathways.

Once again the direction of this work was affected by my being given access to a patient with an unusual condition, namely Melanoma Associated Retinopathy (described in Chapter 5.2), whose many visual symptoms included problems

associated with seeing moving objects. As with the other patients there was a substantial loss of the transient component in the appearance of the band, suggesting transient losses are commensurate with magnocellular damage. Since the appearance of the band does not readily lend itself to quantitative measurement, it was at this point that it seemed sensible to complement the findings with additional psychophysical tests designed to isolate those chromatic and achromatic channels subserved by the parvocellular and magnocellular pathways. These proved effective and were applied not only to other MAR patients, but also to patients with other conditions; congenital stationary night blindness (CSNB) and finally the Cuban neuropathy. The nature of the psychophysical losses, which are discussed in Chapter 5, make some contribution towards understanding these different conditions. However, as is often the case in studying patients with specific functional losses, the findings can throw some light on normal vision. In this case they concern two controversial points, namely (i) which pathway (P or M-cell) mediates achromatic vision at low contrast, low spatial and low temporal frequencies?, and (ii) at the ganglion cell level is it a particular sub-group of the P-cells that has particular responsibility for signalling colour? Hence, the simple puzzle in psychophysics has ended in the controversial territory of the role of the parvocellular and magnocellular pathways in perception!

Since much of the work in this thesis has been published, where this occurs my plan is to introduce the paper, enclose it, and add a commentary on it.

## 1.2 THE ANATOMY AND PHYSIOLOGY OF THE PRIMATE VISUAL SYSTEM

A description of the anatomy and physiology of the human visual system is found in many texts (e.g. Kolb, 1991 and Falk, 1991 from Heckenlively and Arden, 1991) with condensed versions in plentiful supply (e.g. Barlow and Mollon, 1982). However, a brief review of the main components and their relations to each other is given, as this provides a background for the detailed descriptions of the structures of particular relevance to this work. The anatomy and physiology of the retina fall into this latter category. A more detailed description of the two parallel 'P' and 'M' pathways is then given with the emphasis is on the retinal stage. This is followed by a brief description of the geniculo/cortical stages. In addition, although this work is concerned largely with the processing of the optical image, some reference to the characteristics of the optical structures involved is helpful, if one is to be able to separate the optical and neural contributions to the perceived image, whether they be normal or abnormal.

### 1.2.1 THE GROSS STRUCTURES OF THE HUMAN EYE

A horizontal cross section of the eye is shown schematically in Figure 1.2. It is an almost spherical hollow sphere of approximately 20mm in diameter and is composed of three layers or coats. The outer one (the fibrous tunic) consists of the transparent 'cornea' over the anterior surface of the eye and the 'sclera', an opaque membrane that is continuous with the cornea and encloses the remainder of the globe. The sclera is tough, protects and shapes the eye and provides the anchor for the extrinsic eye muscles.

The second layer is the 'vascular tunic' or 'uvea' with the 'choroid' lying directly below the sclera. Its blood vessels provide nutrition to all three coats. It is heavily pigmented and consequently absorbs light, thereby reducing any back-scatter. Anteriorly it differentiates into the 'ciliary body' and the 'iris'. The ciliary body consists chiefly of the annulus of 'ciliary muscles' important in controlling lens shape. The convoluted surface of the body (the ciliary processes) contains a large capillary bed, required since the ciliary epithelium secretes the fluid, the aqueous humour, that fills the cavity of the anterior segment of the eye. The iris is the most anterior part of the uvea located between the cornea and the lens. The pigment in the front surface gives the visible coloration of the iris, whereas the back contains a black, light absorbing pigment. The central opening of the iris, the pupil, can vary in diameter from approximately 2 to 8mm. (Davson, 1949). The size is controlled by two smooth

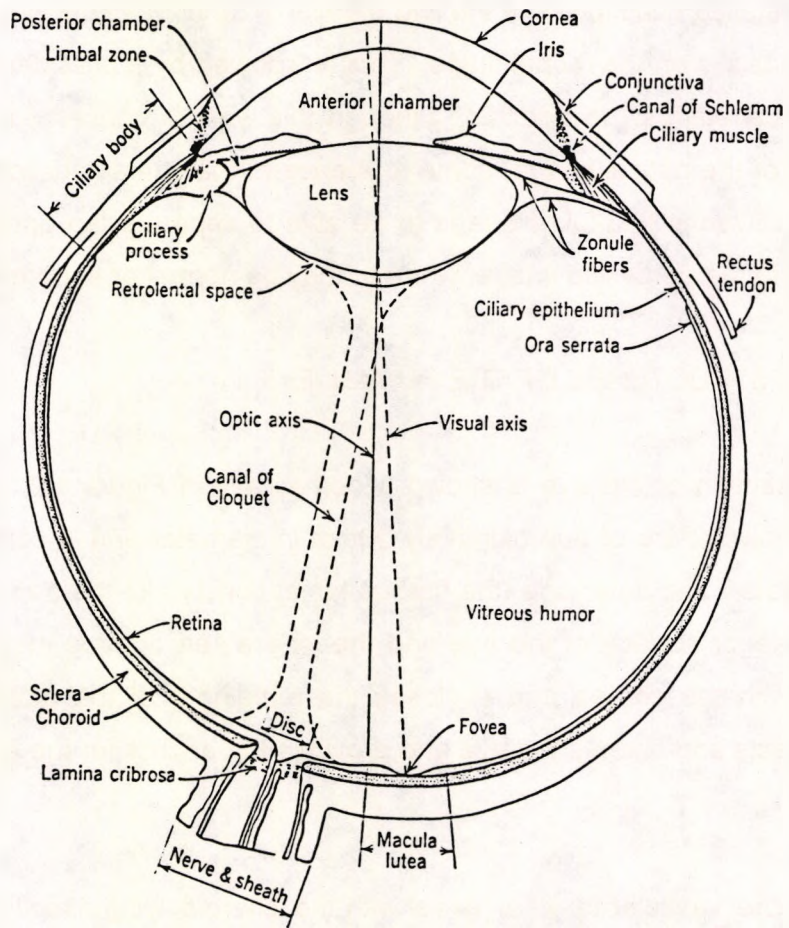


Figure 1.2: Horizontal section of the right human eye. (From Walls, 1942)

muscles in the iris; constriction is controlled by the annular 'sphincter' innervated by the parasympathetic system and dilation by the radial 'dilator' innervated by the sympathetic system.

The crystalline lens is held in position by zonular fibres that attach to the ciliary body. It is a transparent, bi-convex, flexible structure which is supported vertically and separates the liquid aqueous humor in the anterior segment and the jelly-like vitreous humor in the posterior segment (refractive indices 1.336). However, because of the large refractive index between the aqueous humor and the external air, the bulk of the focusing of the image takes place at the cornea (the power of this component is approximately 42 dioptries), whereas the crystalline lens with a refractive index increasing from a value of 1.38 in the outer layers to 1.41 in the inner denser nucleus (Duke-Elder, 1938) and flanked by the two humors contributes, in its relaxed state, a mere 12 dioptries. The curvature of the crystalline lens may be increased by the contraction of the encircling ciliary fibres which produces in the young accommodated eye anything up to an additional 10 dioptries; the lens hardens with increasing age, with a corresponding reduction in accommodative power.

The components of the eye with a specifically optical role are, therefore, the cornea, aqueous humor, iris, lens and vitreous humor. Shown also in Figure 1.2 is the region known as the 'macula lutea', in which a layer of yellow pigment provides a protective UV filter and can also be considered an optical component that removes poorly focused blue light. A two-dimensional optical image of the external scene is created on the retina which is the innermost of the three coats, known as the 'sensory tunic' and it is here that the neural processing of the image is begun. Hence much of the structure of the retina corresponds to that of the central nervous system.

The neural retina is thin (200µm - 400µm) and is separated from the choroid by the retinal pigment epithelium which is firmly attached to the choroid. The pigment epithelium has a secretory role and a special relationship with the photoreceptor visual pigment metabolism. The neural retina is largely transparent, composed of distinct layers, but has only a weak attachment to the pigment epithelium. However, anteriorly the retina is continuous with the ciliary epithelium, posteriorly with the optic nerve and at these positions the retina is firmly anchored. This neural layer is composed of three main types of neurons; photoreceptors, bipolar cells and ganglion cells. The ganglion cell axons leave the retina as a single group known as the 'optic nerve', and the region where they make their right-angled turn to leave the retina is

known as the 'optic disc'. At this point there are no receptors to record the image and consequently there is an associated 'blind spot' in the visual field. The gross anatomy of all these features are shown in Figure 1.2.

## 1.2.2 THE ANATOMY OF THE RETINA

The stained retina in cross-section displays a layered architecture (Polyak, 1941) and reveals the different neural components. A schematic representation in Figure 1.3 shows the conventional numbering of ten sharply defined layers (Polyak 1957). Starting with the outermost layer, they are: (1) retinal pigment epithelium, (2) rod and cone layer, (3) outer limiting membrane, (4) outer nuclear layer, (5) outer plexiform layer (OPL), (6) inner nuclear layer, (7) inner plexiform layer (IPL), (8) ganglion cell layer, (9) nerve fibre layer, (10) inner limiting membrane. In the central foveal region, (Figure 1.4) there is a rod free zone of slender tightly packed cones with the retinal structures abutting the vitreous humor (essentially layers 4 to 9) displaced to the sides; this enables the light to pass almost directly to the photoreceptors. Both these factors, together with the fact that capillaries circumnavigate the region, contribute (under photopic conditions) to the good resolution of the image over that region. The morphology of these different neural components is described and follows the general assessment of Kolb (1991).

**The Pigment Epithelium:** a single layer of pigmented epithelial cells which, like those of the choroid, absorb light and further reduce backscatter. They transport metabolites for the receptors from the choroidal blood supply, in particular vitamin A needed by the photoreceptors; they also act as scavengers, demolishing the discarded discs from the tips of the outer segments of the receptors.

**The Photoreceptors:** The primate retina contains two types of receptor cell whose function it is to catch quanta of light and pass a message to the next stage of integration and processing at the OPL. Rod receptors are in the majority (110-125 million cells: Osterberg, 1935) and operate most effectively in dim light. They peak in density in an annulus approximately 5mm (18 degrees) from the centre of the fovea whereas the cones (6-8 million cells) operate in daylight and are concentrated in the fovea.

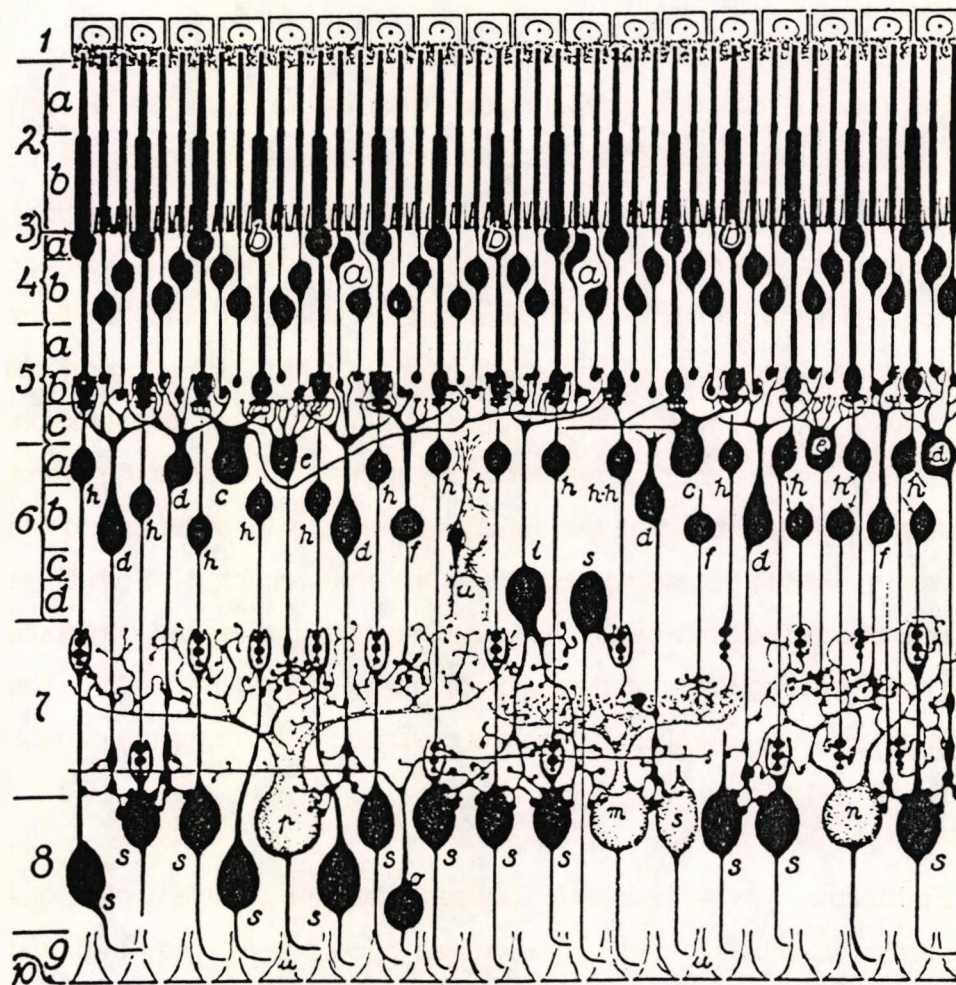


Figure 1.3: Schematic diagram of the neurons of the primate retina and their synaptic relations: h- midget bipolars; s- midget ganglion; d- mop bipolars; a- rods; b- cones; e,f,h- centripetal bipolars; m,n,o,p-ganglion cells; i- centrifugal bipolars; c- horizontal cells. From Polyak, 1957. See text for description of layers.

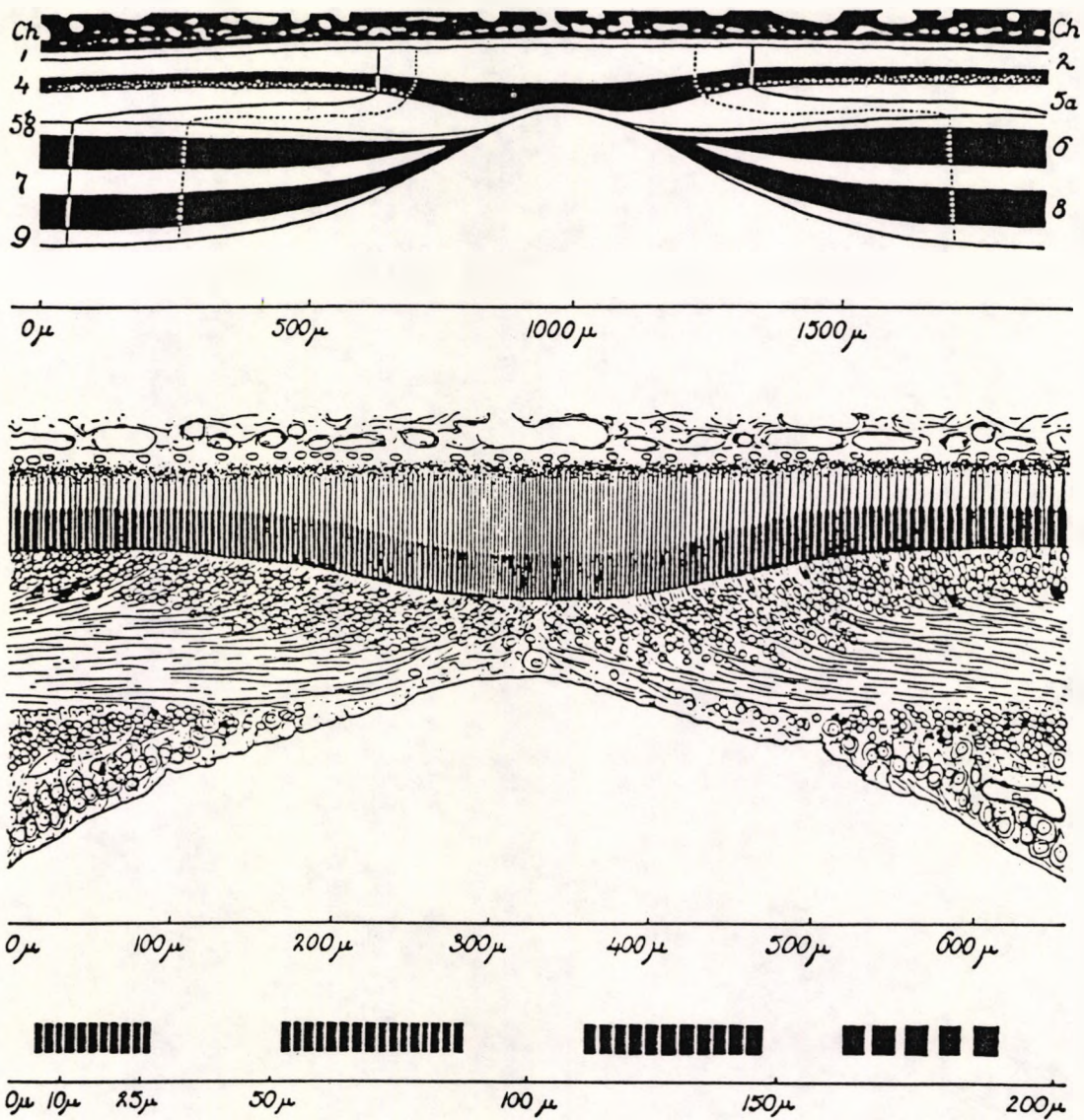


Figure 1.4: Section through the central fovea of the human retina . The central region comprising slim tightly packed cones is rod free. The upper part indicates schematically the manner in which layers 6-9 are displaced to allow the light to proceed through to the photoreceptors with less scatter and less absorption. See text.

Fine structure of photoreceptors: Both cell types are elongated and divided into several regions, termed the outer segment, inner segment, nuclear region, fibre, and synaptic pedicle. The light absorbing pigments are arranged in discs in the outer segments which increases the probability of photon absorption. The inner segments contain numerous mitochondria, required to maintain the metabolism and signalling capacity of the outer segments. The rods are slim cylindrical structures, ranging in thickness from  $1\mu$  near the fovea to  $2.5\mu$  peripherally. The foveal cones are similar in shape to the rods, with a maximum width of  $2.5\mu$ , but as the distance from the fovea increases the inner segments shorten and increase in width to about  $6\mu$ ; the outer segments taper with the characteristic cone shape.

'Receptor nuclei and fibres': The rod inner segments are connected by thin fibres to their cell bodies, which extend from these to the outer plexiform layer. There they terminate in 'spherules', which make synaptic contact with the dendrites of bipolar cells. The inner cone segments make direct contact with the cell bodies, except in the fovea where there are connecting outer fibres. Cone inner fibres extend from the cell bodies to the outer plexiform layer where they terminate in pedicles, many times larger than the rod spherules. Over most of the retina the fibres are oriented perpendicularly to the retinal layers but centrally they radiate from the fovea lying approximately in the plane of the retina, minimising the obstruction to the incident light provided by the cell bodies. It is these inner fibres that probably contain most of the yellow macular pigment molecules and it is the linear arrangement of these molecules that gives rise to the dichroism of this pigment which leads to the polarization of the incident light and the entopic phenomenon of Haidinger's brushes.

'Receptor photopigments': The visual pigments consist of a light-absorbing molecule called 'retinal' bound to a protein called an 'opsin'. There are four distinct types of visual pigment, each having a characteristic kind of opsin protein, which modifies the absorption spectrum of the retinal. In rods it is 'scotopsin', with the whole pigment/opsin complex called 'rhodopsin'. Light absorption causes the retinal-scotopsin combination to break down so the maximum absorption changes to the near UV. This process is described as the bleaching of the pigment. Regeneration then takes place. Cone pigments are known to bleach in the same way as rods, i.e. by the breakdown of the retinal, and in this case the opsin known as photopsin is essentially the same as for rhodopsin. The details of the subsequent regeneration of the visual pigment are not fully known and may differ from the rod model. For all the photopigments, the molecular changes in visual pigments convert light energy into

electro-chemical activity, which in turn leads to changes in the electrical resistance of the outer membrane of the photoreceptors.

There are three types of cone photoreceptors characterised by their single photopigment. The relative intensity of the cone signals is therefore a measure of the wavelength composition of the light, which in turn leads to the sensation of colour. Microspectrophotometry and electrophysiology has shown that they absorb and respond maximally at wavelengths of 420, 531 and 558 nm respectively.

The receptors are arranged in a mosaic, with the cones forming a close packed rectangular lattice in the 'fovea centralis', the region of high acuity, and separating out peripherally. The rods predominate in the periphery and have little representation in this central region. The distribution of cone and rod receptors is shown in Figure 1.5 together with the corresponding photopic visual acuity. However, until recently it was thought that the three cone types had identical morphology; now it has been shown to be possible to distinguish between short and longer wavelength cones. The short-wavelength cones have their lowest density in the foveal pit (3 -5%), a maximum density on the foveal slope of 15%, finally dropping to 8% elsewhere (Ahnelt, 1987). In the monkey, the relative numbers of the medium and short-wavelength cones have been reported (Marc and Sperling, 1977) together with their distribution across the retina. The medium-wavelength are in the majority, 64% in the fovea and 52 -59% elsewhere.

**Outer Plexiform Layer:** Some processing of the image takes place at this first synaptic layer in the retina. Cone pedicles and rod spherules have synapses with various bipolar cell types. In addition, cones pass electrical messages to each other and, by a similar teleo-dendritic pathway, rods communicate with cone pedicles (Nelson, 1977). The processes of horizontal cells are not only postsynaptic to photoreceptors, but also presynaptic, i.e. the H-cell signal "feeds back" and thus modifies the photoreceptor output. Also in the OPL are the synaptic interactions between horizontal cells, cones and rods which provides some feedback.

Bipolar cells: There are 9 types of bipolar cells with the six most common shown in Figure 1.6.

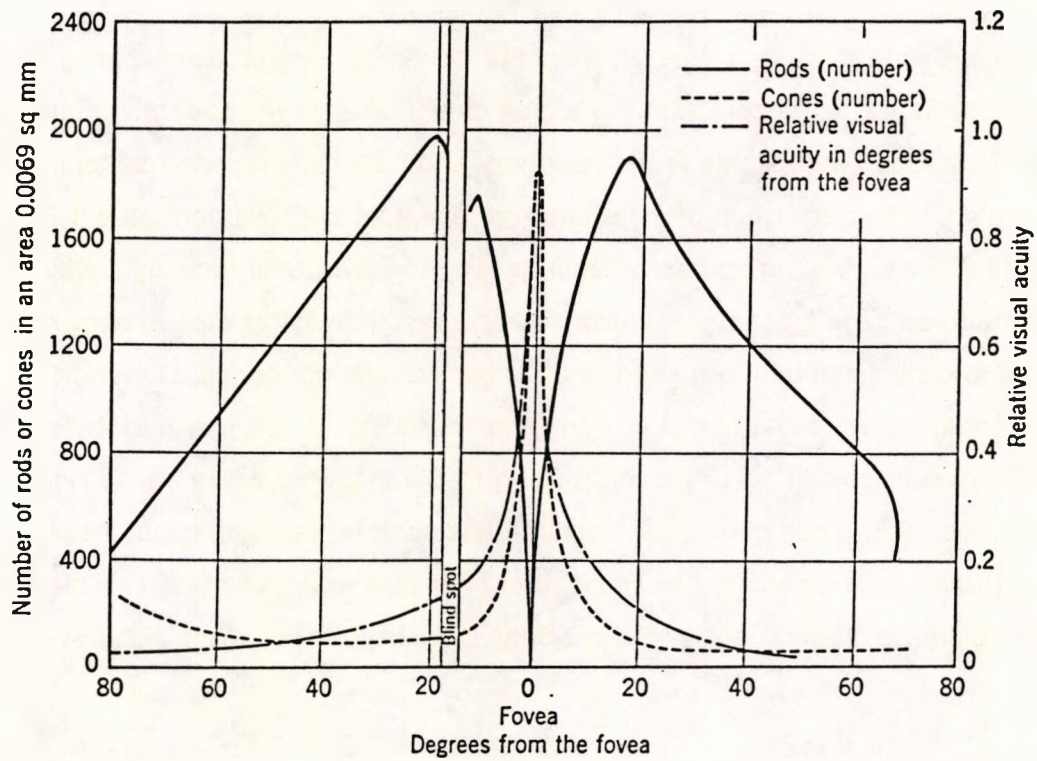


Figure 1.5: Distribution of rods and cones along a horizontal meridian. Visual acuity is included for comparison showing the close relation between cone density and acuity. (From Graham 1965).

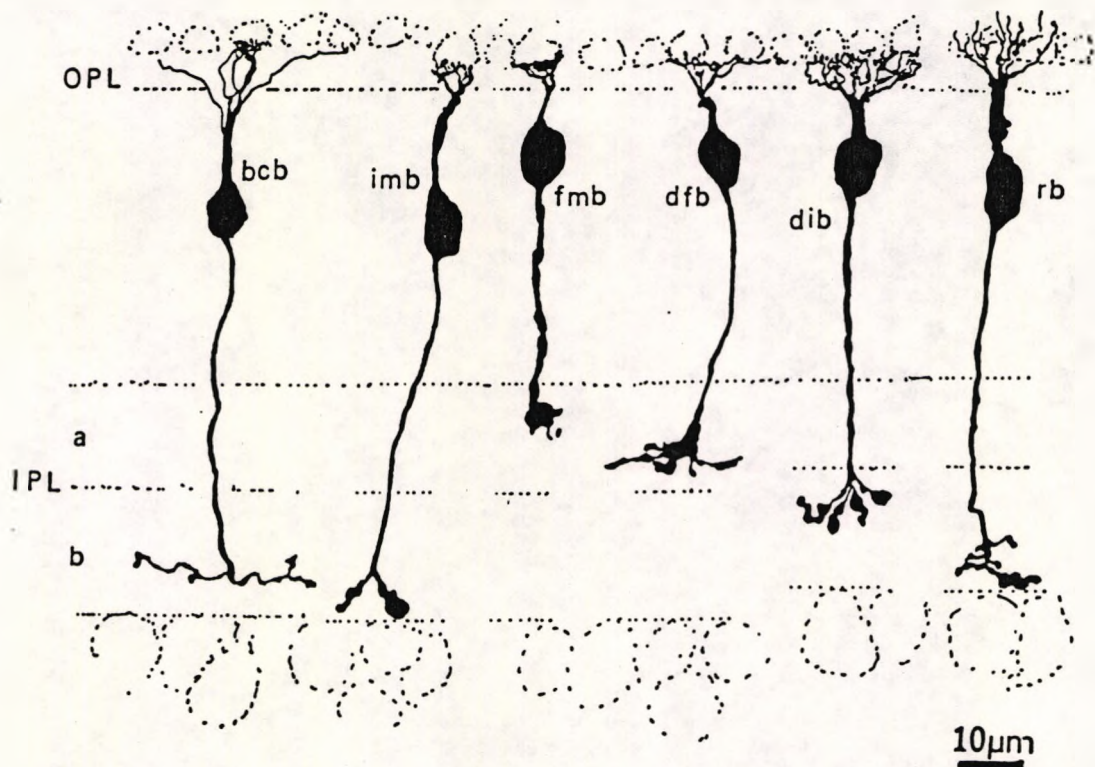


Figure 1.6: Drawings of the six most common types of bipolar cell of the primate retina as seen in vertical views, revealed by Golgi staining. (bcb = blue cone bipolar; imb = invaginating midget bipolar; fmb = flat midget bipolar; dfb = diffuse flat bipolar; dib = diffuse invaginating bipolar; rb = rod bipolar. From Kolb 1991).

Rod bipolar cells: Morphologically, there is a single type (rb) connecting exclusively to rods, with each dendritic terminal invaginating a rod spherule. In the central retina, the tuft of dendrites is small (15um), contacting 15-20 rods. Peripherally, the tuft is larger (30um), contacting 40-50 rods. The rod bipolar cells do not synapse with ganglion cells directly but rather with some amacrine cells in the IPL which allows for divergence and convergence of the rod signals before synaptic output to the ganglion cells.

The cone bipolar cells fall into two categories: depolarising and hyperpolarising and this is described more fully in the following section on physiology (1.2.4). Of the 8 types of cone bipolars, three (not illustrated) are known as 'giant' or 'wide field'. They spread over 70-100um, connecting with as many as 15-20 cones. Little is known of them and they will not be discussed further here. Of the remaining 5 types, there is the common 'diffuse flat' (dfb) and 'diffuse invaginating' (dib) type which collect from several cones (5-7 centrally, and 12-14 peripherally). The junctions involving 'flat' dendritic connections are associated with hyperpolarising or 'off' responses to light, whereas those that are 'invaginating' are associated with depolarising or 'on' responses. The majority of cone bipolars comprise two further types known as 'midget' bipolars that connect to the same single cone, i.e. foveal cones output to 2 midget bipolars as well as the two types of diffuse bipolars. These also are either invaginating (imb) or flat (fmb) in their contact with the cone pedicle. Both the diffuse and the midget flat bipolars terminate in sublamina 'a', whereas the invaginating cells terminate in sublamina 'b'. This separate location for 'on' and 'off' activity has some bearing on the possible site of damage in the Cuban amblyopia which is discussed in Chapter 5. Finally, there is the 'blue cone bipolar' (bcb) which typically connects via several dendrites to a single blue cone and also terminates in sublamina 'b'.

Horizontal cells: Three types of horizontal cells have been distinguished in the retina (Linberg et al 1987). HI is the classic horizontal cell of the primate, first described by Polyak (1941). It is a small field cell (15um-diameter dendritic tree in the fovea, 80-100um in the periphery), with stout dendrites. In the fovea there are 7 distinct clusters of terminals contacting cones, and in the peripheral retina up to 18 clusters. It has a single thick axon that passes laterally in the OPL in a terminal stalk carrying a large number of terminals fanning out and each ending in a rod spherule (Kolb, 1970). HIII cells are similar in appearance but have dendritic spreads that are 1/3 greater. They are asymmetric, with one or two dendrites that are much longer, and because of their bigger field size contact more cone pedicles; it is thought that they too have axons

that terminate at a rod spherule (Kolb 1993). HII cells are quite different; they also have an axon but it is curled and short. Contacts with cones pedicles are by way of wispy terminals.

Horizontal cells are usually thought of as providing the first mechanism which forms the surround of ganglionic receptive fields. They also have a key role in rod-cone interactions in the cat and it is thought to be similar in the human (Nelson, 1977). In addition, recent electron microscopic studies of horizontal cells suggest an involvement in chromatic function (Kolb, 1991). HI primarily contacts red and green cones with a small number of contacts with blue cones. HII cells specifically contact blue cones. HIII cells avoid blue cones.

### **Inner Plexiform Layer**

The axonal endings of bipolar cells transmit information from the OPL to the of the IPL. The bipolar cells communicate with different types of functionally specialised amacrine cells and to dendrites of the various ganglion cells. The amacrine and ganglion cell branching takes a variety of forms. In particular, rod bipolars connect to the AII and A17 amacrine cells which collect enormous numbers of rods in their fields; hence much of scotopic sensitivity is accounted for by this. Cone amacrine cells are of the wide field type, and more restricted. They form complex synapses with bipolar cells, to which they are both post and presynaptic - thus more feedback- and also form sign inverting synapses- thereby helping to shape ganglion cell receptive fields.

Amacrine cells: There are at least 25 different types of amacrine cells in the human retina (Kolb 1991). They are classified by size of dendritic tree. Figure 1.7 shows the main categories. Small ( cells 1-10), medium (cells 10 and 11) and large ( cells 12-15 ); also the branching characteristics and in particular the stratification of the dendrites in the IPL serve to distinguish a number of categories. Their functions are thought to form 'surrounds' (with inhibition), and to modify cell behaviour- e.g. responsiveness to motion.

The neuropil of the IPL was arbitrarily divided into 5 strata by Cajal (1972), and since then this description has been used. An amacrine cell that stratifies in strata S1 and S2 (cell 1) differs from cells that stratify in strata 4 and 5 (cells 4 and 5). Some ramify diffusely through all the strata (cells 11 and 14). Some are monostратified (cell 13).

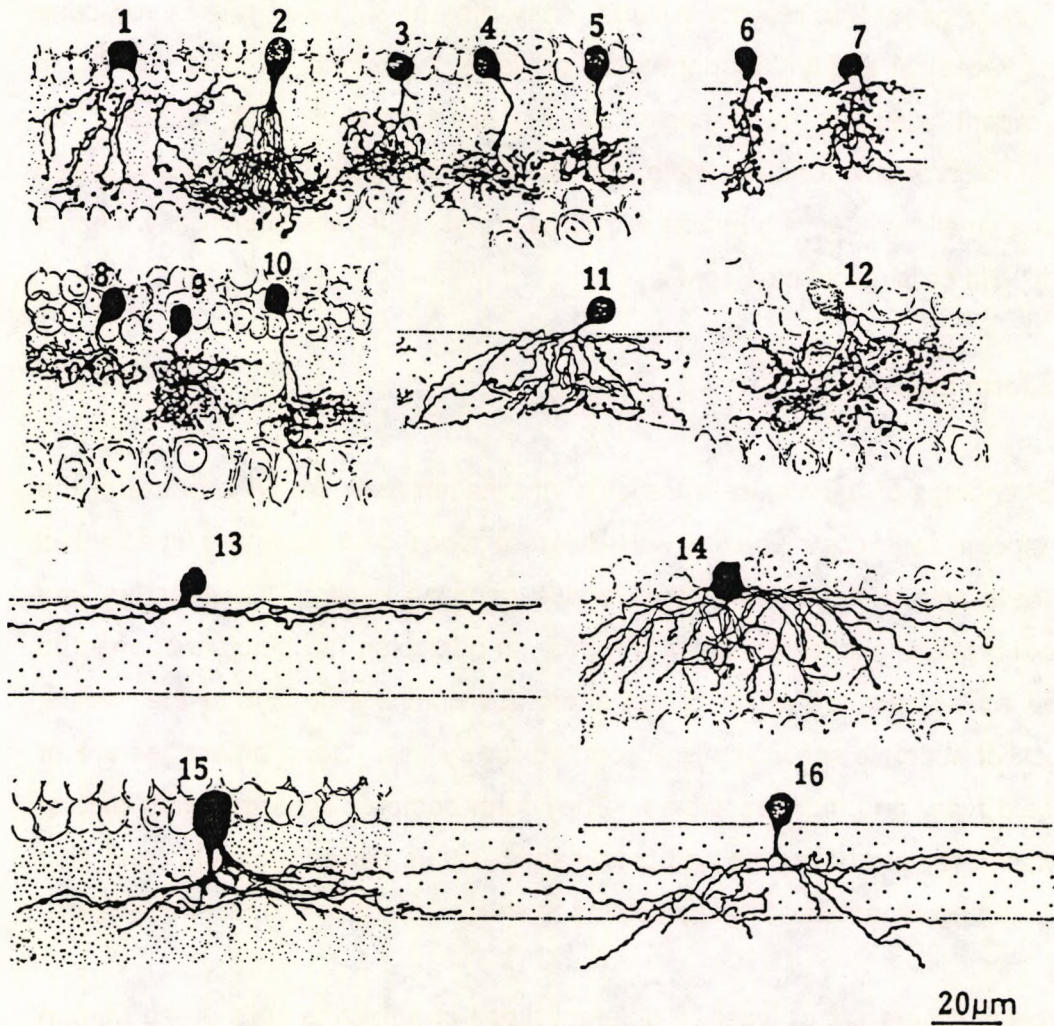


Figure 1.7: Drawings of Golgi-stained amacrine cells in vertical view in the monkey retina. See text for different cell types. (From Polyak 1941).

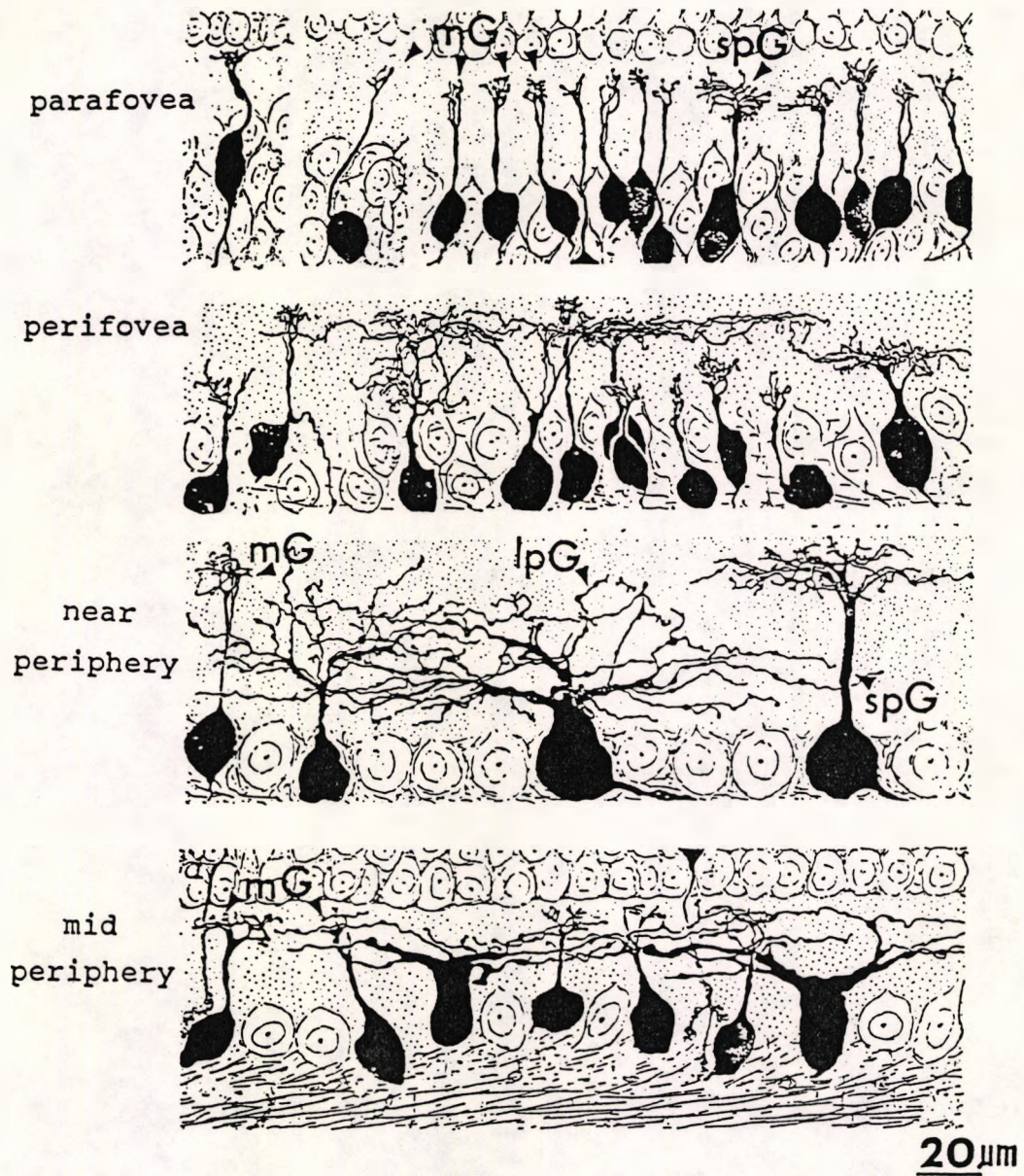


Figure 1.8: Drawings of the most common Golgi-stained ganglion cell types in the monkey retina. (mG = midget ganglion cells; spG = small parasol ganglion cells; lpG = large parasol ganglion cells) (From Polyak 1941).

Finally there are cells running in the reverse direction from the IPL to the OPL known as the 'interplexiform' cells. These may affect a long term re-organisation in dark adaptation and receptive field structure; not much is known about them (Dowling, 1987).

Ganglion cells: Using similar morphological criteria, there are at least 20 types of these (Kolb 1993). Figure 1.8 shows some. As with the amacrine cells the dendritic tree span increases with eccentricity, with the smallest fields in the fovea. Hence any classification has to include eccentricity, and inter-cell comparisons must be made at specific eccentricities. The 3 main categories shown are the 'large parasol' (25-90um), the 'small parasol' (10-35um) and the 'midget ganglion cells' (5-9um). In addition, there are a small number of small and large diffuse ganglion cells, bistratified cells and various large field monostatified with different stratification levels.

### **Nerve fibre layer**

Axons of the ganglion cells turn into the plane of the retina and are segregated into bundles by sheet-like Mueller cell processes and astrocytes. They travel across the surface towards the optic disc from where they leave the eye. Figure 1.9 shows how the blood vessels and the ganglion cell axons temporal to the disc circumnavigate the fovea so as not to degrade the quality of image; also no fibres cross the horizontal meridian. The thickness of the fibre layer is minimal peripherally and thickest at the disc and it is thought that in man the longer fibres lie on the on the vitreal side of the layer at the disc (Minkler, 1980).

### **Glial Cells**

The three basic types are Mueller cells, astroglia and microglia. Mueller cells are the basic supporting structures of the retina, stretching radially across to form the outer and inner limiting membranes and enveloping all the neural processes; interest has centred on them recently because of their role in maintaining the constancy of ionic composition of extra cellular fluid and in generating the ERG and for this reason reference is made to them.

### 1.2.3 CONTRAST, CONTRAST SENSITIVITY AND CONTRAST GAIN

The terms 'contrast', 'contrast sensitivity' and 'contrast gain' are used extensively throughout this work. In order to describe the physiology of the retina, it is necessary to use these terms. In order to define these terms it is helpful to know some physiology! On balance it seems best to interrupt the description of the anatomy and physiology of the retina at this point.

The layman knows exactly what he means by 'contrast' and, if pressed, will volunteer that it is pretty well independent of light level. To the visual scientist, it is a measure of the variation in luminance (temporal or spatial) in a stimulus, compared with mean level of luminance. For an aperiodic stimulus (e.g. Snellen letters), contrast (C) is generally taken as

$$C = (L_{\text{object}} - L_{\text{background}}) / (L_{\text{background}})$$

The threshold value for  $(L_{\text{object}} - L_{\text{background}})$  is often called  $\Delta L$  and hence the threshold of detectable contrast is  $\Delta L / (L_{\text{background}})$ . Weber's law, as applied to stimuli of large area, is that  $\Delta L / (L_{\text{background}})$  is a constant which is sometimes described as the Weber fraction or Weber's contrast.

For a periodic stimulus, contrast (C) is:

$$C = (L_{\text{max}} - L_{\text{min}}) / (L_{\text{max}} + L_{\text{min}})$$

and is frequently called Michelson contrast. For both versions, contrast sensitivity is taken to be the inverse of the threshold contrast.

#### NEURAL RESPONSES:

Kaplan (1991) reviews the work on the nature of neural responses to luminance and contrast. For there to be a relatively stable sensitivity to contrast over different illumination levels, there needs to be some kind automatic gain control. Otherwise the saturating nature of neural responses would lead to a plummeting of contrast sensitivity and a consequent distortion of the visual scene. This follows from the

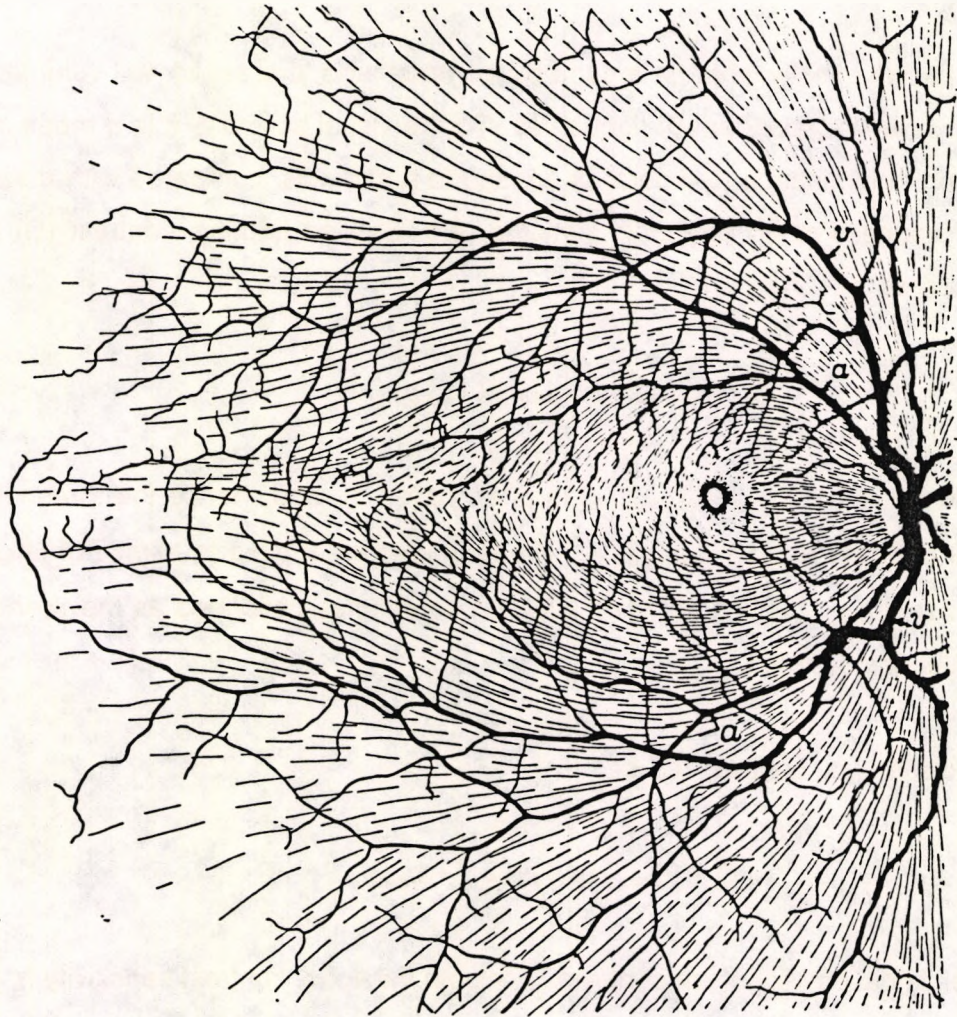


Figure 1.9: Optic nerve fibres and blood vessels (arteries 'a' and veins 'v' ) can be seen to circumnavigate the central fovea in the retina of the macaque monkey. The optic disc is seen on the right. (From Polyak, 1941).

Naka-Rushton equation which links the response (R) of a neuron to the luminance (L) viz:

$$R = L \cdot R_{\max} / (L + L_s)$$

where  $L_s$  is the luminance at which the response reaches half the maximum value  $R_{\max}$ . In situations where incremental stimuli  $L$  are superimposed on a background stimulus of luminance  $L_B$ , the luminance is replaced by  $L + L_B$  and the response is  $R + R_B$ . Since the 'gain' is  $\Delta R / \Delta L$  (or  $dR/dL$ ),

$$\text{Gain} = 1 / (L_B + L_s)^2 \cdot L_s \cdot R_{\max}$$

Where  $L_B \gg L_s$ ,

$$\text{Gain} = (L_s \cdot R_{\max}) / (L_B)^2$$

'Contrast gain' is the response per unit contrast and again for  $L_B \gg L_s$ ,

$$G_{\text{con}} = (L_s \cdot R_{\max}) / L_B$$

This means that the sensitivity to contrast is inversely proportional to the background light level. However, if the retina adapts with an 'automatic gain control' to avoid saturation over the range of illuminations represented in the scene, it has thereby averted the 'saturation catastrophe'. The Naka-Rushton equation can be modified to incorporate a gain factor 'g' that depends on the current luminance  $L$  and the luminance that immediately preceded it. Thus  $g$  is a 'functional' of  $L(t)$ ,  $g = g\{t, L(t)\}$  which can be written more simply as  $g\{L_B\}$ . The modified equation is:

$$\begin{aligned} R / R_{\max} &= (g\{L_B\} \cdot L) / (g\{L_B\} \cdot L + L_s) \\ \text{or } R / R_{\max} &= L / (L + L_s / g\{L_B\}) \\ &= L / (L + L_s'), \quad \text{where } L_s' = L_s / g\{L_B\}, \end{aligned}$$

The effect of adaptation can be thought of as changing the semi-saturation constant to  $L_s'$ , and the modified contrast gain becomes:

$$G_{\text{con}}' = (R_{\max} \cdot g\{L_B\} \cdot L_B) / L_s$$

With an appropriate choice by the adapting mechanisms for the functional 'g', the contrast sensitivity can be maintained.



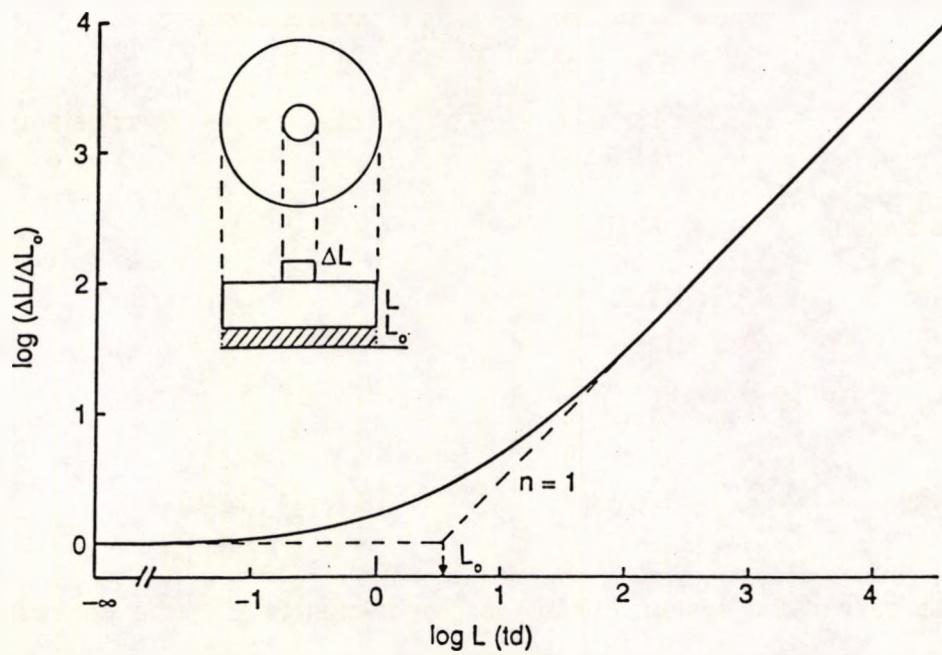


Figure 1.10: Photopic threshold-versus-intensity function based on the Wyszecki and Stiles data, (1982).

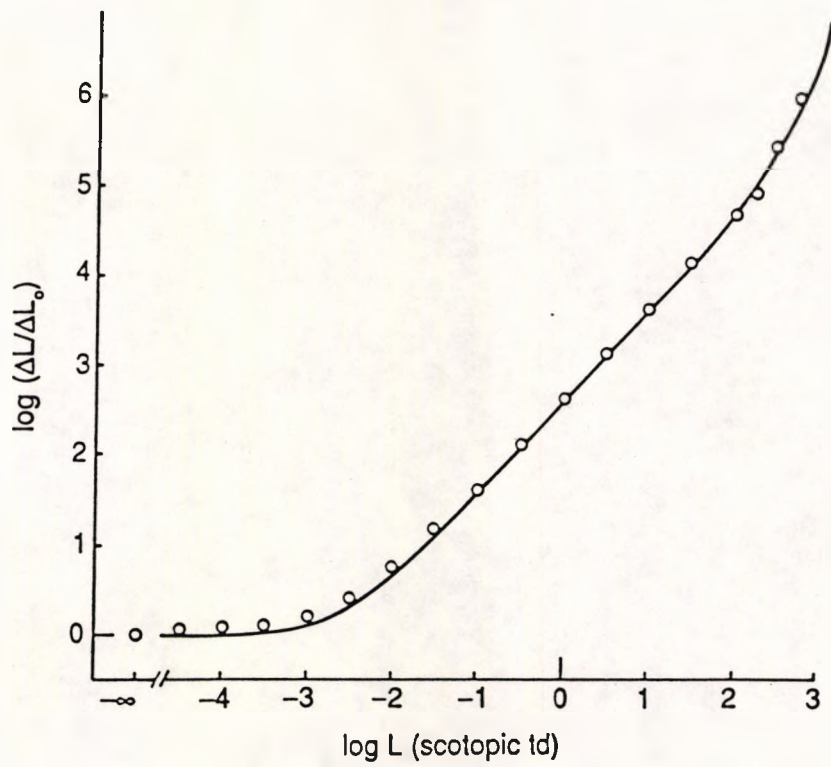


Figure 1.11: Scotopic threshold-versus-intensity function .(From Aguilar and Stiles, 1954).

(Wyszecki and Stiles, 1982). Figure 1.11 shows the equivalent function for scotopic vision with a saturating response at the higher luminances. (Aguilar and Stiles, 1954). The value of  $n = 0.5$  is an efficient gain compression at very low levels of illumination, where photon noise is significant and this is discussed in the next section. The value of  $n = 1$  gives rise to contrast constancy.

Originally, Fechner (1860) explained Weber's law in terms of a logarithmic response of the visual system to luminance. This necessitated a shallow intensity-response function rather than the steeper intensity-response function that is actually found; the sensitivity compression is now attributed to the automatic gain control described above. The possible nature and location of gain mechanisms is discussed in the next section.

#### 1.2.4 THE PHYSIOLOGY OF THE RETINA

Some of the work described in chapter 5 involves patients whose rod pathways are known to be defective at the retinal level and whose colour vision is, in some cases, affected. They see continuous light scintillations as if they have an ongoing intrusion of noise into their perception of images. For this reason, the physiology of the retina is described in some detail.

Part of the understanding of the physiological mechanisms in the human retina has been arrived at indirectly through psychophysics. More recently, methods have been developed both for studying the manner in which the absorption of light in the retinal image activates the system and the subsequent transmission of the signal. This has involved obtaining direct intracellular recordings on the large retinal cells of the lower vertebrates and much of the knowledge acquired is thought to apply to the human retina. Recordings have now been made on primates and much work has been done on extra-cellular recordings from ganglion cell optic nerve fibres or LGN cells. The crucial point is that they are single cell responses. In addition, the multicellular recordings of the human ERG have contributed to the understanding of the retinal mechanisms, although it is more the case that the knowledge of the underlying physiological mechanisms enables the ERG responses to be understood.

## Dynamic Range of the Retinal Response to Light Intensity

The visual system copes with light levels ranging from a total number of quanta entering the pupil at rate of  $100 \text{ s}^{-1}$  on a dark night, to  $10^{14} \text{ s}^{-1}$  on a sunny day. Nerve fibres can only transmit spikes at a rate of up to  $1000 \text{ s}^{-1}$  and alterations in stimulus strength can only be signalled by alterations in spike rate. Very small alterations in light intensity can be seen over a huge range, and so there has to be some kind of gain control applied for images under these extremes of lighting to be perceived at all. The alternative of there being different ganglion cells for different ranges of illumination is known not to apply. Retinal physiology is best appreciated if the problem of matching the dynamic range of visual signals to the limited capacity of nerve fibres is kept in mind. An additional task is to maintain a relatively constant response to a given contrast, so a scene may appear relatively unchanged over a wide range of illumination. This involves a gain control mechanism.

The gradual increase in detection thresholds (or decrease in sensitivity) with increasing luminance level might reflect an increase in noise and/or a reduction in gain. In the previous section, the consequences of possible gain changes were briefly considered in relation to the perception of contrast. A brief reference to 'noise' is now given, in order that the description of the physiology of the retinal components may be seen against this backdrop.

At low levels of light intensity the visual system needs to extract signals from a noisy stimulus (photon noise), noisy receptors (thermal breakdown of photopigments), noisy transmission lines (random release of transmitters). Photon noise is a major factor at the lowest levels of light intensity, with the photon density fluctuating by an amount that is proportional to the square root of the light intensity. Hence, the threshold of detectable change in intensity ( $\Delta L$ ) would be proportional to  $L^{1/2}$ . The psychophysical evidence for the 'square root law' operating in rod vision, i.e. a gain that reduces with the square root of the intensity of signal, indicates an optimal compression in gain in relation to photon noise. The level of noise in the transmitted signal is then independent of light intensity. With increasing light intensity, noise is not deemed to be a major factor in the effect of backgrounds on visual sensitivity (Walraven et al.).

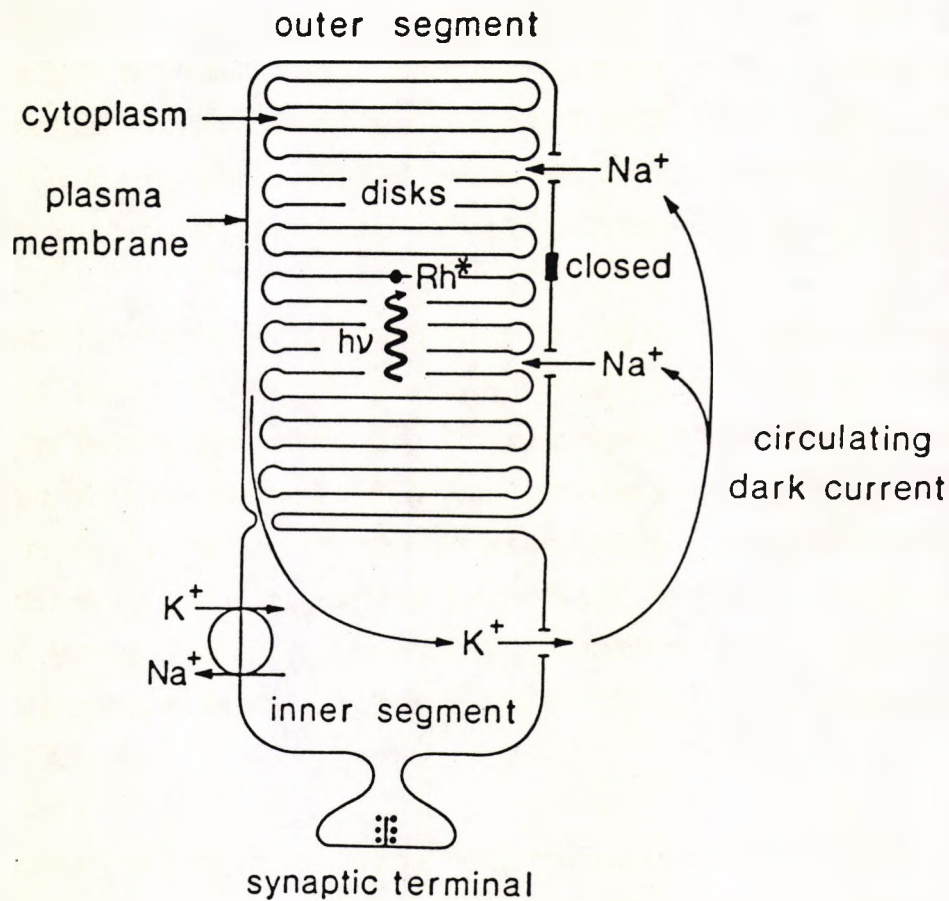


Figure 1.12: Excitation of a rod by the absorption of light.: A metabolic pump in the inner segment extrudes sodium ions; these are then free to enter the outer segment, the membrane of which has a high conductance for sodium ions in its resting state in the darkness. Light absorption by the rhodopsin embedded in stacks of 'disc' membranes leads to the closure of ion channels; the high conductance of the outer segment is transiently decreased. There is a reduction in the circulating current and consequent hyperpolarisation of the cell. (From Lamb, T.D.,1986).

## The Action of Light on Photoreceptors

In darkness there is a steady extracellular current flowing out of the inner parts of the photoreceptors towards the outer segments and then in through the outer segments to return intracellularly to the inner segments. Figure 1.12 shows how, in the case of a rod, this comes about. The inner segment has, in common with all cells, a Na-K pump extruding Na ions and maintaining a negative potential. In the dark, channels in the membrane of the outer segments are open allowing the return passage of cations, chiefly Na and Ca ions. This leaves the cell membrane in a depolarised state. The absorption of light by the outer segments causes these channels to be closed, blocking the re-entry of ions. This results in a hyperpolarisation, i.e. the inside of the cell becomes more negative with respect to the outside than it is in the dark. This contrasts with most sensory receptors which depolarise in response to a stimulus

Figure 1.13 (Baylor 1987) shows the voltage changes in a monkey rods and cones in response to brief flashes of light of increasing intensities. The responses of both the rods and cones have amplitudes that are continuously graded with increasing intensity, until they finally saturate; the relation to intensity is given by the percentage of channel closures. Further increases of light intensity simply result in an extended durations of the response. The time course of the closure of the channels in the outer segments is reflected in the transient decrease in circulating current, which in turn gives rise to leading edge of the a-wave in the ERG as well as dictating its entire time course.

The response of the cones is much faster than that of the rods and is less sensitive to light. 40 times as many photons must be absorbed by a dark adapted cone to give the same photocurrent as a dark adapted rod. The action spectrum of the photocurrents recorded from individual primate cones corresponds to the absorption spectrum of the three different pigments with maxima at 460, 530 and 568 nm whereas the responses of the rods peak at 491 nm and reflect the human scotopic sensitivity curve.

In Figure 1.13 it can also be seen that the rod responses reach half-saturation when each rod has absorbed about 30 photons. Each rod contains about  $10^9$  rhodopsin molecules, so each of these photons passing through the length of the outer limb has a high chance of capture (30% -50%). However, isolated rods can even demonstrate single photon responses, with the responses fluctuating according to a Poisson

distribution. The photocurrent is about 1 pA at its peak, estimated to have come about through the closure of a local patch of 4% of the membrane channels that had been open in the dark (i.e. many channels close as a result of a single photoisomerisation). This represents a very large amplification associated with the phototransduction converting light energy into electrical energy ( a gain of about  $10^6$  ). The rhodopsin is embedded in the stacks of disc membranes, physically separate from the surface membranes, which indicates that there must be an internal transmitter involved. This is now known to be a cyclic nucleotide (cGMP), present in the outer segments that in darkness opens the ion channels. Photoisomerisation of the visual pigment leads to the hydrolysis of cGMP and the resulting reduction in concentration of cGMP leads to closure of ion channels resulting in hyperpolarisation. Restoration of the concentration associated with the dark state involves a another enzyme (cyclase) whose activity is speeded up by the reduction in the calcium concentration. A similar process operates in cones in which the basic mechanisms are similar, more rapid, but operate at lower gain.

Light adaptation in the rods and cones: there appears to be a gain control mechanism by which the gain varies with light intensity (Purpura et al. 1988). This operates even at very low levels of light stimulation, where the amount of bleaching of pigment is so little that the loss of sensitivity with increasing light intensity cannot be ascribed to there being a reduced amount of pigment available for light catching. It is now known to involve a feedback mechanism controlling the concentration of cGMP. Light activates the enzyme PDE which reduces the concentration of cGMP. At the end of the light stimulus the concentration of cGMP rises as it is synthesised by another enzyme, GMP cyclase. The rate of formation of cGMP is controlled by the intracellular free calcium concentration. During a long flash, when channels close, the rate of entry of calcium drops, but it continues to be extruded by a calcium pump. Consequently the calcium concentration falls, and the rate of formation of cGMP by cyclase increases. This feedback mechanism reduces the 'gain' of transduction i.e. the sensitivity of the receptor. Other mechanisms, involving a protein called 'arrestin' and phosphorylation of opsin also may reduce the sensitivity.

Another control of sensitivity is afforded by response saturation. There are a finite number of light controlled channels in the surface membrane. Hence, at low intensity levels, the number of channels closed is proportional to the light intensity. For instance, a quantum causes the closure of about 4% of all channels, leaving the numbers of channels available for closure virtually unchanged. As the intensity

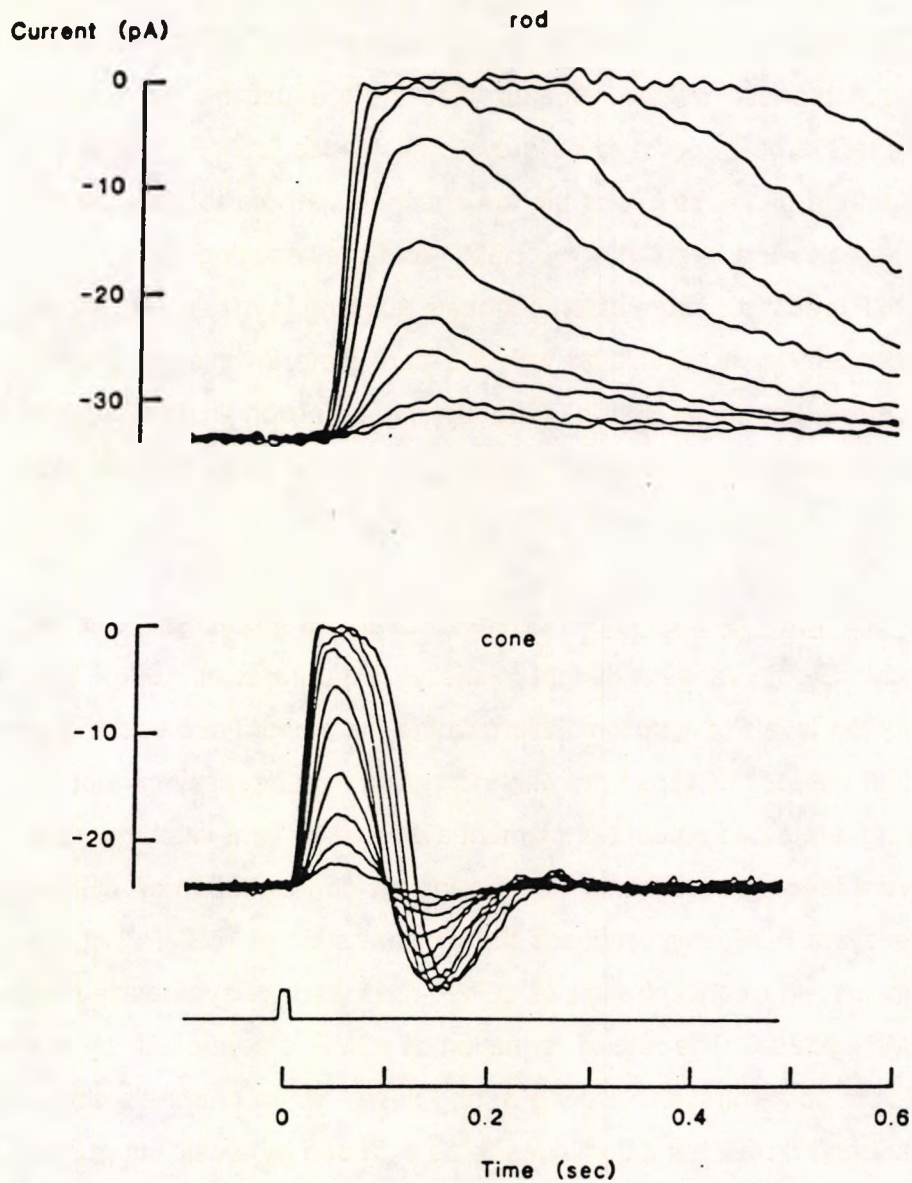


Figure 1.13: Reduction of circulating current through a monkey rod and cone produced by flashes of light flashes of different intensities. The separate intensities vary by a factor of two, with the rod photoisomerisations ranging from 3 to 900, and the cones from 200 to 36000. Timing of flash is shown. (From Baylor, D.A., 1987).

increases and the number of channels available for closure decreases, the sensitivity effectively decreases until saturation is reached when all channels are closed. This manner of sensitivity control accounts for the V/Log I relationship. This implies that the extended range of operation of the retina (i.e. the full extent of the adaptation or gain control) must involve other mechanisms. One of these sites is in the isolated photoreceptor but other sites of adaptation may also occur, possibly at the bipolar level (Falk, 1991).

Light adaptation in rods: The sensitivity (defined above) for primate rods was first reported to be maintained constant for large ranges of adapting lights, and this was unlike the rods of amphibians (Baylor, 1987). However, more recent work (Tamura and Yau, 1991) shows that in primates too, there is a local regulation of sensitivity by background illumination. There may be differences in the 'threshold-versus-intensity' (t.v.i.) curves determined psychophysically, and those derived from direct measurements on rods, which could imply further stages of sensitivity control at postsynaptic sites in the retina.

#### Light adaptation in cones:

The equivalent relationship between the cone system t.v.i. and the individual photon responses of cone receptors has not yet been characterised. However, it is known that there are additional gain control mechanisms as the cones cannot be saturated by steady background.

#### Interconnections of Photoreceptors

Rod-rod coupling; Rods do not operate in isolation. The signal induced in a rod spreads electrically, via gap junction to other rods, with the result that the width of the receptive field of a rod is far greater than a single rod's diameter. Such coupling results in spatial averaging which smoothes out quantal fluctuations. Because the current spreads to other rods, the response of a rod to a single photon is less in a coupled network. However many rod outputs converge at the synapse with the bipolar and horizontal cell resulting in the transmitted signal being at least as great as in the absence of coupling. An additional consequence of this coupling is that, as the signal spreads the temporal response to a single flash of light becomes of shorter duration i.e. the voltage response is more 'transient' than the photocurrent.

Cone-cone coupling: Gap junctions are present in the primate retina implying electrical coupling between photoreceptors. These may however not occur in the foveal cones which connect to midget bipolar cells. (However interactions between different cone types occur postsynaptically through H-cell feedback).

Rod-cone coupling: This exists but is much weaker than rod-rod coupling. For example, in CSNB there is a block of the rod synapse, but somehow rod signals get through to the brain, even though the sensitivity is lower than if the right pathway was operative. It is known that in the cat, rod signals can be detected in intracellular records from single cones (Nelson 1977) and this pathway may be operative in CSNB.

### The Outer Plexiform Layer

Because of the short distances involved, the graded hyperpolarisation produced by light in rod and cone outer segments spreads to the synaptic terminals without any great loss. Absorption of light by the photoreceptors results in a reduction of the transmitter released by the terminals. The intracellular potential of the horizontal cells always moves in the same direction as the receptors (at least in those connected to rods) and therefore the chemical transmitter, released in the dark, has a depolarising action on them and the absorption of light, which results in a reduction of transmitter, has a hyperpolarising action. However the bipolar cells respond in two ways; some of the bipolar cells also hyperpolarise in response to a decrease in transmitter concentration, i.e. when light is absorbed by the underlying receptor cell in the centre of its receptive field. These are called 'off-bipolars' because they drive ganglion cells that fire at light offset. Others known as 'on-bipolars' depolarise when the centre of the receptive field is illuminated i.e they drive ganglion cells that fire at light onset. This parallel processing of increases in light intensity (the on-pathway) and decreases in intensity (the off-pathway) is thought to enhance contrast sensitivity.

Horizontal cells have an apparent large receptive field because of their extensive electrical coupling. This means that large responses are obtained only with large targets as small point images can only give small responses because of the electrical loading by the rest of the coupled network. There are two types of horizontal cells described by some (Falk 1991) as A and B. A has a large soma with thick dendrites and corresponds to the HI cells described by Kolb (1991). Type B has finer dendrites (HII). The dendrites of both make synapses with cones; B has a long axon terminating

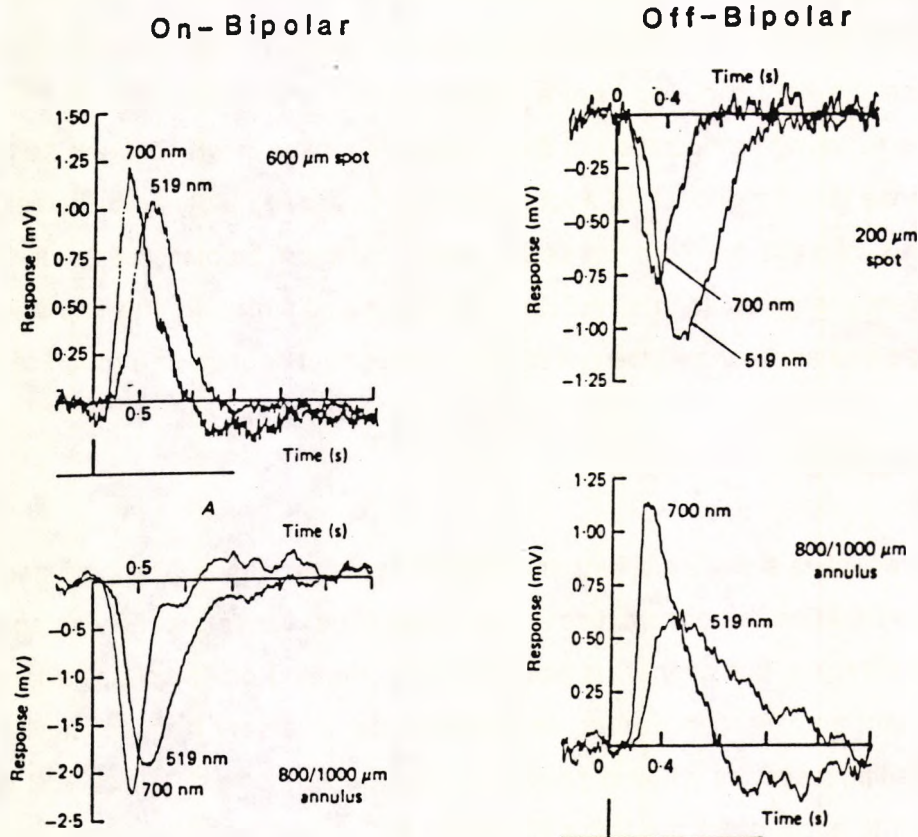


Figure 1.14: Centre-surround organisation of the receptive field of bipolar cells in the salamander retina. The stimuli have been chosen to stimulate selectively either rods or cones with the light intensities chosen to evoke roughly similar response amplitudes. The opposite polarity of the responses to a centred spot of light rather than an annulus is seen for both an on-centre and an off-centre bipolar cell. (From Capovilla et al. 1987). Note also that the response to rods is slower than the response to cones.

in rod spherules. Type A has no synaptic contact with rods, even though both rod and cone signals can be recorded from both types. This mixing of rod and cone signals is thought to arise from low resistance gap junctions between rod spherules and cone pedicles.

With their large receptive fields, horizontal cells are able to provide the antagonistic surround that opposes the centre response of the bipolar cells. Such an arrangement enhances edge detection and underlies colour opponency. Horizontal cells make synaptic contact with the bipolars and feed back synaptically onto cones so as to oppose the light induced centre response of the bipolars. Figure 1.14 shows the centre-surround organization of the bipolar responses in which it can be seen that the response to a small centred spot of light is of opposite polarity to the response to an annulus of light for both on-centre and off-centre bipolar cells. If the target is sufficiently large so as to stimulate both centre and surround, the separate responses oppose one another and the net result is either no response or a much reduced one.

### Synaptic Gain

Photoreceptive signals are further amplified at the synapses. The gain associated with the transmission to horizontal cells and off-bipolars varies greatly with spatial aspects of the stimulus, but overall is about 10 fold. For rod on- bipolars, a large and very significant amplification occurs, and this results in a very high sensitivity to light. A rod bipolar responds when a photon is absorbed by only 1 out of 100 rods. This is thought to account for the large difference in the amount of light required to produce the a-wave of the ERG as opposed to the b-wave (Falk, 1991). Blocking the rod on-bipolars results in loss of b-wave, which is one of the key signs of the MAR and CSNB patients, described in Chapter 5.

Synaptic gain is determined by the strength of signal required to alter transmitter release and on the magnitude of the postsynaptic conductance change resulting from the transmitter. Rods and cones are depolarised in the dark and therefore are operating on the steep part of the curve linking membrane potential and transmitter released. Hence a small change in presynaptic voltage resulting from dim light will produce a large change in transmitter released. The higher gain at the synapse with the on-bipolar cells, which depolarise when rods hyperpolarise, is due to its mode of operation. This type of sign inverting synapse, operates through a cGMP cascade very similar to that in the rod outer limb. The glutamate receptor initiates the enzyme

cascade in the bipolar, while in the rod it is opsin the cascade being a chemical amplifier. The synapse with the rod bipolar cells also sharpens temporal resolution (mentioned above). Probably, similar mechanisms operate at cone-bipolar synapses.

### The Inner Plexiform Layer

The IPL contains amacrine cell processes, bipolar cell processes, and the dendrites of ganglion cells. The axons of ganglion cells, are by comparison few and far between. Some amacrine cells have 'pseudo-spikes', i.e. their membranes are regenerative, with a series of wavelets which last most of 10 ms as opposed to spikes of 1ms duration found with the ganglion cells. The process of inactivation, required for a travelling spike, does not occur. It is in the axons of the ganglion cells that the real action potentials are generated and intensity is signalled by frequency modulation. Recordings made by Kuffler (1953), from a single on-centre ganglion cell in the cat show the centre-surround organization (Figure 1.15). There is a spontaneous maintained discharge in the dark. (A) shows how a small spot of light, centred in the receptive field, causes an abrupt increase in the firing rate, (B) demonstrates how an annulus of light, appropriately sized to fall on the surround of the receptive field, causes a suppression of the firing rate. Removal of the stimulus produces a transient increase in the firing rate. Uniform illumination is seen to have a lesser effect on the firing rate than the small spot since it is reflecting the contributions of both the centre and the surround. For an off-centre ganglion cell the pattern of firing is reversed, with a small central stimulus causing a reduction in firing rate and so on. For both the on- and the off-cells, there are two distinct types of cell; those that respond in a 'linear' or a 'sustained' fashion to a sustained flash of light and those that respond in a 'non-linear' or a 'transient' way to a continuing presentation of the stimulus, i.e. they fade away with time. In addition there are cells that respond only to light that moves across their field in a preferred direction; others are simple motion detectors. A summary of the properties of sustained and transient 'on' and 'off' ganglion cells is shown in Figure 1.16 (Ikeda 1985).

The simplest pathways for the cone system are cone/on-bipolar/on-ganglion and cone/off-bipolar /off-ganglion ( with the bipolar/ganglion synapses being located in sublamina b and sublamina a respectively). Rod bipolars are on-bipolars and yet both on- and off- ganglion cells have rod input. The explanation for this apparent paradox is that rod bipolars do not have direct synapses with ganglion cells but synapse with the A II and A25 amacrine cells in sublamina b. A sign-inverting

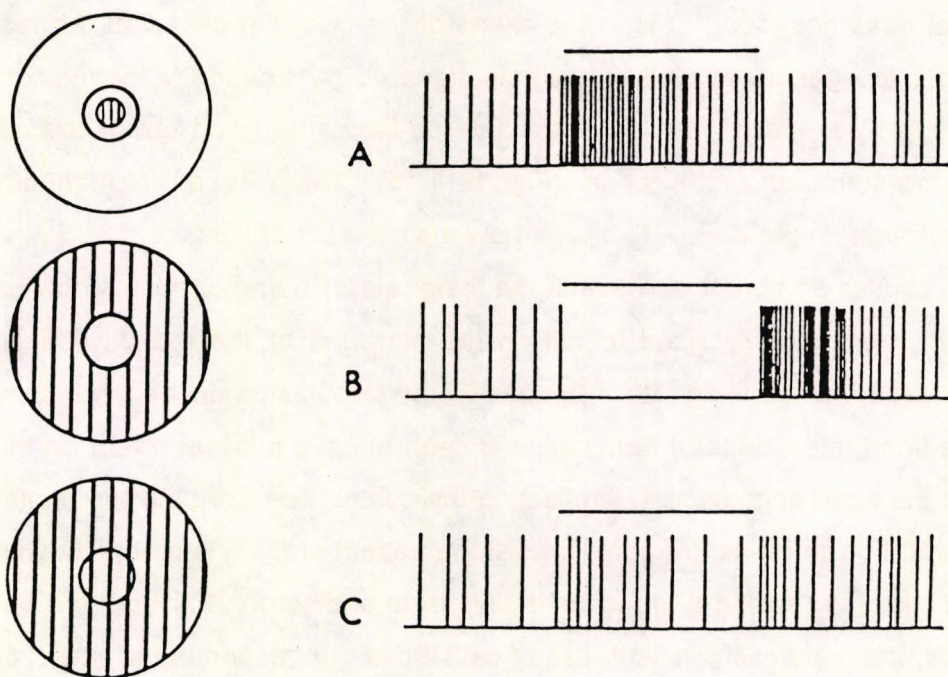


Figure 1.15: Firings of an on-centre ganglion cell in the retina of an anaesthetised cat. (A) shows the increased response rate to a centred spot of light; (B) the suppression of response by an annulus; (C) The substantial cancellation of responses by a large field stimulus. (From Kuffler 1973).

		<u>Sustained (Tonic, X)</u>		<u>Transient (Phasic, Y)</u>	
		On	Off	On	Off
Excitatory Visual Trigger	Centre				
	Surround				
Inhibitory Visual Trigger	Centre				
	Surround				
Synapse Position in IPL		subl. b	subl. a	subl. b	subl. a
Optimal Spot		Small		Large	
Firing to Stationary Optimal Spot		Sustained		Transient	
Receptive Field Size		Small		Large	
Spatial Summation		Linear		Non-Linear	
Peripheral Activation		Ineffective		Effective	
Relative Common Location		Central retina		Peripheral retina	
Morphology		Small soma, dendrite, & axon ( $\beta$ type)		Large soma, dendrite & axon ( $\alpha$ type)	
Axonal Conduction		Slow		Fast	
Destination		LGN		LGN Superior colliculus	
Possible Functional Role		Analysis of spatial detail		Detection of novel or of movement in visual field	

Figure 1.16: Summary of the properties of ganglion cells of the cat's retina.  
(From Ikeda 1985).

synapse occurring between the amacrine cells and the off-ganglion cells provides the off-ganglion cells with their input.

#### 1.2.5 PRIMATE FOVEAL GANGLION CELLS

Much of the work leading to the descriptions and classifications of the cells in the retina has been carried out on lower vertebrates and, in particular, the classification of the ganglion cells through their physiological responses has been based on those of the cat. More recently there has been a major study by Calkins et al. (1995) on the morphology of foveal ganglion cells of the primate, which has a more direct bearing on the interpretation of the data presented in this thesis.

The conventional description is that there are two types of foveal ganglion cell; the P and M, so named because they project to the parvocellular and the magnocellular layers of the LGN. P-cells have a spatially and chromatically opponent receptive field, are sustained and are thought to correspond morphologically to the 'midget' ganglion cell. They are present in the greatest numbers, totalling 90-95% of all foveal ganglion cells (Dacey, 1993). M-cells are achromatic, spatially opponent, are transient and are thought to correspond morphologically to the 'parasol' cells and constitute 5-10% of the foveal ganglion cells (Silveira & Perry 1991). The standard model considers that P-cells not only signal colour, but with their small receptive fields, dense sampling, involving receptive field overlap, and ability to signal high contrast, to subserve high spatial acuity tasks, provided high temporal frequencies are not involved. M-cells have large receptive fields, lower sampling density, low contrast thresholds and although saturating at a low contrast, are thought, at threshold, to subserve the achromatic contrast sensitivity function at low spatial frequencies. The extent to which this model does characterise all the foveal ganglion cells has been recently re-examined by Tsukamoto et al. (1992), and Calkins et al. (1995) and is now described. They examined a population of 157 ganglion cells. The picture differed considerably from the conventional description. 73% were midget cells with a compact dendritic tree and in close association with a single midget bipolar; 27% were non-midget, with larger dendritic trees displaying a variety of types of synaptic contact

**Midget ganglion cells:** Each M and L cone pedicle synapses with both a 'flat' and an 'invaginating' bipolar (Chapter 1.2.2), the former terminating in sublamina 'a', the latter in sublamina 'b'. Every synapse on any given midget ganglion cell comes from one midget bipolar. i.e. there is a private pathway from cone to ganglion cell (Calkins et al

1994) with each M or L cone providing both an off-response in sublamina 'a' and an on-response in sublamina 'b'. Their most striking finding was that there were two distinct categories of bipolar/ganglion connection; one involving approximately 28 synapses and the other approximately 47. They hypothesise that the two synapse arrangements are specific for the two wavelength categories, since the only known difference in the two cone types is their visual pigment. They go on to suggest that it is the circuit with the large number of synapses that connect with the M cones, and those with fewer that connect with the L cones. They base this suggestion on the fact that the average scene provides a spectral input that results in the M cells collecting 10% fewer quanta. Weighting the synapses would balance the strength of signal, thereby reducing chromatic noise.

If they are correct in suggesting that the two circuits are linked to the two cone types, then there is an implication for the nature of the chromatic opponency. Most cones are surrounded by a mixture of other cone types. Spectrally pure antagonism requires spectrally pure lateral connections (Reid and Shapley, 1992). However it is thought that horizontal cells are not spectrally selective (Wässle et al. 1989). Kolb (1991) says they are to some extent. Also the narrow field amacrine cells are also found not to be spectrally selective. (Calkins et al. 1995). Hence pure spectral opponency could, as Lennie (1992) suggests, simply result from a random distribution in the surround.

**Non-midget ganglion cells:** 27% of the foveal ganglion cells are non-midget, a far greater percentage than previous estimations (Calkins et al. 1995). Whilst 75% of them had dendrites in either sublamina 'a' or 'b', and include the parasol cells, 25% are 'bistratified', in that they ramify in both sublamina 'a' and 'b'. Of these there are two types; one type synapses both with the blue cone bipolar, in sublamina 'b' and with diffuse bipolar terminals in sublamina 'a' that have both M and L inputs. This ganglion cell is wired as an ON(S)/OFF(M+L) (Nelson et al., 1978), and probably corresponds to the blue-ON bistratified cell of Dacey and Lee (1994). The other type of bistratified cell collects from diffuse bipolars in both sublaminae and not from blue bipolars. Their specific cone inputs are not known but they could either be an ON-OFF luminance cell or a chromatically antagonistic cell. The latter only requires an uneven weighting of cone types to the on-and off-bipolar cells. Both these bistratified cell types would be candidates for the physiological Type II cells (Wiesel and Hubel 1966, De Monasterio and Gouras, 1975 and Derrington and Lennie, (1984). If they

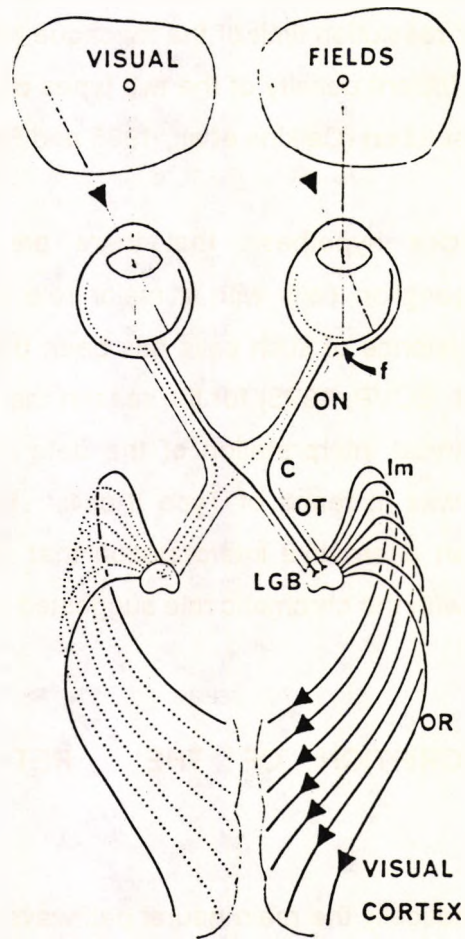


Figure 1.17: A schematic diagram of the main neural pathways involved in vision. It shows excitation of the visual pathway by the left visual field through to the lateral geniculate body (LGB) and visual cortex. f = fovea, Im = loop of Meyer, C = chiasma, ON = optic nerve, OR = optic radiations, OT = optic tract. (From Ruskell1988).

mediate B/Y and R/G colour opponency as suggested by Rodieck (1991), the sampling frequency of their arrays should match the psychophysical observations. Sekiguchi and Williams (1993), established psychophysically that the neural pathways for detecting R/G isoluminant gratings and S cone isolating gratings are spatially similar, with a R/G isoluminant resolution of 20-27 c/degree. This is higher than the resolution limit found by Mullen (1985), and so taking it to be an upper limit and allowing for the lower resolution limit of the macaque (Merigan and Katz, 1990) it appears that there is a sufficient density of the two types of bistratified cells (R/G and B/Y) to account for the resolution (Calkins et al., 1995 and Rodieck 1991).

This shows that Rodieck's hypothesis that there are spatially non-opponent, chromatically opponent ganglion cells with a major role in colour vision might be correct. However, the existence of such cells has been deemed unlikely by Lennie, (private communication at ECVF, 1995) for the reason that no-one has been able to find them again! The initial interpretation of the data on the Cuban Amblyopia, described in Chapter 5, was in terms of Type II cells. Following a suggestion by Lennie, we have given an alternative interpretation that does not depend on the existence of Type II cells with the chromatic role suggested by Rodieck (1990).

#### 1.2.6 A BRIEF DESCRIPTION OF THE RETINOGENICULOCORTICAL PATHWAYS

Figure 1.17 shows schematically the main neural pathways involved in human vision. The optic nerves from the right and left eyes come together at the optic chiasma. At this point the fibres from the nasal half of both retinae cross and join the fibres from the temporal retinae of the opposite eye. This means that information from the right visual field, relayed by the 'lateral geniculate nucleus' (LGN), ends up in the left visual cortex and vice-versa. There is also an 'up-down' reversal. The macular region is arranged differently with half the fibres crossing over so that the fovea is represented in both hemispheres.

In addition some fibres leaving the optic tracts terminate either in the pretectal region or the superior colliculus (Davson 1949). These are thought to be involved with pupillary reflexes and the control of eye movements respectively and will not be considered further in this work.

The lateral geniculate nucleus is arranged in 6 distinct layers shown in Figure 1.18. The cells in layers 1 and 2 are the magnocellular cells receiving input from the M ganglion cells (see section 1.2.5). They are larger than those in layers 3-6, which are known as the parvocellular cells which receive input from the P ganglion cells. It follows that fibres from the fovea end predominately in the central regions of layers 3-6 with the parafovea being represented in all layers. The information from the two eyes is kept separate, i.e. the crossed fibres terminate in layers 1, 4 and 6 whereas the uncrossed fibres terminate in layers 2, 3 and 5. In addition, the retinal topography is substantially retained within the separate layers of the LGN (Le Gros Clark, 1934). The separate fibres from the LGN then project to separate subdivisions of layer 4C of the cortex with this separation being maintained within layer 17. Beyond this there are several visual cortical areas, each with a complete topographical map; these extrastriate areas are thought to subserve different aspects of vision. In particular V4 (in temporal cortex) is thought to be primarily concerned with colour vision (Zeki 1980), and MT (in parietal cortex) with movement (Dubner and Zeki 1971).

Recently interest has focused on two particular subcortical pathways (magnocellular and parvocellular- or M and P pathways), and two cortical pathways (parietal and temporal pathways) and the possible relationship between them. The suggestion is that distinct channels of information arise in the retina and remain segregated up to the highest levels in the cortex with two largely independent subsystems that mediate different classes of visual behaviour. This view is evaluated in a recent review by Merigan and Maunsell (1993).

The M and P pathways excite interest, not only because of the extent to which they dominate vision i.e. they comprise > 90% of the axons leaving the retina (Shapley and Perry 1986), but also because of the curious sharp anatomical segregation and even beyond) layer 4C of VI (striate cortex), described above and shown in Figure 1.19. The extra-striate cortex is also dominated by two pathways. One includes regions in the parietal cortex and is thought to have special responsibility for assessing spatial relationships and object motion; the other chiefly located in the temporal cortex is thought to be involved in visual identification of colours, patterns and objects (Ungerleider and Mishkin 1982). Anatomical, physiological and behavioural evidence has suggested a relationship between these subcortical and cortical pathways which was finally made explicit by Livingstone and Hubel (1987). The idea of such distinct parallel pathways became immediately popular partly because of its simplicity but also because of its ability to account for much psychophysical data.

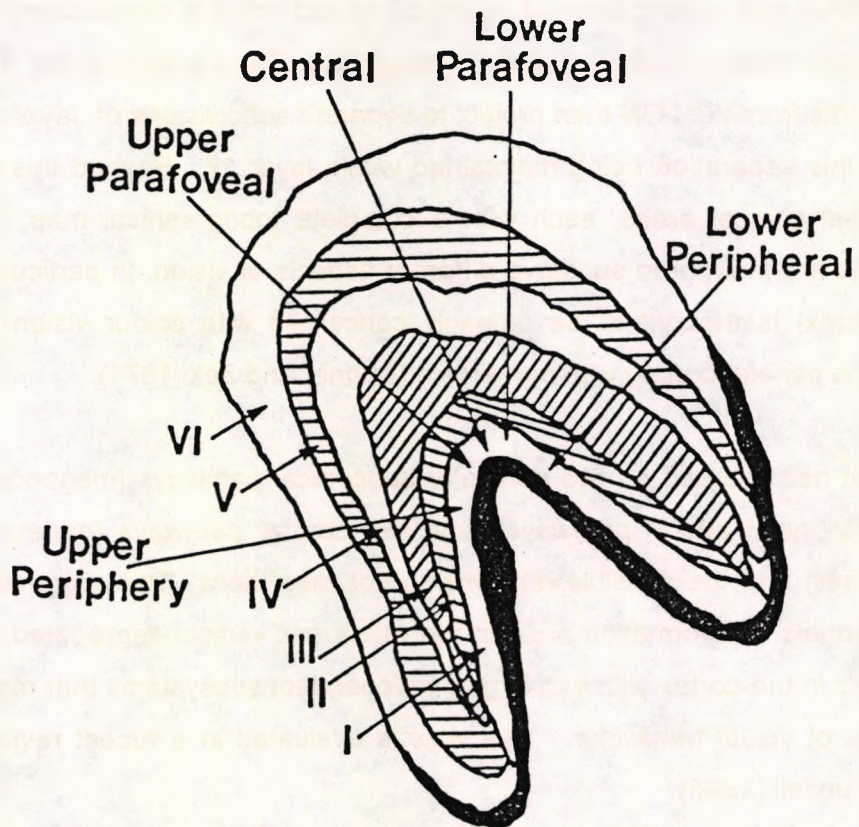


Figure 1.18: Cross sectional representation of the left lateral geniculate body of the Rhesus monkey, showing the six cellular layers and approximate projections of points in the visual field (From Ruddock, 1977)

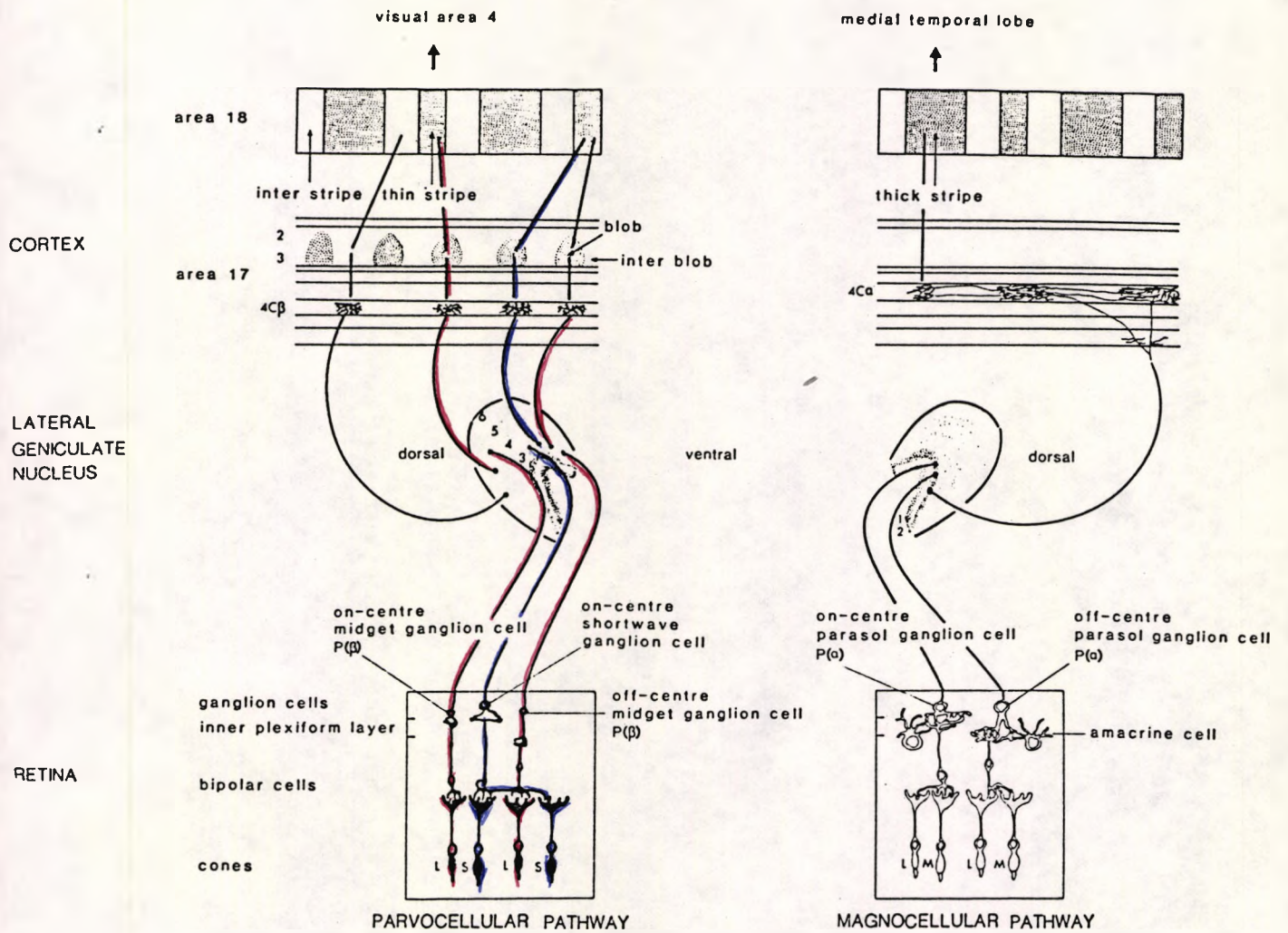


Figure 1.19: The parallel channels of the geniculostriate pathway of the primate visual system. The magnocellular system carries little chromatic information: The large  $P\alpha$  cells of the retina project to the magnocellular layers (1 and 2) of the lateral geniculate nucleus and then to layer 4C $\alpha$  of the visual cortex and the 'thick stripes' of area 18. A second parallelism is represented within the parvocellular system; here the parallelism is between a channel that carries almost pure chromatic information and a channel that carries information about colour and spatial contrast. These two subsystems of colour, represented by blue and red respectively, appear to remain independent at least as far as the 'blobs' of area 17 of the cortex. (From Mollon, 1989).

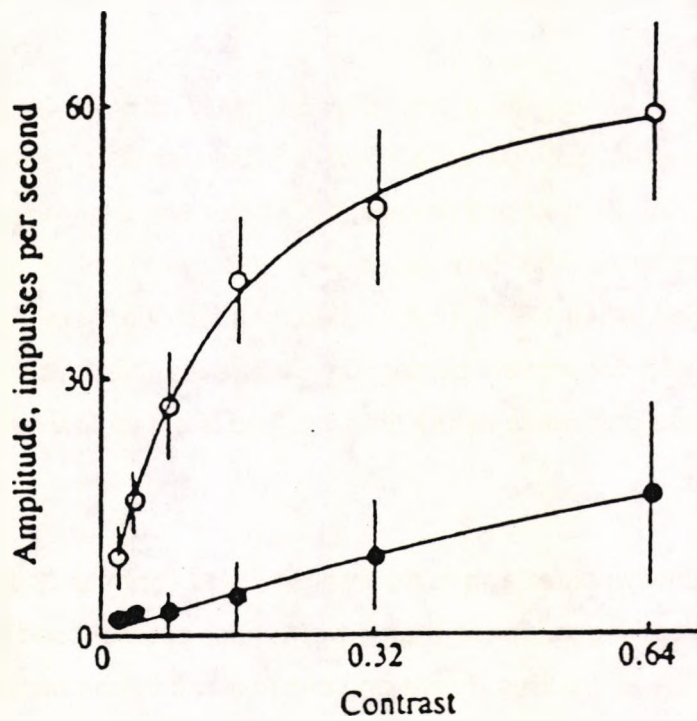


Figure 1.20: Average response-contrast functions for ganglion cells in the rhesus monkey. Recordings were from 28 parvocellular projecting cells (o), and 8 magnocellular (●). The stimulus was a sinusoidal grating of optimum frequency for each cell, drifting at 4 Hz. (From Kaplan and Shapley, 1986).

### Physiology of the P and M pathways: spatial, temporal and chromatic characteristics:

Whilst the anatomical segregation of P and M pathways is essentially complete, the physiological responses of cells in these two pathways are very different in some respects but virtually identical in others. The most obvious difference lies in their response to colour. P pathway neurons show both red/green and blue/yellow opponency, responding to colour differences, quite independently of the accompanying luminance. On the other hand, M cells are described as colour insensitive because of having virtually no response to isoluminant alternating stimuli even though there are some circumstances under which they can give a non-selective or unsigned response to changes in colour.

Another respect in which they are physiologically distinct is in their temporal responses to visual stimuli. M cells show a more transient response than P cells (Purpura et al. 1990, Schiller and Malpeli, 1978) and with their larger axons, conduct impulses more rapidly. This last observation (Gouras 1969; Kaplan and Shapley 1982; Schiller and Malpeli 1978) is often cited as a factor in favour of deeming the M pathway specialised for motion perception. However, the velocity difference may have no functional significance as the time involved is only a few milliseconds (Lennie et al. 1990).

The P and M pathways differ also in their sensitivity to contrast. Kaplan and Shapley (1986) produced striking evidence that (even under optimal conditions) M cells are many times more sensitive than P cells and can respond to contrasts <2%; individual P cells rarely respond to contrasts below 10% (Figure 1.20). This difference has been ascribed to a difference in receptive field size (de Monasterio and Gouras, 1975; Lennie et al., 1990) although there is little difference in the receptive field centre size (Derrington and Lennie 1984). A further distinction is that the M cells saturate at lower contrasts.

Stimulus dimensions in which the P and M cells have different but largely overlapping responses include spatial, temporal and luminance responses. The differences can be small. The claim that the M cells are more sensitive to high temporal and low spatial frequencies is based on differences in peak temporal frequency, cut-off frequency and peak spatial frequencies of as little as 15%. The M cells have a lower luminance threshold but with a large overlap range in which they both respond (Purpura et al.

1988). These responses are considered further in relation to the neural basis of psychophysical channels in Section 1.3.2

#### The temporal and parietal pathways

The evidence from anatomical experiments make a clear case for the distinctiveness of these two pathways, and strongly suggest that the terminations of M and P in V1 and V11. are to a considerable degree routed into different cortical regions (Figure 1.19) However the behavioural and physiological segregation between the cortical pathways is not as striking, and evidence is incomplete. (see Merigan and Maunsell 1993).

### 1.3 INTRODUCTION TO PSYCHOPHYSICS

Psychophysics is the direct quantitative study of sensory performance, and has a key role in the understanding of sensory mechanisms. By systematically manipulating the input to the system and restricting the range of permitted responses, much can be learnt of the response characteristics of the underlying mechanisms. Also, when used in conjunction with human anatomy, animal electrophysiological recordings (in particular primate single cell recording), it provides a powerful tool for understanding human neural networks, both normal and abnormal. It is in this latter activity that there is much controversy.

Since this thesis is based on psychophysics and in particular involves considering the neural implications of psychophysical data, it is helpful to give a background resume not only of psychophysical methods in general as well as those actually used but also to refer to some of the problems associated with attempting to identify physiological substrates of psychophysical channels.

There are many texts on classical psychophysics and psychophysical procedures (e.g. Graham, 1965), with two types of measurement being central to these procedures. The first involves the establishing of a sensory match between two 'input' stimuli that differ physically in some respect, e.g. spectral content. An assumption is made that, if the two stimuli result in physiologically identical signals to the 'brain', they will be seen identically and conversely that, if they are seen identically, it follows that somewhere along the path between the retinal image and the subsequent perceived image there must be identical physiological activity. The second type of measurement involves 'manipulating' the input stimulus until it has reached some threshold value. The threshold might be either an 'absolute' threshold, in which the stimulus or some characteristic of it is just seen or a 'difference' threshold in which the stimulus is just distinguishable from another.

The value of the evidence resulting from sensory experiments has been examined in a definitive work by Brindley (1970). The category above he designates as Class A and argues that the assumption linking physiological activity with psychophysical data is firmly based in these. Another type of psychophysical measurement, Class B, is one in which there is no equality of overall sensation but some aspect of two stimuli are judged equal. For example, two different coloured stimuli could be adjusted until they are deemed equally bright or the luminance difference between two grey stimuli

might be adjusted to equal the difference between two others at a higher overall luminance level. He argues that any attempt to link these perceived 'equalities' to physiological equalities is suspect and that, where possible, Class B experiments should be converted to Class A experiments. The experiments described in this thesis are only Class A experiments and involve mainly the determination of thresholds; Class B experiments will not be considered further here.

Classical psychophysics sees a threshold as a barrier which a stimulus must exceed before it can be perceived and as such provides an inverse measure of the sensitivity of the system to that particular stimulus. Psychometric techniques are used to measure this threshold. More recently it has been recognised that it is not a single stimulus magnitude but a range of values over which there is a varying 'probability of seeing' the stimulus, with this variability reflecting both quantal fluctuations in the low intensity stimuli associated with threshold (which follow a Poisson distribution) and subject variability.

There are many different procedures for identifying the threshold, whether it be described in statistical terms or simply seen as a single value. Each method involves a decision on the part of the subject as to whether or not the stimulus has been seen at each presentation. The problem arises that the threshold found will reflect not only the subjects' sensitivity to that stimulus but also their personal decision-making criteria; e.g. if the response required is a simple 'yes / no', the more cautious observer will register a higher threshold. The subject may also subconsciously or consciously manipulate his own responses. Thus a hysteric can deny the presence of stimulus until it is very intense. Techniques have been devised to eliminate the 'criterion' element, or to make the method more robust in relation to differing skills, actual mistakes, deviousness, or obstructiveness on the part of the observer, but in general increasing the validity carries the price of a lengthier procedure. Clinically, the duration of the test can be a decisive factor. The particular method used in this work, where contrast thresholds are measured (Chapter 5), is known as a Modified Binary Search technique (MOBS) described later, but as a background to this and the work in Chapter 4, several frequently used methods are described first.

Method of Adjustment: This allows the observer to control the changes in stimulus magnitude, whether it be establishing a match or adjusting for threshold. It generally involves swinging back and forth (bracketing) with decreasing step size. It is quick, interesting for the observer but vulnerable to variations in 'criteria' and also to the

observer remembering where the neutral point is in relation to the instrument setting, e.g. knob position, so 'repeatability' can be impressively high! This is the method used in the work described in Chapter 4, in which the angular speed of the rotating striped pattern was adjusted to achieve a given result.

Method of Limits: In this the stimulus magnitudes are controlled either directly by the experimenter or are computer controlled. Essentially the magnitudes are varied systematically in an ascending or descending order or 'staircase', until there is a change in response as to seeing the stimulus. The direction of change is then reversed and the exercise repeated. The number of reversals used depends on the accuracy sought (more reversals = more accurate), offset against tiring the observer (more reversals = less accurate). The mean of the reversal settings is taken as the endpoint. Decreasing the step sizes towards the end point can increase precision efficiently. One of the problems associated with this method is a kind of perceptual inertia resulting in the observer continuing to see and respond in the manner appropriate with the previous setting resulting in overshoot at each reversal. A number of patients will go on saying "yes" to a descending staircase until the stimulus is at zero, and this is the main reason why a single staircase is difficult to employ clinically. Another problem is that the strategy may be detected or even deliberately manipulated by the subject. This can be overcome by a refinement, of presenting 2 different staircases at once (initially ascending and descending) and interleaved randomly by a computer. Simple staircase procedures are widely used clinically, e.g. the Humphrey automated perimeter, which runs 24 abbreviated staircases (or more) simultaneously for different retinal locations but it produces a noisy result, and is inflexible.

Eliminating the 'Decision Criterion' factor: This can be overcome with a 'forced choice' procedure whereby the stimulus is presented alongside a blank with the subject having to select one or the other. It is a response requirement that can be incorporated in a variety of methods of arriving at the threshold value. Caution no longer produces a high threshold! The stimuli, frequently used in this work, were random letters and provided the subject is forced to guess, it constitutes a kind of forced choice procedure.

Method of Constant Stimuli: This involves the presentation of a fixed number of stimuli of different predetermined magnitudes presented in random orders. Threshold can be taken as, for example, the value for which there is a 50% probability of seeing.

Even with preliminary trials to set appropriate limits, the method involves a large number of presentations and is too slow for normal clinical use and frequently too slow for volunteers and therefore is not an option employed except in the experiments described in Chapter 2.2 in which the orientation of an illusory 'band' was established by making a comparison with marker lines randomly orientated at predetermined values.

Signal Detection Theory: An alternative to the classical procedures are a set of methods based on signal detection theory which enable 'sensitivity' and 'decision criteria' to be separated. (see Macmillan, 1991 for a summary). The stimuli are superimposed on a background of noise; the observer is presented with this or pure noise and the request for a yes / no response. 'Hits' or correct 'yes' responses are compared with 'false alarms' or incorrect 'yes' responses giving a 'Receiver Operating Characteristic' (ROC) enabling the sensitivity to be established. The value thus obtained seems relatively invariant over different experimental procedures but the problem remains that establishing ROCs is time-consuming.

Adaptive Procedures: Both the classical psychophysical methods as well as those incorporating signal detection can be speeded up by a procedure in which the stimulus value at any presentation is based on the performance in previous trials. An example of this is the 'modified binary search'. (Tyrnel, 1988)

Modified Binary Search (MOBS): This uses both binary search strategy and the common procedure of manual bracketing. The binary search is the method used in all computer searches and is the most efficient method of locating a value in a list. The set of data is divided into two and half is searched. If the desired object is not found, it must be in the unsearched half. The unsearched half is divided into two. Again one half is searched, and so on. In this case, the procedure is best explained by example. If after the first presentation the stimulus is perceived, the stimulus value is dropped to half. If it is again perceived, the magnitude is dropped to half of the second value, i.e. 1/4 of the first value. However, if at the second presentation the stimulus is not seen, the magnitude is increased to a value that is the mean of the two values in memory, namely 3/4 of the initial value. The third presentation now replaces the first in the memory of the computer. The fourth presentation is the mean of the 2nd and 3rd values. This process continues so that at any given presentation the value is the mean of the two previous values. However, the normal algorithm assumes no mistakes are made, and errors can stop the convergence. The modified

binary search assumes that mistakes are made, and contains an addition to the algorithm that if the same response is made 3 times in a row, a mistake has been made and the search procedure reverses 'up' the " tree " which had been previously established. When the response changes, the search begins again and follows 'down' the tree.

Except in the case of 'forced choice' presentations, the problem remains as to the means of communicating that the stimulus has been 'seen'. In the case of the random letters there is no problem. The letter is right or wrong. Where the stimuli are blobs or gratings that appear and disappear at a given temporal frequency, a simple 'yes' or 'no' is not very satisfactory; there is no evidence that it is true. For these stimuli we made the observer clap or say 'yes' when he could see it. Provided his responses synchronise with the stimuli, it is taken as a correct response. This was a procedure we were glad of in Cuba where none of the patients could speak English! (See Chapter 5).

### 1.3.1 SPATIAL, TEMPORAL AND CHROMATIC PSYCHOPHYSICAL CHANNELS

Over the last few decades vision scientists have drawn increasingly on the concepts and methods of systems analysis and in particular 'linear systems analysis'. The 'frequency response' i.e. the system's ability to transmit sinusoidal modulations of luminance at different frequencies (both temporal and spatial) could, in principal, link the retinal image to the perceived image. Abnormalities in the perceived image could then be described in terms of abnormalities in the response function. There are pitfalls! Firstly, the visual system, after the initial absorption of light, is strongly non-linear in its response to luminance (Hartline and Graham, 1932). There are ways around this. Even a non-linear system behaves in an approximately linear fashion provided the range of input variations is kept small and so in establishing a 'frequency response', provided the 'input' modulations are of small amplitude, linear mathematics can be applied.

The second pitfall is that there is not an 'output' modulation that can be measured; the output is a sensation and all that can be quantified is a response to the stimulus. The technique that is often employed is to measure the threshold of input modulation necessary for detection of the stimuli of the different frequencies. Clearly the sensitivity of the system to any given frequency is inversely related to the threshold

but an additional assumption has to be made in order to link the responses for the different frequencies; i.e. to obtain a 'modulation transfer function' for the system. The assumption made is that at threshold the 'output' modulation is of a fixed magnitude, regardless of frequency, and so the distribution of the inverse of input modulation at threshold against frequency represents such a transfer function. Operating at threshold also satisfies the first requirement of working with small input variations; the various procedures for establishing the thresholds have been described in the previous section.

This approach was pioneered by De Lange (1958) in relation to the detection of flickering lights. In showing that near threshold the visual system behaves approximately linearly, he was able to unify a large body of empirical data. Figure 1.21 shows the temporal frequency response based on data acquired by Kelly (1961) at different levels of mean luminance,  $L$ . The data are plotted in two ways. The input modulation 'm' (or luminance contrast) is taken as

$(L_{\max} - L_{\min}) / (L_{\max} + L_{\min})$  and the second way shows the inverse of the threshold contrast ( $1/m$ ) as a function of frequency which results in responses coincident at low temporal frequencies, reflecting the non-linear Weber's Law in this range. The first way plots the inverse of the absolute amplitude threshold ( $m.L$ ), where  $L$  represents the mean luminance against frequency, which results in a single envelope at higher temporal frequencies. This shows that for temporal frequencies near 'cut-off', the system is behaving linearly.

Subsequently, linear systems analysis was applied to the threshold detection of sinusoidal gratings by Campbell and Robson (1964, 1968) with a comparable impact. The spatial frequency response became known as the 'contrast sensitivity function' or CSF. At about the same time Van Nes and Bouman (1967) investigated the effect of luminance on the CSF. Their results are shown in Figure 1.22(a). The same results are replotted in Figure 1.22(b), to show the manner in which the spatial cut-off frequency varies with retinal illumination depicting an extraordinary linear dependence that saturates abruptly.

Campbell and Robson concluded that the contrast sensitivity function that they had derived, was in fact the envelope of several functionally separate 'channels'. This was based on the comparison of thresholds of square wave gratings and sinusoidal gratings and also on the manner in which the contrast sensitivity function is modified or elevated after adaptation to a particular spatial frequency. The spread of influence

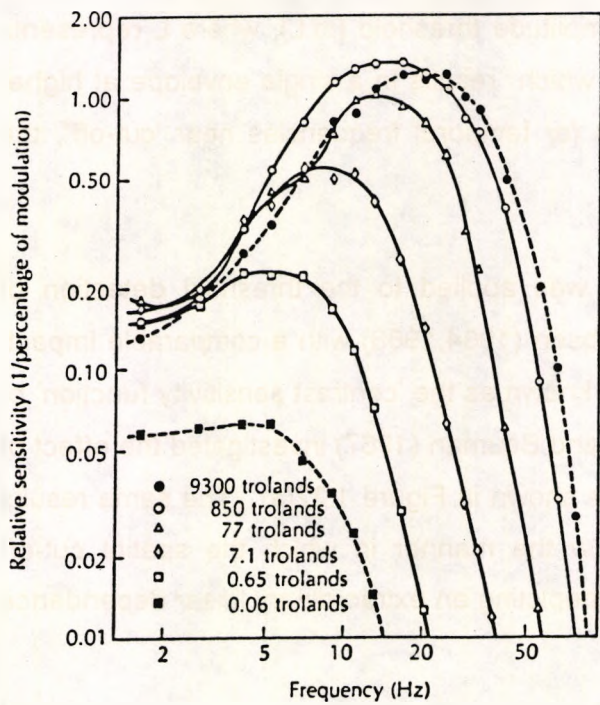
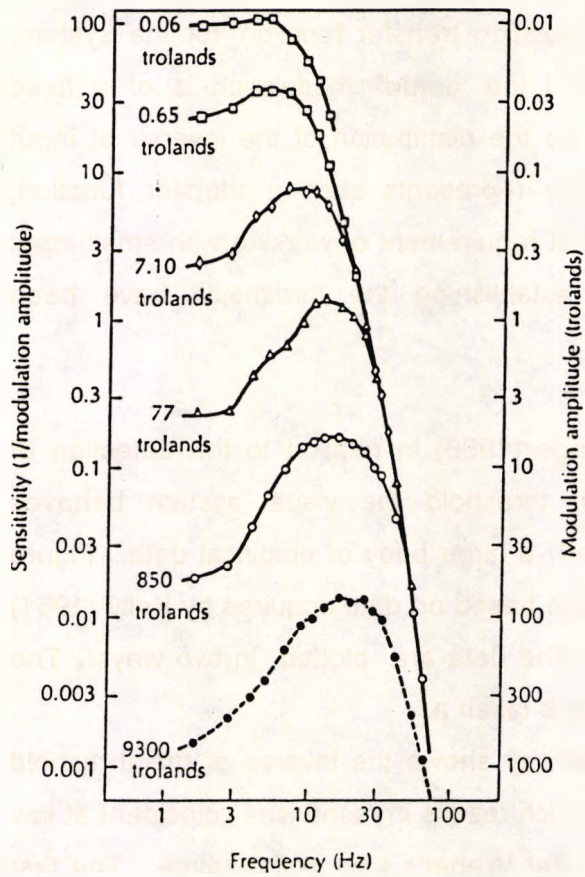


Figure 1.21: Results of Kelly's experiments (1961), plotted in two different ways. The separate curves are for different retinal illuminations.

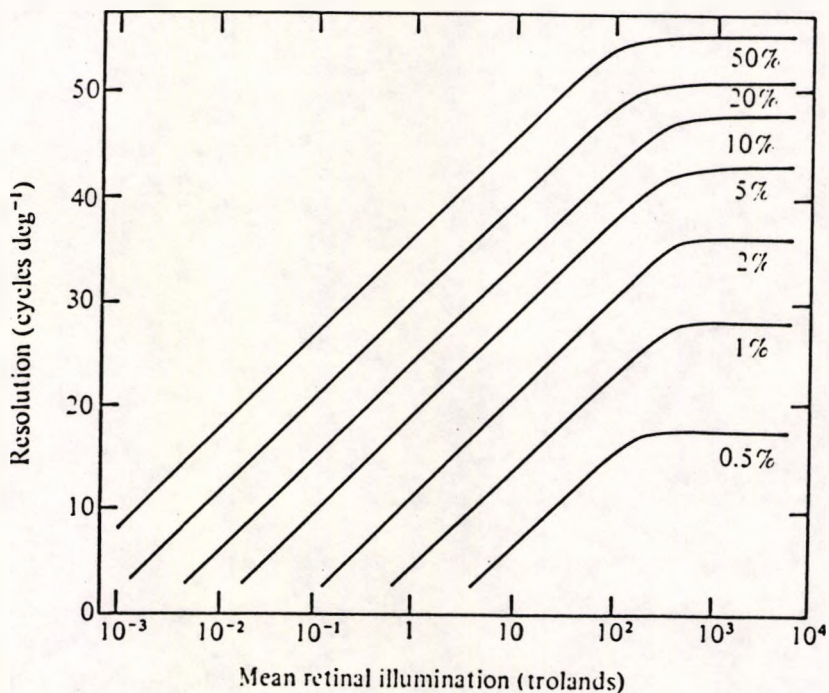
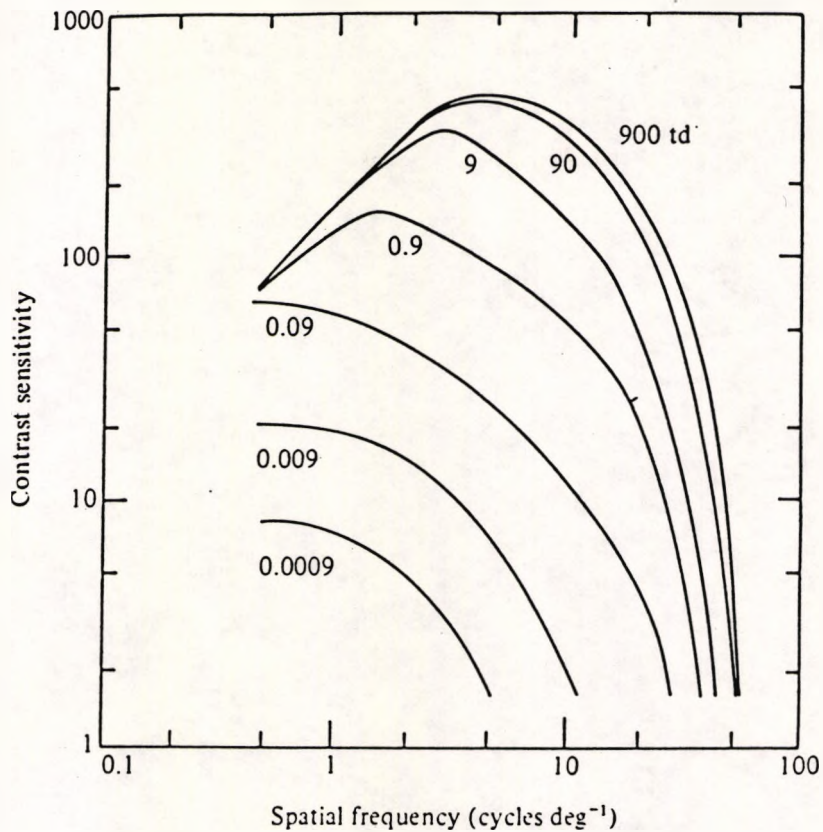


Figure 1.22: (A) Spatial contrast sensitivity (through fixed pupil of 2mm) for a range of different retinal illuminations, illustrating the loss of sensitivity for medium and high frequencies as illumination is decreased. (B) The same results replotted. Note the abrupt cessation of improvement with illumination at approximately 500 trolands. (From Van Nes and Bouman, 1967)

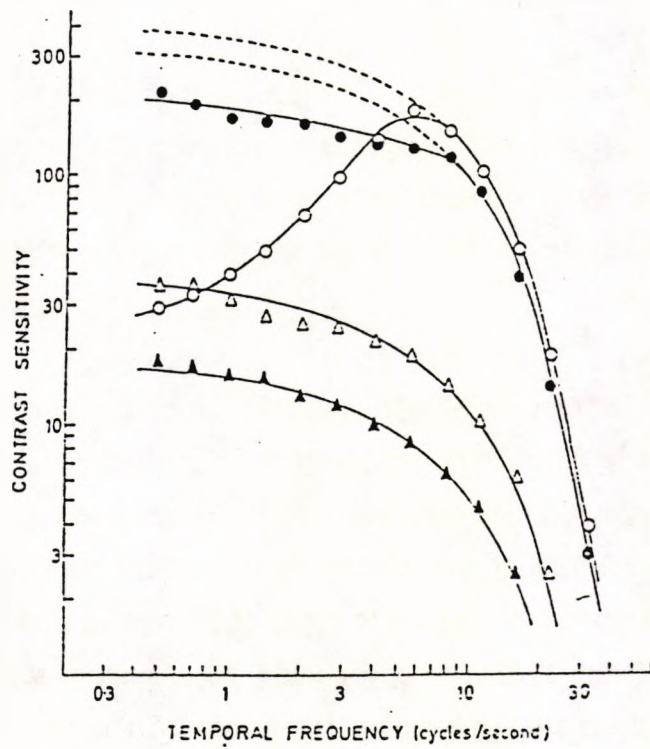
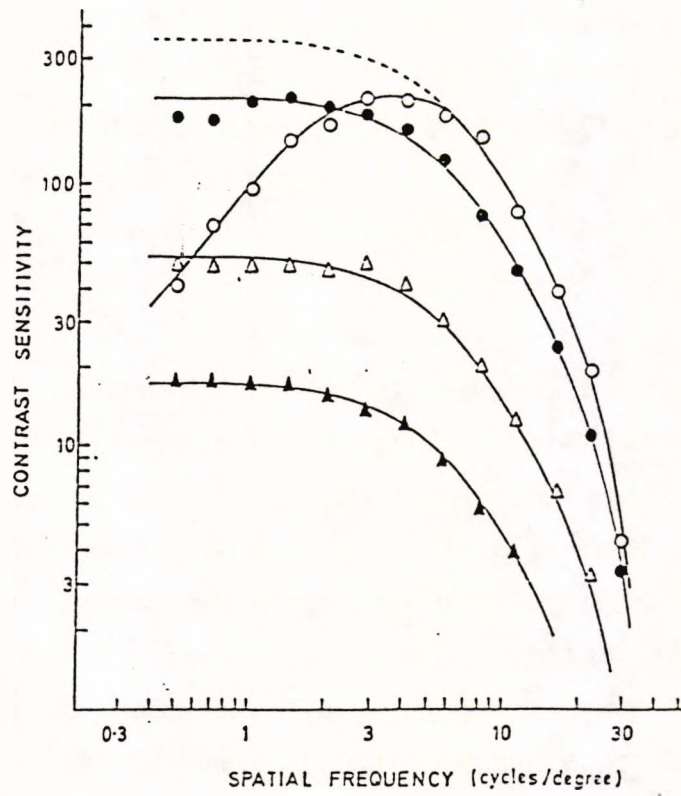


Figure 1.23: (A) Spatial contrast sensitivity functions for different temporal frequencies:

$\circ = 1, \bullet = 6, \Delta = 16, \blacktriangle = 22 \text{ c.s}^{-1}$ . (B) Temporal contrast sensitivity functions for different spatial frequencies:  $\circ = 0.5, \bullet = 4, \Delta = 16, \blacktriangle = 32 \text{ cycles.degree}^{-1}$ . The interdependence of these functions is clear. (From Robson, 1966).

depicts the spatial frequency response of a given channel. These underlying channels were found to have a narrow spatial bandwidth of approximately an octave (Blakemore and Campbell, 1969) and were considered to respond linearly. The vague term 'channel' was thought of as a functional unit, i.e. a group of mechanisms with the same filter characteristic, and carrying no suggestion that there be an equivalent physiological mechanism.

In 1966, Robson investigated stimuli that had combined spatial and temporal components, namely sinusoidal gratings that reversed in a counterphase fashion and figure 1.23 shows contrast sensitivity as a function of both spatial and temporal frequency. There is a clear interdependence between spatial and temporal responses. At high spatial frequencies there is a low pass temporal response, cutting off at lower temporal frequencies whereas at low spatial frequencies there is a higher band-pass temporal frequency response. Temporally, the situation is reversed: at high temporal frequencies, there is a low pass spatial frequency response and at low temporal frequencies, there is a higher spatial band-pass characteristic. The thresholds are best represented as a 3-dimensional spatio-temporal surface.

The next line of enquiry was to establish whether or not there were sub-channels within the overall temporal frequency response analogous to the spatially tuned channels. A variety of methods were used and the general consensus seems to be that, unlike the spatial channels, there are only two or, at most, three independent temporal channels.

Kulikowski and Tolhurst (1973) demonstrated the existence of two distinct classes of detector; the one functioning optimally at high/medium spatial frequencies and displaying a sustained temporal response and the other specialised for low spatial and high temporal frequencies, displaying a transient response. Around this time, adaptation experiments analogous to those of Blakemore and Campbell (1969) were performed by Smith (1971) and repeated by Moulden et al. (1984). Moulden concluded that there are two temporal sub-channels; a low pass filter peaking at 6 Hz and a band-pass peaking at 9 Hz. Smith's data showed a higher peak for the band-pass channel. A different technique involving simultaneous detection and temporal frequency discrimination at threshold (Watson and Robson, 1981) indicated at least two channels on the basis that only two temporal frequencies, one high and one low, can be perfectly discriminated at threshold. Thompson (1983) identified two broadly tuned channels whilst Mandler and Makous (1984) identified three channels using

similar methods. This had followed earlier work on supra-threshold frequency discrimination (Mandler, 1984) in which he was able to demonstrate the possibility of there being 3 temporal channels, whereas Thompson, on repeating this, was only able to identify 2 channels.

Masking experiments using temporally varying noise were found in the case of Pelli (1981) to indicate the presence of 3 channels, the highest peaking at 20-30 Hz. More recently Anderson and Burr (1985) found 2 distinct channels, a temporal low-pass channel that is maximally sensitive to high spatial frequencies and a band-pass channel that is optimum for low spatial frequencies. Of particular interest is that the low-pass masking function extends to the same temporal frequencies as the band-pass function. This could mean that the sustained, low-pass detectors respond to frequencies as high as those of the band-pass detectors, a result which contradicts the findings from other methods. Alternatively, it could imply that the band-pass units actually suppress the activity of the sustained detectors, independently of any masking, and that the reverse does not happen. i.e. there is no suppression of the activity of the band-pass detectors by the low-pass ones. This was suggested by Breitmeyer and Ganz (1976), in a quite different situation, and is important in the interpretation of the appearance of the 'complex band' described in this thesis in Section 3.1

Some of the earlier work on investigating the temporal characteristics of the visual system used a method of subliminal summation. Ikeda and Boynton (1965) devised a method in which a brief subliminal flash was followed by a test flash. The sensitivity to the brief test flash was determined as a function of the time interval and the response was found to be transient. They had used extended targets. When, at a later date, interest focused on the evidence of there being two distinct classes of channels, Tolhurst (1975) adapted the technique to investigate a possible sustained response, by extending the duration of the initial flash. Sinusoidal gratings were used as both stimulus and test flash. Depending on the spatial frequencies chosen, the profile of persistence varied, showing a transient response for the low spatial frequencies and a sustained response for the higher, with both types of response present at intermediate values of 3 cycles per degree. This last conclusion is specifically used in Paper 3.

More recently, Barbur et al. (1981) and Holliday and Ruddock (1983) demonstrated the existence of two spatio-temporal filters in human vision using a background

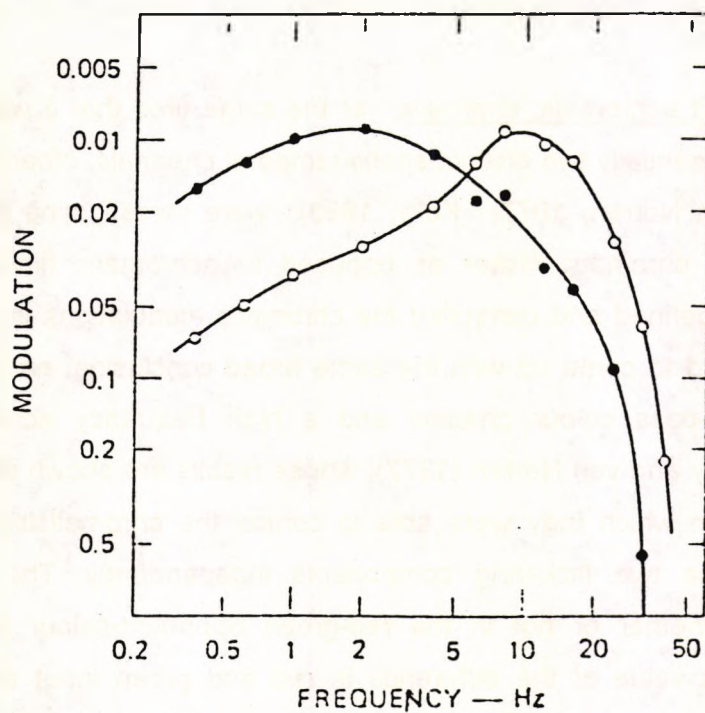


Figure 1.24: Sensitivity to purely luminance flicker (open symbols) and purely chromatic flicker (filled symbols) in a 1.8 degree field; dark surround; AP=2.3mm; retinal illuminance 860 trolands. The stimuli in the two sets of data consisted of the same red/green flickering waveforms that were either in phase to give a yellow luminance flicker or in anti-phase to give a red/ green chromatic flicker. The sensitivities to luminance and chromatic flicker clearly dominate two separate frequency bands (Kelly and van Norren, 1977).

modulation technique. Threshold illumination was found for detecting a target moving across a background that could be modulated, both spatially and temporally. The characteristics of the response mechanisms so revealed were (i) temporal low-pass, spatial band-pass (ST1), and (ii) non-linear temporal band-pass, spatial low-pass (ST2). The ST2 characteristics were similar to the De Lange characteristics, with a peak sensitivity ranging from c. 8 - 20 Hz as the background illumination ranged from 1 to 3 log trolands.

It seems that although there are considerable differences in the results and conclusions of these investigators, there is general agreement that, unlike the spatial domain, there are only 2 or 3 broadly tuned temporal channels.

Chromatic and achromatic channels: at the same time that it was established that there were essentially two distinct spatio-temporal channels, others (De Lange, 1958; Kelly and van Norren, 1977; Kelly, 1983) were investigating the visual systems responses to chromatic flicker as opposed to achromatic flicker. These elegant experiments defined and controlled the chromatic modulations in a variety of ways, but all seemed to come up with the same broad conclusion; namely that there is a temporal low-pass colour channel and a high frequency achromatic band-pass channel. Kelly and van Norren (1977), whose results are shown in Figure 1.24, used a technique in which they were able to control the chromaticities, amplitudes and phases of the two flickering components independently. The intention was to investigate whether or not in the red-green opponent-colour pathways it is the instantaneous value of the difference in red and green input that determines the output. Their general conclusion is that this is the case and that both types of flicker sensitivity are controlled by the pathways of the proximal retina, and not by the cone cells. The spectral sensitivity of these colour opponent and luminance channels was investigated by King-Smith and Carden (1976).

### 1.3.2 NEURAL MECHANISMS UNDERLYING PSYCHOPHYSICAL CHANNELS

Whilst the existence of chromatic and achromatic psychophysical spatio-temporal 'channels' is generally accepted, the relationship of different cell types to these channels is controversial. A popular view is summarised by Schiller et al. (1990) on the basis of lesion experiments; namely that the P-pathway is essential for processing colour, texture, fine pattern and fine stereopsis whereas the M-pathway is crucial for the perception of fast flicker and motion. They claim that brightness discrimination,

coarse shape discrimination and low spatial frequency stereopsis, and more controversially, that contrast sensitivity is subserved by both.

The link between the psychophysical channels and the P- and M-pathways has been studied by Lee and co-workers in a series of experiments of great elegance and persuasiveness; a brief description of them forms the basis of this introduction. In these they compared the temporal characteristics of the chromatic and achromatic channels with direct recordings from the P- and M-cells (Lee et al. 1988, 1989a, 1989b, 1990 and Kremers et al. 1990).

Cells of the M-pathway are much more sensitive to a temporal luminance modulation than those of the P-pathway, and those of the P-pathway are more sensitive to chromatic modulation (Lee et al., 1989a), but linking them to the post-receptoral mechanisms postulated by Kelly and van Norren (1976) is not completely straightforward. Firstly, in comparing psychophysical thresholds with cell sensitivity, assumptions need to be made in order to define the latter. A cell threshold can only be defined in probabilistic terms or alternatively the sensitivity can be described in terms of 'contrast gain' (Kaplan and Shapley 1986). It has also been noticed that the psychophysical threshold corresponds to a firing rate of 10-20 impulses/second which provides another avenue for describing the cell's sensitivity. i.e. the contrast necessary to generate a specified response. A further complication is that the sensitivity of an array of similar single cells may be enhanced by group interactions in the array. It has been argued that the P-pathway is capable of displaying greater luminance contrast sensitivity than the M-pathway because it contains a far greater number of cells: some kind of summation (probability or otherwise) must be invoked, since individual P cells have a low contrast sensitivity (see Chapter 1.2.5).

There is a convincing argument that cells of the M-pathway are the sole substrate of heterochromatic flicker photometry (HFP) based not only on the implausibility of the achromatic channel being built from P-pathway cells but, more strongly, on the precise comparison of physiological and psychophysical detection thresholds (Lee et al 1988; Lee 1990).

Any hypothesis linking M- and P- pathways to post-receptoral channels is greatly strengthened if it holds over a range of conditions. Lee et al. (1990) investigated the temporal frequency responses of both phasic (M-pathway) and tonic cells (P-

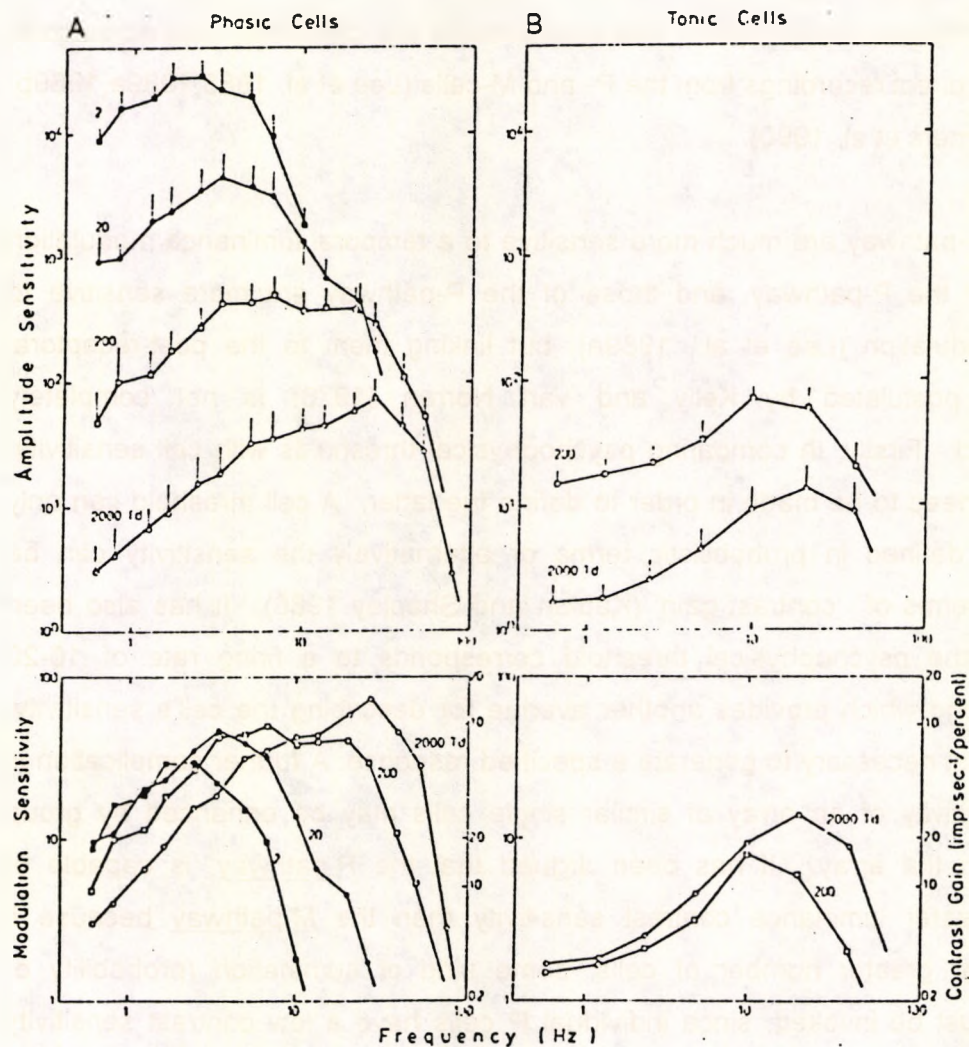


Figure 1.25: Sensitivity of ganglion cells to luminance modulation, expressed both in terms of amplitude sensitivity  $1/(L_{max} - L_{min})$  or Michelson contrast sensitivity / contrast gain:  $(L_{max} + L_{min}) / (L_{max} - L_{min})$ . Sensitivity is expressed as a function of frequency for 4 retinal illuminations. (A) Phasic cells; (B) Tonic cells. Sensitivity was estimated from the modulation required to invoke a 20 impulses/sec modulation. In the lower panels, the luminance is expressed as the luminance contrast required to reach the criterion and also as the contrast gain; the latter is obtained from the gradients of cell responses plotted as a function of luminance contrast. (From Lee et al. 1990)

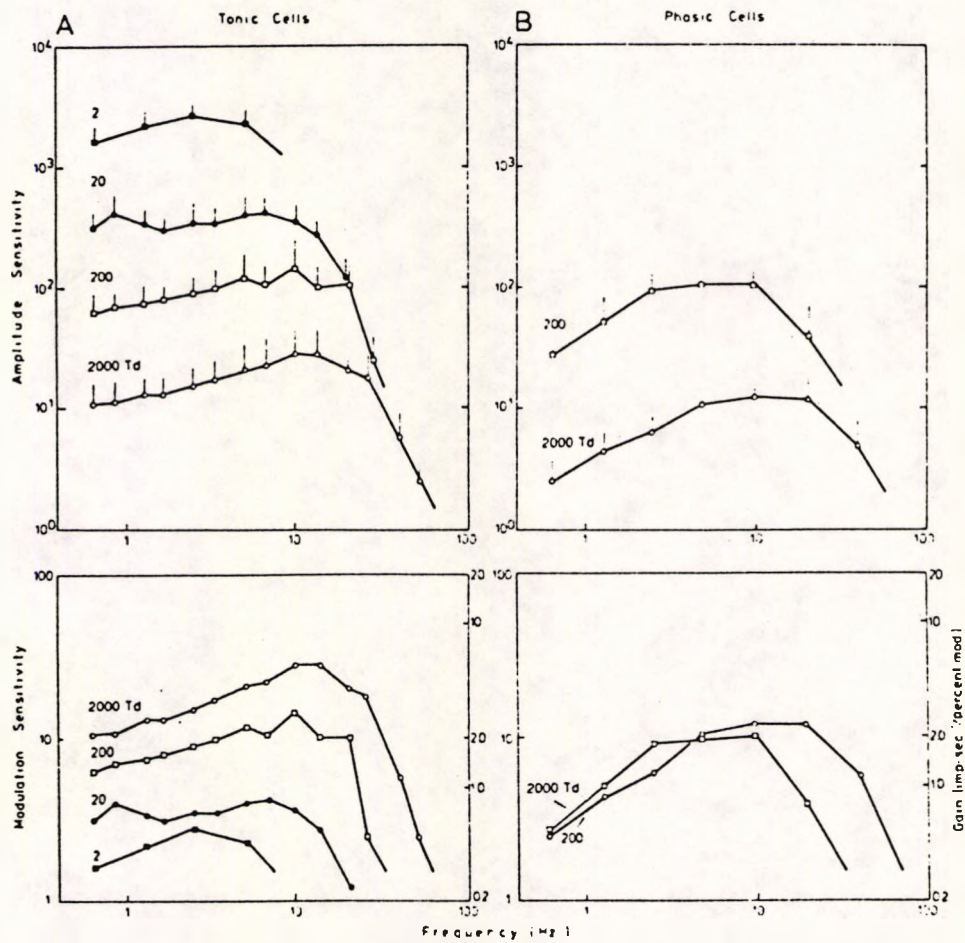


Figure 1.26: Sensitivity of ganglion cells to chromatic modulation, expressed in terms of amplitude sensitivity and modulation sensitivity for different illumination levels. (A) Phasic cells; (B) Tonic cells. Sensitivities were expressed in terms of diode modulation instead of contrast sensitivity. (From Lee et al. 1990).

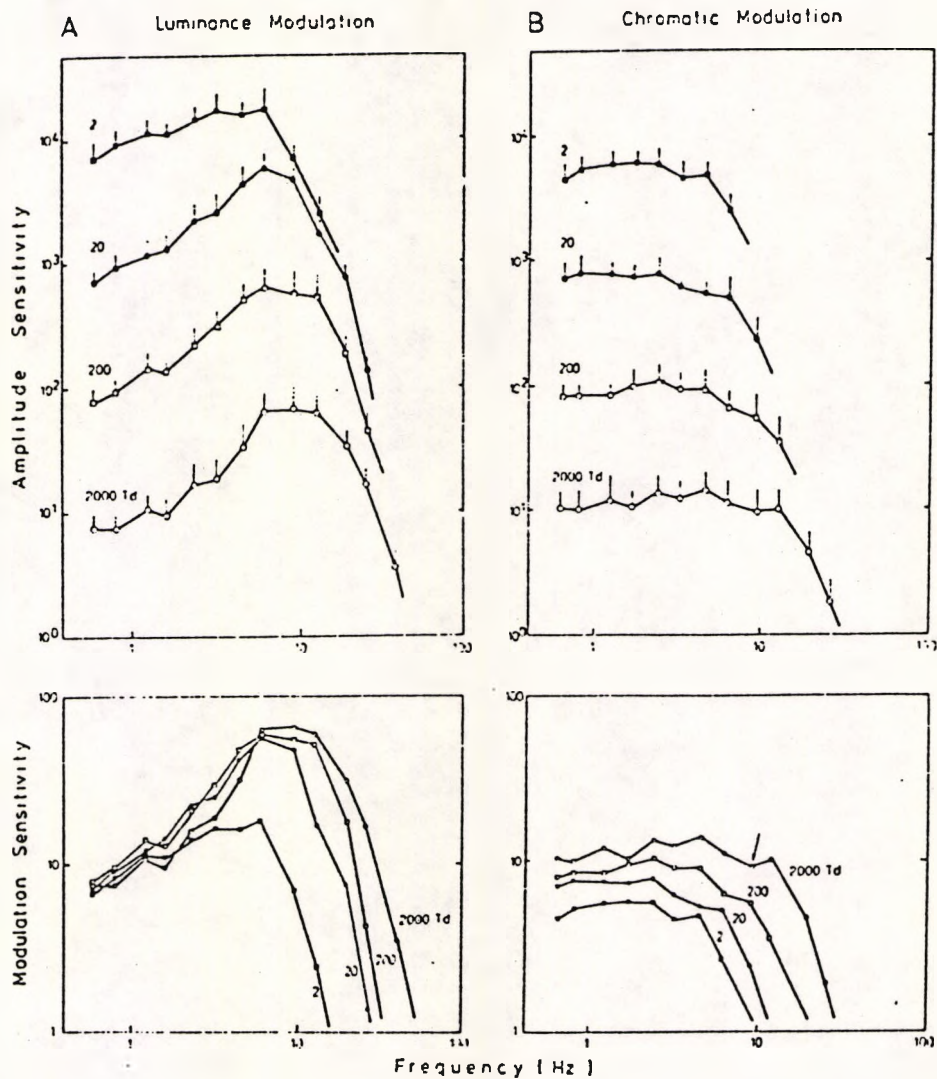


Figure 1.27: Temporal frequency responses for the human visual system. (A) luminance modulation; (B) chromatic modulation. The sensitivity is expressed both as both an amplitude and a modulation sensitivity, as in Figures 1.26 and 1.27. The luminance data plotted as an 'amplitude sensitivity' results in curves that are coincident at high temporal frequencies indicating a linearity of response at threshold, whereas when plotted as a 'relative modulation', coincidence occurs at the low temporal frequencies showing that Weber's Law applies. (From Lee et al. 1990).

pathway) over a range of illumination levels. Their dramatic results are shown in Figures 1.25-1.27. Figure 1.25 shows the sensitivity of both phasic and tonic ganglion cells to luminance modulation, expressed either as an 'amplitude' sensitivity  $1/(L_{\max} - L_{\min})$  or as a 'modulation' sensitivity, given either by the Michelson contrast sensitivity  $(L_{\max} + L_{\min}) / (L_{\max} - L_{\min})$  or the contrast gain. Figure 1.26 shows the sensitivities of ganglion cells to chromatic modulation and Figure 1.27 shows the equivalent psychophysical responses (similar to those of Kelly (1961) already shown in Figure 1.21). The similarity of the cell sensitivity functions and the psychophysical responses gives a convincing indication that the M- and P-cells are the substrates of the psychophysical channels. The same data is also presented as a ratio of the human psychophysical and cell sensitivities. There is, however, one striking difference between the physiological and psychophysical responses. The P-cells respond to chromatic flicker at frequencies greatly in excess of fusion frequencies, the M-cells to a lesser extent. This implies a subsequent cortical mechanism acting as a low pass filter, with the corner frequency for the P-cells being less than that for the M-cells. This conclusion is used in Paper 3.

If it is accepted that the two ganglion cell types mediate chromatic and achromatic vision at threshold, it is not obvious how a stimulus that combines chromatic and luminance components will be handled. Kremers and Lee (1992) compared the sensitivity of ganglion cells and human observers to combined chromatic and luminance modulation using an additivity measure. The results indicate that for the combined stimuli the psychophysical sensitivity is the envelope of independent chromatic and achromatic mechanisms with physiological substrates in the parvocellular and magnocellular pathways respectively. Under these conditions sensitivity seems to be set by a chromatic channel below 3 Hz and an achromatic channel above that frequency. They went on to compare detection thresholds for mixed stimuli with thresholds for the discrimination of colour alternation. Sensitivity to the latter plummeted after 3 Hz lending support to the view that the sensitivity to mixed stimuli was set by the P-pathway up to 3 Hz and the M-pathway after that. In order to compare the psychophysical to physiological sensitivities, instead of the direct ratio used by Lee et al. 1990, they analysed their data in terms of 'additivity' within physiological and psychophysical mechanisms. This led to the same conclusion.

Their conclusions concerning responses to temporal modulations are consistent with some results of the lesion experiments of Schiller (1990) and Merigan (1991). Lesioning the P-pathway produces a loss of sensitivity to chromatic modulation and

lesioning the M-pathway produces a loss of sensitivity to high temporal frequency luminance modulation. However, the lesion experiments that suggest that detection of luminance modulation at low temporal frequencies and low spatial frequencies occurs through the P-pathway is considered by Kremers and Lee to be unlikely, given the extremely low contrast sensitivity at these frequencies. Our own results on the MAR patients also do not support this additional role of the P-pathway; this is discussed in Chapter 5.2.3 and the final discussion.

In spite of the few contradictory views, there seems little doubt that the chromatic and achromatic psychophysical channels associated with large field targets, established by threshold detection, have the P- and M-ganglion cells as physiological substrates respectively.

There has not been an investigation of comparable depth into the physiological substrates of spatial vision, and whilst there are some areas of general agreement, there are considerable differences. The question as to whether the P- and M-pathways have specific roles in the detection of fine and coarse spatial vision has been approached through several avenues; anatomy, physiology or lesion studies on 'behaving' monkeys.

The popular view, referred to by Livingstone and Hubel 1987, and more recently outlined by Schiller, 1992, is that "the size of the colour-opponent receptive field is small" and "by contrast the broad-band cells have much larger receptive fields" (Schiller and Malpeli, 1978; Shapley et al., 1985; De Monasterio and Gouras, 1975)

This was seen as an indicator that the P-cells have a special involvement in fine vision and the M-cells in vision involving low spatial frequencies. Support for this view of the relative field sizes is given by Derrington and Lennie 1984, where they suggest that the M-cell receptive field diameters lie somewhere in the range 1.6 to 3 times larger. This is contradicted by Crook et al 1988, who report that "the resolving ability of tonic, spectrally opponent ganglion cells was usually similar to that of phasic non-opponent ganglion cells at similar eccentricities". They also suggest that their results imply that "the centres of phasic and tonic monkey ganglion cells are similar at most eccentricities."

The casting vote in identifying functional roles seems to lie with the lesion experiments in the LGN. The claim of Schiller et al. (1990) that the colour opponent

channel is essential for the processing of fine pattern is supported by the work of Merigan et al. 1986. In a later work Merigan (1989) reports that the spatial and chromatic vision of the macaques is very similar to that of humans and they also suggest, from the losses resulting from P-lesions, that the P-pathway plays an important role in colour vision at all spatial frequencies as well as achromatic vision at high spatial and lower temporal frequencies. Following M-pathway lesions, Merigan and Maunsell 1990 report that the sensitivity to very low spatial frequencies (achromatic Gaussian blurs) was so severely compromised as to suggest that the M-pathway is the sole substrate for such a stimulus. These three separate conclusions are drawn on extensively in the work reported in Chapter 5 and to a lesser extent in Chapters 2, 3 and 4.

## CHAPTER 2: THE 'ROTATING STRIPES EFFECT'

### 2.1 INTRODUCTION

The odd appearance of a slowly rotating black-and-white pattern of stripes is described briefly in the 'general introduction' (and more fully in Paper 1, section 2.3). The effect seen is a parallel band of clearly resolved stripes, moving around with the pattern as a whole but lagging slightly behind the perpendicular to the stripes, the effect being similar to Fig 1.1. The 'band' was first described by Babington-Smith (1964) and, at a later date, Wade (1974) established that the width of the band varied inversely with the angular velocity. Barbur (1980) accounted for this using a simple model. He argued that the perceived image was simply the integration of the persisting images over the duration of the integration time, these component images being rotated with respect to each other. It follows that at any one moment, the edge of the band, where the stripes appear totally smeared, would be at a distance from the centre such that the retina would be subjected to one black and one white stripe during the integration time. For a greater angular velocity, the distance from the centre would be less for this to be achieved; there would be an inverse relationship between width of band and angular velocity.

At greater speeds the parallelism begins to break down with the band being narrow at the centre and fanning out towards the edge (Figure 2.1) and at even greater speeds the resolved stripes degenerate into concentric circles. In all these cases the appearance can be computed from a knowledge of the persistence of the observers vision and consequently could be used as a means of gaining insight into this persistence. However, it is only in the case of the slowly rotating stripes (parallel bands) that there is a simple relation between appearance of the band and the persistence of the images. This is discussed in Paper 1, although Figure 2.2 shows why it is so. At any given moment in time, any given point (x,y) on the grating rotating with an angular velocity ' $\omega$ ', has a velocity (perpendicular to the stripes) that is given by  $\omega x$ ; i.e. proportional to 'x' and independent of 'y'. This means that, at any moment in time, the stimulus is in effect providing a series of mini-columns of stripes, each travelling with a velocity that is proportional to the distance along 'x'. The band is therefore parallel sided and the boundary simply lies where the column is travelling too fast to be resolved.

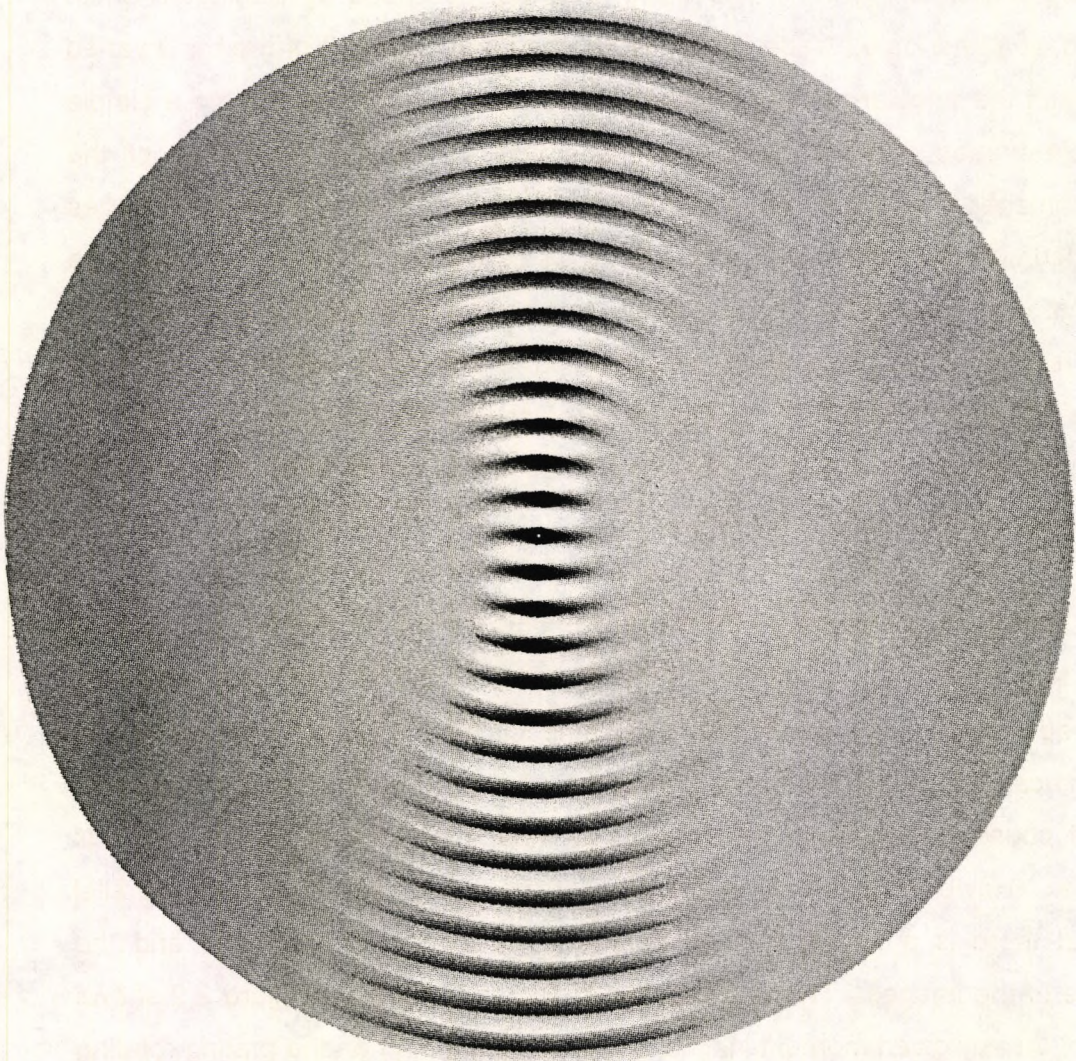


Figure 2.1: Predicted appearance of the 'rapidly' rotating grating ( $3.75 \pi \text{ rad.s}^{-1}$ ).  
See Paper 3 for details.

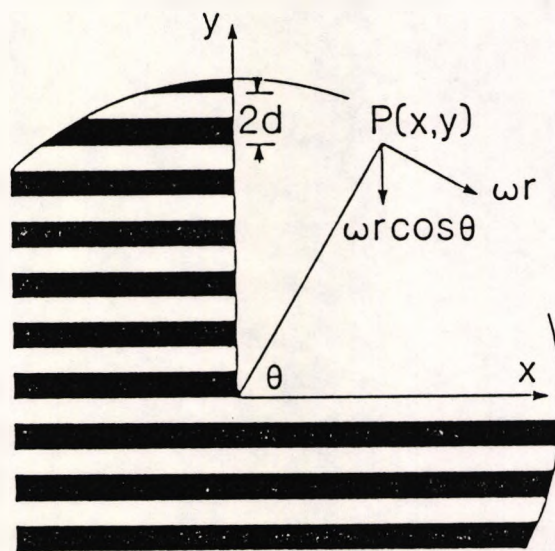


Figure 2.2: Rotating striped pattern, with the origin of the Cartesian system at the centre of rotation and the x,y-axes fixed on the pattern. With a constant angular velocity ' $\omega$ ', the point P(x,y) travels with a constant speed  $\omega r$ . The component of velocity perpendicular to the stripes,  $\omega r \cos \theta = \omega x$  will produce the blurring of the stripes.

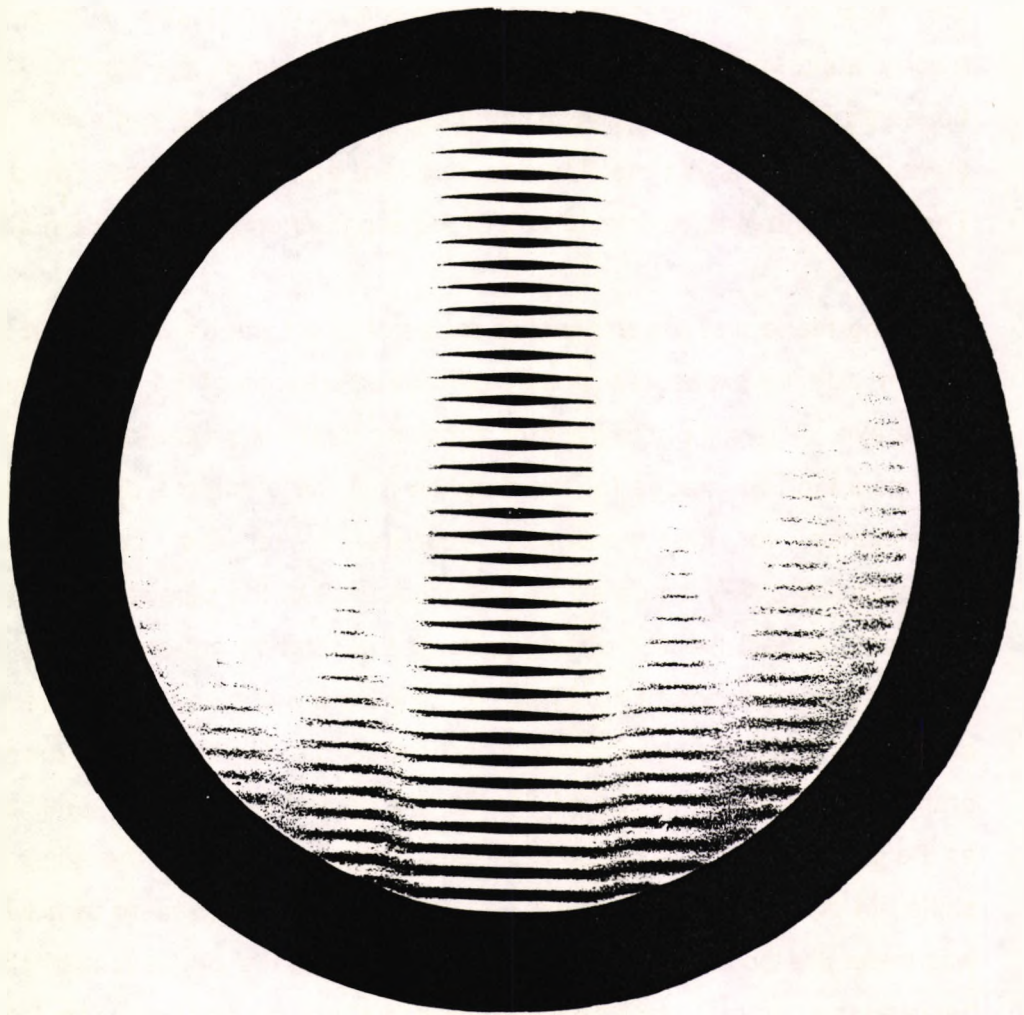


Figure 2.3: Single exposure photograph (60ms) of a 'slowly' rotating ( $3.28 \text{ rad.s}^{-1}$ ) square waveform grating showing the parallel sided band, flanked by secondary bands of half the width of the central band and of alternating phase i.e. black stripes are adjacent to white stripes. The contrast across the bands is in the form of a 'sinc' function (see Chapter 2.3).

In some preliminary experiments, reported in the next section, the relationship between the width of the band, angular speed and luminance was investigated. The intention was to use the effect simply as a method of obtaining the integration time of the visual system under different conditions of illumination. However it was very quickly apparent that there was a substructure within the band. An inner band appeared to lie obliquely across the wider band, a feature that might be expected if there were two distinct mechanisms involved, each with its associated persistence. The widths and relative orientations of the separate components were also studied.

Following these first experiments, a series of photographs were taken of the moving pattern, with the exposures chosen to include durations of the known persistence time of the eye. Any still photograph of a moving target is smeared as a consequence of the integration of images for the duration that the shutter is open. The appearance corresponds to the perceived appearance of the same moving target neurophysiologically 'smeared' as a consequence of the persistence of vision. Hence one could expect the still photographs of the rotating pattern to look similar to the perceived appearance of it. They do! Figure 2.3 shows this. However, there is a difference. The photographs display secondary bands flanking the main band, each of the same width but of half the width of the central band, and of diminishing contrast as the distance from the centre increases. The stripes within the adjacent bands are shifted in phase by 180 degrees; i.e. a black stripe is adjacent to a white stripe. It was these photographs that led to the awareness of the simple relationship that exists between the contrast across the pattern and either the temporal impulse response of the of the observer's visual system or, in the case of the camera, the 'exposure function'. It is not simply the duration of the persistence of the image to a brief flash of the pattern (the integration time), nor the time the shutter is recording, but the manner in which the persisting image builds up and fades away or, in the case of the camera, the profile of the transmission of the shutter as it opens and shuts. The subsequent theoretical analysis showed that, assuming linearity, the contrast across the pattern is a direct display of the complex temporal modulation transfer function and was published as two separate papers. Each paper is introduced, summarised and included in Section 2.3.

The data from the initial experiments, whilst initially obtained with a view to obtaining a simple 'integration time', was re-examined in terms of the temporal 'cut-off' frequency following the theoretical analysis. The cut-off frequency is the inverse of the integration time.

## 2.2 PRELIMINARY EXPERIMENTS TO INVESTIGATE THE 'BAND' CHARACTERISTICS FOR NORMALS

It has already been shown in Chapter 2.1 (Figure 2.2) that the pattern, rotating with an angular velocity ' $\omega$ ' radians/sec, can be considered to be a series of columns of stripes, which, at any moment in time and any given distance ' $x$ ' from the centre, are travelling with a velocity (perpendicular to the stripes) that is equal to  $\omega x$ . This means that they are exposing the underlying retina to a temporal frequency of  $f = \omega x / 2d$  where ' $2d$ ' is the width of a pair of stripes (black and white). The edge of the perceived band is at a distance from the centre where the temporal frequency generated is too great to be resolved (the cut-off frequency ' $f_{cut}$ '). It follows that the width of the band ( $2x$ ) is given by:  $4d \cdot f_{cut} / \omega$ .

The experiments undertaken were:

- (i) to investigate the relation between the width of band ( $2x$ ) and the angular velocity ( $\omega$ ) for different luminances
- (ii) to establish the cut-off frequency of the both the 'inner' and 'outer' band as a function of luminance for different retinal eccentricities
- (iii) to measure the orientations of the 'inner' and 'outer' bands in relation to the line perpendicular to the stripes.

### 2.2.1 EQUIPMENT:

The stimulus consisted of a high contrast black and white square-wave grating (5.2mm for one black and white pair of stripes) printed on glossy paper and mounted on a disc that could be rotated at a variable speed in either direction. A servo-motor with 24V servo-amplifier was used with a manual speed control (multiturn potentiometer). This was calibrated using an infra-red beam, interrupted at time intervals dictated by the rotation rate. The disc was illuminated with a tungsten/halogen lamp and a 6-12V stabilised power supply. In order to reduce specular reflections, the lighting was oblique to the surface. Luminance was controlled with neutral densities placed in front of the light source with maximum luminance being approximately  $640 \text{ cd.m}^{-2}$ ; the observers used a chin rest and viewed the stimulus binocularly through a artificial pupils of 5mm diameter from a distance of 1.5m. The fundamental spatial frequency of the grating was  $3.4 \text{ c.deg}^{-1}$ .

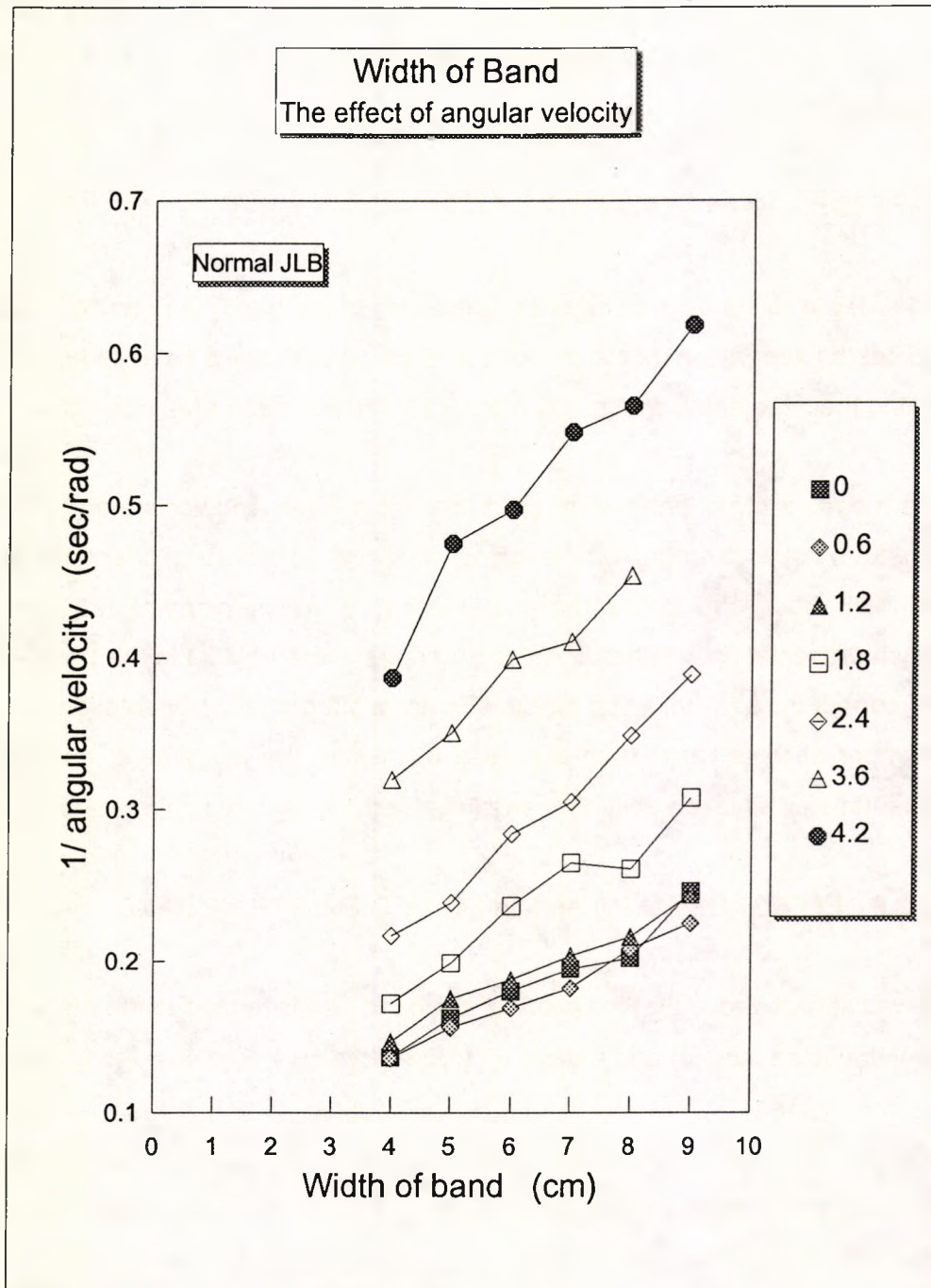


Figure 2.4: The inverse angular velocity of the rotating grating is shown as a function of the width of the band generated. The linear relation is seen to hold for different illuminations. The maximum illumination is  $650 \text{ cd. m}^{-2}$  and filter densities are shown in the legend. The fundamental spatial frequency is  $3.4 \text{ c/deg}$ ; the grating is viewed binocularly with artificial pupils of 5mm.

To identify the edge of the band, there were two parallel-line markers mounted on the pattern. These could be arranged to lie parallel at any chosen separation and at any orientation.

#### METHOD:

In order to relate angular speed to the width of the band, in practice it was necessary to set the separation of the markers and adjust the speed so as to have the band just filling the intervening space. All readings were the mean of 4 settings.

To measure the orientation of the band, for a given angular speed ( $3.3 \text{ rad.s}^{-1}$ ), the markers were arranged to lie along a range of different orientations (chosen in random order) and presented many times. The observer was required to judge on each presentation whether or not the markers were parallel to the band. The number of correct trials ( $n$ ) for each orientation are plotted against orientation ( $x$ ). The overall number of trials varied with the ease of making the judgement, and the subjective orientation was taken as the mean of the distribution curve  $(\sum n.x) / (\sum n)$ .

#### 2.2.2 EFFECT OF ANGULAR VELOCITY ON WIDTH OF BAND

It was shown above that the width of the band ( $2x$ ) is related to the angular velocity ( $\omega$ ), the stripe size ( $d$ ) and the cut-off frequency ( $f_{\text{cut}}$ ) by:  $2x = (4d f_{\text{cut}}) / \omega$

$$\text{i.e. } 1/\omega = 2x / (4d f_{\text{cut}})$$

Figure 2.4 shows the inverse relation between the width of band and the angular velocity, which holds well over the range of illuminations used. Since the slope of the line connecting the points is inversely proportional to  $f_{\text{cut}}$ , the increase in slope and consequently the reduction in cut-off frequency  $f_{\text{cut}}$  with decreasing illumination is clearly visible.

An interesting feature of the graphs is that they do not (extrapolated) pass through the origin which could be caused by an underestimation of the width of the band. The cut-off frequency can be calculated from the data in two ways:

(i) from the gradient:  $f_{\text{cut}} = 1 / (2d \cdot \text{gradient})$

(ii) separately:  $f_{\text{cut}} = \omega \cdot x / (2d)$

Since the retina is not homogeneous, the gradient method, based on a series of different widths and consequently a series of different eccentricities, carries a potential source of error. Hence the estimates for  $f_{cut}$  have used the individual values.

### 2.2.3 TEMPORAL FREQUENCY 'CUT-OFF' FOR THE 'INNER' AND 'OUTER' BANDS SEEN BY NORMALS: THE EFFECT OF (1) LUMINANCE AND (2) ECCENTRICITY

The technique described in Section 2.2 for obtaining the width of a band was again employed. The width of the band was defined by markers and the speed of rotation was increased until the edge of either the inner band or the outer boundary just touched them. The cut-off frequency was then calculated for that particular width of band. A series of different separations were used which, in effect, gave the cut-off frequency for a range of different eccentricities. For each width of band, the experiment was repeated for a range of different luminances; the results for two normals are shown in Figure 2.5 (outer band), Figure 2.6 (inner band), and Figure 2.7 (both bands). At higher luminances the 'outer' cut-off frequencies are approximately 40 Hz whereas the inner band is cutting off at approximately 12 Hz. As the luminance decreases the 'inner' cut-off does not change greatly, but the 'outer' cut-off reduces and approaches that of the 'inner' band. It can also be seen that for both normals, there is a gradual increase in the temporal cut-off frequency for increased eccentricity that is particularly marked in the 'outer' band.

The relationship between the 'outer' cut-off frequency, luminance and retinal eccentricity has certain similarities with the some of the early flicker investigations. In these the stimulus generally involved an opaque sector disc interrupting the illumination of a test field; hence the contrast of the flickering stimulus was 100% and fusion frequency corresponds in principle to the cut-off frequency on the temporal frequency response curves of De Lange and the cut-off frequency of the 'outer' band. Figure 2.8 shows the results of Hecht and Verrijp (1933), in which critical frequency is shown for three different eccentricities of a  $2^\circ$  stimulus, over a range of retinal illuminations. The similarity with Figure 2.5 is striking. For comparison, arrows have been added to show the range of retinal illuminations used with the rotating stripes. The eccentricity of the bands of width 4cm to 9cm for the viewing distance of 1.25m

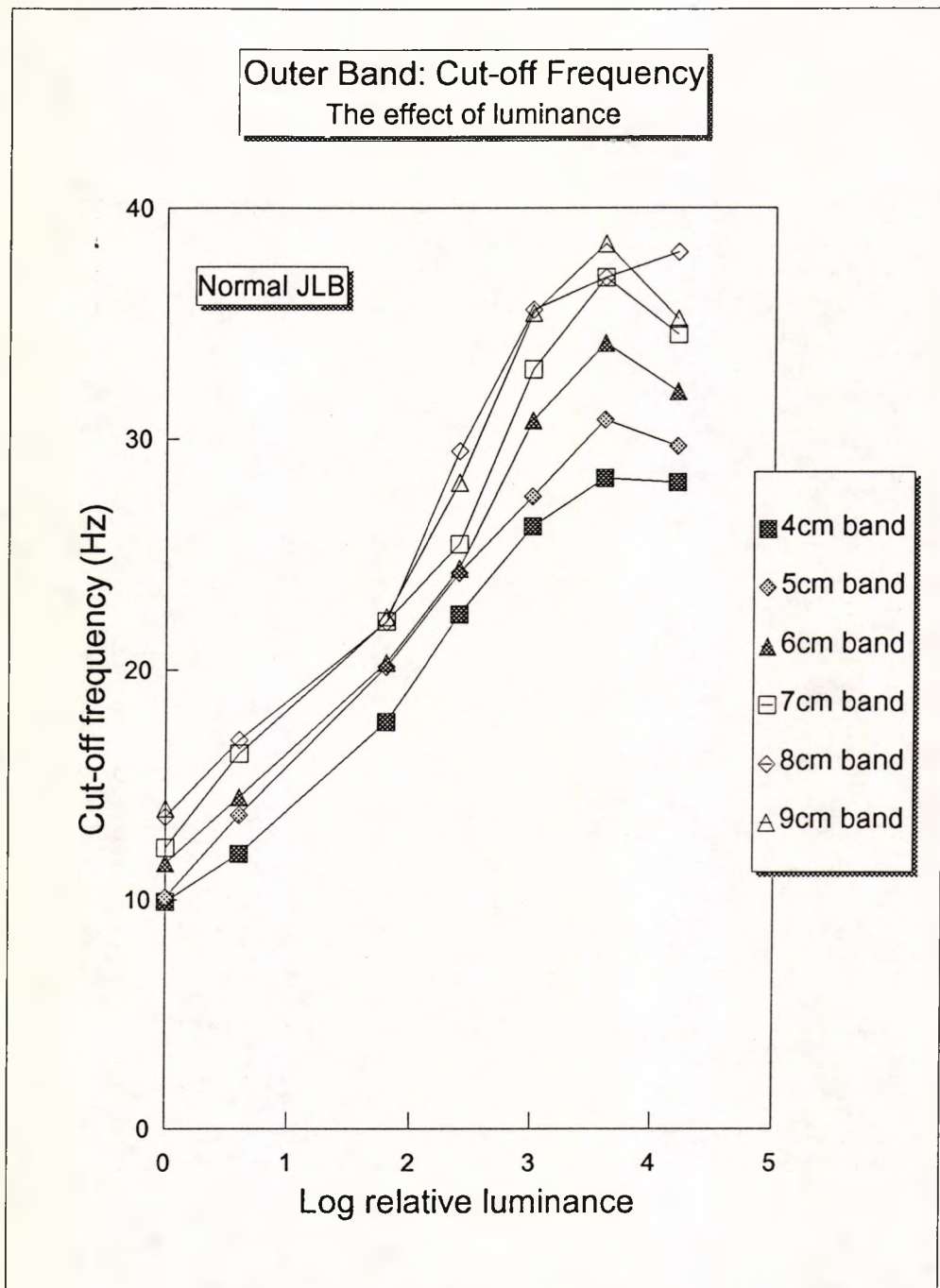
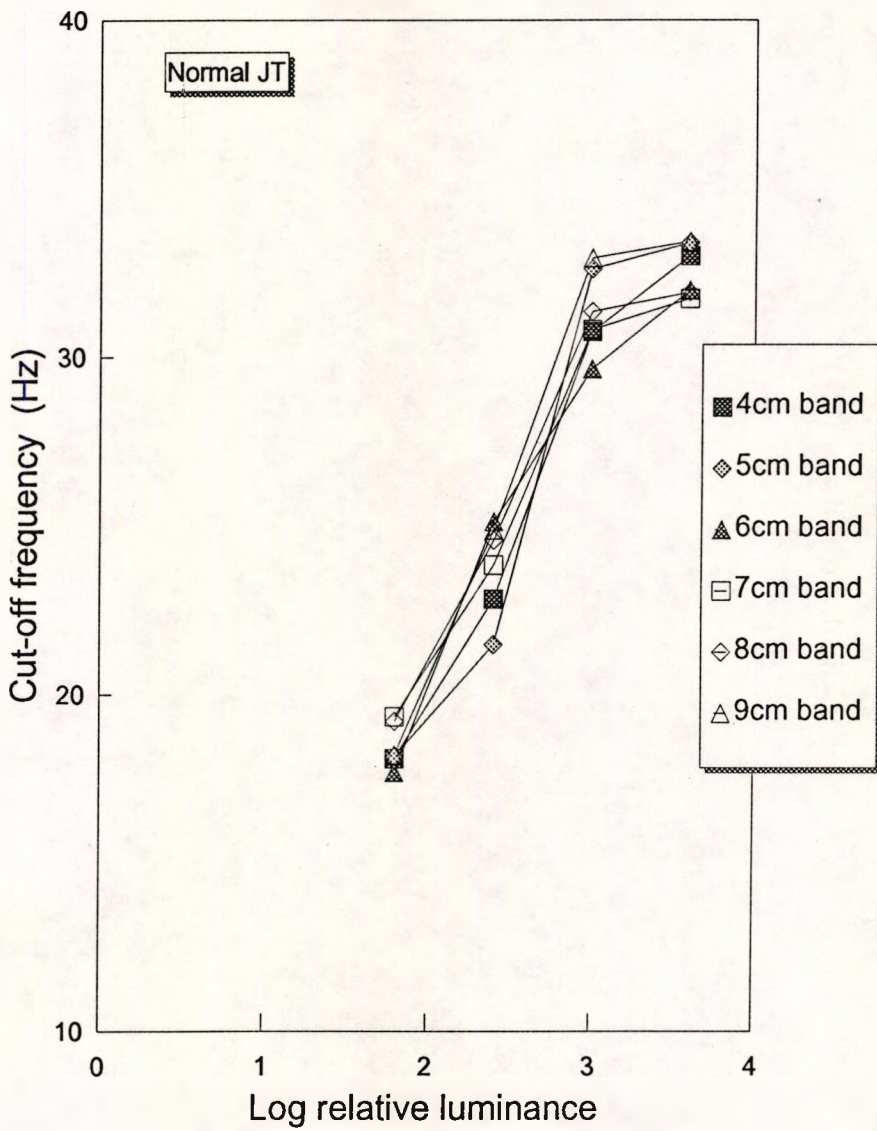


Figure 2.5: The cut-off frequencies for the 'outer' bands are shown as a function of luminance (maximum:  $650 \text{ cd. m}^{-2}$ ) for a series of different widths of band. Both observers display an increase in cut-off frequency for increased luminance. Subject JLB shows a drop at the highest luminance. It is also apparent that there is a gradual increase in cut-off frequency with increasing widths of band i.e. with increased eccentricity. The fundamental spatial frequency is  $3.4 \text{ c/deg}$ ; the angular velocity is  $3.78 \text{ rad. s}^{-1}$  and the grating is viewed binocularly through an artificial pupil of  $5\text{mm}$ .

Outer Band: Cut-off Frequency  
The effect of luminance



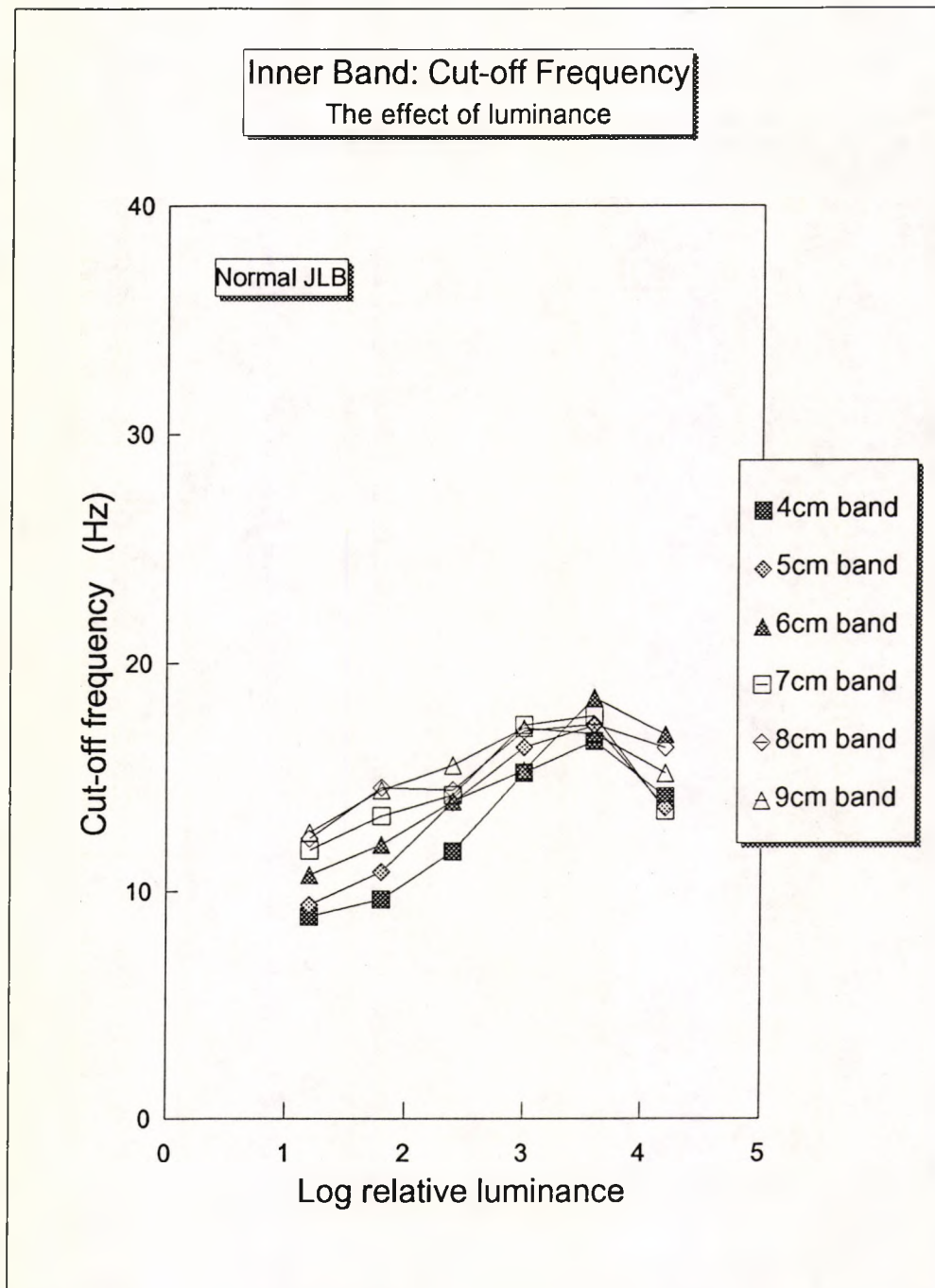
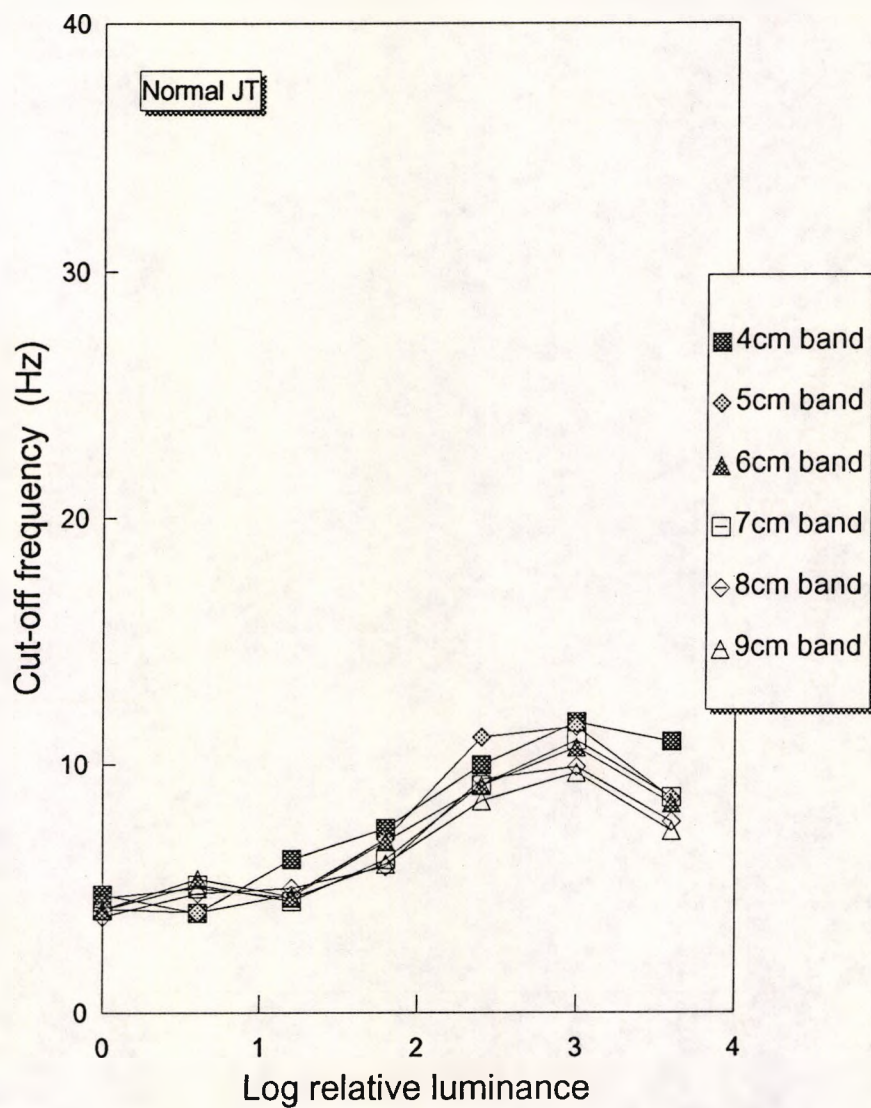


Figure 2.6: The cut-off frequencies for the 'inner' bands are shown as a function of luminance (maximum:  $650 \text{ cd. m}^{-2}$ ) for different widths of band. As with the 'outer' bands, both observers display an increase in cut-off frequency for increased luminance (less than for the 'outer' bands) and again subject JLB shows a drop at the highest luminance. Cut-off frequency increases with increased eccentricity.

### Inner Band: Cut-off Frequency The effect of luminance



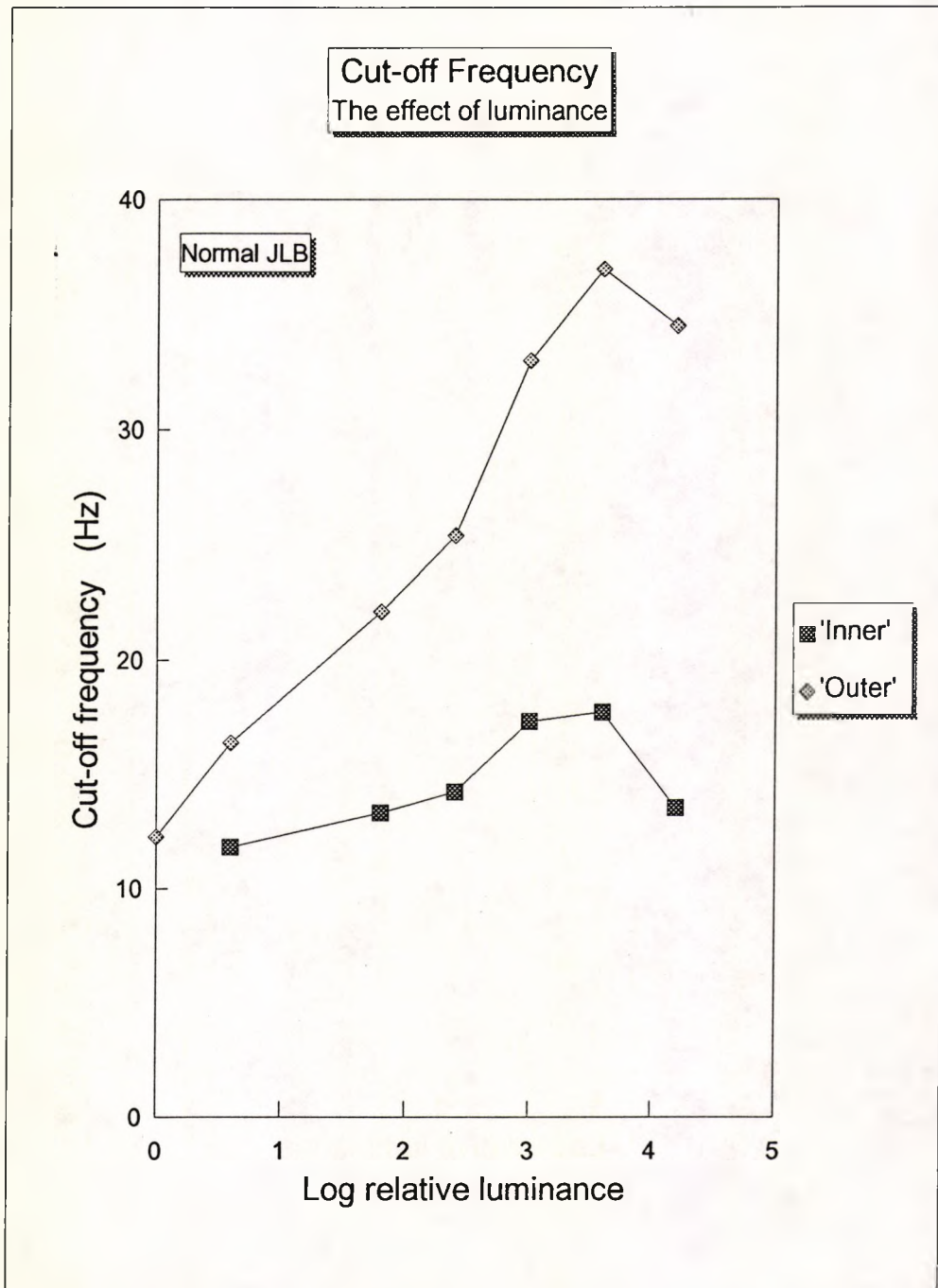
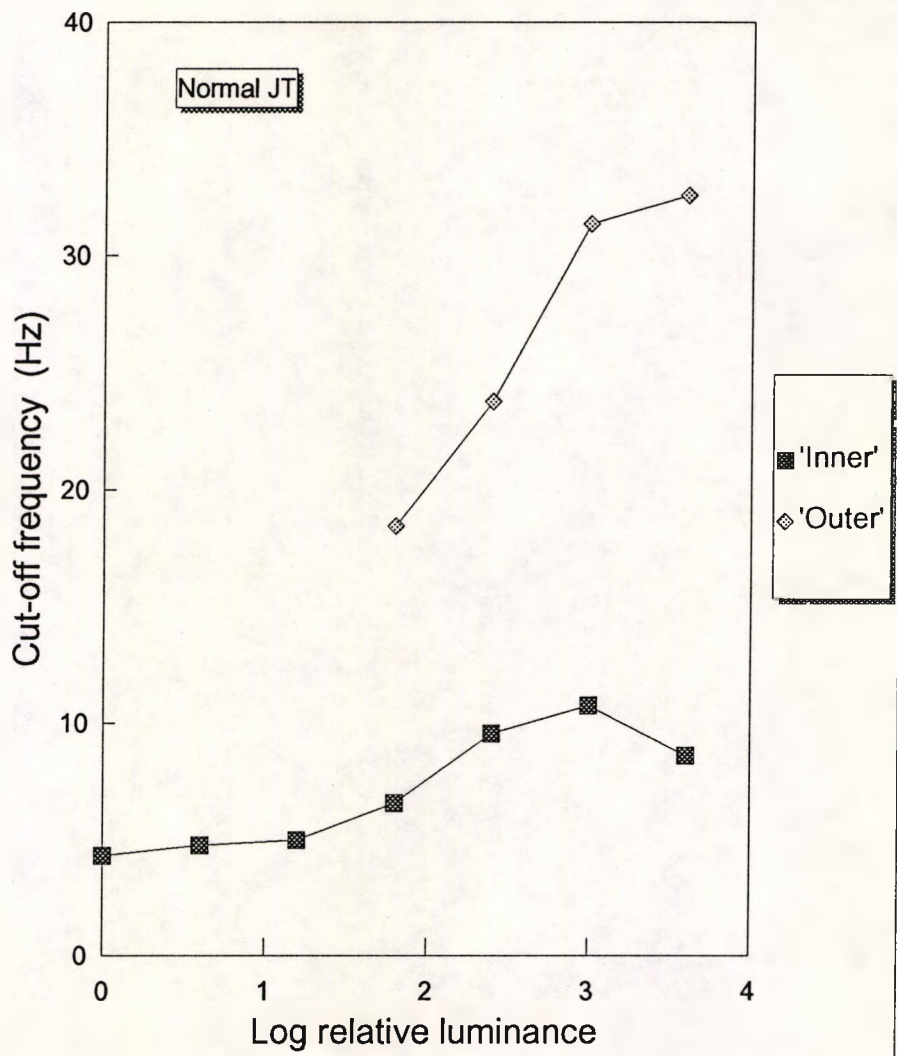


Figure 2.7: The cut-off frequencies for both the 'outer' and 'inner' bands are shown as a function of luminance for a single width of band (7cm). Both observers display a decrease in cut-off frequency for decreased luminance, with the values merging at the lowest luminances (1.2 cd. m<sup>-2</sup>). Again the fundamental spatial frequency is 3.4 c/deg; the angular velocity is 3.78 rad s<sup>-1</sup>.

Cut-off Frequency  
The effect of luminance



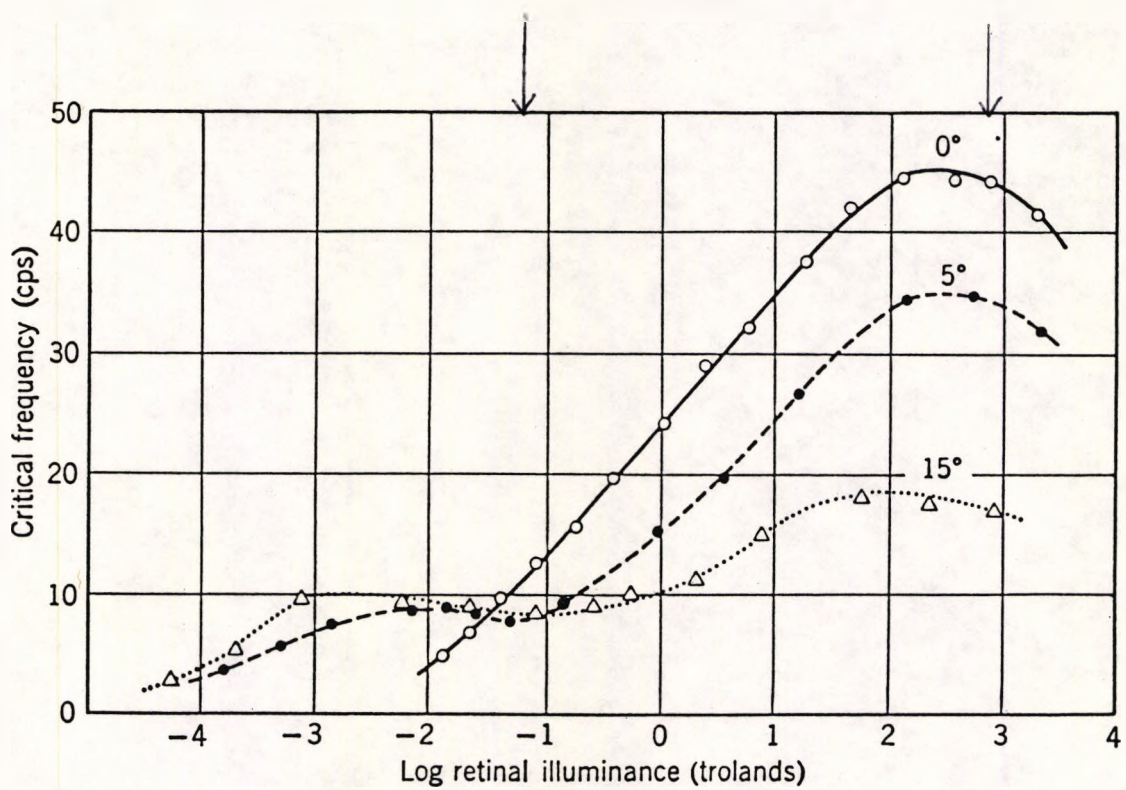


Figure 2.8: Relation between critical frequency and log retinal luminance for white light for three different retinal eccentricities; 0°, 5° and 15°. The arrows indicate the range of retinal illuminations used in the comparable investigation using the rotating stripes. The peripheral data display a distinct low luminance branch attributed to rod function (from Hecht and Varijp, 1934).

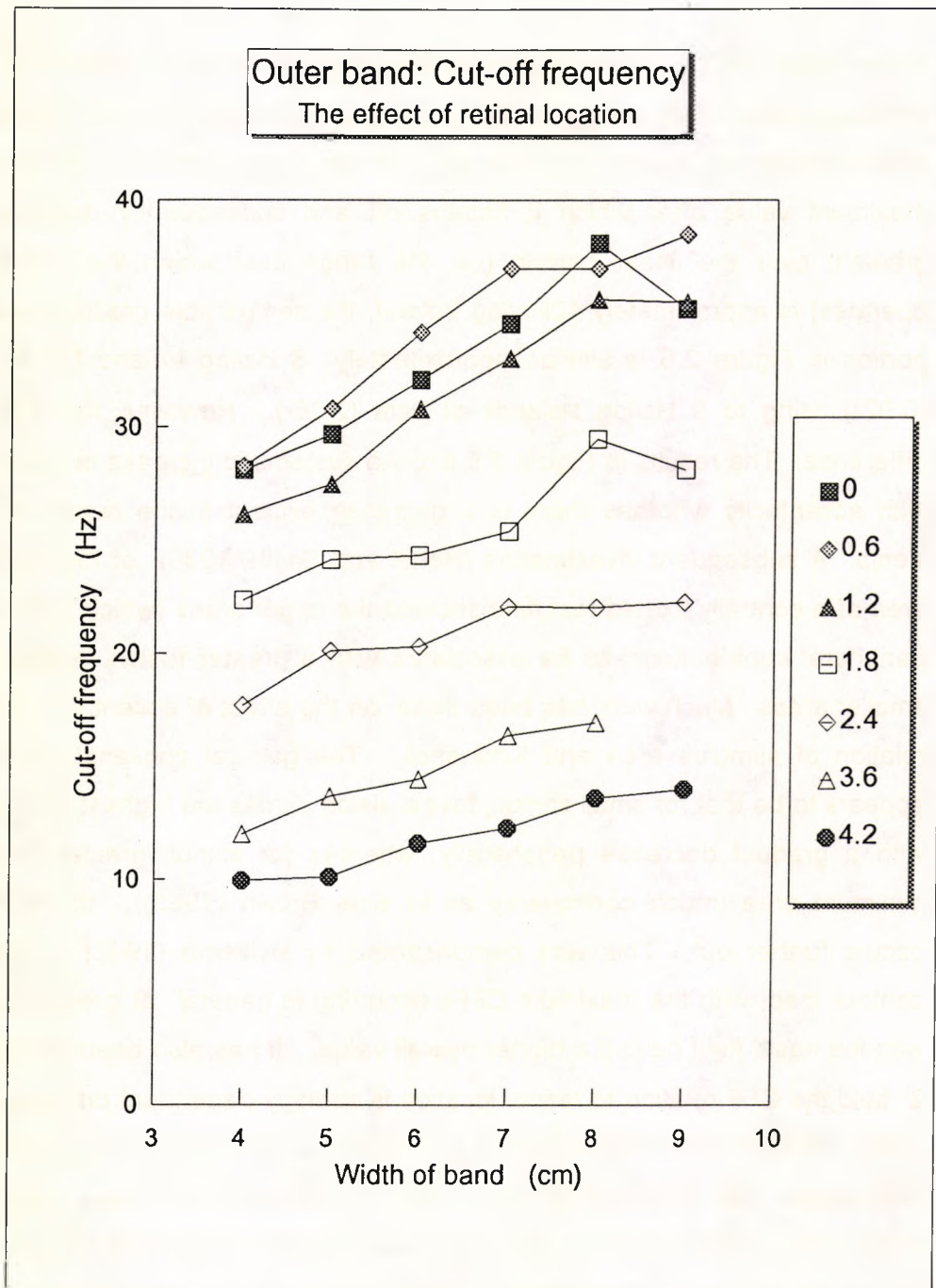


Figure 2.9: The cut-off frequencies of the 'outer' band replotted as a function of eccentricity for different retinal illuminations (filter densities are shown in the legend). The rate at which the cut-off frequencies vary with eccentricity is virtually unaffected by luminance. The spatial frequency of the grating is 3.4 c/deg and the angular velocity is 3.78 rad.s<sup>-1</sup>; binocular viewing through artificial pupils of 5mm.

ranges from  $0.92^\circ$  to  $2.06^\circ$ , and so the two most relevant graphs are those of  $0^\circ$  and  $5^\circ$  eccentricity. The results of Hecht and Verijp show that the critical frequency increases with log illumination in an approximately linear fashion over 4 log units to a maximum value after which it flattens off and subsequently drops slightly. The gradient over the linear portion (i.e. the range over which the Ferry-Porter Law operates) is approximately 10Hz/log troland; the comparable gradient over the linear portion in Figure 2.5 is similar: approximately 8 Hz/log troland for the 4cm band ( $0.92^\circ$ ) rising to 9 Hz/log trolands at 9cm ( $2.06^\circ$ ). However, there is one major difference. The results in Figure 2.5 show a systematic increase in cut-off frequency with eccentricity whereas there is a decrease evident in the results of Hecht and Verijp. A subsequent investigation (Hecht and Smith, 1936) of the influence of the area of a centrally fixated test field showed the larger areas (which in turn have more peripheral contributions) to be associated with a greater fusion frequency than the smaller areas. Much work has been done on the effect of eccentricity, and the interrelation of stimulus area and luminance. The general consensus (Landis, 1954) appears to be that for small stimuli, foveal vision carries the highest critical frequency, with a gradual decrease peripherally, whereas for stimuli greater than a certain minimum area (much controversy as to size- Brown (1965)), the maximum CFF occurs further out. This was demonstrated by Hylkema (1942) in the form of a contour map, with the maximum CFFs occurring in general at greater eccentricities, with the nasal field having a higher overall value. It has also been claimed that for a  $2^\circ$  field the CFF relation to retinal location is strongly dependent on luminance (Ross, 1936). At high luminances, the CFF decreases towards the periphery whereas at low luminances the reverse is true, with an intermediate value resulting in an independence of luminance. This does not occur for the rotating stripes. Figure 2.9 shows the rotating stripes data replotted to show cut-off frequency as a function of eccentricity for a series of different luminances. Inspection shows that luminance has little effect.

More recently, it has been recognised that the visual field is represented topographically in the striate cortex in a manner whereby the scale of the map changes with eccentricity. For increasing eccentricity there are decreasing lengths of cortex surface associated with a given extent of visual field. The scale is known as the cortical magnification factor (M) and there are many examples in which, if a stimulus is magnified at peripheral locations in inverse proportion to the cortical magnification, the variation in visibility with eccentricity vanishes. Rovamo and

Raninen (1984) showed that if the spatial parameters of a flickering stimulus is M-scaled there is still a reduction in critical frequency with eccentricity and only when there is an additional scaling applied to the luminance, is constancy maintained across the field.

In addition, stimuli have been used that employ both temporal and spatial sinusoidal luminance variations (e.g. drifting or counterphase gratings). The cortical magnification factor (M-scaling) has again been applied to threshold responses in different retinal locations; in particular luminance responses and spatial and temporal contrast sensitivity. Virsu et al., 1982 found that for drifting gratings, where M-scaling is applied spatially, there is little change in temporal sensitivity across the field for drifting gratings. Wright and Johnston (1983) found (without using a scaling factor in stimulus area) a linear decrease in contrast sensitivity across the retina which depended on the spatial frequency content, but they also concluded that there was an independence of temporal frequency. This suggests that the CCF variation with eccentricity, could simply be attributed to a spatial factor.

Clearly the spatial content of the stimuli used in the early flicker experiments is completely different from that of the rotating stripes. In spite of this, the results of Hecht and Verijp (1933), Hecht and Smith (1936), and in particular Hylkema (1942) are broadly consistent with the cut-off frequency results obtained with the 'stripes'.

In relation to the effects of eccentricity, there is less similarity between the 'stripes' results and the conclusions of the more recent work on drifting and counterphase gratings. However, the different authors do not agree as to whether or not there is a temporal variation across the field. Conventional methods for measuring the temporal cut-off frequency stripes at different eccentricities, using linearly drifting (or counterphase gratings), have had to compromise between having a sufficient area of stripes to qualify as stripes and a small enough patch to isolate a particular eccentricity. Differences can arise here. There is no such problem with the rotating pattern, as the edge of the band has a very narrowly defined eccentricity.

The 'stripes' results, that show an increased temporal sensitivity with increasing eccentricity, are consistent with the psychophysical results of Sharpe (1974) and with the ganglion cell data of Ikeda and Wright (1972) in which they demonstrate (in the cat) that there are relatively more transient ganglion cells peripherally. The connection with the density of ganglion cell types is discussed further in Chapter 3.1.

#### 2.2.4 ORIENTATION 'LAG' ASSOCIATED WITH 'INNER' AND 'OUTER' BANDS

The relative lag of the inner band with respect to the outer band represents a relative time delay, which is either (i) the direct consequence of the relative 'transport' time or (ii) results indirectly from the different persistence times or (iii) both. This relative lag is conceptually easy to appreciate. However, the orientation of either of these bands, is established by its being parallel to a line marker fixed to the pattern. For each, this represents a relative time delay, this time between the perception of the either band and the marker. Since the marker is a physical object, whose image is subject to de-blurring (Burr, 1980), this indicates that the de-blurred image is seen near the leading edge of the trail of persisting images. It is the same marker used for identifying both the inner and outer orientations, and so any time factors (advancements or delays) associated with the markers cancel out.

Figure 2.10 shows the 'lags' associated with both the 'inner' and 'outer' bands. For both investigations, the angular velocity was fixed at  $3.3 \text{ rad.s}^{-1}$ , with 1 degree representing a time delay of 5.3 ms.

Inner Band: The lags differ for the three subjects, ranging from approximately 11 degrees for observer (JT) to 7 degrees for observers (JLB) and (JW). The differences between individuals could represent a real difference in their delay (approx. 21ms), but is more likely to represent a difference in criterion as to what constitutes the boundary of the 'inner' band. The 'inner' band itself has a further substructure and if the observer concentrates on a more central component corresponding to a more persisting component, then that sub-band will inevitably be seen later in time. This seems to be what has happened. The observer (JT) with the greater lag (11 degrees) was also recorded as having a narrower 'inner' band as shown in Figure 2.6; i.e. his cut-off frequency at the same luminance was found to be approximately 9Hz as opposed to approximately 15Hz for (JLB). Assuming a rectangular temporal impulse response function, this cut-off frequency corresponds to approximate integration times of 110ms instead of 67ms. For a rectangular temporal impulse response function, the orientation of a band would be mid-way between the grating position at the beginning and end of the integration time which would impose a relative time delay in one band of  $(110/2) \text{ ms}$  and  $(67/2) \text{ ms}$  for the other. The relative delay would be approximately 20ms which would account for the difference in 'lags'.

Outer Band: This was a far harder observation to make and again there is considerable difference between the observers. The results of (JLB) and (JW) indicate a lag of approximately 3 degrees, whereas the less experienced observer (JT) perceived a lag of approximately zero. The first observations made by (JT) were strange. These are also shown in Figure 2.10, in which he observes a lead of 4 degrees clockwise and 9 degrees anti-clockwise. A difference of 5 degrees represents an asymmetry of approximately 26 ms which I ascribe to a calibration/setting error. I have included them for a different reason. Apart from any asymmetry, the 'lead' is of interest. No mechanical slip in the scale marks on the disc or error in the speed calibration could account for this as both directions produce a lead. For some reason there is a relative delay in the perception of the markers. His readings taken at a later date (at a similar time to those of (JLB) and (JW)) no longer show the strong asymmetry, which would be consistent with there having been an earlier error in the potentiometer setting, but although there is no longer the pronounced lead (approx. zero), there is in relation to the 3 degree lag of (JLB) and (JW). I can offer no explanation as to why he perceives the outer boundary 3 degrees in advance, i.e. 16ms in advance of (JLB) and (JW).

These results show a lag in the 'inner' band with respect to the 'outer' band:

- (i) 5.0 degrees for (JW) which represents a delay of 27ms
- (ii) 3.5 degrees for (JLB) which represents a delay of 18.6ms
- (iii) 9.5 degrees for (JT) which represents a delay of 50 ms

Clearly these preliminary measurements show that there is repeatability in the readings of the individual subjects, but at the same time, there are difficulties of establishing the same criteria amongst the different observers. This problem is addressed in Section 3.1. Nevertheless, the luminance effects, eccentricity effects and time delays associated with the 'inner' and 'outer' bands throw some light on possible physiological mechanisms underlying the perceived effects. Discussion of this is deferred until Chapter 3, which specifically concentrates on the complex band.

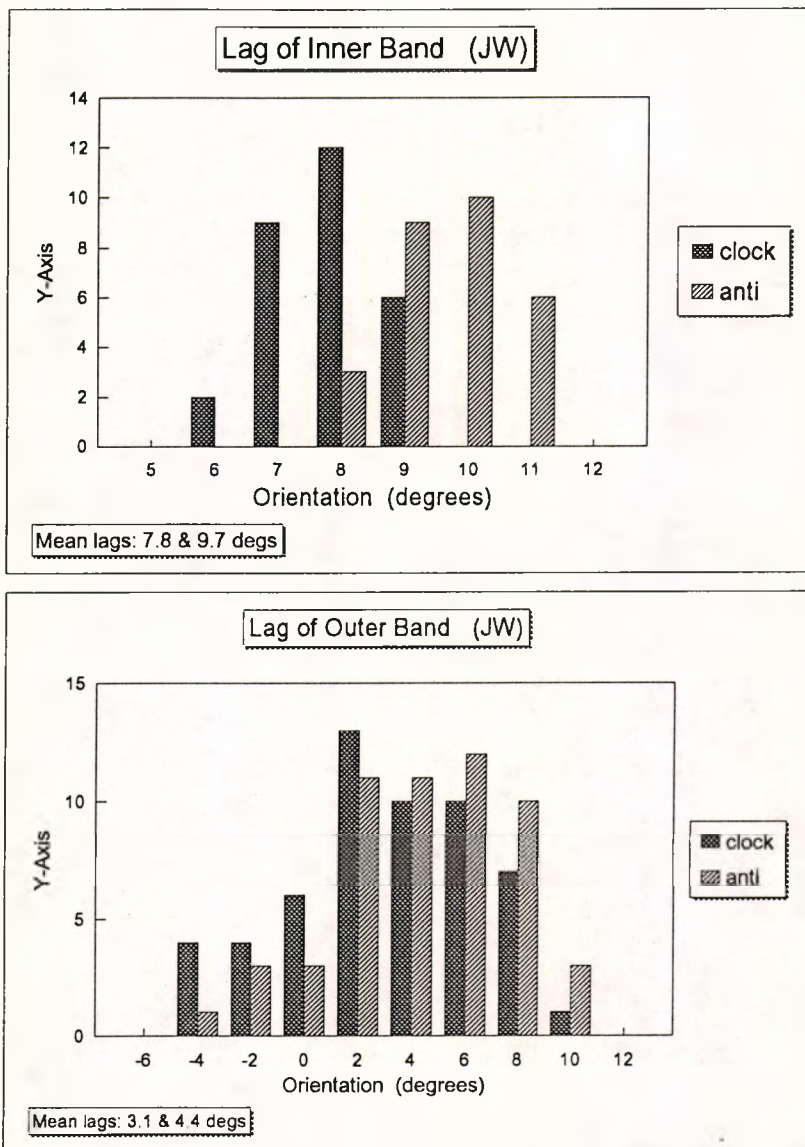
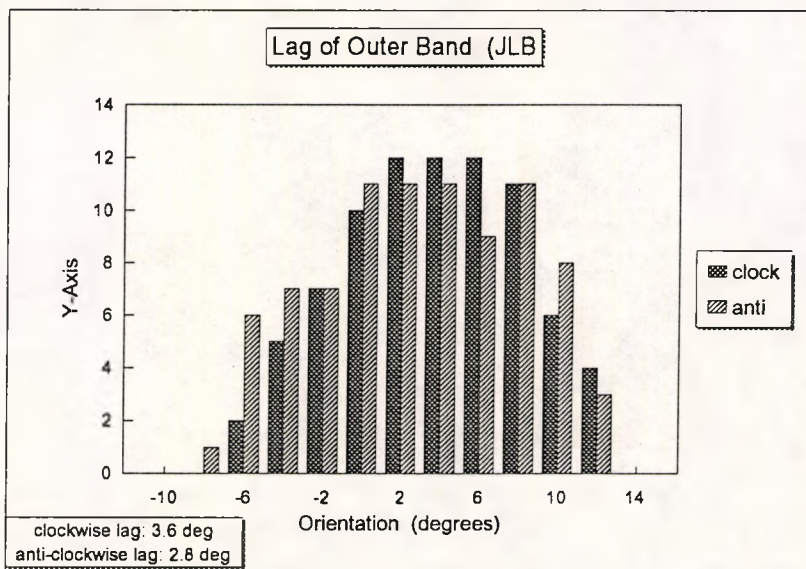
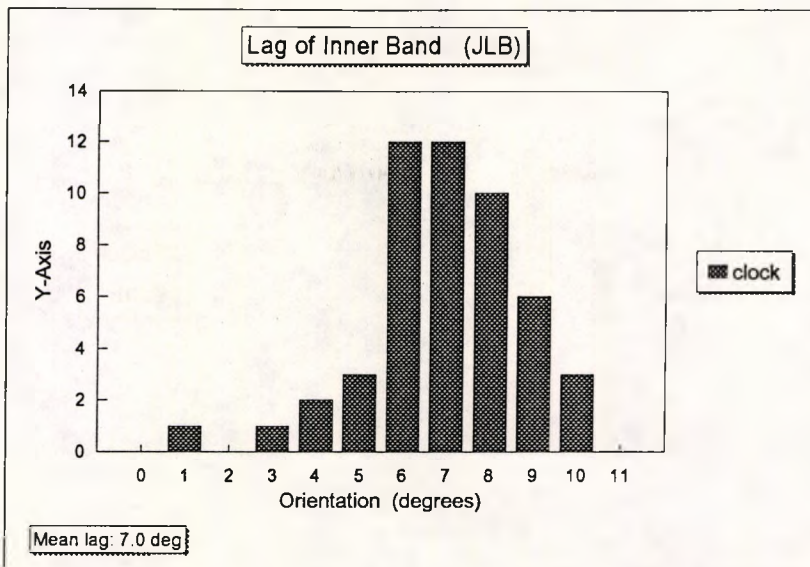


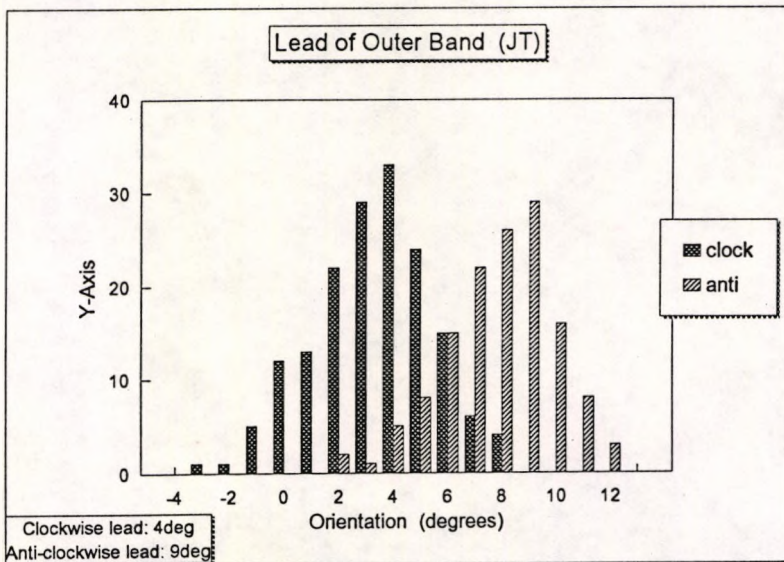
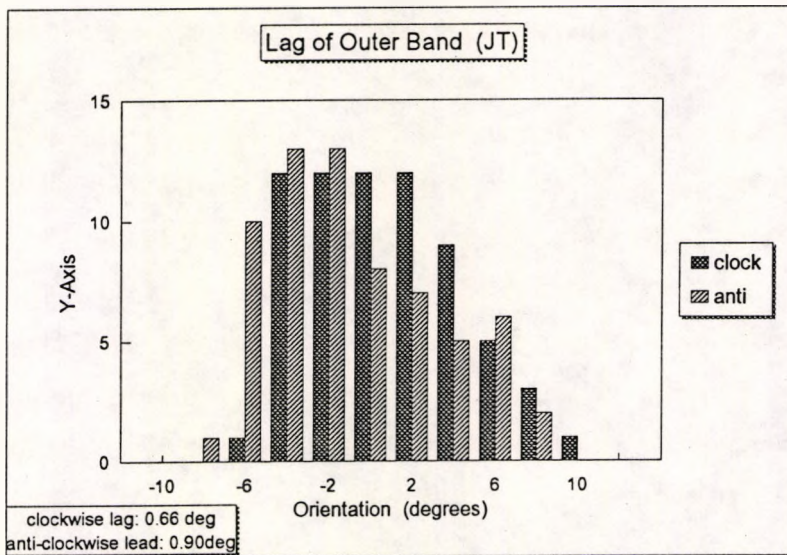
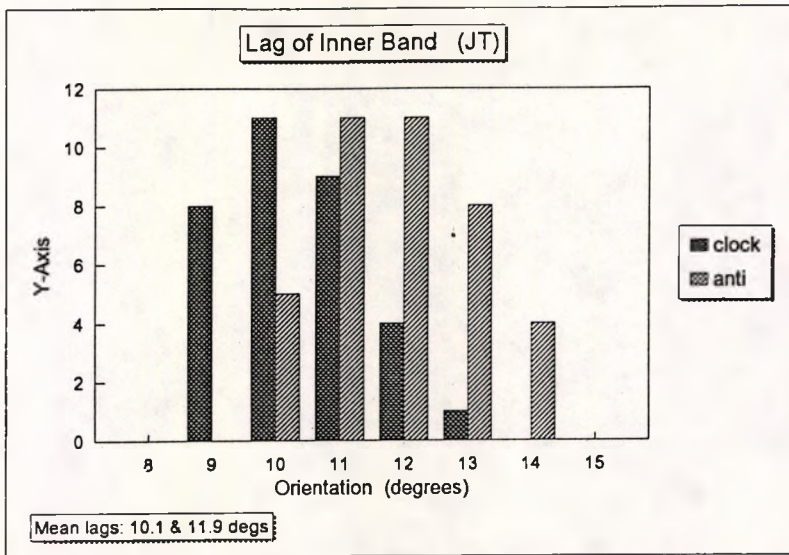
Figure 2.10: The orientations of the 'inner' and 'outer' bands established using a pair of markers presented at a variety of orientations; the observer judges on each presentation whether or not they are orientated correctly. The angular velocity is fixed at 3.3 rad/sec. Hence 1 degree represents a delay of 5.3ms. The difference in relative time delay for each observer can be ascribed to different criteria being applied as to what constitutes the boundary.

(A): Subject JW: The 'inner' band displays a mean lag of 8.75 °; the 'outer' band 3.25 °. The relative lag of 5 ° represents a time delay of 27ms.



(B): Subject JLB: The 'inner' band displays a clockwise lag of 7°; the mean lag of the 'outer' band is 3.2°. The relative lag of 3.8 deg. represents a time delay of 18.6ms.

(C): Subject JT: The 'inner' band displays a mean lag of 8.75 °; the mean lag of the 'outer' band is -0.78 ° (i.e. a lead). The relative lag of 9.5 °. represents a time delay of 50ms.



## 2.3 THEORETICAL ANALYSIS OF THE 'BAND EFFECT' SEEN UNDER UNIFORM ILLUMINATION

### 2.3.1 Introduction to Paper 1: Rotating stripes and the impulse response of the eye: Uniform illumination

This first paper establishes theoretically the simple relationship between the appearance of the band seen and the temporal characteristics of the human visual system. It was already established in the previous section (Figure 2.2) that, at any given moment in time, the stimulus is in effect providing a series of mini-columns of stripes each travelling with a velocity that is proportional to the distance along 'x'. It follows that these columns of stripes of increasing velocity are exposing the retina to a 'sweep' of temporal frequencies. The perceived contrast of each column depends on the ability of the system to transfer that particular frequency and so it follows that the perceived contrast across the band is a direct display of the temporal modulation transfer function of the observer's visual system with the edge of the band (zero perceived contrast) giving the temporal cut-off frequency. Linearity has been assumed, and since the visual system is not linear and the contrast is supra-threshold over most of the band, it is more precise to consider the perceived contrast distribution as a display of the 'describing function'. However, at the edge of the band, the contrast is at threshold; any non-linearity does not therefore interfere with the estimate of cut-off frequency.

If there is a delay associated with any particular temporal frequency, that portion of the band would be seen later in time. There would be a perceived kink in the stripes or, phrasing it more formally, the anti-symmetric distortion of the lines within the band is a direct measure of the phase transfer function. The orientation of the band can provide information on 'transport delay'.

The analysis is illustrated (and validated!) with photographs of the rotating stripes. The equivalence of still photographs of rotating gratings, blurred because of the finite exposure, and the perceived appearance of the same rotating grating, blurred because of the persistence of vision, has already been referred to in the introduction to Chapter 2. The manner in which the shutter opens and closes is analogous to the form and duration of the persistence function (or impulse response) of the visual system. The particular shutter used for the photographs shown in Paper 1, opened

abruptly, stayed open for a known period and closed abruptly, and consequently the resulting photographs correspond to that of an idealised eye with a rectangular temporal impulse response. The predicted contrast for a rectangular impulse response follows a distinctive pattern (a sinc function) which can be seen in the photographs. Although this is both discussed and illustrated in the paper, the larger photograph of Figure 2.3 shows more clearly the manner in which the contrast varies across the pattern. The contrast is given by the sinc function:

$$C=C_0\{\sin(\pi\omega xT/2d)\}/(\pi\omega xT/2d)$$

which gives a central band of twice the width of the flanking bands, together with an oscillating but diminishing contrast. This can be seen in the photograph. The phase change of 180 degrees at each band can also be seen, i.e. a black stripe in one band is replaced by a white in the neighbouring band. Since the real visual system does not have a rectangular impulse response, there are some differences between the photographs and the appearance actually perceived; however the features that are independent of the precise profile of the temporal impulse response, such as the effect of speed of rotation, are well illustrated.

A Fraunhofer diffraction pattern associated with a single slit has a similar form. Assuming the slit has a uniform transmittance (i.e. a rectangular aperture function), the amplitude distribution across the pattern also follows a 'sinc' function distribution. The analysis of the appearance of the rotating stripes draws on this analogy and establishes that the perceived contrast distribution across the rotating striped pattern relates to the temporal impulse response of its imaging system in the same way as the amplitude distribution in a Fraunhofer diffraction pattern relates to the aperture function. As an analogue, Fraunhofer diffraction is attractive, not only because it has been exhaustively studied, but because diffraction patterns also provide a visual display of the underlying features which have both spatial and temporal aspects.

In general moving objects are not seen as blurred ( Burr, 1980). This immediately raises the question as to the relationship between the real and perceived position in space of any moving object. As the band is described as 'lagging' behind the perpendicular to the stripes (i.e. parallel to a marker fixed to the striped pattern and lying obliquely to the perpendicular to the stripes), the effect throws some light on this question. The band is not an object, but rather a direct manifestation of persisting images with no deblurring; if deblurring were operating, there would be no band! The marker is deblurred. The implication of the apparent lag is discussed in the paper.

Finally the paper considers possible binocular effects that would arise in the event of there being a superposition of the two images, where there is relative transport delay between the two eyes. The mathematics again draws on the diffraction analogy.

### 2.3.2 Paper 1:

## Rotating stripes and the impulse response of the eye: I. Uniform illumination\*

JANET E. WOLF

*Department of Optometry and Visual Science, The City University, London EC1V 0HB*

Received 17 September 1986; revised 31 March 1987; accepted 29 July 1987

**Abstract**—A rotating striped pattern produces an unexpected visual effect: a band of relatively high contrast is seen obliquely across the striped pattern, moving steadily around with the pattern and lagging behind the perpendicular to the stripes. Photographs of the moving pattern display similar effects. An analysis of the effect (based on a simple linear model) shows that the perceived contrast observed at any instant across the pattern represents the temporal modulation transfer function of the eye and the asymmetrical shape of the lines is a display of the phase transfer function. The analysis establishes and uses an analogy with the amplitude distribution in a Fraunhofer diffraction pattern. The temporal impulse response of the eye is related to the perceived contrast in the same way that the aperture function is to the amplitude distribution in the diffraction pattern. The binocularly perceived contrast distribution is considered as the interference or phasor addition of the two monocularly perceived effects, and the clinical potential of this approach is illustrated. In addition, since the band itself is not an object with a physical boundary, but a perceptual consequence of blurring and spatial averaging, the effect provides a means for investigating the perceived location of moving objects in general.

### INTRODUCTION

Rotating any one-dimensional striped pattern produces the startling effect of a clearly resolved central band lagging slightly behind the perpendicular to the stripes. This effect was initially described by Babington-Smith (1964) who named it the 'band of heightened intensity'. He suggested that the effect was some kind of manifestation of the persistence of vision and that what is seen can be considered to be a summation of images formed over some non-zero time. In his paper, he suggested that the effect was a Moiré fringe pattern resulting from the superposition of two discrete images, namely that image most recently perceived superimposed on the lingering positive after-image of the stripes in a previous position, the two images being separated in time by the persistence time and in space by the rotation during the persistence time.

At one time, it was considered (e.g., Wade, 1974) that such a Moiré pattern would be consistent with a 'travelling moment' or 'travelling window' or 'persistence' hypothesis and that the band effect could therefore be used to test the persistence hypothesis. In fact, if the travelling moment or persistence hypothesis is valid, the eye would perceive the sum of a succession of images displaced by the rotation and not the two discrete

---

\*A summary of the material contained in this report was presented at the joint meeting of the Experimental Psychology Society and the Netherlands Psychonomic Foundation, Amsterdam, July 1984; and at the Applied Vision Association meeting on Mathematical and Statistical Techniques, London, October 1984.

images required for the production of a Moiré band. So the observation that the width of the band does not conform to that of a simple Moiré band does not invalidate the persistence hypothesis. As will be shown here, the persistence hypothesis *can* be used to predict the effect. It was further suggested by Wade (1974), as an alternative hypothesis, that the band effect might be explained in terms of a 'resolution hypothesis', namely that the resolution of faster moving targets is reduced; this would mean that the extremities of the pattern would be blurred, leaving a clear central band. However, reduction in resolution of a moving target also follows from a persistence hypothesis.

Nevertheless, it was established unequivocally (Wade, 1974) that the width of the band decreased with increasing angular velocity for a given striped pattern. This observation was then predicted by a simple model proposed by Barbur (1980). In this model, he assumed complete temporal integration over a fixed period of time, the weighting of the successive images over that period being constant; in effect he assumed a rectangular form of temporal impulse response with linear summation. This assumption then explained not only the inverse relation between perceived width and angular velocity, but also the inverse relation between the perceived width and the temporal integration period and the spatial frequency of the pattern. However, a more accurate prediction of the observed effects would require a better approximation of the temporal response properties of the mechanisms involved in the detection of the pattern.

In the present paper, linearity is again assumed, but in conjunction with a general form of temporal impulse response of the eye. The model analytically predicts the appearance resulting from such an impulse-response function, thereby providing a technique for determining the form of this function. The analysis is tested on a system with a rectangular impulse response and the strength of the analysis may be seen from the close similarity with photographic recordings. The model itself is tested to the extent that the existing psychophysical observations of Babington-Smith (1964), Wade (1974) and Barbur (1980) are all predicted by it.

The model is then extended to encompass any relative time delays between the two monocular images; a linear summation is again assumed. Finally, the clinical implications of these various perceived effects are touched on.

#### THE TEMPORAL IMPULSE RESPONSE

The temporal impulse response of the eye is the perceptual response of the eye to an infinitesimally short flash of light on the retina expressed as a function of time. Integration of light intensities is assumed to take place over this time interval, sometimes described as the *persistence time* or the temporal extent of the *travelling moment*. A target moving with respect to the retina leaves a trail of images, and the perceived image will, therefore, be smeared by this persistence in much the same way that a still photograph of a moving target is smeared by the non-zero shutter opening time. The extent of the smear is given by the product of the velocity and the overall persistence time (or shutter opening time) and in both cases, if linearity is assumed, the final appearance will simply be the perceived intensity distribution of the stationary target convolved with the impulse response scaled or stretched by the velocity. Since the camera exposure function is approximately rectangular, the appearance of the photographs would correspond to the appearance of the target perceived by an eye with an idealized rectangular impulse response function. In general, extracting the form of the impulse response function from the smeared image would be laborious. In the

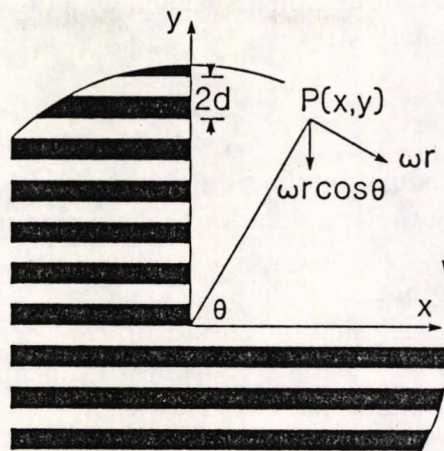


**Figure 1.** Rotating striped pattern, with the origin of the Cartesian system at the centre of rotation and the  $x$ ,  $y$ -axes fixed on the pattern. With a constant angular velocity  $\omega$ , the point  $P(x, y)$  travels with a constant speed  $\omega r$ . The component of this velocity perpendicular to the stripes,  $\omega r \cos \theta = \omega x$ , will produce the blurring of the stripes (see text).

special case of a moving target consisting of a rotating striped pattern, however, the information is readily accessible.

#### THE EFFECT OF ROTATION

The effect of rotation is illustrated in Fig. 1 which shows a one-dimensional pattern of stripes. When this pattern rotates with a constant angular velocity, any point on it will travel round with constant speed increasing proportionally with distance from the centre of rotation. It is, however, the velocity component perpendicular to the stripes that will determine whether or not the eye's perception of the stripes is blurred. Figure 1 shows the pattern with the origin of the Cartesian system at the centre of rotation and the  $x$ ,  $y$ -axes fixed on the pattern. It can be seen that this velocity component (along the  $y$ -axis) for any point  $P(x, y)$  is instantaneously given by  $dy/dt = \omega r \cos \theta = \omega x$  and is independent of  $y$ ; i.e. the blurring component of the velocity is constant for a particular value of  $x$  and the clear region, therefore, lies within a parallel sided band. There is a non-zero rotation  $\Delta\theta$  of the coordinate axes during the integration time interval  $\Delta T$ , which will be small for low angular velocities. The boundary of constant blurring (i.e. the edge of the band) follows the contour that provides a fixed  $\Delta y$  over this interval  $\Delta T$ , the boundary being straight if  $\Delta\theta$  is sufficiently small for  $\sin \Delta\theta = \Delta\theta$ . In addition, the non-zero rotation (necessary for the existence of the band effect) means that the orientation of the band lags behind the instantaneous position of the stripes in the retinal image. The possible significance of this lag is considered later. At this stage the analysis is concerned with the contrast distribution across the centre of the pattern where it is unaffected by lag.

#### COMPLEMENTARY ANALYSES OF THE EFFECT

This paper attempts to provide an explanation of the band effect by means of a linear systems analysis, which can be approached in two complementary ways.

One way is to consider that, as the distance  $x$  from the centre of rotation increases, the velocity component perpendicular to the stripes ( $\omega x$ ) increases, causing the retina to be presented with alternating light and dark images of increasing temporal frequency

$(\omega x/(2d))$ . The luminance modulation associated with this temporally varying input is the contrast of the stationary stripes,

$$\frac{(L_{\max} - L_{\min})}{(L_{\max} + L_{\min})},$$

and it is this temporal modulation that is attenuated by the persistence of the impulse response. This gives an 'output' modulation that consists of the perceived (or recorded) contrast, this contrast being a measure of the system's ability to transmit that particular temporal frequency component.

An alternative way of analysing the effect is to consider the retina being presented with a uniform pattern of fixed spatial frequency with an input modulation that again is the contrast of the stationary pattern. However, because of the increasing perpendicular velocity as the distance  $x$  from the centre is increased, this constant spatial frequency has its modulation reduced by an increasing spatial spread function, namely the temporal impulse response 'scaled up' by the velocity. The output modulation at any distance  $x$  from the centre is once again the perceived contrast. So, either we can consider the target as providing a range of temporal frequencies increasing linearly with  $x$ , their modulation depths being smoothed or attenuated by an impulse response of fixed temporal extent, or we can consider the modulation depth of the fixed spatial frequency being smoothed by a spread function that increases in spatial extent linearly with  $x$ . Whereas both approaches in effect apply temporal filtering to a linear system, it is the latter approach, where the temporal blurring function has been converted into a spatial spread function, that gives the most easily appreciated assessment of the appearance. This is probably because we tend to describe the appearance of any moving target in terms of its spatial distribution at a given point in time rather than in terms of the temporal activity at a given point in space. However, a more general approach, which is effectively a combination of the two, is to consider the target as providing a travelling wave profile whose perpendicular velocity increases linearly with  $x$ , the profile being 'time averaged'. All these approaches are shown in Appendix 1, although it is the second and third approach, where the spatial pattern is considered, that leads most simply to the striking analogy with Fraunhofer diffraction effects.

#### PHOTOGRAPHIC DEMONSTRATION

The similarity of photographs smeared by a non-zero exposure time and the visual appearance at any instant in time smeared by the persistence time enables us to use the former to demonstrate both the main characteristics of the visual rotating-pattern effect and the main features of the analysis.

By assumption, the equivalence in appearance holds for any form of camera exposure function and corresponding temporal impulse response of the eye, provided that any asymmetry in the camera exposure function is reversed in the impulse response. For example, if a camera aperture opens slowly and then shuts abruptly, it will record a picture that is equivalent to that seen by an eye whose impulse response rises abruptly and tails off slowly. In the photographs shown here, the durations of the opening and closing times were sufficiently small that the exposure departed very little from a uniform rectangular function. The exposure was controlled by means of a Uniblitz electromagnetic shutter with opening and closing times of less than 4 ms. The triggering of the shutter was achieved by monitoring continuously the rotation of the disc by means of an infra-red optical switch.

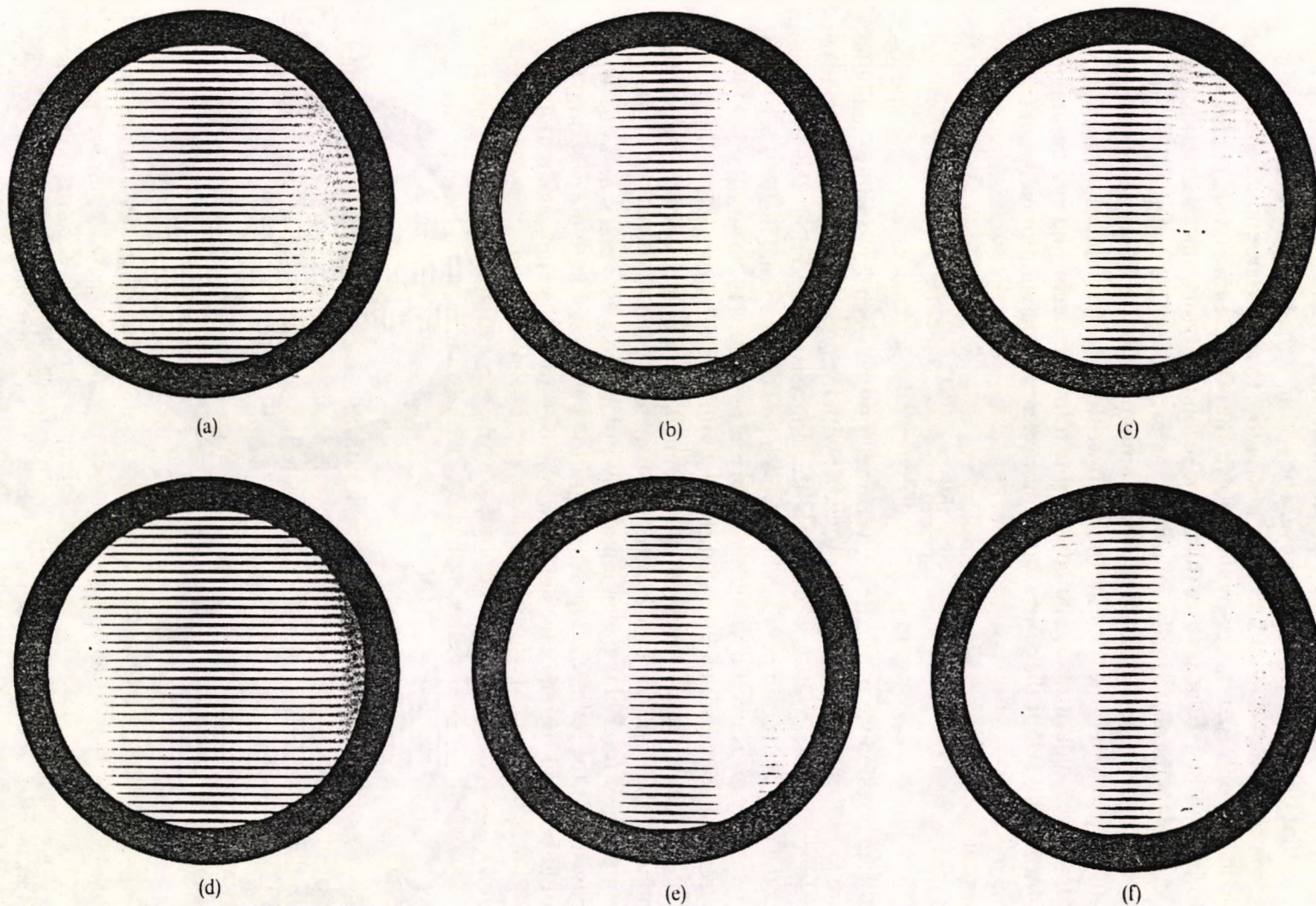


**Figure 2.** Single exposure photographs of the striped pattern of square waveform and line width 2.6 mm. The first three photographs are for exposures of 30 ms and increasing angular velocities (a)  $2.54 \text{ rad s}^{-1}$  (b)  $3.78 \text{ rad s}^{-1}$  (c)  $5.02 \text{ rad s}^{-1}$ . The second three photographs are for an angular velocity of  $3.28 \text{ rad s}^{-1}$  and increasing durations (d) 20 ms (e) 40 ms (f) 60 ms. These photographs show a contrast distribution across the pattern that is in the form of a sinc function which corresponds to the amplitude distribution in a diffraction pattern associated with a single slit.

The first type of photograph taken was a single exposure simulating, in effect, an eye with an idealized rectangular impulse response. Figure 2 shows a series of single exposure photographs of the rotating pattern for varying angular velocities  $\omega$  and varying exposure times  $T$ . In all these photographs there is a main high-contrast band similar to that observed with the real eye. The width of the band varies inversely with angular velocity  $\omega$  and exposure time  $T$ . In addition, the photographs show secondary bands of lower contrast, not seen by the real eye, the explanation of which follows later. The width of the main band is twice that of the secondary bands and the contrast varies with increasing  $x$  in a gradually reducing and oscillatory fashion; the phase of the second band is opposite to that of the main band (i.e. a black stripe appears beside a white stripe), the third is the same and so on. If we simplify the situation by considering a pattern of sinusoidal stripes, and considering a linearly recording system, it can be shown (Appendix 1) that the contrast distribution across the pattern is that of the sinc function

$$C = C_0 \frac{\sin(\pi\omega x T / (2d))}{\pi\omega x T / (2d)}. \quad (1)$$

From this expression we predict the inverse relation between band width and either exposure time  $T$  or angular velocity  $\omega$ , together with the phase reversals, as recorded in the photographs of Fig. 2; this reinforces the analysis. In addition, the expression predicts the inverse relation between band width and either spatial frequency  $1/(2d)$  or angular velocity  $\omega$ , as psychophysically observed by Wade (1974) and Barbur (1980).

Also from this expression we see that the first minimum occurs at a position  $x$  given by  $x = 2d/(\omega T)$  giving an overall width of the main band of  $4d/(\omega T)$ . This first minimum corresponds to the position of the band edge predicted by Barbur (1980) on the basis of his assumption of total blur occurring at any point where one black and one white stripe pass across the retina during the integration period. By the same criterion, total blur would occur in regions exposed to two black and two white stripes, and so on,

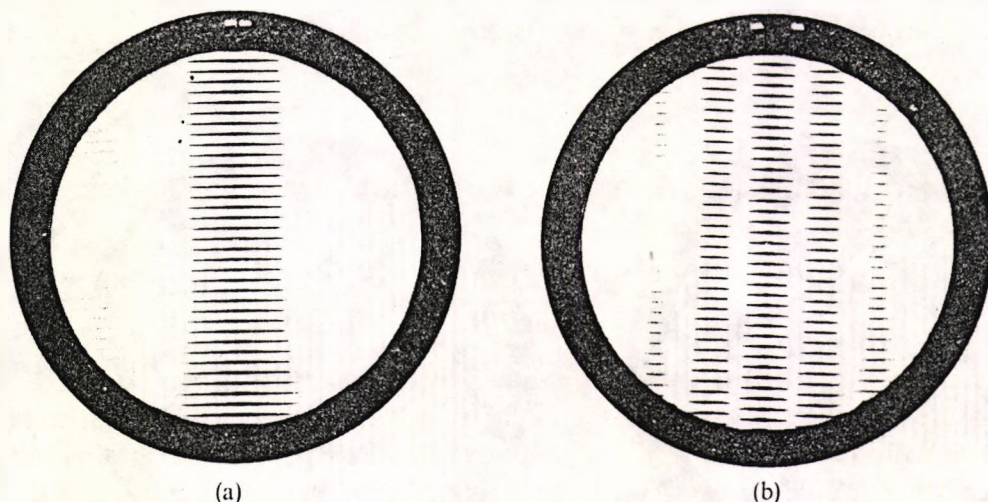


**Figure 3.** Double exposure photographs, each exposure being of 16 ms, separated by a time interval (a) 19 ms and (b) 54 ms, the exposure durations being indicated by white marks on the black surround. The angular velocity for each is  $3.28 \text{ rad s}^{-1}$ . This type of photograph simulates two similar mechanisms whose outputs combine linearly, one of which is delayed with respect to the other. The contrast distribution across the pattern can be seen to be in the form of a cosine function modulated by a sinc function, which corresponds to the diffraction pattern associated with 2-slit interference.

which would lead to the prediction of repeating bands recorded by the camera. Indeed, if intermediate regions exposed, say, to one white and two black stripes, etc., had been included, a sine profile across the whole pattern would have been predicted.

The second type of photograph was intended to simulate two similar mechanisms whose outputs are delayed by different amounts before being perceived, as might be encountered in a binocularly perceived image in which the image of one eye is delayed with respect to the other. This involved exposing the film twice, each exposure being of time  $T$ , with the second exposure being delayed in time by a short interval  $T_{\text{del}}$ . Figure 3 shows two such double exposures in which only  $T_{\text{del}}$  differs. The contrast distribution can be shown to be

$$C = C_0 \frac{\sin(\pi\omega x T / (2d))}{\pi\omega x T / (2d)} \cos(\pi\omega x T_{\text{del}} / (2d)). \quad (2)$$

In both photographs, the form of the overall sinc function associated with the single exposure can still be seen, but this has been broken down into a series of bands (governed by the cosine function), their width being determined by the relative delay in the formation of the separate images. From equation 2, this width is seen to be  $2d/(\omega T_{\text{del}})$ , which is independent of the form of the impulse response.

For both of these types of temporal impulse response (single rectangular and double rectangular), the contrast distribution amounts to the Fourier transform of the overall impulse response. Similarly, for a more general form of impulse response, the contrast distribution across the pattern would again be of the same form as the Fourier transform of that impulse response, i.e. it represents the temporal amplitude transfer function of the system. This is established in Appendix 1.

#### THE DIFFRACTION ANALOGY

The analogy with Fraunhofer diffraction effects is apparent. The distribution of the amplitude  $A$  across the diffraction pattern due to a single slit of aperture  $a$ , expressed as a function of the angle  $\theta$  (see Fig. 4), is given by

$$A = A_0 \frac{\sin(\pi a(\sin \theta)/\lambda)}{\pi a(\sin \theta)/\lambda},$$

whereas the amplitude distribution for two-slit interference, the slits being of width  $a$  and separation  $D$ , is given by

$$A = A_0 \frac{\sin(\pi a(\sin \theta)/\lambda)}{\pi a(\sin \theta)/\lambda} \cos(\pi D(\sin \theta)/\lambda).$$

This analogy can be understood qualitatively. Consider both the single rectangular exposure function and the single rectangular aperture function of Fig. 4(a) and (b). The resultant modulation of the light is the sum of all the elementary wavetrains and, in any given direction  $\theta$ , is effectively the original modulation smoothed out by the rectangular function of width  $a \sin \theta$ , the resulting modulation in this case being the final amplitude of the light. In the case of the rotating pattern, the moving profile of stripes is analogous to the wavetrains of light. The original spatial modulation is the actual contrast which is smoothed out in this case by the rectangular function of width  $\omega x T$ , the resulting modulation being the perceived contrast at a distance  $x$  from the centre.

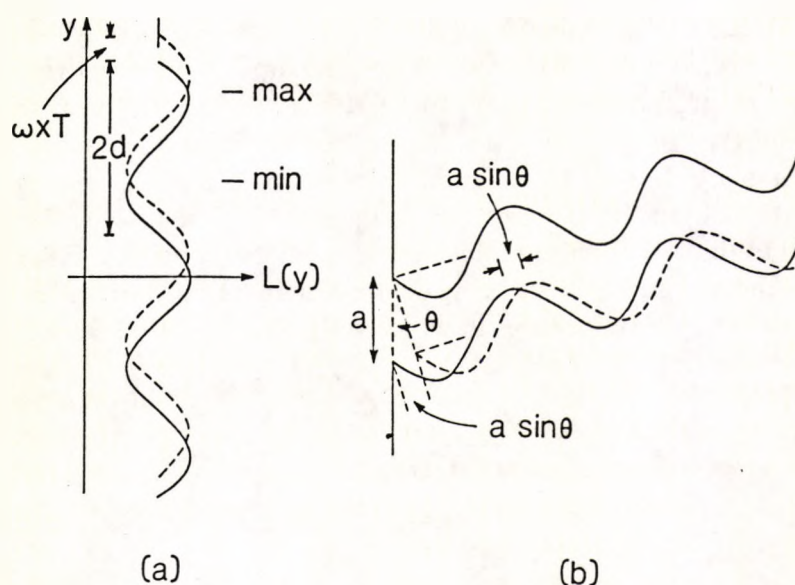


**Figure 4.** Illustration of the origin of the analogy between the perceived contrast of the rotating stripes as a function of the distance  $x$  from the  $y$ -axis and the amplitude distribution in a Fraunhofer diffraction pattern as a function of  $\theta$ . (a) The actual modulation or contrast of the stripes at a distance  $x$  from the  $y$ -axis is attenuated by the rectangular function  $\omega x T$  as a consequence of integration over the duration  $T$  of the impulse response. (b) The amplitude of the light in direction  $\theta$  is attenuated by the rectangular function  $a \sin \theta$  as a consequence of integration of wavelets across the aperture of width  $a$ .

In considering the Fraunhofer diffraction system to be an analogue model of the visual system, we see that the aperture function is analogous to the impulse response function. In particular, for the rectangular function  $a$  is equivalent to  $T$  and the separation  $D$  of the slits is equivalent to the relative delay time  $T_{\text{del}}$  prior to superposition. Also the spatial frequencies  $u = (\sin \theta)/\lambda$  that constitute the spectrum of the aperture function have been replaced by the temporal frequencies  $\nu = \omega x/(2d)$  that constitute the spectrum of the impulse response. There has in effect been a complete exchange of temporal and spatial factors.

#### PHASE EFFECTS

The phase associated with each aperture spatial frequency represented in the diffraction pattern (i.e. with each direction  $\theta$ ) has its equivalence in the band effect. If the diffraction aperture is shifted in space there would be a linear phase shift in each frequency component, the magnitude of each phase shift being proportional to the frequency (shift theorem). If the impulse response is shifted in time (i.e. an additional delay added to the system), there would be a corresponding phase shift at each temporal frequency. Again this is proportional to the particular temporal frequency, which, in turn, is proportional to the distance  $x$  from the centre of rotation, so the phase shift would be proportional to the distance  $x$ . Since the phase shift manifests itself as a shift in the  $y$ -direction of the pattern, any phase shift that increases linearly with distance  $x$  amounts to an overall rotation of the lines. In other words the pattern would be perceived or recorded later in time. Apart from this rotation, the pattern would be indistinguishable from the unshifted version. However, any delay and consequent phase shift at a particular temporal frequency or group of frequencies would result in a rotation of that localized section of the pattern. This would show as a kink in the

straight lines of the pattern. The magnitude of the kink or displacement at any value of  $x$  (associated with temporal frequency  $\omega x/(2d)$ ) is proportional to the phase shift and so the shape of the line is a display of the phase transfer function of the system. This follows from Appendix 1(b).

#### SYMMETRY IN THE AMPLITUDE AND PHASE TRANSFER FUNCTIONS

Any real function may be split unambiguously into a 'real even' and a 'real odd' part. The transforms of these functions are 'real even' and 'imaginary odd' (e.g., Bracewell, 1983). This leads to the original function having an 'even' amplitude transfer function and an 'odd' phase transfer function. Following from this, a Fraunhofer diffraction pattern displays a symmetry of amplitude distribution about the origin regardless of any asymmetry in the light transmission across the aperture. The negative side of the pattern can be thought of as corresponding to the negative frequencies in the spectrum of the aperture function. Any asymmetry in the aperture function manifests itself as an 'odd' phase distribution about the same origin.

Analogous features appear in the rotating pattern effects. For an asymmetric temporal impulse response or exposure function, the contrast distribution along the  $x$ -axis will again be symmetrical about the centre of rotation. One side of the origin can be considered to be displaying positive temporal frequencies and the other negative, and so the contrast on either side represents the symmetrical weighting of positive and negative frequencies in the impulse-response spectrum. In this case the concept of negative frequencies has a physical reality in that any temporal frequency results from the movement of the pattern, and the velocity on one side of the origin is in an opposite direction to that on the other. As with the Fraunhofer effects, any asymmetry in the temporal impulse response will manifest itself as an 'odd' phase transfer function resulting in the locus of the central lines having an 'odd' pattern symmetrical about the origin.

#### DISCUSSION

An important feature of this study has been to show that a formal analysis of the visual effects produced by the rotation of a sinusoidally striped pattern is equivalent to a formal analysis of Fraunhofer diffraction in so far as the eye (or camera) operates linearly. Since Fraunhofer diffraction has been so exhaustively studied, as an analogue it is attractive. Although many other linear systems might share this common formal description, Fraunhofer diffraction has the particular advantage of providing a visual display of the features underlying the analysis.

In analysing the special case of the effects resulting from a rectangular temporal impulse response function we have seen that the width of the main band is inversely proportional to the angular velocity  $\omega$ , the exposure time  $T$  and the spatial frequency  $1/(2d)$ , the overall width of the main band being  $4d/(\omega T)$ . However, it follows from the Similarity Theorem (e.g., Bracewell, 1983) that, for any form of impulse response  $f(t)$ , whereas the contrast distribution across the pattern will be peculiar to that particular impulse response form, the dimensions of this distribution will again be inversely proportional to the angular velocity, spatial frequency and the temporal extent of the particular impulse response. The dimension that is of particular interest is the 'width of band' which, of course, refers to the extent of this pattern or contrast distribution that is deemed resolvable. For a real eye with a temporal-frequency cut-off of  $\nu_c$ , the edge of the band will be at a position  $x$  where the orthogonal velocity of the drifting stripes

provides a frequency  $\nu_c$ . At the edge of the band  $x_c = 2d\nu_c/\omega$ , which is half the overall width of the band; so it follows that the resolvable band width seen by a real eye also varies inversely with angular velocity and spatial frequency. This corresponds to the psychophysical observations of Barbur (1980) and Wade (1974). It should, however, be emphasized that the eye does not see the repeating bands recorded by the camera and noted, but not explained, by Babington-Smith (1964) and Wade (1974). This is because the repeating bands are a manifestation of the rectangular response function, whereas the single band visually observed implies a smoothly varying band-limited impulse-response function.

The width of band, in spite of being inversely related to the temporal extent of the impulse response, cannot give us the actual extent (without knowing the form of the contrast distribution across the whole pattern). Nevertheless, it can provide a useful means of comparing persistence times that might differ because of some other physical factor (e.g., luminance or wavelength of light), the differences manifesting themselves as proportional changes in band width. More importantly, if the observer's two eyes have different persistence times, this fact will manifest itself by there being a narrower band when viewed by the eye with the greater persistence.

Although a particular feature of this analysis is its conversion of temporal blurring into spatial blurring, it is well known that there are circumstances where the spatial smear that forms the basis of this analysis simply does not appear (Burr, 1980). However, it is for target forms (e.g. spots of light) where a trailing blur would produce a significantly different outline from the stationary target that this partial or total deblurring appears to operate. It has been suggested that targets are seen at a position corresponding to the weighted mean of the trail of persisting images (Morgan, 1980). Photographs of such moving targets, on the other hand, do show the smear, the photographs not having a deblurring mechanism. However, for moving sinusoidal stripes, persistence without deblurring produces only a reduction of the perceived or recorded contrast, the outline, i.e. spatial frequency, being unchanged. So it seems that for this periodic target deblurring of the visual image does not take place, given the striking similarity between visual and photographic effects.

In so far as the band effect is a manifestation of blurring, this effect has a bearing on the question of where a moving deblurred image of a non-periodic target is actually seen in space. The band itself, whether visually perceived or photographically recorded, would be expected to have an appearance (orientation as well as contrast) that is dictated by the positions and relative intensities of the elementary patterns that go to make the integrated pattern. This is illustrated for the case of the rectangular exposure function. The stripes in the band would be expected to lie midway between their positions at the opening and closing of the shutter and this can be seen in the photographs. The band is lagging behind the final recorded position of the stripes. If the exposure function were to vary in time in a non-rectangular fashion e.g., increasing linearly with time, we would expect the resulting band to occupy a position that reflects this variation in weighting; a spatial averaging is reflected in the orientation. In so far as deblurring does not occur, we would expect the same for the visually perceived band as for the photographically recorded band. In fact, observers describe the band as 'lagging', and Babington-Smith (1964) called it 'oblique'. But lagging or oblique with respect to what? It transpires that the lag is referred to any markers, either black or white, associated with the central perpendicular to the stripes. If a line is placed perpendicularly across the centre of the stripes, the band will be seen to lie obliquely

with respect to it. If the marker were seen at its spatially averaged position, it ought to appear approximately parallel to the band. The fact that it leads so strikingly would be consistent with the deblurred marker's position being seen nearer to the leading edge of its own trail of persisting images.

It is, however, in the clinical field that the band effect may have the most useful application. In providing an immediate display of the complex temporal transfer function, the rotating pattern is virtually a temporal equivalent of the single contrast sensitivity grating of varying spatial frequency and contrast (Campbell and Robson, 1982). Preliminary investigations have already been made on a patient with a Snellen acuity of 6/6 in both eyes and with no symptoms other than a recently acquired distortion in the appearance of the position of moving objects. The band width was found in one eye to be approximately half that in the other, indicating a ratio of persistence times of approximately 2 to 1.

Unlike the Pulfrich effect (Rushton, 1975), the band effect provides a nice distinction between relative delays in the perception of the two monocular images caused by differing persistence times, and relative delays that are the result of differing conduction velocities. The former produce different monocular band widths in the two eyes, whereas the latter do not. The relative delay manifests itself simply as a rotation of one band with respect to the other: the binocular impression of the band represents the interference of the two patterns. On the assumption of a linear summation of the monocular images, there would be cosine striations of width  $2d/(\omega T_{del})$ . These striations would lie within the width of the monocular band whose edge is at  $x = 2dv_c/\omega$ , provided that the relative temporal delay  $T_{del} > 1/2v_c$ .

In the more likely event of the two eyes differing both in persistence times and in conduction velocities, the separate monocular patterns taken in conjunction with the binocularly perceived pattern will, by phasor addition, provide information on the differences in the conduction velocity. Should the combination of the two monocular images be substantially non-linear, a relative delay would still produce a visible interference in the structure of the separate monocular bands.

#### Acknowledgements

I am grateful to Professor F. W. Campbell for helpful discussion and advice, and to my colleague Dr J. L. Barbur for constant help and constructive criticism. This study was assisted by a grant from the Science and Engineering Research Council.

#### REFERENCES

- Babington-Smith, B. (1964). On the duration of the moment of perception. *Bull Br. Psychol. Soc.* 17, 27A.
- Barbur, J. L. (1980). Quantitative studies of some dynamic visual effects. *Perception* 9, 303-316.
- Bracewell, R. N. (1983). *The Fourier Transform and its Applications*. McGraw-Hill, Japan, pp. 13-18.
- Burr, D. (1980). Motion smear. *Nature* 284, 164-165.
- Campbell, F. W. and Robson, J. G. (1982). Printed by Nigel Durrant and Associates for Pilkington Optical and Ophthalmic Lenses.
- Dainty, J. C. and Shaw, R. (1974). *Image Science*. Academic Press, London, pp. 211-213.
- Morgan, M. J. (1980). Analogue models of motion perception. *Phil. Trans. R. Soc. Lond. B* 290, 117-135.
- Rushton, D. (1975). Use of the Pulfrich pendulum for detecting abnormal delay in the visual pathway in multiple sclerosis. *Brain* 98, 283-296.
- Steward, E. G. (1983). *Fourier Optics: An Introduction*. Ellis Horwood, Chichester, pp. 61-70.
- Wade, N. J. (1974). Some perceptual effects generated by rotating gratings. *Perception* 3, 169-184.

## APPENDIX 1: CONTRAST DISTRIBUTION ACROSS THE PATTERN

(a) *Summation of complex amplitudes*

*General impulse response  $f(t)$ .* Any point  $P(x, y)$  on the pattern has a velocity component perpendicular to the stripes given by  $\omega x$  (Fig. 1). At a given distance  $x$  from the centre of rotation, during the integration time  $T$ , the retina will record a series of elementary images approximating to those of a travelling sine wave profile whose luminance distribution is given by

$$L(y, t) = a + b \cos(2\pi y/(2d) - 2\pi vt),$$

where  $v = \omega x/(2d)$ , or the real part of

$$L(y, t) = a + b e^{i2\pi vt} e^{-i2\pi y/(2d)}.$$

Each interval of time  $dt$  provides a stimulus of complex amplitude  $b f(t) e^{i2\pi vt}$ . The resultant complex amplitude, assuming that summation can be performed over the integration time  $T$ , is  $b \int_0^T f(t) e^{i2\pi vt} dt$ . The contrast of the stationary pattern  $(L_{\max} - L_{\min})/(L_{\max} + L_{\min})$  is  $b/a$ , and the recorded contrast of the moving pattern  $(L'_{\max} - L'_{\min})/(L'_{\max} + L'_{\min})$  is  $(b/a) \int_0^T f(t) e^{i2\pi vt} dt$ , i.e.

$$C = C_0 \int_0^T f(t) e^{i2\pi vt} dt.$$

*Rectangular impulse response.* The resultant complex amplitude is

$$\begin{aligned} & b \int_0^T \frac{1}{T} \text{rect}\left(\frac{t}{T}\right) e^{i2\pi vt} dt \\ &= b \left| \frac{e^{i2\pi vt}}{i2\pi vT} \right|_0^T \\ &= b e^{i\pi vT} \frac{e^{i\pi vT} - e^{-i\pi vT}}{i2\pi vT} \\ &= b e^{i\pi vT} \frac{\sin(\pi vT)}{\pi vT}. \end{aligned}$$

If we choose the phase origin to be at time  $T/2$ , we have a resultant complex amplitude of  $b \sin(\pi vT)/\pi vT$ . (Note that the area under the impulse response is taken as unity; hence the factor  $T$ .) The time-averaged travelling wave is therefore given by

$$L'(y, t) = a + b \frac{\sin(\pi \omega x T/(2d))}{\pi \omega x T/(2d)} \cos 2\pi(\omega x t/(2d) - y/(2d)).$$

The contrast of the stationary pattern  $C_0$  is  $b/a$ , and the recorded contrast of the moving pattern is

$$C = C_0 \frac{\sin(\pi \omega x T/(2d))}{\pi \omega x T/(2d)}.$$

(b) *Fourier analysis—varying temporal frequency and fixed temporal spread function*

*General impulse response  $f(t)$ .* In this approach we consider the rotating pattern as providing a temporally varying input luminance at any point on the retina or film, given by

$$L(t) = a + b \cos(2\pi vt),$$

where  $v$  is the temporal frequency given by  $\omega x/(2d)$  and  $\omega x$  is the perpendicular velocity. The input modulation  $M_{\text{in}} = (L_{\max} - L_{\min})/(L_{\max} + L_{\min}) = b/a = C_0$ , the contrast of stationary stripes. The temporally varying output  $L'(t)$  will simply be the input convolved with the temporal spread or exposure function  $f(t)$ , i.e.

$$\begin{aligned} L'(t) &= L(t) * f(t) \\ &= (a + b \cos(2\pi vt)) * f(t) \\ &= a + M(v) b \cos(2\pi vt + \phi(v)), \end{aligned}$$

where  $M(v)$  and  $\phi(v)$  are the modulus and phase of the visual transfer function, i.e.  $F(v) = M(v)e^{-i\phi(v)}$  (e.g., Dainty and Shaw, 1974). The output is sinusoidal and has the same frequency as the input. The output modulation is

$$M_{\text{out}} = \frac{L'_{\text{max}} - L'_{\text{min}}}{L'_{\text{max}} + L'_{\text{min}}} = M(v)M'_{\text{in}}.$$

Therefore

$$C = M(v)C_0.$$

*Rectangular impulse response.* Let the impulse have duration  $T$ , i.e.

$$f(t) = \frac{1}{T} \text{rect}\left(\frac{t}{T}\right).$$

Then

$$\begin{aligned} M(v) &= \frac{\sin(\pi v T)}{\pi v T} \\ &= \frac{\sin(\pi \omega x T / (2d))}{\pi \omega x T / (2d)}. \end{aligned}$$

Therefore

$$C = C_0 \frac{\sin(\pi \omega x T / (2d))}{\pi \omega x T / (2d)}.$$

(c) *Fourier analysis—fixed spatial frequency and varying spatial spread function*

*Rectangular impulse response.* Let the impulse have duration  $T$ , i.e.

$$f\left(\frac{y}{\omega x}\right) = \frac{1}{\omega x T} \text{rect}\left(\frac{y}{\omega x T}\right),$$

where the temporal impulse response function is scaled by the velocity. Then

$$M(u\omega x) = \frac{\sin(\pi u\omega x T)}{\pi u\omega x T}.$$

Therefore

$$C = C_0 \frac{\sin(\pi \omega x T / (2d))}{(\pi \omega x T / (2d))}.$$

## 2.4 THEORETICAL ANALYSIS OF THE 'BAND EFFECT' SEEN UNDER STROBOSCOPIC ILLUMINATION

### 2.4.1 Introduction to Paper 2: **Rotating stripes and the impulse response of the eye: Stroboscopic illumination**

This second paper deals with the effect perceived when the rotating striped pattern is stroboscopically illuminated. This results in multiple parallel bands being seen across the rotating stripes, with each band appearing to rotate about its own centre. The paper analyses the effect and shows how stroboscopic lighting can be thought of as sampling the temporal impulse response function in the same way as the slits in a diffraction grating sample the aperture.

In the case of a diffraction grating, increasing the number of slits in a fixed size grating (thereby decreasing the slit separation) results in each of the multiple diffraction patterns remaining the same size, but appearing further apart, whereas keeping the slit separation fixed and increasing the number of slits (thereby making a diffraction grating of increasing size) results in the individual patterns decreasing in size, but remaining in the same place. When the rotating pattern is photographed under stroboscopic illumination, increasing the flash rate with a fixed shutter time produces bands that are further apart, but keeping a fixed flash rate and increasing the shutter time results in fixed position bands of decreasing width. Figure 2.11 shows the striking analogy between 'band' patterns and diffraction patterns; Figure 2.12 shows the multiple bands in greater detail. Even the secondary bands associated with a diffraction grating can be identified!

The relationship between the sampling rate and the resulting quality of apparent motion is also discussed in the paper.

### 2.4.2 Paper 2

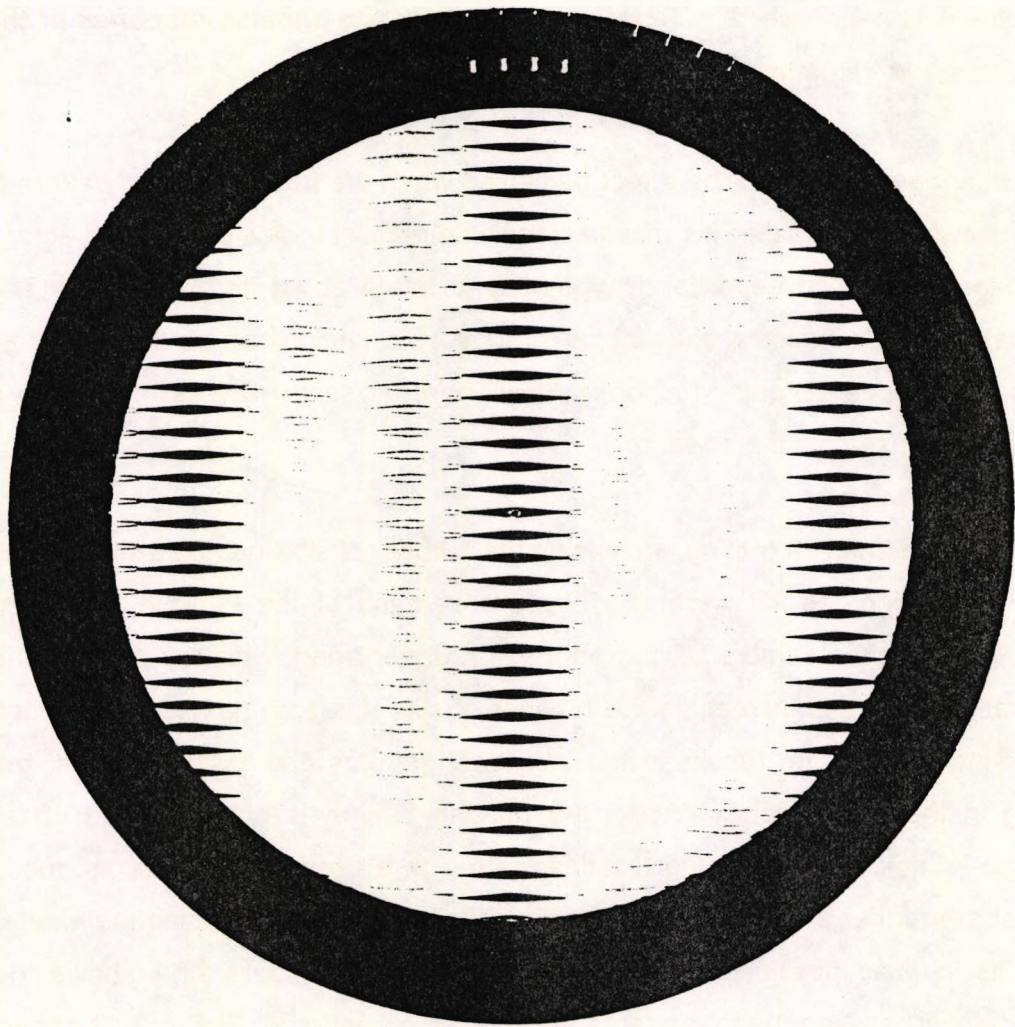


Figure 2.11: Photograph of a stroboscopically illuminated grating, rotating slowly at  $3.28 \text{ rad.s}^{-1}$ . A marker on the pattern illustrates its locations at the moment of exposures. The overall exposure time  $T = 81 \text{ ms}$  and the flash interval  $T_{\text{del}} = 20 \text{ ms}$ . This results in 4 flashes during the exposure time. The contrast distribution across the pattern can be seen to be analogous to the amplitude distribution across a Fraunhofer diffraction pattern across a 4 slit grating. Note the  $(N-2)$  secondary bands of alternating phase lying between the principal bands.

## Rotating stripes and the impulse response of the eye: II. Stroboscopic illumination

JANET E. WOLF

*Department of Optometry and Visual Science, The City University, London EC1V 0HB*

Received 23 September 1986; revised 31 March 1987; accepted 29 July 1987

**Abstract**—The visual effect perceived when a rotating sinusoidally striped pattern is viewed under stroboscopic illumination consists of a band of relatively high contrast repeated at intervals across the pattern. On the basis of a previous linear model (Wolf, J. E., 1987, *Spatial Vision*, Vol. 2, pp. 199–211), the contrast distribution is shown to correspond to the Fourier transform of the temporally sampled impulse response of the eye, the stroboscopic illumination providing such a sampling. The analysis uses the analogy of these perceived contrast effects with the amplitude distribution in a Fraunhofer diffraction pattern established earlier (Wolf, 1987), and in this situation the stroboscopic illumination temporally samples the impulse response of the eye in the same way that the slits sample the 'aperture function' in a diffraction grating.

### INTRODUCTION

Babington-Smith (1964) first noted that the effect of stroboscopic illumination on a rotating striped pattern was to produce a visual effect that was quite different from the effect obtained with uniform illumination. Uniform illumination gives rise to the appearance of a central band of clearly resolved stripes, lagging slightly behind the perpendicular to the stripes and moving around with the whole pattern, whereas stroboscopic illumination gives rise to a series of these bands, parallel to one another, of approximately equal width and spaced at intervals across the grating. Wade (1974) noted that the number of bands depended on the flash rate for a given angular velocity. Further inspection reveals two additional characteristics. First, as the stroboscopic flash rate increases and these bands are spaced further apart (so that there are fewer across the pattern) they nevertheless retain the same width. Second, the appearance of each of these multiple bands is approximately the same as the appearance of the single central band associated with uniform illumination in both width and internal structure.

For uniform illumination of the pattern, the effect was analysed in terms of the integration of the continuous trail of persisting images (Wolf, 1987). Similarly, the discrete images resulting from the stroboscopic illumination, each displaced in space and time, are assumed to be integrated by the eye, the relative strengths of the elementary images following the form of the temporal impulse response. The equivalence with still photographs, where the images are integrated over the exposure time, is also assumed, and implies that the temporal impulse response and the camera exposure function are of the same form.

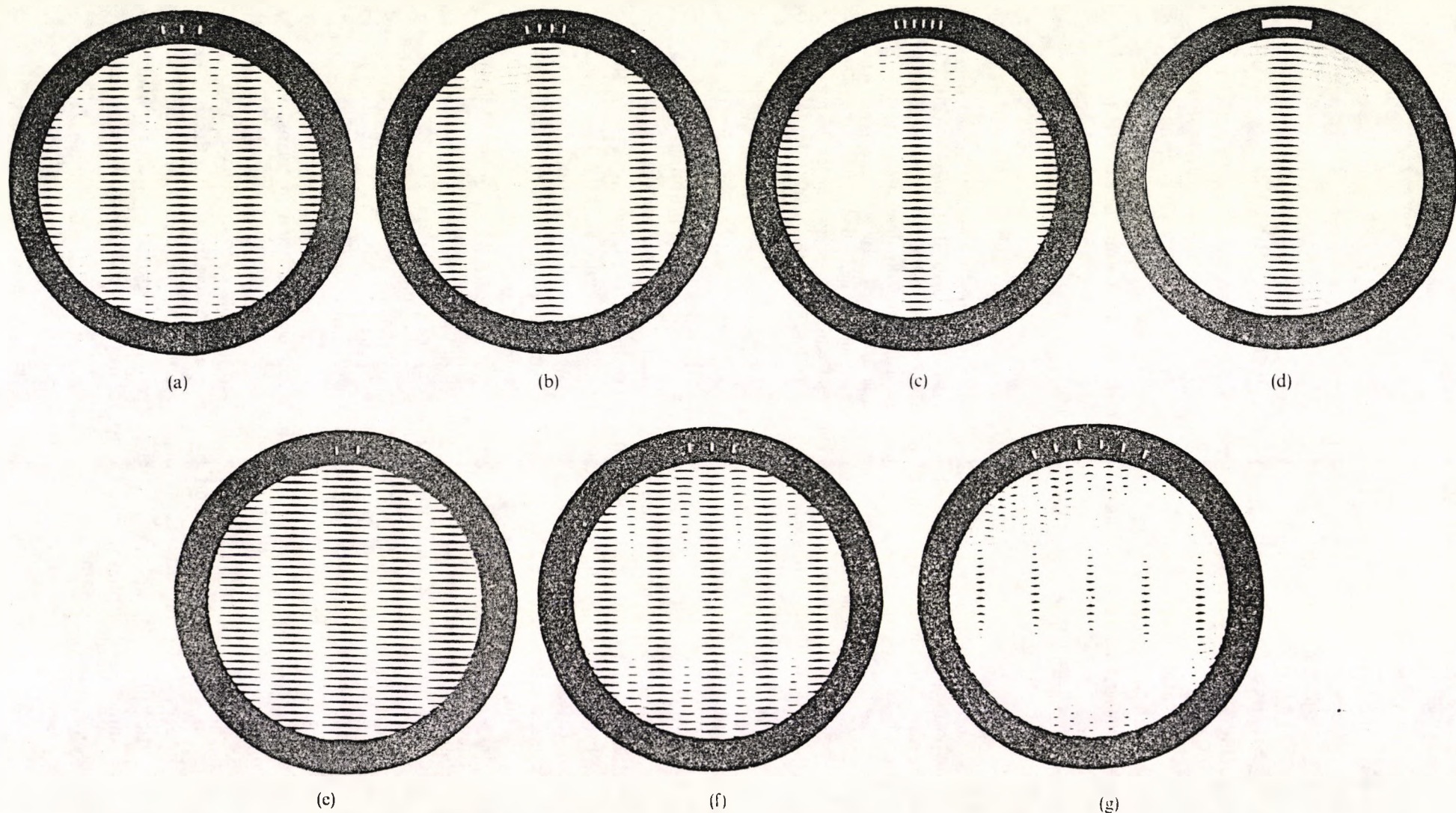


**Figure 1.** Photographs of the stroboscopically illuminated stripes moving with a constant angular velocity  $\omega$ . A marker on the pattern illustrates its locations at the moments of exposure. If the exposure time  $T$  is kept fixed (100 ms in (a)–(d)) and the flash interval  $T_{del}$  is gradually decreased (34, 25, 17.0 ms in (a)–(d)) so that the product of the number of flashes recorded and the flash interval is constant, we have constant-width bands each similar to (d), the band associated with a uniform exposure of  $T$ , but appearing at increasing separations. The exposure function is sampled by the flashes in the same way that a diffraction grating has its overall aperture function sampled by the slits. The contrast distribution across the pattern is thus analogous to the amplitude distribution in the pattern of the grating. However, if the flash interval is fixed ( $T_{del} = 40$  ms in (e)–(g)) and the exposure time is varied ( $T = 80, 120, 240$  ms in (e)–(g)), the bands remain in the same position but decrease in width. This is comparable to the diffraction pattern obtained with a grating of fixed slit-separation and increasing overall aperture.

### PHOTOGRAPHIC DEMONSTRATIONS

To demonstrate the essential features of the effect for an eye with an idealized rectangular impulse response, a rectangular camera exposure function was used, but this time with stroboscopic illumination. Two types of photograph were taken. The first type was one in which the angular speed and the exposure time was fixed whilst the flash rate of the stroboscopic illumination was varied. Figure 1(a), (b) and (c) show the effect of increasing the flash rate, whereas Fig. 1(d) shows the corresponding pattern with uniform illumination but with the same angular velocity and overall exposure time. The angle of rotation can be seen from the marks on the border which in the case of stroboscopic illumination are shown as a series of small lines, spreading over an angle governed by the angular speed and the shutter opening time, the number of marks indicating the number of flashes captured in that given exposure time. In the case of the uniform exposure the marks appear simply as a smear of the same angular spread and can be thought of as corresponding to an infinite flash rate.

Corresponding closely with the visual effects perceived, the photographs show that, for increasing flash rates, the high contrast bands retain the same width but are separated by distances that vary inversely with the flash rate. They also show that the bands are of the same form as the single band associated with uniform illumination. In addition, between these bands of maximum contrast there are some fainter bands, not observed by the real eye. For photographs involving  $N$  flashes, there appear to be  $N-2$  secondary bands between the principal bands, the phases of these adjacent bands being reversed (i.e. a dark stripe in one band is adjacent to a white stripe in the neighbouring band).

The second type of photograph involved fixing the angular velocity and the flash rate and varying the exposure time. Figure 1(e), (f) and (g) show the effect of increasing the exposure time which in turn increased the number of flashes captured in each exposure. In these photographs, the bands remain centred at fixed separations, but as the total exposure increased, the width of the bands decreased. With regard to the corresponding visual effect, increasing the exposure time amounts to increasing the integration time of the eye, which might be achieved in practice by altering the adaptation level.

### ANALYSIS OF THE STROBOSCOPIC EFFECT

At a distance  $x$  measured along the stripes from the centre of rotation (the origin of the  $x$  and  $y$ -axes), the velocity perpendicular to the stripes is given by  $\omega x$  for an angular velocity  $\omega$ . It is this component that affects the contrast, whether by a continuous smear or the summation of discrete persisting images; movement along the direction of the stripes has no effect on this perceived contrast. Since this perpendicular velocity increases proportionally with the distance  $x$  from the centre of rotation, the separation of the discrete images increases linearly with  $x$ .

If we again simplify the situation and consider the profile of the stripes to be sinusoidal, the recorded profile will still be sinusoidal and of the same spatial frequency but with an amplitude (or contrast) that is modified by the phase of the successive discrete images. The resulting contrast of the stripes for that given value of  $x$  can be established simply by considering each discrete image to be a sinusoidal travelling wave pattern whose complex amplitude is described by a phasor, the modulus of this complex amplitude representing the actual contrast and the phase representing the displacement between successive images. Appendix 1a shows that by summing these complex amplitudes over the persistence time of the eye or the exposure time of the

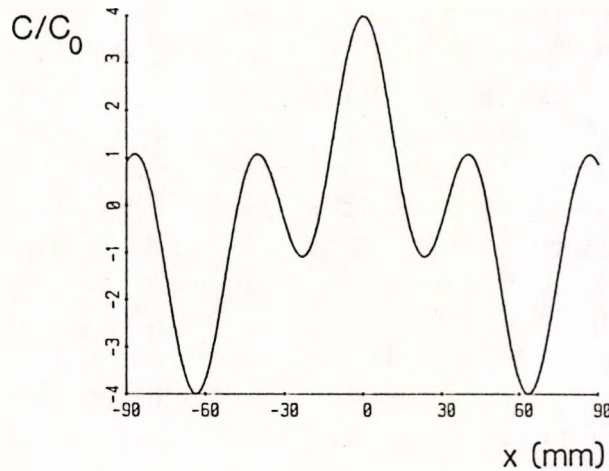


Figure 2. Perceived contrast distribution across the rotating pattern according to the function

$$\frac{C}{C_0} = \frac{\sin(\pi\omega x \bar{T}) \sin(\pi\omega x N T_{del}/(2d))}{\pi\omega x \bar{T} \sin(\pi\omega x T_{del}/(2d))}$$
 illustrated for the parameter values shown in Fig. 1(b) where angular velocity  $\omega = 3.28 \text{ rad s}^{-1}$ , duration of flash  $\bar{T} = 10 \mu\text{s}$ , flash interval  $T_{del} = 25 \text{ ms}$ , and number of flashes in the exposure  $N = 4$ .

camera we obtain an expression for the perceived or recorded contrast  $C$  across the pattern thus

$$C = C_0 \frac{\sin(\pi\omega x \bar{T}/(2d)) \sin(N\pi\omega x T_{del}/(2d))}{\pi\omega x \bar{T}/(2d) \sin(\pi\omega x T_{del}/(2d))}, \quad (1)$$

where  $C_0$  is the contrast at  $x = 0$ , i.e. the value of the perceived contrast of the same pattern when it is stationary;  $\bar{T}$  represents the duration of the flash, and  $T_{del}$  represents the time interval between flashes. Figure 2 illustrates Equation (1) and has used the particular values of the parameters that correspond to Fig. 1(b) in which  $N = 4$  flashes are captured during the exposure time. Equation (1) predicts the appearance of the repeating parallel bands separated by distances of  $2d/(\omega T_{del})$  and each of width (up to the position of first zero contrast) of  $4d/(\omega N T_{del})$  or  $4d/(\omega \bar{T})$ . Hence the photographs involving a fixed exposure time ( $N T_{del} = \text{constant}$ ) as shown in Fig. 1(a)–(c) show bands whose separation varies inversely with  $T_{del}$ , the width of the bands remaining constant because  $N T_{del}$  is constant. However, the photographs involving a constant flash rate ( $T_{del}$  fixed) but varying exposure ( $N T_{del}$ ) result in a series of bands centred at fixed positions but of widths varying inversely with  $N$  as shown in Fig. 1(e), (f), and (g).

The appearance of secondary bands of alternating phases can also be predicted from Eq. (1), again illustrated in Fig. 2. The numerator  $\sin(N\pi\omega x T_{del}/(2d))$  falls to zero more frequently than the denominator  $\sin(\pi\omega x T_{del}/(2d))$  giving  $N - 1$  additional minima between the principal maxima and  $N - 2$  secondary maxima. The alternating phases of all adjacent bands illustrated in Fig. 2 manifest themselves in the photographs by the stripes in any one band being shifted through half a cycle with respect to those in the adjacent bands.

#### THE DIFFRACTION ANALOGY

The phenomenon of the repeating bands can be predicted very simply from the diffraction analogy established by Wolf (1987). The distribution of the perceived

contrast  $C$  across the rotating pattern represents the temporal frequency response of the system in the same way that the distribution of the amplitude  $A$  across a Fraunhofer diffraction pattern displays the spatial frequency content of the aperture function. The flashing light can now be considered to be sampling the camera exposure function or impulse response in the same way that the slits can be considered to be sampling the aperture function in a diffraction grating. Hence the corresponding expressions for the amplitude  $A$  and the perceived contrast  $C$  of the sampled rectangular functions apply:

$$A = A_0 \frac{\sin((\pi a \sin \theta)/\lambda) \sin((\pi N D \sin \theta)/\lambda)}{(\pi a \sin \theta)/\lambda \sin((\pi D \sin \theta)/\lambda)} \quad (2)$$

$$C = C_0 \frac{\sin(\pi \omega x \bar{T}/(2d)) \sin(\pi \omega x N T_{\text{del}}/(2d))}{\pi \omega x \bar{T}/(2d) \sin(\pi \omega x T_{\text{del}}/(2d))} \quad (3)$$

Here we see the analogy between the effects on contrast of either decreasing the stroboscopic flash interval or increasing the overall exposure function and the corresponding diffraction effects. Decreasing the slit separation ( $D$ ) in a fixed size diffraction grating results in the various orders moving apart whereas increasing the size of the grating for a fixed slit separation leaves the position of the principal maxima unchanged but narrows the separate orders. Also, as with the contrast patterns, there are  $N - 2$  secondary maxima between the principal maxima.

The equivalence between the stroboscopically illuminated travelling wave profile and light passing through a diffraction grating may also be appreciated qualitatively. The grating may be thought of as an aperture that has been blocked off in strips, the slit apertures sampling this overall aperture at regular intervals. The wavetrains of light emerging from the individual slit apertures reinforce each other for certain angles, cancel at other angles, and so on, resulting in the well-known repeating amplitude distribution. It is common to think of this distribution as representing the spatial spectrum of the *sampled* aperture function. The unsampled or open aperture would produce its own particular amplitude distribution representing the spatial spectrum of that particular aperture. Provided that this spectrum is 'band-limited' (i.e. the pattern does not extend indefinitely) and provided that the sampling interval or slit separation is sufficiently fine for the repetitions not to overlap, the repeating patterns are identical with the unsampled version. In the case of an overall rectangular aperture, the spectrum is not strictly band-limited; the sinc function spreads to infinity, so the repeating function is not quite identical to that of an unsampled aperture, and follows the form of Eq. (1).

For rotating stripes viewed by an eye with a general (as opposed to a rectangular) impulse response  $f(t)$ , the spectrum of the sampled function  $f_s(t)$ , which is reflected in the perceived contrast distribution across the pattern, is given (see Appendix 1(b)) by

$$C = C_0 [F(v) * \text{comb}(v T_{\text{del}})] \frac{\sin(\pi v \bar{T})}{\pi v \bar{T}}, \quad (4)$$

where  $v = \omega x/(2d)$ . The convolution of  $F(v)$  with the comb function gives a repeating contrast pattern with the principal maxima at values separated by the distance  $x_s = 2d/(\omega T_{\text{del}})$ . The displacements of the pattern over the intervals  $T_{\text{del}}$  are multiples of  $2d$ , and so the motion is effectively frozen at these positions. The envelope  $\sin(\pi v \bar{T})/(\pi v \bar{T})$  results from the non-zero duration  $\bar{T}$  of the flashes.

The manner in which the separation of these bands varies inversely with flash

interval fits well with the visually observed effects recorded by Wade (1974). However, the separations, of  $2d/(\omega T_{del})$ , are independent of the temporal characteristics of the eye and simply reflect the positions of frozen motion.

With uniform illumination, the contrast distribution represents the temporal frequency response of the system and hence the edge of the band corresponds to the cutoff frequency  $\nu_c$ . The magnitude of the distance from the centre is given by  $x_c = 2d\nu_c/\omega$ . Provided that there is such a cutoff frequency (i.e. the impulse response is band-limited) and provided also that the flash interval is sufficiently short for the bands not to overlap ( $x_s \geq 2x_c$ ), the repeating patterns will be identical with the unsampled version. For this the flash-frequency  $\nu_s$  would have to be such that  $\nu_s \geq 2\nu_c$ . This can also be thought of as providing a sampling interval of the temporal impulse response function that is finer than the Nyquist interval. A flash frequency of  $\nu_s < 2\nu_c$  results in an overlap of bands (e.g., Bracewell, 1983), the physical meaning of which is examined below.

#### DISCUSSION

The sampling action of stroboscopic light can be considered in two quite distinct ways: (a) as temporally sampling the moving target, the resulting image being processed according to the temporal impulse response of the eye or uniform camera exposure; or (b) as sampling the impulse response or exposure function, this modified function then filtering the moving target that is taken to be uniformly illuminated. The implications of both of these approaches will be examined as much work has been done on apparent motion using the former, whereas the latter is particularly appropriate in investigating the impulse response of the eye.

In the first approach, any point on the retina at a given distance  $x$  from the centre of rotation, and which under uniform illumination would be subjected to a 'true' temporal frequency  $\nu$ , would experience an input that, as a consequence of the sampling of the temporal variations, consists of a series of discrete temporal frequencies

$$\{\nu + n\nu_s\}, \quad -\infty < n < \infty,$$

where  $n$  is integral and  $\nu_s$  is the flash rate. Assuming  $\nu_s \geq 2\nu_c$  (i.e. the bands do not overlap), the regions that correspond to the repeated bands that would be unresolved under uniform illumination are seen as resolved as a consequence of the 'true' temporal variation being under-sampled. For each  $|\nu + n\nu_s| < \nu_c$ ,  $-\infty < n < \infty$ , these temporal modulations are visible. This approach has a physical reality in that the temporal variations have been slowed and are seen as such by the eye whose 'temporal window' (Watson *et al.*, 1983) has been unaffected by the flashing light.

In the second approach, the action of the stroboscopic light physically results in an input consisting of a series of images displaced in space and time, each spatial displacement being  $\omega x/\nu_s$ . This is formally equivalent to the pattern being convolved with a sampled impulse response that has been scaled for velocity. Thus, in this spatial approach, the appearance at this same distance  $x$  that would be blurred under uniform illumination (i.e. where the spatial smear is too great for the particular spatial frequency) becomes resolvable because the stripes are now smoothed only by a sampled spread function. In effect, the sampling of the spatial smear or spread function produces a repeating set of 'spatial windows', the perceived spatial frequency of the target remaining unchanged. In a physically meaningful way we can consider either a sampled temporal variation to be convolved with an unsampled temporal impulse response, or

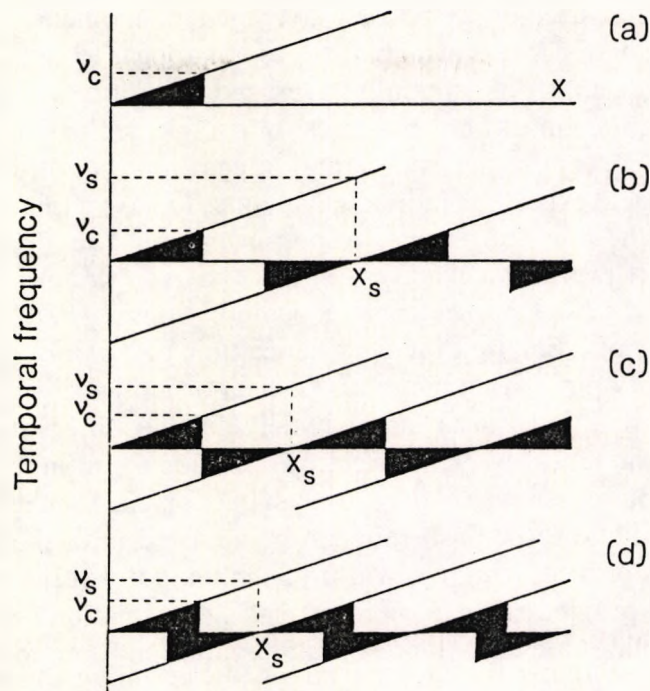


**Figure 3.** (a) Display of the temporal frequencies (plotted as a function of  $x$ ) that are presented to the eye by the rotating pattern illuminated with uniform light; (b), (c) and (d) display the additional frequencies that result from temporal sampling. In (b) and (c),  $\nu_s \geq 2\nu_c$ , so that for any value of  $x$ , there is never more than one temporal frequency lying within the temporal window of limit  $\nu_c$ . In (d),  $2\nu_c > \nu_s > \nu_c$ , so that there are ranges of  $x$  for which there are two conflicting frequencies. In these ranges there is no apparent smooth motion.

an unsampled spatial variation to be convolved with a sampled scaled impulse response.

Figure 3 illustrates the relationship between the two approaches. The 'adequate' sampling of the impulse response function resulting in separated bands is demonstrated in Fig. 3(b) and (c) where  $\nu_s \geq 2\nu_c$ . The same diagram illustrates the undersampling of the temporal variations associated with the repeat bands, the undersampling producing at any one position  $x$  a series of discrete frequencies only one of which is not filtered out. Figure 3(d) illustrates undersampling of the impulse-response function ( $\nu_s < 2\nu_c$ ) in which the bands overlap; within this overlap region the undersampling of the temporal variations results in two simultaneously perceived, conflicting (i.e. opposite sign) temporal frequencies corresponding to two sinusoidal waves travelling at different speeds in opposite directions. It is at these low flash rates that the visual impression is one in which there appear to be residual nuclei of bands continuing to rotate, separated by regions in which the motion has broken down into a flickering-jumble. It seems that smooth apparent motion survives over regions where there is only one visible frequency, but breaks down in the overlap region where there are conflicting messages.

A related feature of interest is the visual appearance under stroboscopic illumination of a thin line marker fixed centrally and perpendicular to the stripes. It is seen as a fan of radial lines. Wolf (1987) discussed the appearance under uniform illumination of such a marker. There, the line marker appeared as a single deblurred line consistent with the deblurring described by Burr (1980). The orientation of the band appeared to lag behind the line, suggesting that the deblurred line was being seen nearer to its leading

edge, since the band itself is a spatially averaged phenomenon. However, under stroboscopic illumination, the central band does not appear to lag, suggesting that the marker is being seen at its spatially averaged position. At greatly increased stroboscopic rates, the fan of lines collapses to a single deblurred marker.

Using the same concept of persistence and integration that underlies the whole of this analysis, we would expect the individual fan lines to have a relative brightness that reflects the form of the temporal impulse-response function. The effect *does* appear to be one in which there is a variation in line brightness, the stronger lines being nearer to the leading edge and the fainter ones trailing behind. Allport (1970) used this 'radius display' as a means of estimating the persistence time or 'span of simultaneity', even though he was of the opinion that there was no clear ordering of brightness in the lines. However, he conceded that it was "an extremely difficult observation to make".

To summarize, the repeating band effect can provide a continuous monitor of the sampling of the impulse response of the eye when phenomena such as the radial display are observed. In addition, the flash rate can be adjusted until the bands abut, thus providing a means of measuring the width of the temporal transfer function. More generally, the effect provides a means of investigating the relation between the impulse response, the sampling rate, and the resulting apparent motion, for a pattern of any given spatial frequency.

#### *Acknowledgements*

I am grateful to Professor F. W. Campbell for helpful discussions and advice, and to my colleague Dr J. L. Barbur for constant help and constructive criticism. Some of the equipment used in this investigation was provided by a grant from the Science and Engineering Research Council.

#### REFERENCES

- Allport, D. A. (1970). Temporal summation and phenomenal simultaneity: Experiments with the radius display. *Q. Jl. exp. Psychol.* **220**, 686-701.
- Babington-Smith, B. (1964). On the duration of the moment of perception. *Bull. Br. Psychol. Soc.* **17**, 27A.
- Bracewell, R. N. (1983). *The Fourier Transform and its Applications*. McGraw-Hill, Japan, pp. 189-202.
- Burr, D. (1980). Motion smear. *Nature* **284**, 164-165.
- Dainty, J. C. and Shaw, R. (1974). *Image Science*. Academic Press, London, pp. 211-213.
- Steward, E. G. (1983). *Fourier Optics: An Introduction*. C. Grey Morgan (Ed.). Ellis Horwood, Chichester, pp. 67-70.
- Wade, N. J. (1974). Some perceptual effects generated by rotating gratings. *Perception* **3**, 169-184.
- Watson, A. B., Ahumada Jr., A. J. and Farrell, J. (1983). The window of visibility: a psychophysical theory of fidelity in time sampled visual displays. NASA Technical Paper, No. 2211. Ames Research Center, Moffett Field, California 94035.
- Wolf, J. E. (1987). Rotating stripes and the impulse response of the eye: 1. Uniform illumination. *Spatial Vision* **2**, 199-211.

#### APPENDIX 1 CONTRAST DISTRIBUTION ACROSS THE PATTERN FOR STROBOSCOPIC ILLUMINATION

##### *(a) Summation of complex amplitudes*

*Rectangular impulse response.* At any given distance  $x$  from the centre of rotation, the pattern of stripes (considered here to have a sinusoidal intensity profile) provides in effect a sinusoidal wave travelling with a velocity  $\omega x$  perpendicular to the stripes. The illumination of this travelling wave is a succession of

discrete flashes, each considered to be of zero duration and time interval  $T_{\text{dec}}$ . The modification for flashes of non-zero duration will be considered later. The underlying retina or film will record the succession of these images that occur during the overall integration time (or exposure time), each image being displaced in space by a distance  $\omega x T_{\text{dec}}$ . We consider the stationary pattern to have a luminance profile at time  $t = 0$  of

$$L(y) = a + b \cos(2\pi y/(2d)),$$

and each of the successive images to be displaced in phase spatially by an amount  $\delta$  such that  $\delta = 2\pi\omega x T_{\text{dec}}/(2d)$ . The contrast of each stationary image would be given by

$$C_0 = \frac{L_{\text{max}} - L_{\text{min}}}{L_{\text{max}} + L_{\text{min}}} = \frac{b}{a}.$$

Each elementary image may be considered to have a complex amplitude of  $b e^{-in\delta}$ . Summing the complex amplitudes over the total number of flashes  $N$  gives the resultant complex amplitude which is

$$\begin{aligned} & \sum_{n=0}^{N-1} b e^{-in\delta} \\ &= b(1 + e^{-i\delta} + \dots + e^{-i(N-1)\delta}) \\ &= b \frac{1 - e^{-iN\delta}}{1 - e^{-i\delta}} \\ &= b \exp[-i(N-1)\delta/2] \frac{\sin(N\delta/2)}{\sin(\delta/2)} \\ &= b \exp[\underbrace{-i\pi(N-1)\omega x T_{\text{dec}}/(2d)}_{\text{phase}}] \frac{\sin(N\pi\omega x T_{\text{dec}}/(2d))}{\sin(\pi\omega x T_{\text{dec}}/(2d))}. \end{aligned} \quad (\text{A1})$$

If we consider the phase origin to be at time  $T/2$  and take the number of flashes to be  $N = 2M + 1$ , symmetrically displaced about the phase origin, the resultant complex amplitude is

$$\begin{aligned} & b \sum_{n=-M}^{+M} e^{-in\delta} \\ &= b \frac{\sin(N\delta/2)}{\sin(\delta/2)} \\ &= b \frac{\sin(N\pi\omega x T_{\text{dec}}/(2d))}{\sin(\pi\omega x T_{\text{dec}}/(2d))}. \end{aligned}$$

The linear phase shift present in Eq. A1 amounts to a displacement in  $y$  that is proportional to  $x$ , which simply corresponds to a rotation of the overall pattern. Selecting a phase origin that is central for a rectangular impulse response results in the simpler expression. Hence the recorded luminance profile is given by

$$L'(y) = a + b \frac{\sin(N\pi\omega x T_{\text{dec}}/(2d))}{\sin(\pi\omega x T_{\text{dec}}/(2d))} \cos(\pi y/d).$$

The recorded contrast

$$\begin{aligned} C &= \frac{L'_{\text{max}} - L'_{\text{min}}}{L'_{\text{max}} + L'_{\text{min}}} \\ &= \frac{b \sin(N\pi\omega x T_{\text{dec}}/(2d))}{a \sin(\pi\omega x T_{\text{dec}}/(2d))} \\ &= C_0 \frac{\sin(N\pi\omega x T_{\text{dec}}/(2d))}{\sin(\pi\omega x T_{\text{dec}}/(2d))}. \end{aligned}$$

The individual complex amplitudes of the component phasors may be modified to take account of the non-

zero duration  $\bar{T}$  of the separate flashes (assumed rectangular in form). Each flash by itself would give rise to a contrast distribution.

$$C = C_0 \frac{\sin(\pi\omega x \bar{T}/(2d))}{\pi\omega x \bar{T}/(2d)}$$

(Wolf, 1987). Hence the modified contrast distribution would be given by

$$C = C_0 \frac{\sin(\pi\omega x \bar{T}/(2d)) \sin(N\pi\omega x T_{del}/(2d))}{\pi\omega x \bar{T}/(2d) \sin(\pi\omega x T_{del}/(2d))}$$

(b) *Fourier analysis—fixed spatial frequency, varying spatial spread function  $f(y/\omega x)$*

As assumed in (a), the input is represented by

$$L(y) = a + b \cos(2\pi u y)$$

where  $u = 1/(2d)$ . The output  $L'(y)$  is obtained by convolving the input with the *sampled* spread function,

$$\begin{aligned} L'(y) &= L(y) * f_s\left(\frac{y}{\omega x}\right) \\ &= a + M(u\omega x) b \{\cos(2\pi u y + \phi(u\omega x))\}, \end{aligned}$$

where  $M(u\omega x)$  and  $\phi(u\omega x)$  are the modulus and phase of the OTF of the sampled spread function (see Dainty and Shaw, 1974). Taking account of the non-zero flash duration  $\bar{T}$ , the sampled spread function is given by

$$f_s\left(\frac{y}{\omega x}\right) = \left\{ f\left(\frac{y}{\omega x}\right) \frac{1}{\omega x T_{del}} \text{comb}\left(\frac{y}{\omega x T_{del}}\right) \right\} * \left\{ \frac{1}{\omega x \bar{T}} \text{rect}\left(\frac{y}{\omega x \bar{T}}\right) \right\},$$

which leads to an OTF of

$$F_s(u\omega x) = F(u\omega x) * \left\{ \text{comb}(u\omega x T_{del}) \frac{\sin(\pi u\omega x \bar{T})}{\pi u\omega x \bar{T}} \right\}.$$

Hence the perceived contrast is given by

$$C = C_0 \left[ F(v) * \left\{ \text{comb}(v T_{del}) \frac{\sin(\pi v \bar{T})}{\pi v \bar{T}} \right\} \right]$$

which is a repeating pattern of interval  $x_s = 2d/(\omega T_{del})$ , each pattern corresponding to the spectrum  $F(v)$  of the general impulse response  $f(t)$  (e.g., Bracewell, 1983, p. 193).

## CHAPTER 3: THE COMPLEX 'BAND'

### 3.1 INTRODUCTION

Psychophysics has shown there to be at least two distinct spatio-temporal channels and these have been described in some depth in Section 1.3.1; a channel with sustained, low pass characteristics cutting off at lower temporal frequencies and a transient band pass channel with a higher cut-off frequency. This third paper interprets the appearance of the 'inner' and 'outer' bands in terms of the linearity, chromatic characteristics and the interaction of two frequency-tuned channels.

The characteristics of the two bands are very different. The inner band or Zone 1 is of high contrast, lags behind the band as a whole and cuts off at a low temporal frequency. The flanking or 'outer' band is of low contrast, cuts off at a higher temporal frequency, has a fragmented quality and appears to be 'frequency doubled'. This region is called Zone 2. Beyond that lies Zone 3. Perhaps the most interesting difference between Zone 1 and Zone 2 is that when the whole rotating disc is illuminated by a pale desaturated coloured light (e.g. Lee filter 106 'primary red'), the whites of Zone 1 take up the colour of the illuminant, as does Zone 3. The whites of Zone 2 remain white. The loss of perceived colour associated with one of the channels over the particular frequency range in which the other channel is active indicates a suppression of one by the other. This is not a new idea. It has already been suggested by Tolhurst (1975), Anderson and Burr (1985) and Breitmeyer and Ganz (1976) as a possible explanation for some of their data, that the activity of the transient channel can suppress that of the sustained channel. It should be emphasised that the word 'zone' is reserved for a particular region on the pattern which corresponds to a particular frequency range. It should not be confused with the word 'channel' as more than one channel could be contributing to the appearance of a particular 'zone'. In practice, the boundary of Zone 1 is taken to reflect the cut-off of the sustained channel as any activity extending into the frequency range of Zone 2 which is subsequently suppressed is only of academic interest. The boundary of Zone 2 identifies the edge of the transient channel.

The arguments for the parvocellular pathway providing the physiological substrate of the more sustained chromatic channel, concerned also in signalling high contrast achromatic stimuli of high spatial and low temporal frequency, and with the magnocellular pathway having a major role in signalling achromatic stimuli with a

higher temporal frequency content, have been discussed extensively in Section 1.3.2. The two pathways seem likely contenders for mediating the two zones. It might seem that the low temporal cut-off frequency of Zone 1 is inconsistent with the activity of the P-cells. However, the apparent suppression of the output of the parvocellular pathway over the higher temporal frequency range has been ascribed to a cortical filter (Lee et al. 1989), leaving the achromatic magnocellular pathway in sole charge over that frequency range. This would, in addition, account for the loss of colour in Zone 2.

Whilst it is the apparent suppression of the high temporal frequency output of P-cells that is generally cited as evidence of cortical filtering, there is also evidence that the maximum flicker rate for M-cell firing is greater than flicker fusion frequency. The P- and M-cell 'de Lange' functions are shown in Figure 1.26 and have been discussed in Chapter 1.3.2. From these graphs, the cut-off frequencies of both cell types can be plotted as a function of luminance (Figure 3.1) and compared with the results of Figure 2.7. The similarity is not impressive! All that can be said from this, in support of the suggestion that the M-cells signal Zone 2 and the P-cells signal Zone 1, is that at lower luminances the cut-off frequencies merge, and also the rate at which the M-cell cut-off increases with increasing luminance is greater than that for the P-cells as is the rate at which the cut-off frequency of Zone 2 increases compared with that of Zone 1. Of greater interest is the dissimilarity in the two sets of data. Unlike the physiological data, the psychophysical data (JLB) show a sudden decline in cut-off frequencies for the highest luminances, (referred to in section 2.1). This could be optical; on the other hand, if it is accepted that there is cortical filtering lowering the perceived cut-off frequencies, then the high luminance reduction of perceived cut-off frequencies could be explained by a filter whose attenuation increases with luminance.

The preliminary experiments, described in Chapter 2.2, identify an additional difference in the characteristics of the two zones. Figures 2.6 and 2.7 show how the cut-off frequency of Zone 2 increases with eccentricity more rapidly than that of Zone 1. This, coupled with the other differences, implies two distinct mechanisms. If the transient Zone 2 is, in fact, mediated by the magnocellular pathway, an improvement in cut-off frequency with increasing eccentricity suggests an increasing proportion of M-cells with eccentricity. However, there are conflicting estimates on the distribution of cell types with eccentricity; Silveira and Perry (1991), Calkins et al. (1995) and Livingstone and Hubel (1988) find little change across the field. Ikeda and Wright

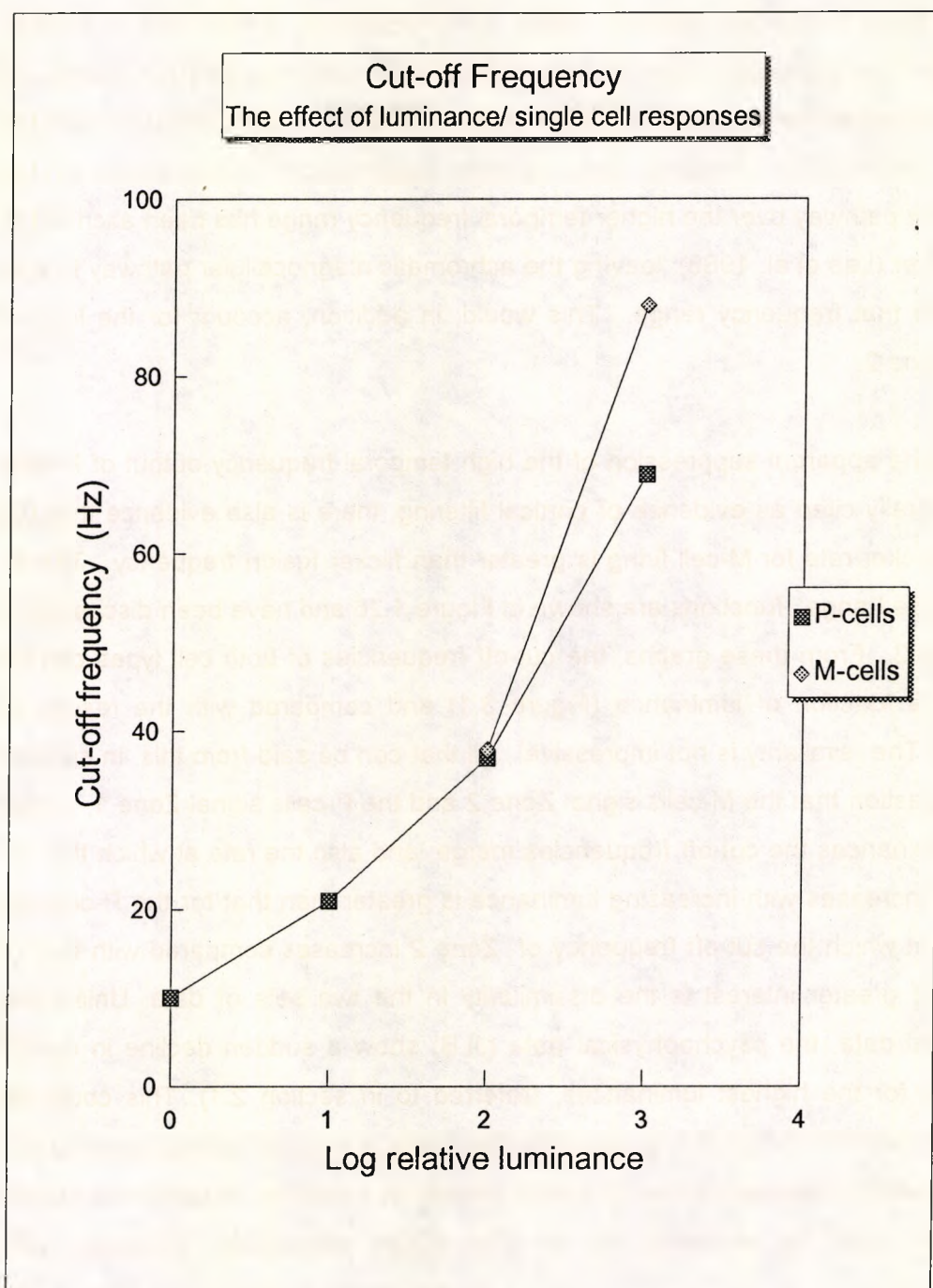


Figure 3.1: The temporal cut-off frequencies for single P- and M-cells plotted as a function of luminance, taken from the data of Lee et al. (1990), already shown in Figure 1.26. Note the the similarity of both P and M cut-off frequencies at the lower luminances, with differences only emerging at higher luminances. Note, also, the higher values compared with any psychophysically determined estimates.

(1972) find an increased percentage of transient cells peripherally in the case of cats. However, Silveira and Perry (1991) do show that the nasal quadrant has the greatest preponderance of M-cells. Taken in conjunction with the work of Ikeda and Wright (1972) and the flicker work of Hylkema (1942), in which maximum CFF values were found in the nasal quadrant, it suggests that flicker fusion values and, in the case of the stripes, the cut-off frequencies are a pointer to M-cell density.

Linking cell types to psychophysical channels is controversial territory, but there are several indicators that, in the normal eye, Zone 1 and Zone 2 reflect the separate activity of the parvocellular and magnocellular pathways and that this simple device of a rotating striped pattern is providing a window into the activity of these two pathways. There is one problem associated with this 'window' and it is that of knowing what the observer is actually seeing. The width and the orientation of the bands, seen by the observer, can be ascertained using parallel markers fixed to the rotating pattern (a procedure which was discussed in section 2.2). Establishing the contrast distribution across the band is more difficult. The solution described and demonstrated in the following paper is that of modelling possible underlying channel characteristics and comparing a simulation based on the composite model with the effect actually perceived.

## 3.2 COMPUTER SIMULATION OF THE COMPLEX 'BAND'

### 3.2.1 Introduction to Paper 3: **Rotating stripes provide a simultaneous display of sustained and transient channels**

A basis of the simulation can be understood from Figure 3.2. At any moment in time each point 'P' on the retina is stimulated by the amount of light falling on the retina at that moment together with the lingering stimulation provided by the grating in its previous positions for the duration of the integration time of the eye. The contributing intensities lie along an arc traced out from 'P' with the length determined by the product of the angular velocity and the integration time. Figure 3.3 shows the simulation that results from a rectangular impulse response (i.e. an idealised eye in which the persisting images are of constant strength over their duration). The contrast distribution can be seen to follow the expected 'sinc' function (discussed in Section 2.3) which indicates that the computation is correct.

Very simple models are chosen for the sustained and transient channels. Even with such simplified characteristics, the essential features of the complex band are identified. The paper illustrates this. However, until such time as there is a system designed to allow the observer to adjust the model until the simulation is close to the actual effect, the method has limited use in establishing detailed channel characteristics; the potential lies rather in the testing of models. The paper also refers to the possible use in clinical cases where there are gross pathological changes involved which produce significant changes in the effect. Under these conditions, even the simplified models will identify the key features. It should also be noted that where the abnormalities take the form of a greatly increased persistence time, this is equivalent to speeding up the rotating pattern. The requirements for a parallel band are lost, together with the simple link between appearance and temporal characteristics. Under these conditions, the simplest link between channel characteristics and appearance of the pattern is by means of a simulation.

Finally the possible physiological substrates for these sustained and transient 'zones' are discussed. It is argued that these zones reflect the separate activity of the parvocellular and magnocellular pathways.

### 3.2.2 Paper 3:

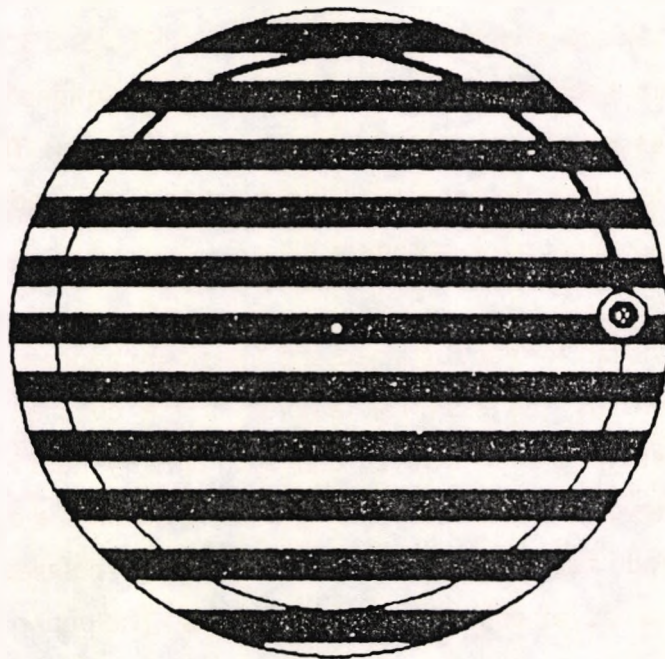


Figure 3.2: The rotation of the grating results in any point on the retina, at a given moment in time, being exposed to a fluctuating luminance, whose profile can be seen along the arc extending from 'P'. The arc length is determined by the product of the angular velocity and the integration time.

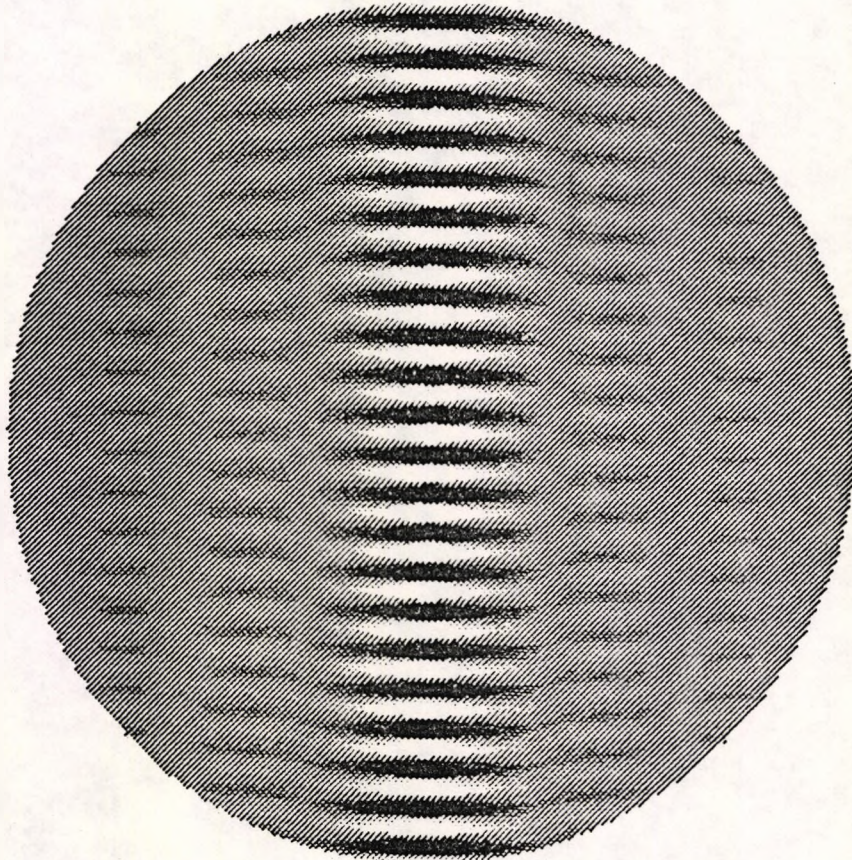


Figure 3.3: Predicted appearance of the rotating grating for an imaging system whose temporal impulse response is rectangular (e.g. an idealised eye whose persisting images are constant for their duration). Angular velocity is  $\pi \text{ rad.s}^{-1}$ ; integration time is 30 ms. Note the similarity with figure 2.3; again the contrast distribution is in the form of a 'sinc' function.

## Rotating stripes provide a simultaneous display of sustained and transient channels

JANET E. WOLF and NICHOLAS G. LUSTY

*Department of Optometry and Visual Science, City University, London EC1V 0HB, UK*

Received 23 May 1991; revised 25 February 1994; accepted 10 March 1994

**Abstract**—A slowly rotating striped pattern provides an instantaneous display of the temporal response characteristics of the visual system. The effect seen is that of a central column of clearly resolved stripes. The distribution of contrast across the width of the band displays the temporal frequency response; the spatial phase of the resolved stripes shows the temporal phase response of the mechanisms involved; and the orientation of the band indicates the transport delay. This band consists of two distinct regions, which suggests that there are at least two independent channels involved. At low temporal frequencies, a linear channel capable of carrying colour information mediates the appearance; at higher temporal frequencies, a nonlinear, achromatic channel predominates. The chromatic response to the pattern suggests that there is some interaction between channels. Computer simulation of a sustained and a transient channel produces an output similar to that perceived, thereby reinforcing the notion that this simple device enables one to display simultaneously the properties of the sustained and transient channels.

### 1. INTRODUCTION

Any moving target producing a moving retinal image will have an appearance which to some extent displays the activity of the underlying spatio-temporal channels of the visual system. The separate contributions within a trailing blur are generally obscure, and in some cases filtered out (Burr, 1980). With a target consisting of a one-dimensional striped pattern, rotating slowly (in this case a black and white square wave grating printed on an illuminated surface), these contributions are visually distinct: the purpose of this paper is to indicate why this is so and to indicate how such a stimulus provides a means of studying the behaviour of these channels. The effect seen is one of a central column or 'band' of clearly resolved stripes moving around with the disc as a whole; the borders of this band are approximately parallel and lag slightly behind the perpendicular to the stripes, the general appearance corresponding to that of Fig. 1. If, on the other hand, the pattern rotates quickly (i.e. the period of rotation is less than the persistence time of the eye), a pattern of concentric circles is seen. Finally, if the speed of rotation lies somewhere between these two extremes, there is a central region of clear stripes but the boundaries are no longer parallel; the band is narrow at the centre and fans out towards the edge, similar to Fig. 2.

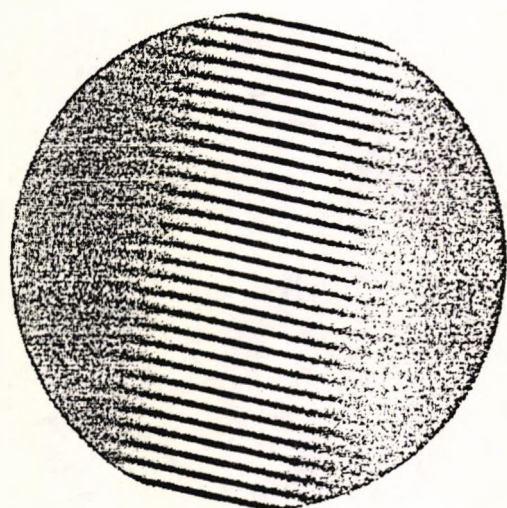
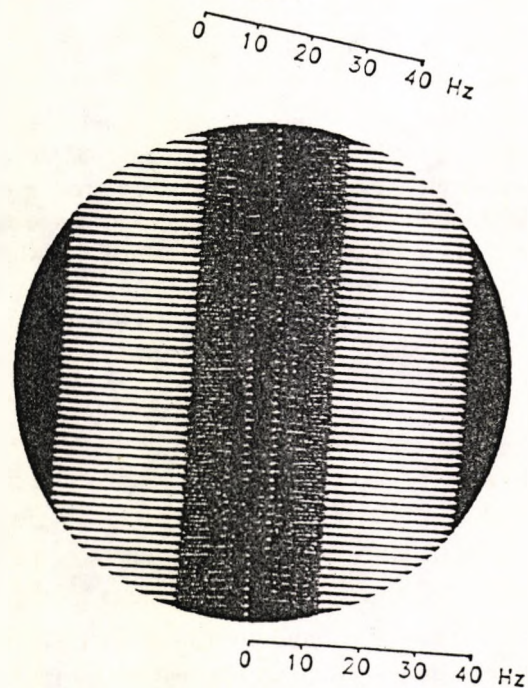
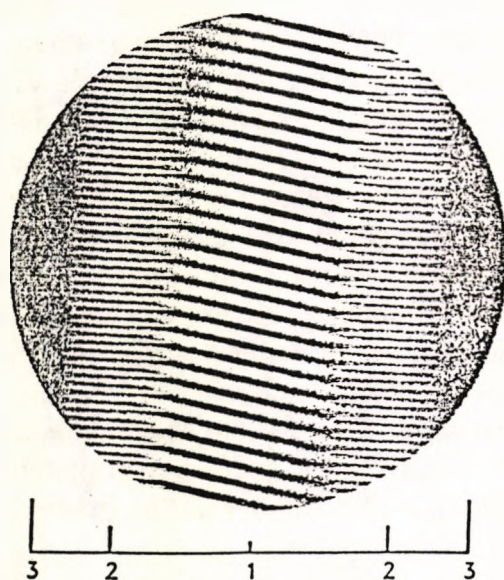


Figure 1. Predicted appearance of the grating rotating slowly ( $\pi \text{ rad s}^{-1}$ ) in an anti-clockwise direction and filtered by:

(i) the sustained channel: a high-contrast parallel band with its boundary at a low temporal frequency ( $\approx 12 \text{ Hz}$ );



(ii) the transient nonlinear channel: a fragmented low-contrast parallel-sided image with band-pass characteristics, displaying frequency doubling and with a higher temporal cut-off frequency ( $\approx 36 \text{ Hz}$ );



(iii) the combined sustained and transient channels. The image corresponding to the sustained channel lags behind that for the transient channel providing a clear demarcation of the zones.

(N.B. The frequency scale ( $F(x) = \omega x/2d$ ) is calibrated for an angular velocity  $\omega$  of  $\pi \text{ rad s}^{-1}$  and rotated in each figure to lie along the perceived stripes.)

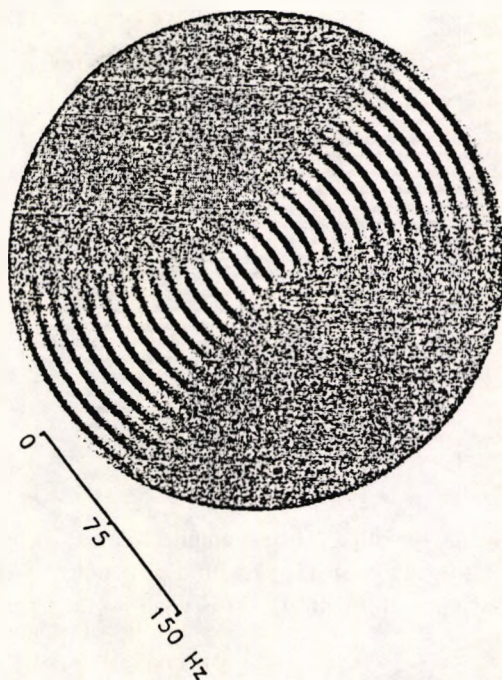


**Figure 2.** Predicted appearance of the rapidly rotating grating ( $3.75\pi \text{ rad s}^{-1}$ ) for the sustained channel. The band is no longer parallel and there is no simple display of the system's temporal transfer function.

The gross appearance for all these conditions is predictable from a knowledge of the persistence of vision or, more precisely, the temporal impulse response of the visual mechanisms involved. Consequently, these effects can all be used as a means of gaining insight into the temporal characteristics of the visual system. However, it has been previously shown that it is the *slowly* rotating pattern that is of especial interest, for it is under these conditions that there is a very simple relationship between the appearance of the band and the temporal characteristics of the visual system (Note 1; Glunder, 1987; Wolf, 1987). The perceived contrast distribution along the stripes provides an instantaneous display of the temporal frequency response, the width of the band indicating the temporal cut-off frequency (see Fig. 3). The anti-symmetric shape of the stripes in the band provides a graphical display of the temporal phase response, and the orientation of the band can provide information on 'transport delay'. This means that the temporal characteristics of a single channel are contained in the width, contrast and orientation of a two-dimensional shape. If there is more than one channel involved in detecting the image, each with its own spatio-temporal characteristics, we would expect to see some kind of substructure corresponding to a superposition of the separate bands, each with a distinct width and orientation. Simple experimentation demonstrates that this is the case. The band *is* complex; we see an inner band apparently superimposed on and lagging slightly behind a wider band, suggesting that we are seeing the action of at least two independent mechanisms or channels.

The difficulty in extracting any quantitative information from the appearance lies in establishing what the appearance actually is! Modelling the properties of possible underlying channels or mechanisms and comparing a simulation with the perceived

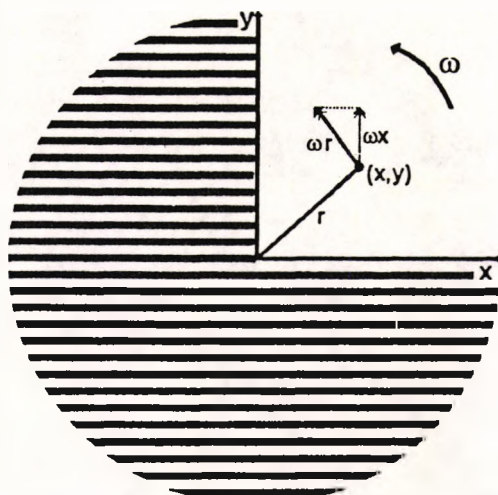


**Figure 3.** The pattern, rotating slowly with a constant angular velocity  $\omega$ , is in effect providing stripes of a fixed spatial frequency moving at any point  $(x, y)$  with a perpendicular component of velocity of  $\omega x$ . The instantaneous temporal frequency at a point  $(x, y)$  is equal to the perpendicular velocity divided by the spatial period ( $2d$ ),

$$F(x, y) = \omega x / (2d).$$

Since the stripes are of fixed contrast along their length, the perceived contrast, at any distance  $x$  from the centre, is a measure of the imaging system's response to that particular temporal frequency, with the boundary identifying the temporal cut-off frequency.

effect is the method used in this study. Even with a very simplified version of channel characteristics, the essential features of the complex band are identified, and, whilst this technique has limited use in establishing detailed psychophysical channel characteristics, its potential lies in the testing of models. This technique can be applied both to normal vision and to clinical cases where pathological changes cause significant changes in channel parameters and consequently to the appearance of the pattern. For example, in the event of there being a significant deficit in the temporal frequency response of one eye, this shows up instantly with a different width of band for each eye (Note 2). However, should the channel abnormality take the form of a *substantially* increased persistence time, the parallel band and the simple mathematics of the 'slowly' rotating grating are lost and a simulation based on numerical convolution provides the most direct way of linking channel characteristics to perceived appearance and vice versa.

## 2. THE COMPLEX 'BAND'

The perceived pattern consists of three distinct areas, the general appearance corresponding to Fig. 1(iii). There is an inner band, 'zone 1', lying obliquely across the rest of the band; in this the stripes are well defined and of high contrast. Surrounding this central band lies a region, 'zone 2', in which the stripes are much less well defined but appear to be doubled in spatial frequency. Furthermore, when the pattern is illuminated by unsaturated coloured light (e.g. pink), the white stripes of the illuminated

target in this outer region look white; this is in marked contrast to the appearance of zone 1 in which the white stripes of the target adopt the colour of the illuminant. Flanking zone 2 is a region, 'zone 3', which is fully blurred and, as in the case of zone 1, adopts the colour of the illuminant. For a spatial frequency of  $3 \text{ cyc deg}^{-1}$ , zone 1 contains frequencies up to  $\approx 12 \text{ Hz}$ . Zone 2 contains frequencies extending from the cut-off value for zone 1 to  $\approx 36 \text{ Hz}$  (Note 2) and zone 3 all frequencies above  $\approx 36 \text{ Hz}$ .

The appearance of zones 1 and 3 may be explained by a single linear channel that carries both luminance and colour. However, since no simple channel could exhibit the behaviour of both zones 1 and 2, we assume that at least two channels are required.

We designate the channel responsible for zones 1 and 3 as the 'sustained' channel since a strong low-frequency response implies a sustained step response. The channel responsible for zone 2 we designate the 'transient' channel, as it has no visible low-frequency response, and thus has a transient step response. It exhibits frequency doubling, and if this is accepted, then there is no option but to use a nonlinear temporal response function. We also hypothesize that it is achromatic.

This leaves unexplained the loss of colour in zone 2, since it would be expected that the sustained channel would either produce a modulated, correctly coloured output (as in zone 1) or an unmodulated correctly coloured output (as in zone 3) depending on the channel bandwidth. The explanation that we favour is that there is some interaction between the channels, with the strong activity in the transient channel inhibiting the output of the sustained channel, whether it be modulated or invariant. The idea of there being a suppression of the activity in the sustained channel by high frequency stimuli has already been used by Anderson and Burr (1985) and Breitmeyer and Ganz (1976). It would also be consistent with the abrupt change from zone 1 to zone 2.

The high temporal frequencies of zone 3 lie beyond the modulation range of both channels and are effectively filtered out. The transient band-pass channel would produce no output and the sustained channel would produce an invariant sustained output leading to an accurate rendering of the colour of the illuminant.

The essential feature of our interpretation is that we see some form of superposition of the separate images mediated by the two channels. Many workers have concluded that there *are* two distinct temporal channels, 'sustained' operating at moderate to high spatial frequencies and 'transient' at moderate to low spatial frequencies (Robson, 1966; Kulikowski and Tolhurst, 1973; Holliday and Ruddock, 1983; Holliday *et al.*, 1983; Anderson and Burr, 1985). The spatial frequency actually used in our initial observations was  $3 \text{ cyc deg}^{-1}$ , a value which is considered to stimulate both sustained and transient channels (Tolhurst, 1975). Also, since it is well established that the temporal characteristics of these channels vary with a range of stimulus parameters (luminance, colour, contrast, retinal location, and spatial frequency), we would expect the appearance of the bands to reflect this. We find this to be so. For example, reducing the illumination on the grating reduces the width of zone 2, until it finally merges with zone 1. There seems little doubt that in zone 1 and zone 2 we are seeing the activity of two distinct 'frequency-tuned' channels.

### 3. MODEL

We will consider that the contributions of the sustained channel end at the boundary of zone 1, which avoids having to incorporate inhibition into the summation of the two images. Our channel characteristics are, in effect, based on the post-inhibition behaviour, should inhibition be operating.

The sustained channel is modelled using a 20th-order critically damped low-pass filter. Initially first- and second-order filters were simulated but the roll-off was too slow giving a highly diffuse edge to the pass-band. Although the exact order of the filter is not critical, the 20th-order chosen provides a typical value for the gradient of neural temporal frequency cut-off (Victor, 1987).

De Monasterio (1978) showed that transient Y-cells give a positive response for both rising and falling edges. Rectification of the input waveform would correspond to this and would give rise to frequency doubling; we shall use this source of frequency doubling as the basis for our simple transient channel. The transient channel is modelled using a step response of one cycle of sine wave, which approximates to a one-octave band-pass filter.

The characteristics of both these filters are shown in Fig. 4. Negative frequencies are included as they have a physical reality; the motion of the stripes producing the temporal variation is in opposite directions on each side of the origin. The channel characteristics bear a qualitative similarity to the 'pattern and movement' channels of Kulikowski and Tolhurst (1973), the sustained and transient channels of Anderson and Burr (1985), and in particular the ST1 and ST2 mechanisms of Holliday and Ruddock (1983) and Holliday *et al.* (1983). The time constants of each have been chosen to give the appropriate zone widths for an illuminance of  $\approx 4 \log T_d$  (cut-offs at approximately 12 and 36 Hz), comparable to the bandwidths of ST1 and ST2.

The output of the two channels may be superimposed. A relative rotation between the two images can be arbitrarily imposed, corresponding to a transport delay in the sustained channel in excess of the delay in the transient channel. With no rotation imposed, there would still be an obliquity or lag between the boundaries of zone 1 and zone 2, which would reflect the difference in duration and form of the two temporal impulse-response functions; that is, the boundary of the band produced in the sustained channel, with its greater persistence, would still lag behind that of the transient channel. It follows that, in general, the relative obliquity that results is the sum of these two separate rotations.

### 4. SIMULATION OF THE PERCEIVED IMAGE

The luminance distribution across the perceived image, at a given moment in time, may be computed by calculating, at each point on the retinal image, the temporal luminance profile that had preceded that moment in time and convolving it with the temporal impulse response function (Appendix 1).

## 5. RESULTS

The results of the convolutions are shown in Fig. 1(i) and (ii) with the contrast distribution resulting from the two filters displaying a similar form to their amplitude frequency responses (Fig. 4). The similarity in form is in spite of the stimulus being of square waveform and simply illustrates the dominance in the stimulus of the fundamental spatial frequency. The images are superimposed in Fig. 1(iii), with no relative transport delay incorporated. The lack of delay was prompted by the results of Sestokas *et al.* (1987), in which they found that the chief factor underlying the apparent delay associated with sustained X-type geniculate cells, as opposed to the transient Y-type geniculate cells, was the relatively slow build-up in the response to the onset of light of the X-type ganglion cells, together with the rapid response rise time of the Y-type geniculate cells.

Clearly the resulting black-and-white image cannot demonstrate the loss of colour associated with a desaturated coloured illuminant resulting from the inhibition of the sustained channel by the transient channel. With this limitation, the composite image is similar to that actually perceived, displaying not only the abrupt change from the high contrast region of zone 1 to the fragmented, poor contrast region of zone 2, but also the overall lag or obliquity of the narrow central band with respect to the outer bands.

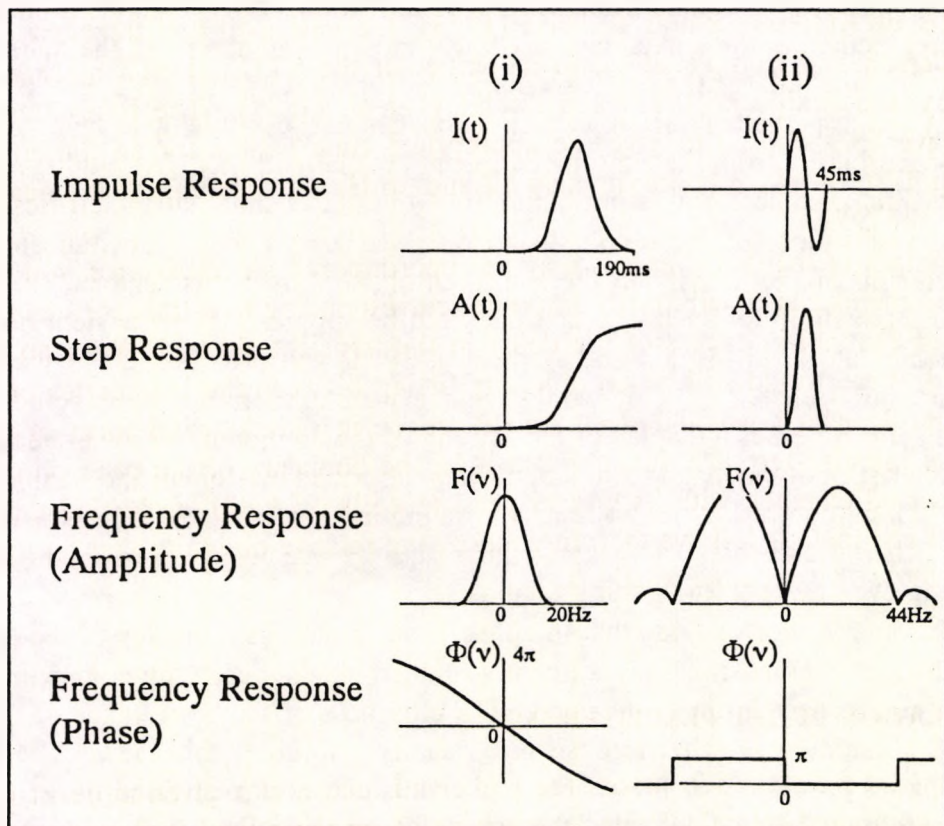


**Figure 4.** Filter characteristics of the two channels: (i) The sustained channel is modelled using a 20th-order critically damped low-pass filter; (ii) The transient channel is modelled using a rectified band-pass filter.

## 6. DISCUSSION

The stimulus of the rotating pattern is unusual in providing a method of displaying the supra-threshold response of the observer to the whole range of temporal frequencies *simultaneously*. It is this that enables the zone boundaries and zone characteristics to be apparent, despite some frequency shifts associated with different stimulus characteristics (contrast, luminance, spatial frequency, retinal position) or even different observers. For example, although it was proposed originally that the sustained channel subserved pattern detection and the transient channel motion detection, later evidence suggests that both channels signal motion (Green, 1981; Murray *et al.*, 1983; Thompson, 1983; Harris, 1984; Anderson and Burr, 1985). Both channels signalling motion is consistent with the steady motion observed across zones 1 and 2, which is apparent simply because both regions *are* seen simultaneously. In addition the apparent loss of colour in zone 2 is only noticed *because* all frequencies are seen simultaneously; with direct comparison, the colour differences show up easily.

We now ask whether the appearance of the complex band provides any additional evidence towards the controversial question of whether specific physiological pathways can be identified as substrates of the psychophysical sustained and transient channels. It seems so. Zone 1 displays the activity of a sustained channel, and the appearance of colour suggests that the neurones involved are colour-coded. This is the region of low velocities and Livingstone and Hubel (1987) claim that the sustained channel mediating the appearance of slowly moving patterns is, in the main, handled by the parvocellular pathway. It seems likely, therefore, that zone 1 may be assigned chiefly to the parvocellular projection. This does not preclude there being a low contrast contribution from the achromatic magnocellular pathway. It would simply be far less visible in zone 1 and is not incorporated in our channel characteristics.

The visible loss of the colour in zone 2 has been taken as an indication of the suppression of the activity in the sustained channel over this region. There is evidence that activity of sustained neurones can be suppressed by transient neurones at the geniculate level (Singer and Bedworth, 1973) and possibly in the visual cortex (Stone and Dreher, 1973). It would seem plausible, therefore, to conclude that the achromatic zone 2 is a display of the activity of the dominant transient neurones. The characteristics of the magnocellular pathway described by Kaplan and Shapley (1986), namely high-contrast sensitivity and low-saturation contrast, would be consistent with zone 2 being a display of magnocellular activity and would correspond to zone 2 existing even at very low grating contrasts.

In summary, we conclude that in zones 1 and 2 there is a display of the activity of two distinct channels; namely a linear sustained channel carrying colour information and a nonlinear achromatic channel. The closeness of the appearance of the results of the simulation to what is observed visually reinforces this view. The temporal and spatial properties of these neural channels can be investigated by adjusting the parameters in the model so that the simulation predicts the effects observed experimentally and this method could be used in clinical cases there are abnormal channel parameters giving an abnormal appearance. It also provides a means of investigating the relative latencies of the two channels. We suggest finally that the loss of colour

in zone 2 provides a direct display of the suppression of the activity of the sustained channel within the active range of the transient channel.

### Acknowledgements

We are grateful to Professor G. B. Arden and Professor J. L. Barbur for their helpful advice and constant encouragement.

### NOTES

1. Wolf, J. E. A method of measuring the impulse response of the eye. Presented at the Applied Vision Association workshop: 'Mathematical and statistical techniques', London, October 1984.

2. Wolf, J. E. The clinical application of the 'rotating stripes' effect. Paper presented at the Applied Vision Association conference: 'Advances in the assessment of visual function and structure', London, July 1988.

### REFERENCES

- Anderson, S. J. and Burr, D. (1985). Spatial and temporal selectivity of the human motion detection system. *Vision Res.* **25**, 1147-1154.
- Breitmeyer, B. G. and Ganz, L. (1976). Implications of sustained and transient channels for theories of visual pattern masking, saccadic suppression, and information processing. *Psychol. Rev.* **83**, 1-36.
- Burr, D. (1980). Motion smear. *Nature* **284**, 164-165.
- Glunder, H. (1987). Rotating gratings reveal the temporal transfer function of the observing system. *J. Modern Optics* **34**, 1365-1374.
- Green, M. (1981). Psychophysical relationships among mechanisms sensitive to pattern, motion and flicker. *Vision Res.* **21**, 971-983.
- Harris, M. G. (1984). The role of pattern and flicker mechanisms in determining the spatio-temporal limits of velocity perception. 1. Upper movement thresholds. *Perception* **13**, 401-407.
- Holliday, I. E. and Ruddock, K. H. (1983). Two spatio-temporal filters in human vision. *Biol. Cybernet.* **47**, 173-190.
- Holliday, I. E., Ruddock, K. H. and Skinner, P. (1983). Spatial filtering of retinal images by the human visual system and its consequences for visual thresholds. SPIE Vol. 467, Image Assessment: Infrared and visible (Sira).
- Kulikowski, J. J. and Tolhurst, D. J. (1973). Psychophysical evidence for sustained and transient detectors in human vision. *J. Physiol. (Lond.)* **232**, 149-162.
- Kaplan, E. and Shapley, R. M. (1986). The primate retina contains two types of ganglion cells, with high and low contrast sensitivity. *Proc. Natl. Acad. Sci. USA* **83**, 2755-2757.
- Livingstone, M. S. and Hubel, D. H. (1987). Psychophysical evidence for separate channels for the perception of form, color, movement and depth. *J. Neurosci.* **7**, 3416-3468.
- de Monasterio, F. M. (1978). Centre and surround mechanisms of opponent-color X and Y ganglion cells of retina of macaques. *J. Neurophys.* **41**, 1418-1434.
- Murray, I., MacCana, F. and Kulikowski, J. J. (1983). Contribution of two movement detecting mechanisms to central and peripheral vision. *Vision Res.* **23**, 151-159.
- Robson, J. G. (1966). Spatial and temporal contrast-sensitivity functions of the visual system. *J. Opt. Soc. Am.* **56**, 1141-1142.
- Sestokas, A. K., Lehmkuhle, S. and Kratz, K. E. (1987). Visual latency of ganglion X- and Y-cells: a comparison with geniculate X- and Y-cells. *Vision Res.* **27**, 1399-1408.
- Singer, W. and Bedworth, N. (1973). Inhibitory interaction between X and Y units in the cat lateral geniculate nucleus. *Brain Res.* **49**, 291-307.

- Stone, J. and Dreher, B. (1973). Projection of X and Y cells of the cat's lateral geniculate nucleus to areas 17 and 18 of the visual cortex. *J. Neurophysiol.* **36**, 551-567.
- Thompson, P. (1983). Discrimination of moving gratings at and above detection thresholds. *Vision Res.* **23**, 1533-1538.
- Tolhurst, D. J. (1975). Sustained and transient channels in human vision. *Vision Res.* **15**, 1151-1155.
- Victor, J. D. (1987). The dynamics of the cat retinal X-cell centre. *J. Physiol.* **386**, 219-246.
- Wolf, J. E. (1987). Rotating stripes and the impulse response of the eye: 1. Uniform illumination. *Spatial Vision* **2**, 199-211.

#### APPENDIX 1

Because of the rotation of the pattern, the temporal luminance profile must be computed along a circular path, and then convolved with the temporal impulse response of the visual system. The algorithm makes use of the fact that, for a pattern of white and black stripes, the convolution is reduced to a simple integration of the impulse response of the system over those areas that are white. Provided that the impulse response can be analytically integrated, the convolution may be performed as a series of finite integrations of the impulse response. Each integration is more easily achieved by measuring the change in step response, over each period, since the step response

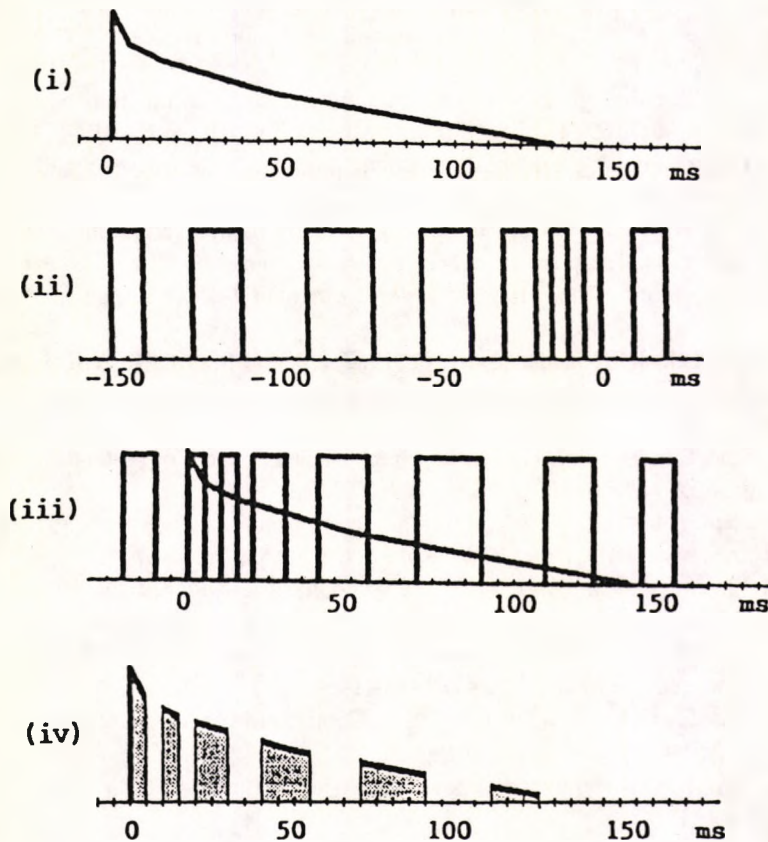


**Figure A1.** (i) Typical temporal impulse response function; (ii) temporal profile of luminance input to receptor; (iii) time-reversed input superimposed on typical impulse response; and (iv) the area under the curve equals the total convolution value and consequently the luminance at that point.

is the integral of the impulse response. This algorithm means an accurate *continuous* convolution can be achieved, without recourse to numerical integration. Figure A1(i) shows an example of an impulse response and Fig. A1(ii) the input to a particular point on the retina. The convolution is performed by reversing the time axis, and integrating the product of the two waveforms shown superimposed in Fig. A1(iii). Since the input waveform is either 'on' or 'off', it is only necessary to integrate the temporal impulse response itself over the periods that the input is 'on'. The convolution result is thus given by the shaded area in Fig. A1(iv). If the input waveform at point  $(x, y)$  turns 'on' in the periods  $-t_0 > t > -t_1$ ,  $-t_2 > t > -t_3$ ,  $-t_4 > t > -t_5$ , and the impulse function is  $I(t)$ , where  $t$  is time, then the value of the convolution  $C(x, y, 0)$  (i.e. at time  $t_0$ ) is

$$C(x, y, 0) = \int_{t_0}^{t_1} I(t) dt + \int_{t_2}^{t_3} I(t) dt + \int_{t_4}^{t_5} I(t) dt + \dots$$

If the anti-derivative  $A(t)$  of  $I(t)$  is known, the convolution is further simplified to

$$C(x, y, 0) = A(t_1) - A(t_0) + A(t_3) - A(t_2) + A(t_5) - A(t_4) + \dots$$

Thus the calculation required for the convolution has been reduced to two function evaluations for each time a white stripe is crossed during the period of the impulse function.

The changes from 'on' to 'off' occur at values of  $y$  given by  $d/2, 3d/2, 5d/2, \dots$ , where  $d$  is the width of one stripe. Hence for a given radius  $r$ , these discontinuities occur at values of  $\phi$  given by

$$\sin \phi = (2n + 1)d/(2r). \quad (\text{A1})$$

Since the disc is rotating at a constant angular velocity, the input waveform will have the same temporal profile as the angular rotations of Eqn (A1).

## CHAPTER 4 CLINICAL APPLICATION OF THE 'ROTATING STRIPES EFFECT'

### 4.1 OPTIC NEURITIS AND MULTIPLE SCLEROSIS

After it was apparent that the complex band was a direct display of the transient and sustained channels, there was the opportunity of showing the 'stripes' to a patient with optic neuritis who had specifically complained of problems in seeing moving targets. Immediately he was able to judge that the band in the more affected eye was approximately half the width of the other, consistent with the reduced flicker fusion frequencies associated with optic neuritis. This warranted a fuller and quantitative investigation into his perception of the 'bands'. Similar measurements were made on a person with multiple sclerosis.

Case 1: A 52-year old man (living in East Germany) was diagnosed as having optic neuritis in August 1986. He complained that 14 months previously to my tests he had suddenly lost vision in the Left eye, and further that (i) he had the impression he was looking through a misty glass, (ii) stationary objects seemed to move and (iii) when playing tennis he could no longer hit the ball. On examination in August 1986 his reduced acuity, and reduced visual field had been noted, but there was no obvious change to the retina or optic nerve, even with fluorescein angiography.

Following treatment of Dexamethasone injections and Prednisolone orally, the first two symptoms disappeared, the visual acuity improved and the visual field returned to normal. In July 1987 he was re-examined by Professor Marion Marré with the following assessment:

	RE	LE
Colour vision:	Congenital deuteranopia	Acquired blue deficiency
Visual acuity:	1.0	0.8-1.0
Fundus:		Paler optic nerve head
Photopic VECP:		Relative delay:5ms upper field 15ms lower field
Contrast sensitivity losses (log scale):	0.2-0.3	0.1-0.5





zone adopted the colour of the illuminant. The whites in the outer zone remained white. However, using the affected eye, she volunteered that she now only saw one band (no 'inner' and 'outer') and the band no longer seemed to be lagging. She explained this, to her own satisfaction, by saying that there was nothing for it to be judged against! This supports there being only one zone. Two are needed to be aware of a relative lag. Also, with the coloured illuminant, she no longer had the impression of a zone differently coloured. This would be expected if Zone 2 were absent as it is the comparison of the two regions that enables the judgement to be made.

#### CONCLUSIONS:

In 'case 2', the transient zone of the band (Zone 2) was absent in the affected eye. This means that either the transient channel is also absent or sufficiently reduced in cut-off frequency so as to be rendered invisible. If it is true for normals that it is the magnocellular pathway whose activity is reflected in Zone 2, then this could indicate magnocellular damage. There also seems to be a fairly general consensus that the magnocellular pathway has a special involvement with movement detection and both these patients had problems with moving objects.

Whilst it might be true to say that magnocellular damage interferes with motion perception, defective motion perception can be achieved without selective damage to the magnocellular pathway. All that would be necessary would be a non-selective damage to one optic nerve (i.e. not confined to P- or M-axons). There need only be a delay in the transmission velocity from one eye, with respect to the other, to account for disturbances in the perception of moving objects. Demyelination of the optic nerve is known to be associated with ocular defects in MS and has the effect of slowing the transmission of nervous impulses, which would account for the difficulties experienced, although a transport delay would not account for reduction in transient channel frequency cut-off (i.e. the loss of Zone 2). However, demyelination also extends the time course of the response to a flash of light (the temporal impulse response) and can therefore reduce the cut-off frequency as well. It is quite plausible that this increased sluggishness would manifest itself in the response to rapidly flickering stimuli rather than the slower ones, which would result in a reduction in the transient channel (i.e. Zone 2) cut-off frequency. If the low cut-off frequency of Zone 1 (in normals) is a result of cortical filtering, there is no need for this 'plausible' argument. At the LGN level, both pathways could have a reduction in cut-off

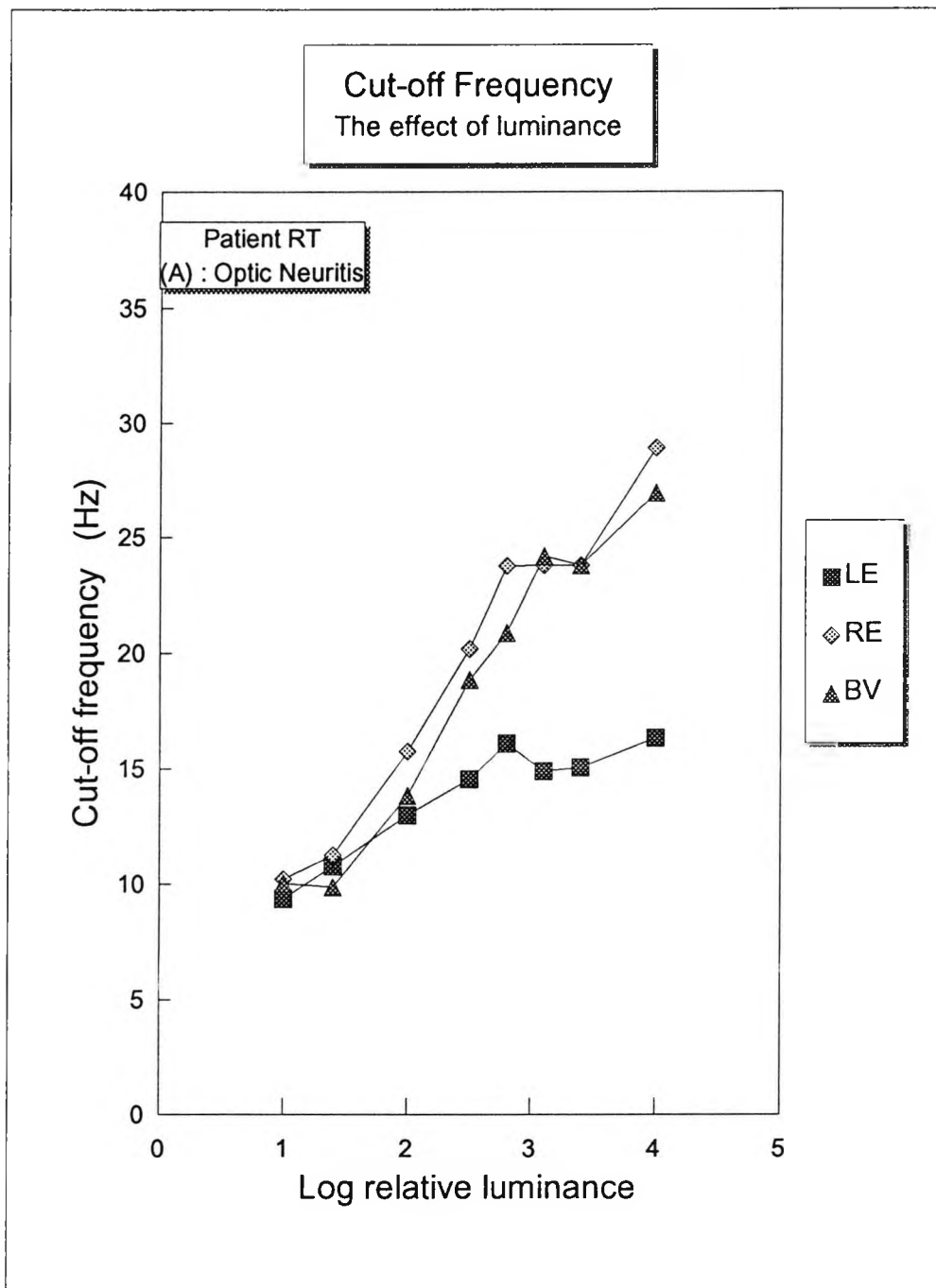


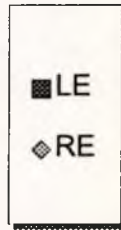
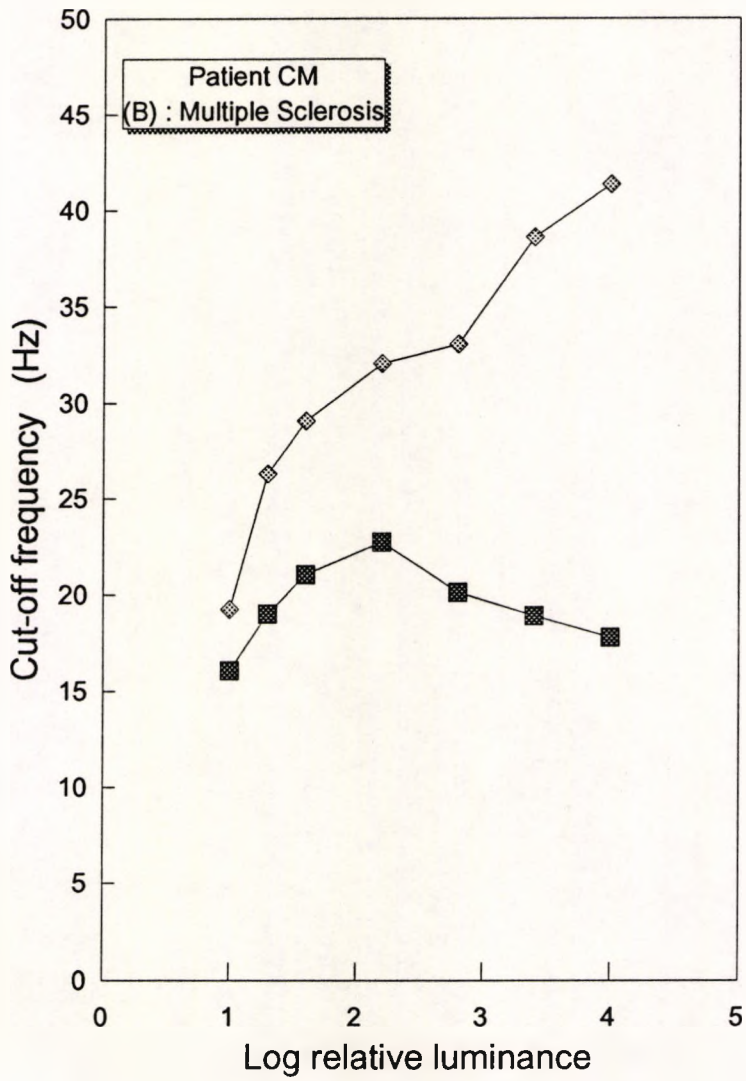
Figure 4.1: The cut-off frequencies for the 'outermost' band are shown as a function of luminance (maximum:  $650 \text{ cd. m}^{-2}$ ) for each eye.

(A) Optic Neuritis: The cut-off frequencies in the affected eye are greatly reduced; similar luminance dependence as Zone 1 of the normal eye, shown in (C).

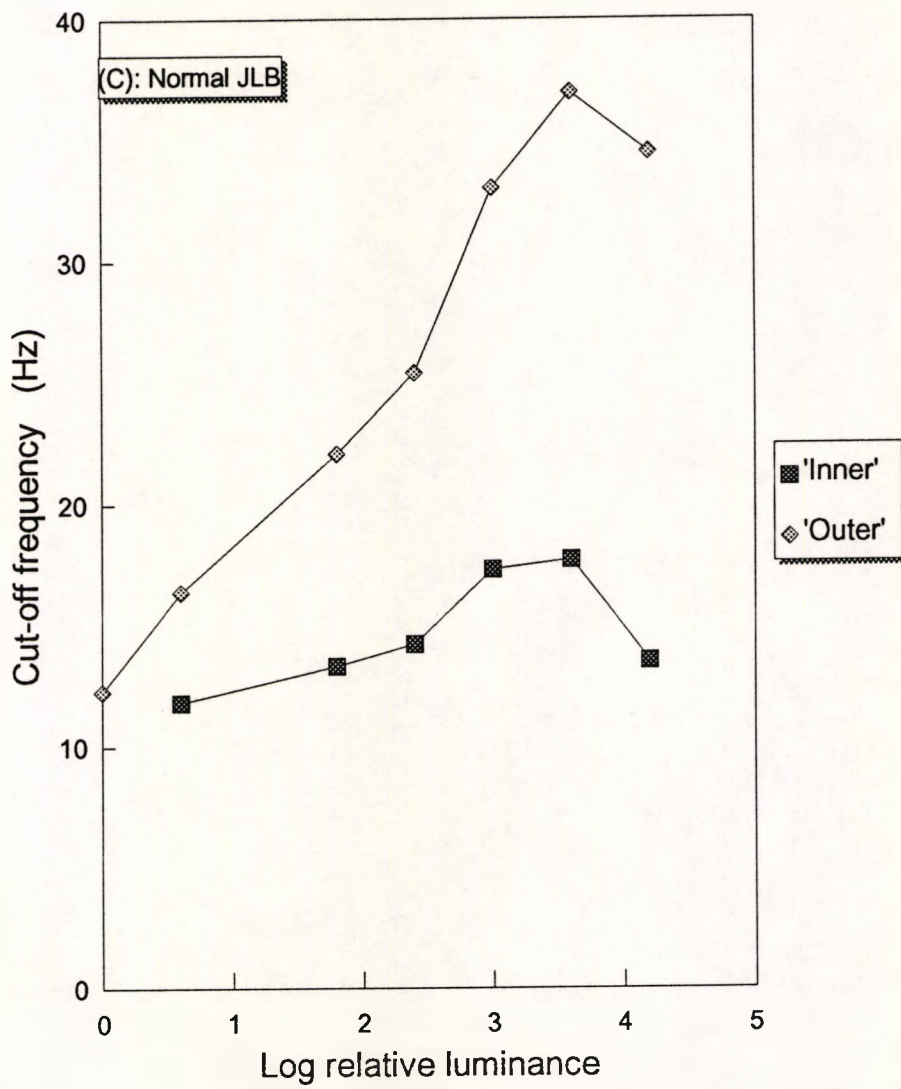
(B) Multiple Sclerosis: The cut-off frequencies in the affected eye are again greatly reduced; some similarity with the luminance dependence of patient (RT) shown in (A). See text for interpretation.

(C) Normal data from Figure 2.7: included so that a comparison may be made between the characteristics of the 'inner zone' of a normal and the outermost zone of the affected eyes .

**Cut-off Frequency**  
The effect of luminance



Cut-off Frequency  
The effect of luminance



frequency, which would go unnoticed in the case of Zone 1 since the responses to the higher frequencies, whether or not they are reduced, are filtered out.

The VER results in 'Case 1' show a substantial delay in the affected eye, sufficient to account for all the problems with moving objects. The similarity of the width of band with that of 'Case 2' suggests that the same factor that causes the time delay is also responsible for the reduced cut-off of Zone 2.

The observations of these two patients show that where there is a unocular disorder or a more pronounced loss of function in one eye, the difference in function of the two eyes is immediately apparent from the width of the two bands. Since the same person is judging both, the 'criterion problem' does not arise.

In addition, the results have the double effect of (i) reinforcing the conclusion that the visibly distinct bands correspond to the separate spatio-temporal channels with specific roles, and (ii) that there is some diagnostic potential in having some simple way of exposing channel loss.

#### 4.2 MELANOMA-ASSOCIATED RETINOPATHY (MAR)

A description of this condition and the subsequent investigation is described in detail in Chapter 5. However, the MAR patient who had complained of problems with moving objects was given the rotating stripes to look at, and so the brief investigation is included in this section. He had no perception of a band within a band and this was interpreted as damage to the transient magnocellular pathway. The more detailed psychophysical investigations (chapter 5) led to the same conclusion. In addition, a red/green grating, illuminated with a red and a green beam of light, produced an interesting result. The normal observer sees a central zone of brilliant colour contrast with a very faint region corresponding to Zone 2. The MAR patient saw the well resolved band of red/green stripes but of greater width. His cut-off frequency for that component was higher than normal. Being speculative, this could be accounted for, if the normal inhibition of the sustained channel by the transient channel (Anderson and Burr 1985; Breitmeyer and Ganz, 1976) and is no longer operating, allowing the colour-carrying region of Zone 1 to be extended. Figure 4.2 shows the MAR patient's cut-off frequency extending up to 28 Hz, in marked contrast to the normal's boundary of approximately 12 Hz.

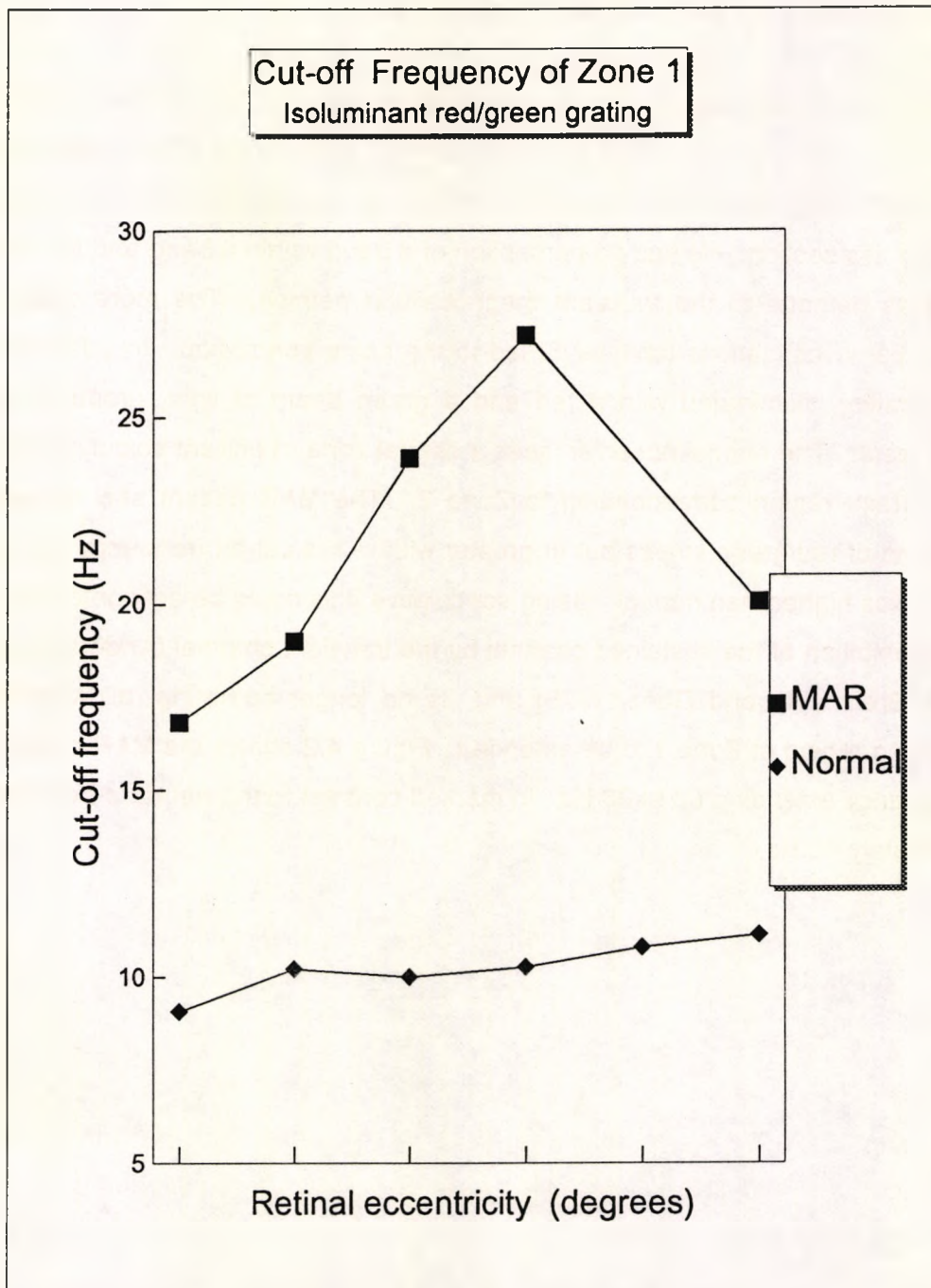


Figure 4.2: An isoluminant red/green rotating grating is used; cut-off frequencies are shown for different eccentricities. Only Zone 1 is visible to normals. The MAR cut-off frequency was considerably higher, suggesting that suppression normally exerted on the P-pathway at the higher temporal frequencies (i.e. over the range of Zone 2) has not taken place.

## CHAPTER 5: FURTHER PSYCHOPHYSICAL TESTS TO IDENTIFY SPECIFIC PATHWAY LOSSES: MAGNOCELLULAR AND PARVOCELLULAR DAMAGE

### 5.1 INTRODUCTION

Even in its present crude form, there is some potential in using the 'rotating stripes effect' as an immediate pointer to major functional losses, particularly where there is a difference in the temporal responses of the two eyes. More quantitative psychophysical tests can then be used, directed by this initial screening. In the case of a patient diagnosed as having MAR, there appeared to be a loss of function in the transient channel, and so some simple psychophysical tests were chosen to isolate the P- and M-pathways with a view to testing this. A description of the symptoms and characterising features of MAR are given first. The reasoning behind the choice of tests, the essential features of the tests and the equipment used are then summarised briefly, although a much fuller description follows in Paper 4. In particular, the basis of the conclusions are argued extensively in the paper, although the conclusions are also summarised in the 'results & conclusions' section (5.2.3).

Having used the tests successfully on MAR patients, they were then applied to several other conditions. This was partly to see whether the very specific losses found in MAR were present in other conditions. The first comparison made was with Congenital Stationary Night Blindness (CSNB), for the additional reason that it is a condition which has many similarities to MAR; it is accompanied by night blindness and the patients have very similar electrophysiological responses, in particular no rod b-wave. The tests were then applied in a routine way to Cuban Amblyopia. These two investigations are reported as both conditions seemed to demonstrate a specific channel loss. A brief clinical description is given of each condition and, where the circumstances required a modification of the tests, this is also described. The results and conclusions for each condition are summarised.

## 5.2 WHAT IS MELANOMA - ASSOCIATED RETINOPATHY?

Several types of paraneoplastic syndromes affect the central and peripheral nervous system. Two in particular affect the retina; they are associated with different types of malignancies and are known as 'cancer-associated retinopathy' (CAR) and 'melanoma-associated retinopathy' (MAR). CAR is associated with epithelial cancers, the most frequent being the small cell carcinoma of the lung. It is characterised by a gradual onset of night blindness with progressive retinal degeneration that may lead to an extinguished electroretinogram that is similar to that of retinitis pigmentosa. The condition can be detected before the underlying carcinoma is detected. In contrast MAR, is characterised by a sudden onset of photopsias associated with night blindness in patients that have already been diagnosed as having cutaneous melanoma. Unlike CAR the condition remains stable over many months and also, unlike CAR the patients may have high visual acuity.

Initially it was established that in MAR the flash ERG for the dark adapted eye shows a reduced b-wave amplitude with a relatively preserved a-wave resulting in a 'negative' wave form, similar to that seen in patients with 'congenital stationary night blindness' (CSNB). There are further striking similarities between the two conditions. They both have normal rhodopsin kinetics and a normal EOG suggesting normal functioning of the rod outer segments and that the visual abnormalities are a defect in signal transmission between rod photoreceptors and 2nd order neurons (Ripps, 1984; Berson, 1988). CSNB patients also have a selective reduction in the cone b-wave and in both abnormalities this is accompanied by a defective ERG 'on-response' suggesting a loss of function in the 'on' bipolar cells (Alexander, 1992; Young, 1991; Miyake 1987; Houchin 1991). It is this selective reduction of 'on-response' (as opposed to 'off-response') that is thought to cause the abnormal b-wave. An abnormal PERG p-50 amplitude, which is also observed, is consistent with damage at the inner retinal level.

Initially it was shown in 2 MAR patients that their serum contained antibodies against an antigen that cross reacts with bipolar cells in the retina (Milam, 1993). A more extensive study has shown that 10 of 12 patients had circulating autoantibodies (IgG class) that react specifically with rod bipolars but although this pattern would account for the abnormal rod bipolar function, the disease mechanism remains unknown (Milam, 1994).

### 5.2.1 THE TESTS:

It is already known that in MAR there is damage to rod bipolars and since these are on-bipolars the possibility arises that the loss of function might involve on-bipolars in general. Since on-bipolars are thought to mediate the detection of increments of light intensity rather than decrements, the contrast thresholds for brief increments and decrements were found. The targets used were large Snellen letters. There was no difference between the sensitivity to increments and decrements, which suggests that any selectivity of loss was not linked to the on- or off- system. Nevertheless, the results were interesting. The threshold was surprisingly high. Since this was accompanied by a high acuity, i.e. a relatively low contrast threshold to small targets, this suggested a spatial frequency selectivity. Hence, the achromatic spatial frequency response was the next characteristic to be investigated; this demonstrated a dramatic reduction in sensitivity to the low spatial frequencies. Since this suggested a possible channel loss, the 'rotating stripes' were used at that stage. There appeared to be no transient zone, which coupled with the patient volunteering that he experienced difficulty with seeing moving objects, pointed to an M-cell loss. At this point it seemed sensible to attempt to design tests that would isolate, and assess the integrity of the two pathways, M or P.

The M- and P- pathways have very different spatial and chromatic characteristics, described already in Section 1.3.3. and the stimuli were chosen to exploit these differences. The targets were either coloured and isoluminant with their background, or black-and-white. They took the form of (i) Snellen optotypes (c.3 degrees) that simply appeared and disappeared at 1 Hz (duty cycle 20%), (ii) Gaussian blurs that reversed sinusoidally in time over a range of temporal frequencies, (iii) sinusoidal gratings that also appeared and disappeared or (iv) that oscillated at 6 Hz. Chromatic contrast thresholds for low spatial frequency, isoluminant stimuli were assumed to involve exclusively the P-pathway, whereas contrast thresholds for achromatic stimuli of the same spatial and temporal content were taken to be mediated by the M-pathway. The justification for these assumptions are argued in detail in Paper 4. Displacement thresholds for the oscillating achromatic gratings were assumed primarily to involve the M- pathway, given the low spatial frequency involved.

## 5.2.2 EQUIPMENT AND PROCEDURE

Stimuli were generated on a computer graphics system (Arden, Gunduz and Perry 1988) with a refresh rate of 94 Hz and a 24-bit colour palette. The monitor was an NEC6GF, with a 24 inch screen. The colours used lay along the red/green colour confusion line of protanopes and the blue/yellow of tritanopes. Colours could be altered without change of luminance. The system allows for individual subjects to equate the relative luminances of the R/G and B/G phosphor outputs (using heterochromatic flicker photometry at 22 Hz) to compensate for differences between their spectral sensitivity and that of the CIE standard observer. Thus isoluminant colours may be generated for each person tested. Since the MAR patients were unable to see flicker at 22 Hz, this refinement had to be omitted for them.

Colour contrast ( as a percentage) is expressed as a fraction of the maximum colour separation possible along a given confusion line, using the given phosphors. It is defined as:

$$\frac{(X_1, Y_1) - (X_2, Y_2)}{(X_1, Y_1)_m - (X_2, Y_2)_m} \cdot 100$$

where  $(X_i, Y_i)$  refers to a position in CIE colour space along a line of colour confusion, and the subscript 'm' refers to the maximum separation of colour along this line achievable with the phosphors; the centre of the colour confusion line has coordinates give by:  $((X_1, Y_1) + (X_2, Y_2))/2$ .

For large values of colour contrast, it should be remembered that ( X,Y) space is not isotropic.

Contrast or displacement thresholds were measured using a 'modified binary search' routine (MOBS) described in Chapter 1.3; these were either achromatic (i.e. luminance contrast) or chromatic contrast thresholds or, as in the case of moving targets, displacement thresholds. The MOBS routine allows for indecisions and errors on the part of the patient, and, in those with poor sight, is slower to use, but more precise than a truncated staircase method. The subjects viewed the target with free eye movements, i.e. in whatever manner was most comfortable and were seated 1-3 m from the monitor.

### 5.2.3 RESULTS & CONCLUSIONS IN MAR

The key results for MAR are shown in Paper 4, Figures 5.1-5.4. Figure 5.1 shows that the contrast thresholds for increments and decrements of light intensity are the same, indicating that whatever the nature of the losses, they are not confined to the on- or off-pathway. The contrast sensitivity function (Figure 5.2) shows the pronounced losses in the low spatial frequency range and Figure 5.3 shows how these sensitivity losses extend over a large range of temporal frequencies. It is generally accepted that for low spatial frequencies (see Paper 4) at the higher temporal frequencies, the thresholds are set by the magnocellular pathway. It follows that the sensitivity losses at the higher temporal frequencies are reasonably attributed to magnocellular losses. However, the virtually constant loss of sensitivity extending down to the low temporal frequencies, suggests that even at the low temporal frequencies the thresholds are set by the same mechanisms. Coupled with the very low contrast threshold for 'normals' at these low temporal frequencies, the results suggest that under the conditions of measurement, (e.g. eyes free to move around), the threshold was set by the magnocellular pathway, with the loss of function in MAR being essentially confined to that pathway. This conclusion is reinforced by difficulties experienced by MAR patients in detecting motion. Figure 5.4 illustrates this. For low contrast stimuli, which would ordinarily be signalled by the M-cells, the displacements necessary to detect motion are very large; for high contrast stimuli, capable of involving the P-cells, the displacements tend towards normal.

The normality of the responses to the R/G isoluminant stimuli is striking. Figure 5.5 shows the R/G colour contrast thresholds for the Gaussian blurs reversing at a range of temporal frequencies to be substantially normal. Also studied, but not included in Paper 4, is the spatial colour contrast sensitivity. This was substantially normal in the case of the red/green gratings and in particular, there was no loss of sensitivity in the low spatial frequency range as there was for black and white gratings. Calkins et al. (1995), deny that there is any great over-representation of P cells in the fovea and the visual fields of the patients showed very little loss of sensitivity in the central 10 degrees. Therefore, it is unlikely that the apparently selective loss of visual function can be ascribed to the preservation of a small central retinal region.

This normality would follow if the R/G cells of the P- system are spared. The high acuity is taken to reflect P-cell activity which suggests that the midget ganglion cells

are functioning. There are substantial losses in sensitivity to blue light and it is argued in Paper 4 that, in addition to the rod bipolar damage, there is:

- (i) M-cell damage
- (ii) Sparing of midget ganglion cells
- (iii) Large ganglion cell vulnerability: e.g. bistratified B/Y cells

The chief conclusion is that disease can be selective in targeting neurons in specific pathways. The other conclusion relates to the achromatic 'contrast sensitivity function' of 'normals'; namely, that the thresholds for the low spatial frequencies are determined by the M-cells. This second conclusion is considered more fully in the final discussion (Chapter 6).

### 5.3 CONGENITAL STATIONARY NIGHT BLINDNESS

Congenital stationary night blindness (CSNB) refers to a group of genetically determined, non-progressive disorders, characterised by a variety of scotopic defects. The mechanisms and sites of loss are described by Sharpe et al. (1990). In some instances scotopic activity is completely absent, although it is more common that either the rate of return of sensitivity is delayed and/or the final threshold is elevated. Cone function may be normal or abnormal. It seems that although the cone receptors are present and functional to some extent, it is the central connections that are disturbed and this distinguishes it from other retinal degenerations in which it is known that the photoreceptors die. There are subdivisions of CSNB according to the inheritance pattern: autosomal dominant, X-linked recessive or autosomal recessive, with a further subdivision based on retinal appearance. This may appear (i) normal, (ii) take up a golden colour in the light adapted state, returning to normal in the dark adapted state (Oguchi's disease) or display small white dots scattered throughout the fundus. The patients studied in this investigation had 'complete', recessively inherited, congenital stationary night blindness.

#### 5.3.1 RESULTS & CONCLUSIONS FOR CSNB

The highly selective losses found in MAR were not found in CSNB. As with most retinopathies, the CSNB losses were present in chromatic and achromatic vision, and at high and low spatial frequencies.

#### 5.3.2 Paper 4

**Paper 4: VISION RESEARCH: IN PRESS**

**Selective Magnocellular damage in Melanoma-Associated  
Retinopathy: Comparison with Congenital Stationary Night Blindness**

by

Janet E. Wolf MSc, DIC(1) and Geoffrey B. Arden PhD, FRCOphthal.(2)

(1)Applied Vision Research Centre, City University, and

(2) Department of Electrophysiology and Psychophysics, Institute of Ophthalmology  
and the Electrodiagnostic Department, Moorfields Eye Hospital, London ,UK.

Running Head: Magnocellular damage in MAR

Keywords: Melanoma, Retinopathy, CSNB, Magnocellular, Spatio-temporal.

Correspondence to: Janet E. Wolf, Applied Vision Research Centre, City University,  
311-319 Goswell Road, London, EC1 V 7DD, UK.

Tel +44 71 477 8000, Fax +44 71 477 8355

## Abstract

Psychophysical methods for isolating and evaluating the function of specific neural pathways are used to characterise the visual losses in patients with melanoma - associated retinopathy ( MAR ). These are compared with those of congenital stationary night blindness (CSNB), a condition which displays a similar grossly abnormal ERG and loss of rod function. In MAR patients achromatic contrast sensitivity was greatly reduced in the low spatial frequency range. Stimuli chosen to isolate the magnocellular pathway were seen badly, whereas stimuli signalled primarily by the midget of the parvocellular pathway (isoluminant red/green or achromatic high spatial frequencies) were seen normally. This selective loss was not found in patients with CSNB. In MAR there is a selective loss of function subserved by magnocellular cells coupled with preservation of function subserved by the midget type 1 parvocellular cells.

A few patients with metastasising cutaneous malignant melanoma remain well for long periods, probably because the patient's immune system produces antibodies against the melanoma. Some of these patients develop Melanoma Associated Retinopathy (MAR) first reported in 1984 (Ripps Carr Siegel & Greenstein 1984; Berson and Lessel 1988). We report on three such patients whose clinical histories have been described elsewhere (Kellner Bornfeld and Forster 1994; Kim Retsas Fitzke Arden and Bird 1995). They have good visual acuity, sensitivity losses outside the central 10 degrees and suffer from night blindness and photopsiae as well as other more subtle disturbances of vision. The ERG is abnormal, with no rod b-wave and a very large negative "PIII", consistent with loss of rod bipolar function. This rare combination is also found in the ERG of patients with recessively inherited complete congenital stationary night blindness (CSNB) (Sharpe Arden Kemp & Bird 1990; Noble Carr & Seigel 1990). An abnormal antibody in MAR patients' serum binds selectively to rod bipolars (Milam Saari Jacobson Lobinski, Feun & Alexander 1993; Milam & Saari 1994). Since rod bipolars are all on-bipolars, the possibility arises that the visual disturbances reported by MAR patients might be selective to on-bipolars in general (Schiller 1982; Schiller 1984; Schiller Sandell & Maunsell 1986; Perry & Silveira 1988), with the patients' ability to see increments of light intensity being impaired, relative to the ability to see decrements (Chan & Tyler 1993). However our results did not confirm this but showed other losses of photopic function in MAR not found in patients with CSNB (although the scotopic losses are similar in the two conditions). Our interpretation of the subsequent results is that MAR causes damage to one of the retinal parallel pathways, analogous to that which can be produced by central lesion experiments in primates.

Studies in macaques and humans have shown there to be two main retino-geniculate types of neurone, parvo and magnocellular (P and M), that operate in parallel and have different morphologies and functional roles (Wiesel & Hubel 1966; de Monasterio & Gouras 1975; Schiller and Malpeli 1978; Derrington & Lennie 1984; Kaplan & Shapley 1986; Purpura Kaplan & Shapley 1988; Watanabe & Rodieck 1989; Lee, Pokorny, Smith, Martin & Valberg 1990). In addition psychophysical studies, on both species, have identified two distinct temporal channels; a sustained and a transient (~~Robson 1966~~, Kulikowski & Tolhurst 1973; Tolhurst, 1975) with the former (low-pass) signalling colour and the latter (band-pass) being achromatic (Kelly & van Norren 1977; Merigan 1989; Wolf & Lusty 1994). The relationship between these psychophysical channels and the different cell types is controversial, but in spite of some disagreement there is much common ground, exploited in the present work.

Usually, P and M ganglion cells have receptive fields with a concentric, antagonistic centre/surround organisation (Wiesel and Hubel 1966; de Monasterio and Gouras 1975 ; Zrenner 1983). The P-cells, about 80% of the total, seem to be a specific primate development. ( For summaries see Perry, Oehler and Cowey 1984; Lee 1995) They are colour-opponent and most can be described as "midget". In the fovea and para-fovea, the receptive field centre of each midget ganglion cell is driven by only one cone (long or medium wavelength). Inevitably, the receptive field centre of the ganglion cell must be colour specific. The surrounds of the midget ganglion cells are colour-opponent to the centres. In some colour-coded P cells with larger dendritic expansions, there is no spatial antagonism of the opponent colour mechanisms ( type II) (Wiesel and Hubel 1966; Calkins Schein Tsukamoto and Stirling 1995). Blue/yellow ganglion cells do not have spatial antagonism and have larger receptive fields. Specific "blue" bipolars connect to such cells (Kolb 1991,1994; Rodieck 1991). The existence of type II red-green cells has been questioned but it is possible that there is a continuum between spatially non-opponent and spatially opponent red-green cells (Kremers Lee and Yeh 1994) and it is these cells which may be primarily concerned with transmission of colour information, while other midget cells may serve primarily to distinguish very small targets (Rodieck 1991). 10% of R/G parvocellular cells may be spatially non opponent. This would be sufficient to explain the psychophysical properties of the chromatic channels (Calkins et al 1995). He also finds that in a block of primate fovea , where every cell was identified, 115 ganglion cells were midget, and 11 of the remaining 42 non- midget ganglion cells were found to be bistratified, i.e. non midget, and might form a substrate for red/ green type II cells.

P-cells have a relatively low contrast sensitivity and show a linear relation between contrast and firing rate up to high contrast (Kaplan & Shapley 1986; Purpura et al. 1988). Their spatial resolution is high and the temporal resolution of the pathway (at least at the cortical level) is relatively poor (Derrington & Lennie 1984; Lee et al 1990). By contrast, the M-cells are primarily concerned with achromatic and luminance signals. For any given eccentricity they have large cell bodies and dendritic fields, and correspondingly large receptive fields than P-cells, (Croner and Kaplan 1994; Perry et al 1984) ( although even this has been questioned by Crook et al 1988) which, coupled with a lower sampling density, makes them respond optimally to low spatial frequencies (Wiesel & Hubel 1966; de Monasterio & Gouras 1975; Derrington & Lennie 1984; Watanabe & Rodieck 1989). They are particularly sensitive to low

luminances and low contrast (Kaplan & Shapley 1986) although their responses saturate at relatively low contrast. In addition, with their larger axons, more rapid conduction velocities, greater proportion of cells with transient responses and greater temporal resolution (Shapley & Perry 1986), they provide the main projection to the cortical motion centres (Schiller & Logothetis 1990). In this work, the differences in response characteristics listed above were exploited and stimuli designed so at threshold they were seen only by one or the other of the pathways. The stimuli were similar (where possible) to those used in behavioural and single-cell experiments in macaques in order to facilitate the comparisons (Lee 1991) with such data. An exception to this was that the monkeys maintained steady fixation (Merigan 1989; Merigan & Maunsell 1990; Schiller et al. 1990). and testing patients under such circumstances was not practicable. In addition the stimulus was in the retinal periphery.

## METHODS

### Subjects.

The 3 MAR patients' clinical data has been fully described elsewhere (Kim et al 1995; Kellner et al. 1994). 5 age matched normals were used for comparison (mean age 61): these included the authors, who are experienced observers. Results were also obtained from 5 persons with CSNB: all were aged between 30 and 40: a description of these has been given (Sharpe et al 1990). Their results were also compared to a group of 4 normal persons of average age 26. All subjects were treated according to a Standard of Best Practice, and the protocol was approved by the local ethical committee.

### Psychophysical stimulation.

The stimuli used were generated on a computer graphics system (Arden Gunduz & Perry 1988) with a refresh rate of 94 Hz and a 24-bit colour palette. The colours used lay along the red/green colour confusion line of protanopes and the blue/yellow of tritanopes. Colours were altered without change of luminance. Thus when colour changed the magnitude of stimulation of all 3 cone types altered simultaneously. The system allows for individual subjects to equate the relative luminances of the R/G and B/G phosphor outputs (using heterochromatic flicker photometry at 22 Hz) to compensate for differences between their spectral sensitivity and that of the CIE standard observer. Thus isoluminant colours may be generated for each person

tested. Since our MAR patients were unable to see flicker at 22 Hz, this refinement had to be omitted for them. Contrast or displacement thresholds were measured using a 'modified binary search' routine (MOBS); these were either achromatic (i.e. luminance contrast) or chromatic contrast thresholds or, in the case of moving targets, displacement thresholds. The MOBS routine allows for indecisions and errors on the part of the patient, and in those with poor sight is slower but more precise than a truncated staircase method. Colour contrast is expressed as a fraction of the maximum colour separation possible along a given confusion line. Achromatic contrast is defined in the conventional manner. Colour contrast thresholds are given as a percentage of the maximum colour separation achievable along the colour confusion line, using the given phosphors. For large values of colour contrast, it should be remembered that (X,Y) space is not isotropic. The subjects viewed the target with free eye movements, i.e. in whatever manner was most comfortable.

Stimuli were chosen to stimulate selectively particular pathways: thus, the sudden brief appearance on a grey field of large lighter grey object (a Snellen optotype or a Gaussian blur) selectively stimulates cells which respond to brightening, i.e. cells with on-centres, whereas the brief appearance of a darker object selectively stimulates cells with off-centres. When the image disappears, any off-response induced in the first case (or on-response in the second) will be small, since cells with central receptive fields which respond to darkening will not have fully adapted to the brief brightening (Kelly 1969). In order to establish the spatial frequency response, vertical sinusoidal gratings were used. These appeared and disappeared with a temporal sinusoidal profile of 0.5 Hz; the contrast was either in the luminance of the grating, or in its colours. The stimulus chosen to isolate the M-cells was a low-contrast, achromatic Gaussian blur reversing from light to dark on a mid-grey background. The stimulus was then modified so as to isolate the P-cells: the hue reversed (with no change in luminance) from either red to green or blue to yellow on a mid-colour background, and the minimum detectable colour difference (in CIE space) was determined. The moving stimulus used was an achromatic low spatial frequency grating filtered spatially with a Gaussian blur. The whole pattern oscillated at 1 Hz.

In two MAR patients additional colour discrimination thresholds were found by means of a luminance masking technique (Barbur Harlow & Plant 1994). The stimulus consisted a set of vertical coloured bars on a background. The average luminance of the bars and the background were equal. The entire pattern was constructed from a series of elements, and the luminance of each element varied randomly and

independently of the chromaticity. The background was maintained at a constant chromaticity (white, near the centre of the chromaticity diagram), while the chromaticity of the bars could be moved in any direction in colour space away from the chromaticity of the background. The minimum colour change required for the patient to recognise the coloured bars was determined. In normal trichromats, the luminance modulation does not affect the chromatic displacement thresholds for the detection of the vertical bars provided chromatic signals are involved. Dichromats (with abnormal spectral sensitivity) cannot detect bars in the presence of random luminance masking even though chromatic changes are so great that they are limited by the phosphors of the display, (providing these changes lie along the appropriate colour confusion lines).

## RESULTS

A summary of the MAR patients' clinical data is shown in table 1.

Common to all was the presence of night blindness and photopsiae. Patient 1 spontaneously described difficulties with detecting moving objects. He had normal visual acuity, and nearly 1 log unit loss of sensitivity determined in the Humphrey field. Patient 2 unfortunately had a congenital red/green colour defect. Humphrey perimetry indicated a rise of threshold of 2.5 log units in the central 10 degrees and a vision of 6/12. Acuity in normal young adults is reduced to this level if 2.5 log units of neutral density filter are placed before the eye. The third patient with the highest titre of circulating antibody (Milam & Saari 1994), had developed posterior uveitis, which in one eye had seriously reduced the visual acuity. However, in the better eye, 6/18 could be obtained, Thus the photopsiae do not seem to affect visual acuity; the Humphrey estimates of threshold may be increased from the normal because the small flashing targets are confused with the photopsiae.

Table 1

Name	IF	RP	G. R-C
date of birth	19.8 29	28.2.33	1.7.49
Sex	M	M	M
diagnosis of melanoma	March 1991	May 1992	Dec 1989
metastases seen?	Y	Y	Y
onset of retinopathy	Feb 93	Jan 1993	June 1991
Deceased	May 1995	May 94	_____
other eye condition?(preceding)	exfoliative glaucoma †	deuteranope	
presenting symptoms	Photopsiae	Photopsiae	Photopsiae; loss of VA
VA	1.0 1.0	0.5 , 0.66	0.05, 0.5‡
Fundus appearance	Normal	Normal	Vitreous haze
Dark adapted thresholds	elevated 3 LU	elevated 3 LU	Elevated 3 LU
average photopic field (+/-10 degrees) sensitivity loss§	7 dB loss*	25 dB loss	8 dB loss
Antibodies present?	Y	Y	Y
progression of retinopathy	colour vision improved after 1 year	?	uveitis progresses, fluctuates
other systemic disease.	Rheumatoid arthritis, pulmonary embolus		

\* Blue field: white unreliable due to confusion with photopsiae.

† one eye only affected : psychophysical tests on other eye

‡ tested eye

§ Humphrey field tester

Electroretinograms were obtained on all patients, and all, including the 3 MAR patients, showed the classic changes associated with complete CSNB (Riggs 1954; Hirose 1956; Miyake 1989; Sharpe et al. 1990; Noble et al. 1990; Noble Carr & Siegel 1990). They were identical with those previously reported for MAR (Alexander Fishmann & Peachey 1992) and therefore are not reported in detail.

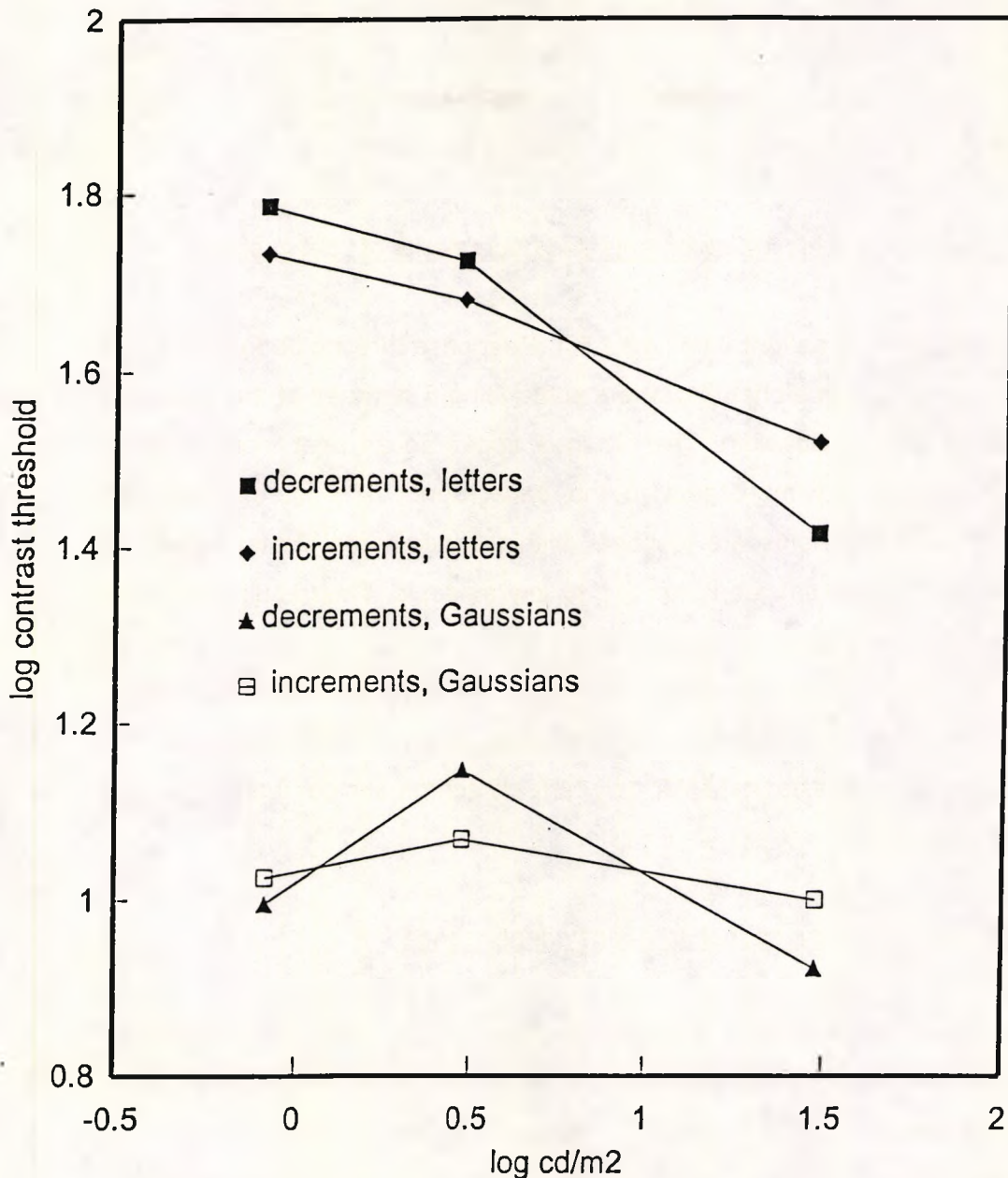
#### Achromatic contrast thresholds for increments and decrements of light intensity.

Such results are shown for patient 2 in figure 5.1. Response thresholds for two types of stimulus are shown: large alphabetic letters subtending 5 degrees at the pupil and Gaussians with a similar half-width. The images appeared as brief increments or decrements of luminance with respect to the background. The incremental and decremental contrast thresholds are identical (within experimental limits), over a range of mean luminances between photopic to low mesopic. This result eliminates the possibility of the damage being specific to the "on" system. However, they are all grossly abnormal. MAR 1 gave similar results, but was only tested in the photopic region. The poor performance with these large targets, taken in conjunction with the patients' good acuity, suggests that MAR only affects achromatic contrast sensitivity at low spatial frequencies.

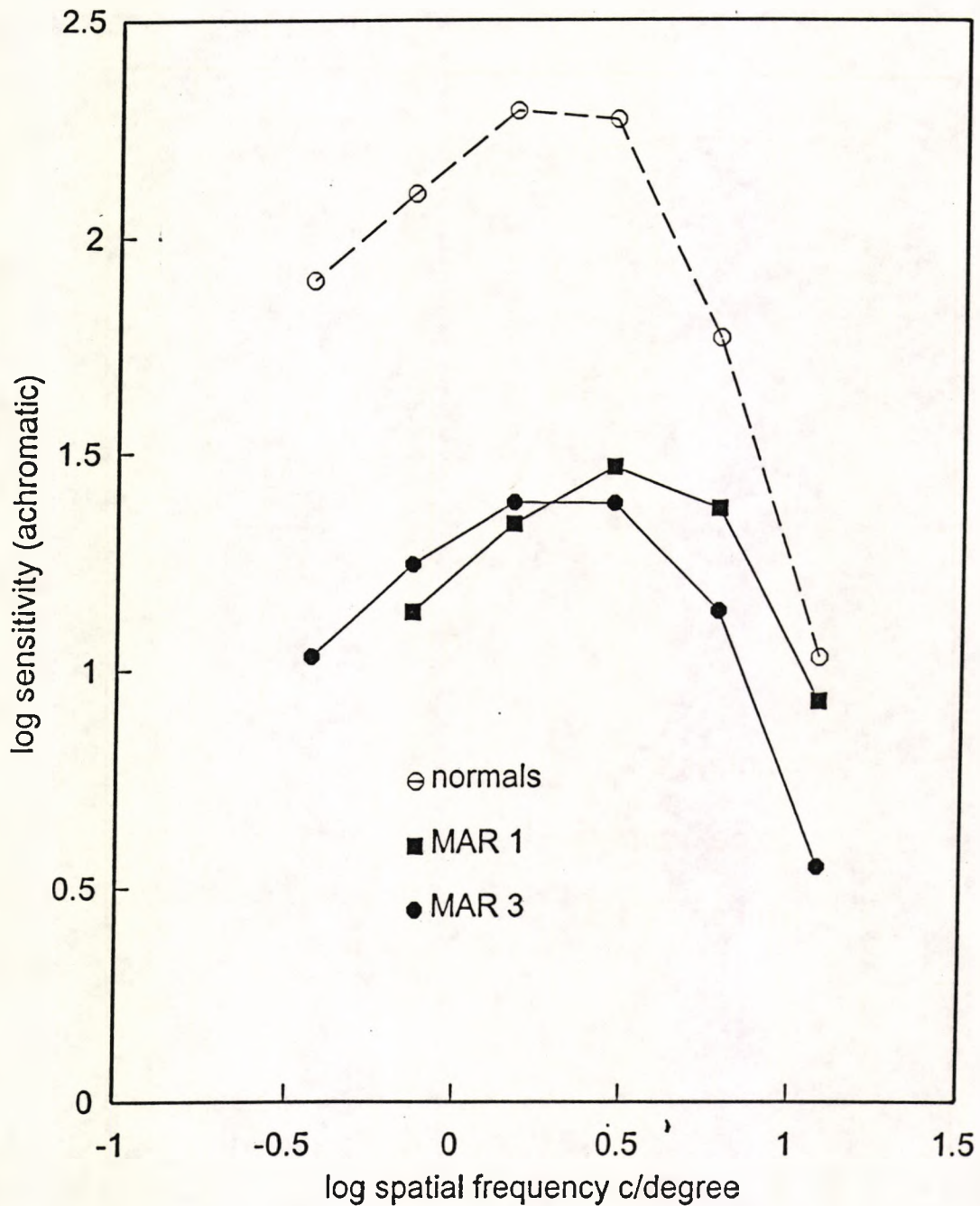
#### Achromatic contrast sensitivity: spatial frequency dependence.

Figure 5.2A compares MAR patients 1 and 3 with age matched normals. The normal values are similar to published data (Swanson, Wilson and Geise 1984). The patients have a massive loss of luminance contrast sensitivity in the low spatial frequency range, while the losses at higher spatial frequency (even in the patient with posterior uveitis) are not so great: this result is consistent with the relatively good acuity, determined with a conventional test-type. The results from the second patient were similar to the others, but since he has a grossly elevated visual threshold on the Humphrey perimeter (see table 1) the comparability of the normal data might be questionable. The standard errors of the mean results are included in the 5. captions in this and subsequent figures.

Figure 5.2B shows the results for this test obtained with five CSNB patients. This group were much younger than the MAR patients, and the normal control group was age-matched. For comparison, the contrast sensitivity functions of the older normals are also shown in 5.2B. There is a loss of contrast sensitivity across all spatial frequencies which appears to be greatest at the higher spatial frequencies tested.

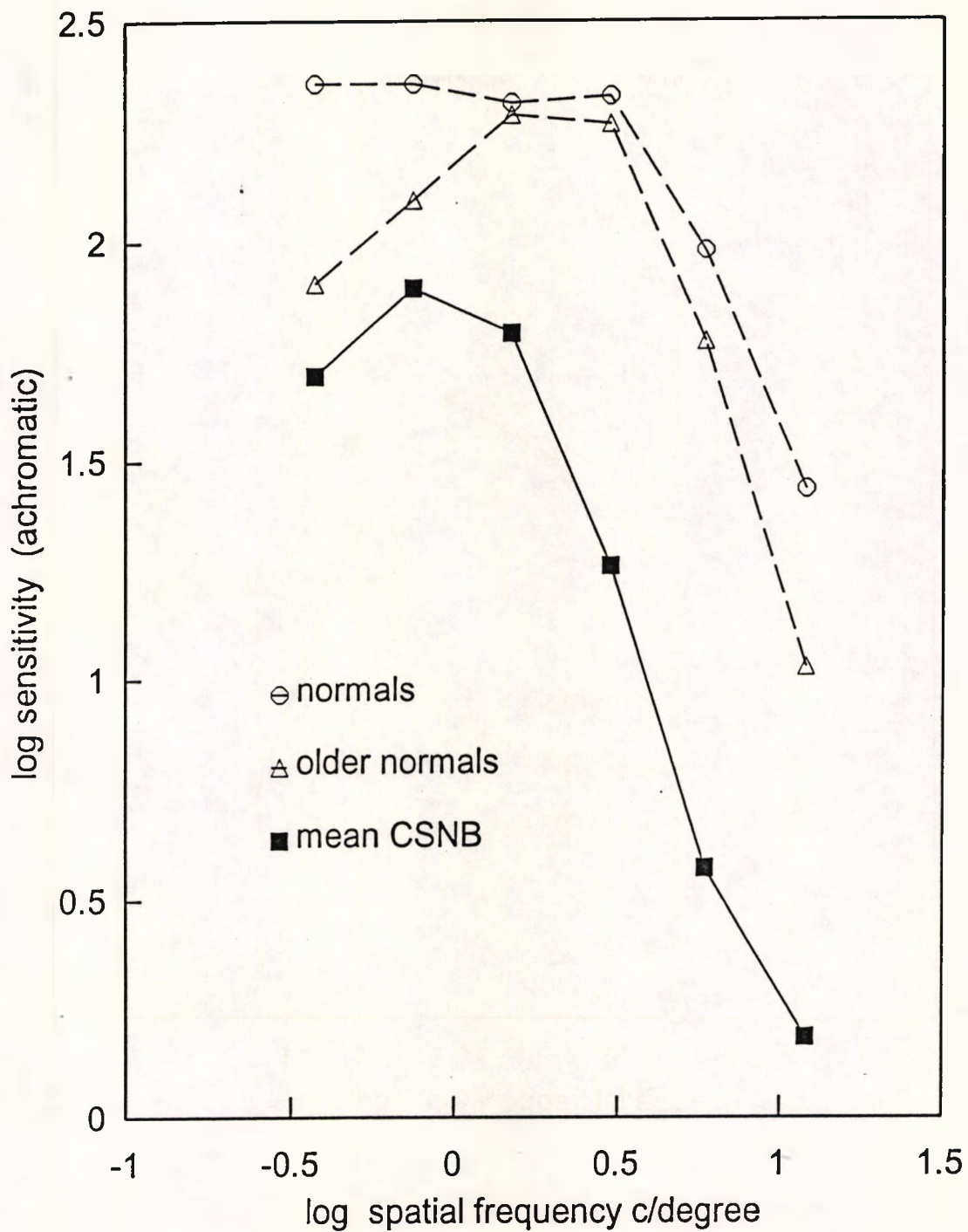


**Figure 5.1:** Contrast thresholds for briefly presented achromatic stimuli that were either of a lighter or darker grey than the background. The targets were either large random letters (6 degrees presented for 20 ms at 200 ms intervals), or large Gaussian blurs whose contrast varies temporally with a sinusoidal profile of 1 Hz. The contrast thresholds are all very high: for the letter targets, > 30%, and for the Gaussians >10%. However, the threshold does not change greatly with luminance, and for each type of target increment and decrement thresholds are seen to be the same. Note these results were obtained in a patient MAR2 whose visual thresholds (determined in a Humphrey perimeter) were elevated by 2.5 log units. The exact linear spatial frequencies used in this and other figures are : 0.33: 0.75: 1.5:3.0: 6.0: 12.0 cycles /degree.



**Figure 5.2:** The achromatic contrast sensitivity function: The stimulus consisted of sinusoidal stripes, modulated at 0.5Hz, extending over a field of 6 degrees.

A: MAR patients 1 and 3 compared to 5 age matched normals ( mean age 60.8, SD 4.4 yr.) . There is a massive reduction in sensitivity at low spatial frequencies tending towards a normal value at high spatial frequencies. Note MAR3 has a vitreous flare which reduces acuity and contrast sensitivity at higher spatial frequencies due to optical causes. The variance of the normal results is greatest for the highest and lowest spatial frequencies where twice the standard error of the mean thresholds illustrated (SEM)s alter the sensitivity by 0.1 of a logarithmic unit ( LU).



B : 5 CSNB patients. These patients were younger than the MAR, and a separate group of normals was employed- the normal data from fig 2A is introduced for comparison. Note, that unlike the MAR patients, the CSNBs have the greatest loss at high spatial frequencies. The variance of the young normals at the highest spatial frequency is similar to that of the older group ( Fig 2A), but for the other points is within the symbols. Twice the SEM of the CSNB patients shifts mean values by 0.2 LU

This is consistent with their known poor visual acuity. The difference between these patients and MAR is quite clear.

In summary the MAR patients have a marked selective low-frequency achromatic loss of spatial contrast, which is not seen in normals or in CSNB. In the low spatial frequency range, young normals have an achromatic contrast threshold as low as 0.4%, which indicates that the threshold is determined by the M-cells (Kaplan & Shapley 1986; Purpura et al. 1988). Thus one explanation for the abnormality in the patients could be that they have a defect of the magnocellular system, and the next experiments introduced stimuli intended to isolate the two systems. The relatively good test-type acuity and contrast sensitivity at high spatial frequencies suggests parvocellular sparing (Merigan 1989; Schiller et al. 1990).

M-cell isolating stimulus: achromatic Gaussian blur reversing from light to dark on a grey background:

Figure 5.3A shows that the temporal variation in achromatic contrast sensitivity for a low spatial frequency (part of the de Lange curve) in normals and in three MAR patients. The range of frequencies investigated is limited by the refresh rate of the monitor. However, the reduction in contrast sensitivity is sustained at a fixed level over a wide range of temporal frequencies. This is consistent with the threshold being determined by the same mechanisms over the range of temporal frequencies investigated. At 10 Hz this must be the M-cell pathway since it is known that such reversing stimuli cannot be seen at all by monkeys with M-cell lesions (Merigan & Maunsell 1990). Thus the result of 5.3A results strongly suggests that the losses at low temporal frequencies are also due to substantial M-cell damage in our patients. It follows that in the normals at threshold, perception of low spatial frequency and low temporal frequency achromatic targets must be determined by the M cells. (see discussion). CSNB patients do not have such losses in temporal contrast sensitivity (fig 3B).

M-cell isolating stimulus: Achromatic low spatial frequency sinusoidal stripes oscillating at 1 Hz.

Figure 5.4 shows grossly abnormal threshold displacements (MAR 1) for sinusoidal gratings (1 c/degree) which oscillated at 1 Hz. Such images are assumed to be processed by the M-pathways. At higher contrasts the displacement threshold tend

towards normal at high contrasts, but such gratings are sufficient to stimulate the P-pathways. At low contrast, where the grating would be in normals detected preferentially by the M pathway, the patient's thresholds rise. Other grating spatial frequencies and oscillation rates were used, and also red-green isoluminant gratings: the elevated displacement threshold seen in Figure 5.4 was not observed when colour contrast gratings were used. This patient was also shown the "frequency doubling illusion": When (for example) 4 periods of a low spatial frequency grating is contrast-reversed at 20 Hz, a normal person sees 8 bars of the grating, and this is attributed to M cells which respond to each half-wave. MAR 1 could not see the stimulus until the contrast was 100%, when he saw 4 bars.

#### P-cell isolating stimulus : Gaussian blur reversing chromatically.

The same Gaussians, described in figure 5.3, were modified so that the luminance remained constant whilst the hue changed, reversing between either green and red or between blue and yellow. Thus the spatial and temporal features were identical to the achromatic stimulus. As described in Methods, precise determination of colour discrimination requires removal of luminance clues, and usually equiluminance is achieved by a flicker method. MAR patients were unable to see flicker at 22 Hz. Therefore it was necessary to assume their spectral sensitivity matched that of the standard observer. If this not the case, a small luminance component will be introduced into the nominally isoluminant coloured stimuli. However, with the Gaussians where the MAR patients suffer a loss of achromatic (luminance) contrast, this luminance component cannot be significant. Figure 5.5A shows, over this same range of temporal frequencies, that the red/green chromatic contrast sensitivity is relatively normal for the two MAR patients whose colour vision was known to be normal prior to developing MAR. Also in CSNB, there is little loss of red/green contrast sensitivity (fig 5B). Figure 5.6A shows very variable losses of sensitivity to the blue/yellow stimuli for the 3 MAR patients. In CSNB the losses are less but again very variable (fig 6B).

#### P- cell isolating stimuli: Chromatic isoluminant gratings.

When coloured gratings of higher spatial frequency are employed, the normal threshold colour contrast is much higher than for Gaussians, and therefore any residual luminance clue in the display (see the paragraph above) may become important. Therefore we only briefly report the results obtained in MAR and CSNB with such stimuli. MAR 2 had a congenital red/green defect. In MAR 1, red/green

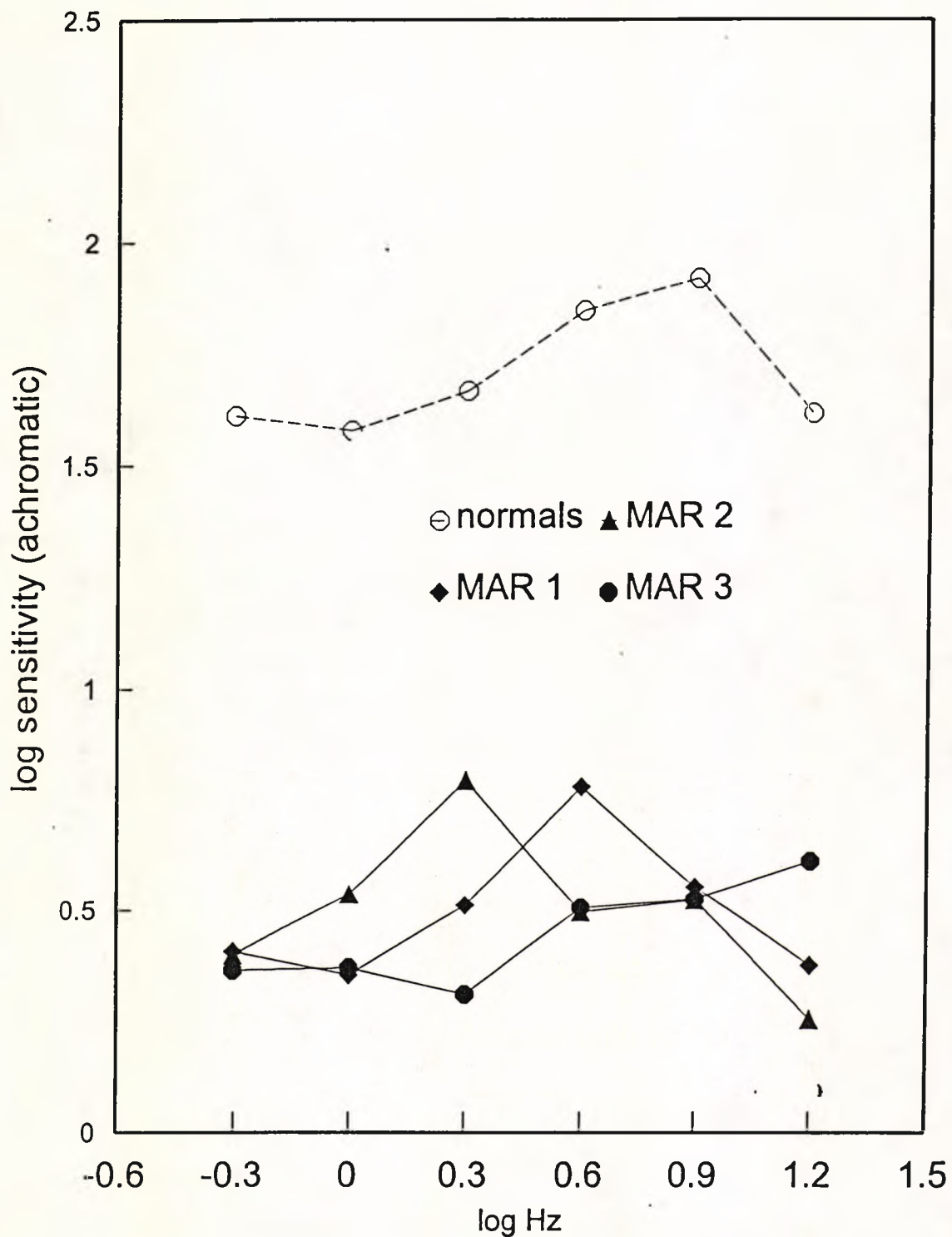
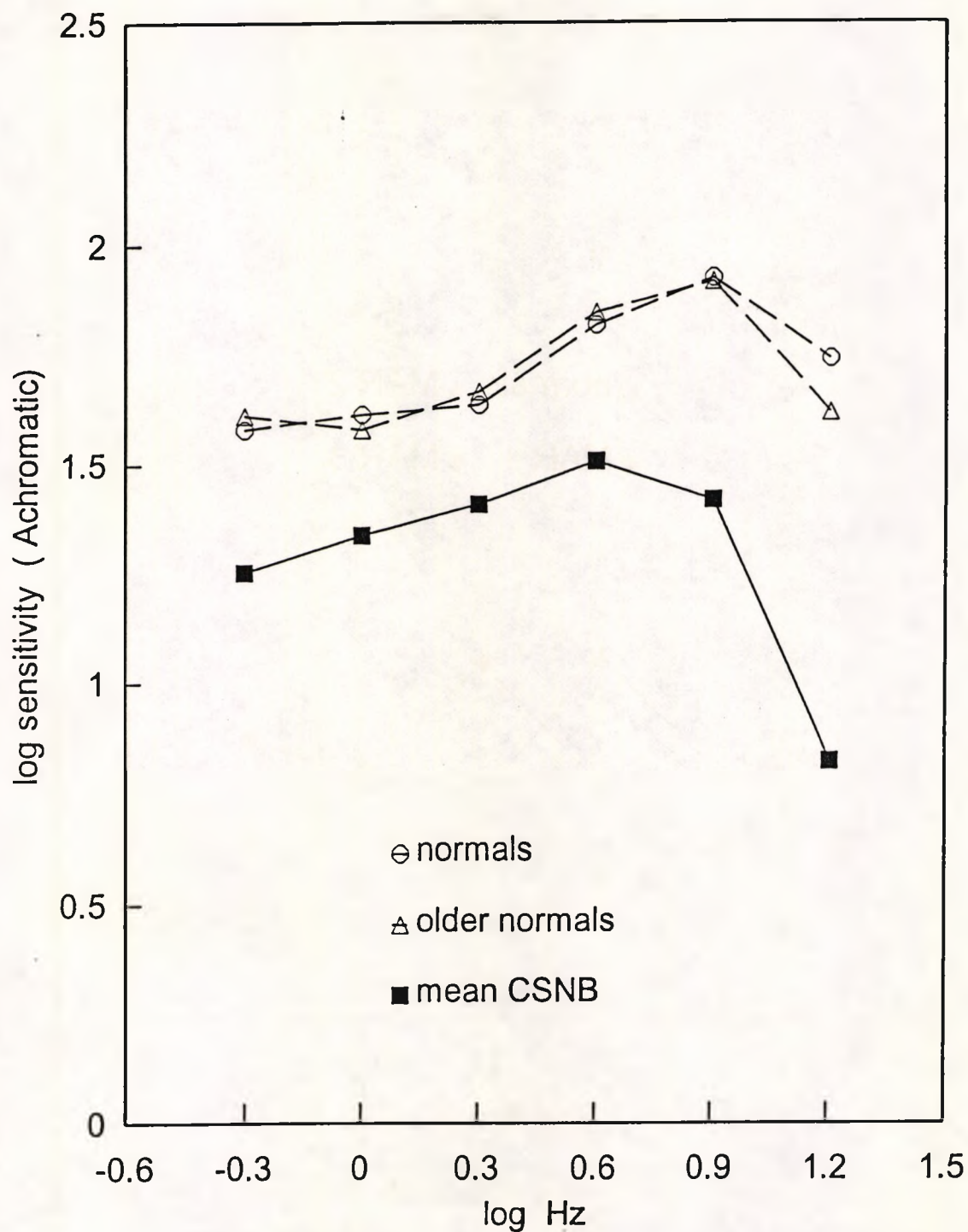


**Figure 5.3:** Achromatic temporal contrast sensitivity: The stimulus was an achromatic Gaussian blur subtending approximately 4 degrees at half maximum contrast, reversing sinusoidally in time. This stimulus selectively excites the magnocellular system. The exact linear temporal frequencies used in this and later figures were : 0.5:1:2:4:8: 16 Hz.

A: 3 MAR patients compared to age matched normals. The variability of the normal result: twice the SEM of the mean normal values is 0.2 LU or less for all frequencies.



B: Temporal contrast sensitivity in CSNB patients compared to age matched normals. The stimulus was the same as for figure 3A. Note, the sensitivity losses of MAR are not found in these patients. Normal variances - as for fig 4. twice the SEM of the mean values shown for the CSNB varies from 0.22LU at 0.5 Hz to 0.36LU at 16 Hz.

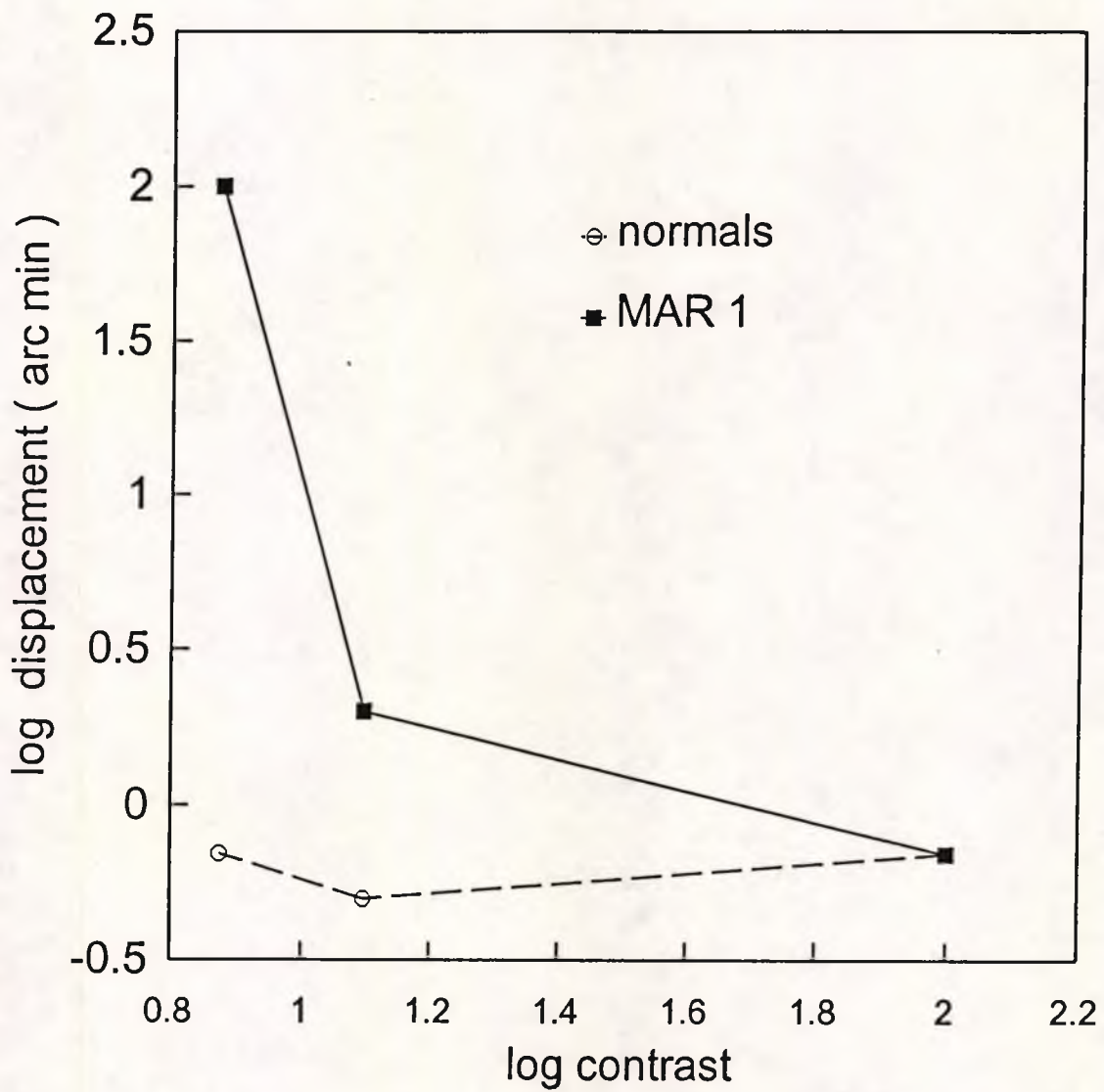


**Figure 5.4:** Displacement thresholds as a function of achromatic image contrast. in MAR 1 compared to normal. The stimulus was a vertical 1 c/degree sinusoidal grating, oscillating sinusoidally in the horizontal axis at 1 Hz.

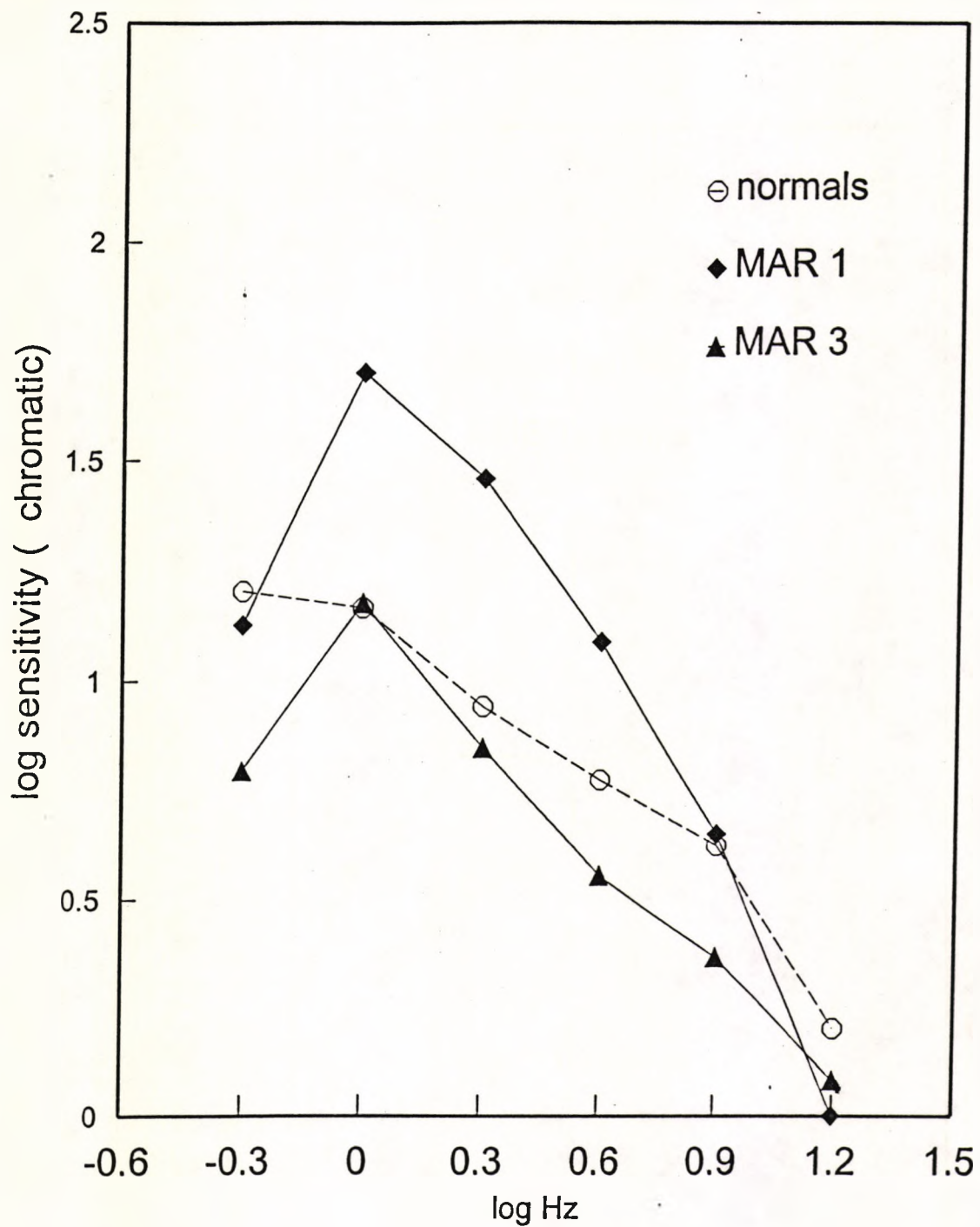
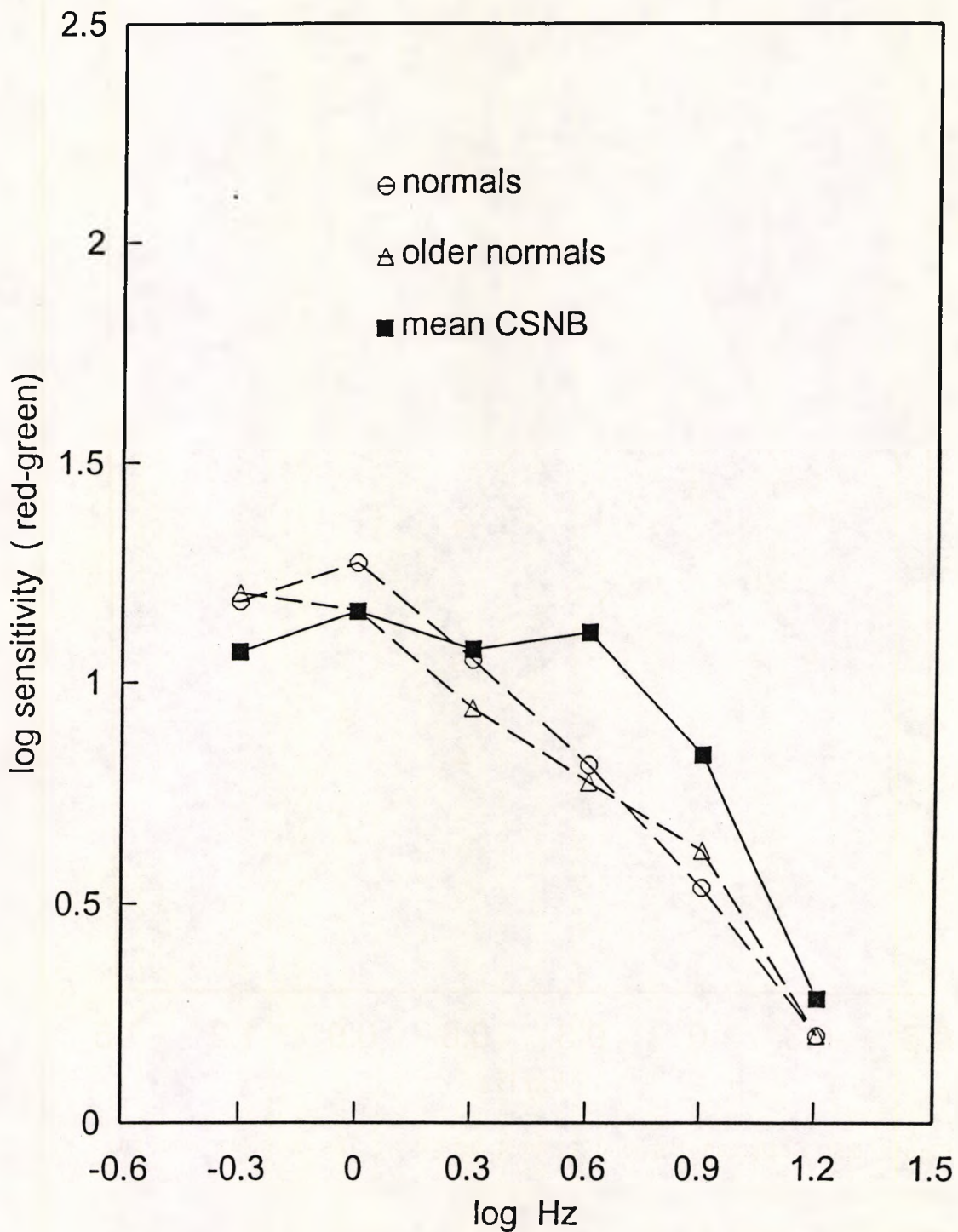


**Figure 5.5:** Red/green temporal contrast sensitivity: The stimulus was an isoluminant, red/green chromatic Gaussian blur which selectively excites the parvocellular system. It subtends approximately 4 degrees at half maximum contrast, reversing sinusoidally in time. Spatially and temporally the stimulus is equivalent to figure 3; the stimulus colours are on a protanopic colour confusion axis.

A: MAR patients 1 and 3 (without congenital red-green defects) compared to age matched normals. Note that the contrast sensitivity losses are small. Twice the SEM of the normal mean values ranges from 0.12 LU at 16 Hz, 0.24 LU at 4 and 2 Hz, to 0.16 LU at 0.5 Hz



B: 5 CSNB patients; the normal comparisons are age matched. Note, the younger normals used for these comparisons were naive, while the older normals whose data are shown in fig 5A included 2 experienced observers with low thresholds. As with MAR, the losses are small. The variance of the normal data for the elderly group is as given in 5A. Twice the SEM of the mean data for young normal adults is 0.19 LU at 0.5 Hz, 0.27 LU for 1,2, and 4Hz, 0.14 LU at 8 Hz and 0.09 LU at 16 Hz. The CSNB data for all frequencies have a corresponding 2 x SEM of 0.14 LU at 0.5Hz, 0.12 at 1 Hz and 0.02 for other data points.

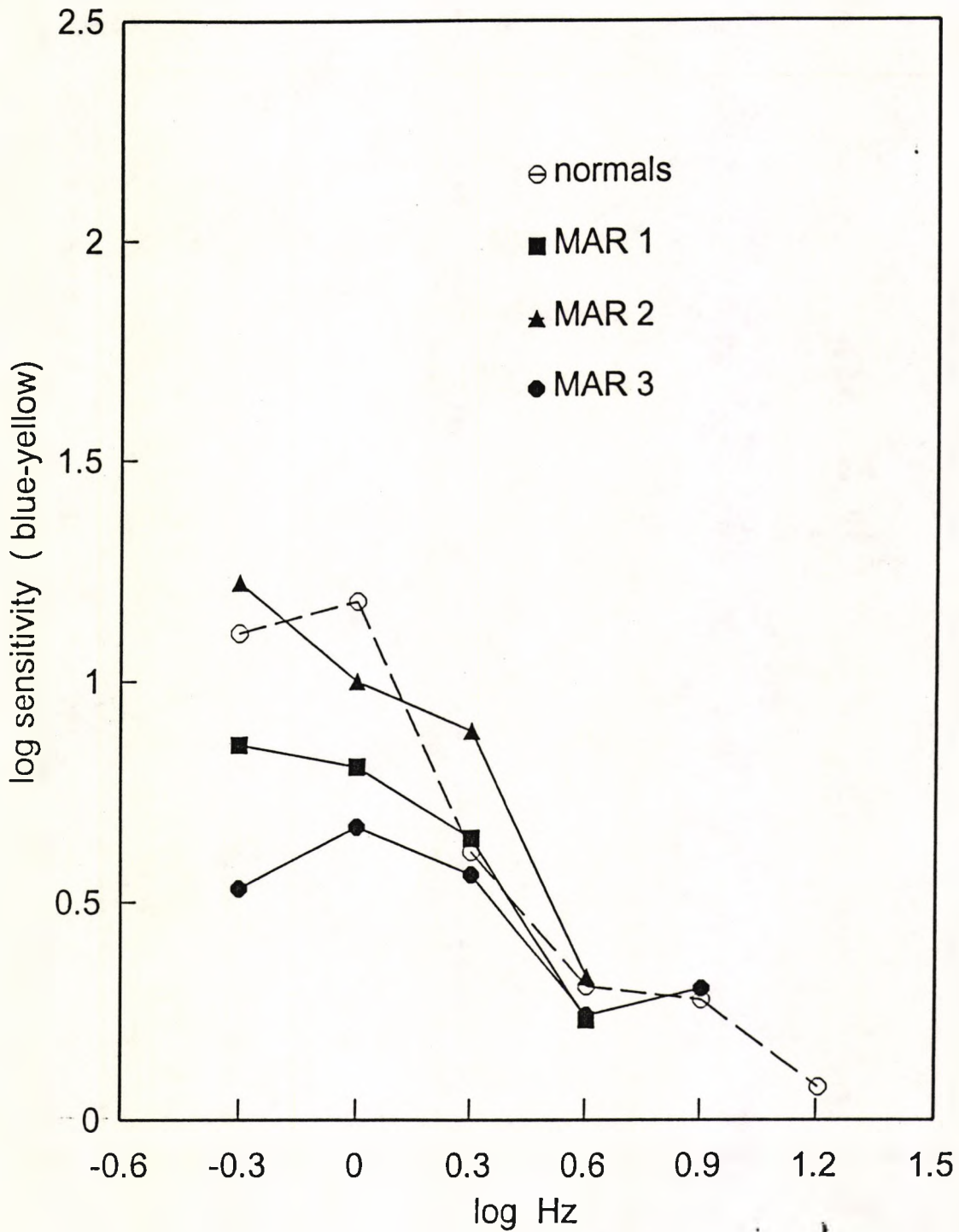
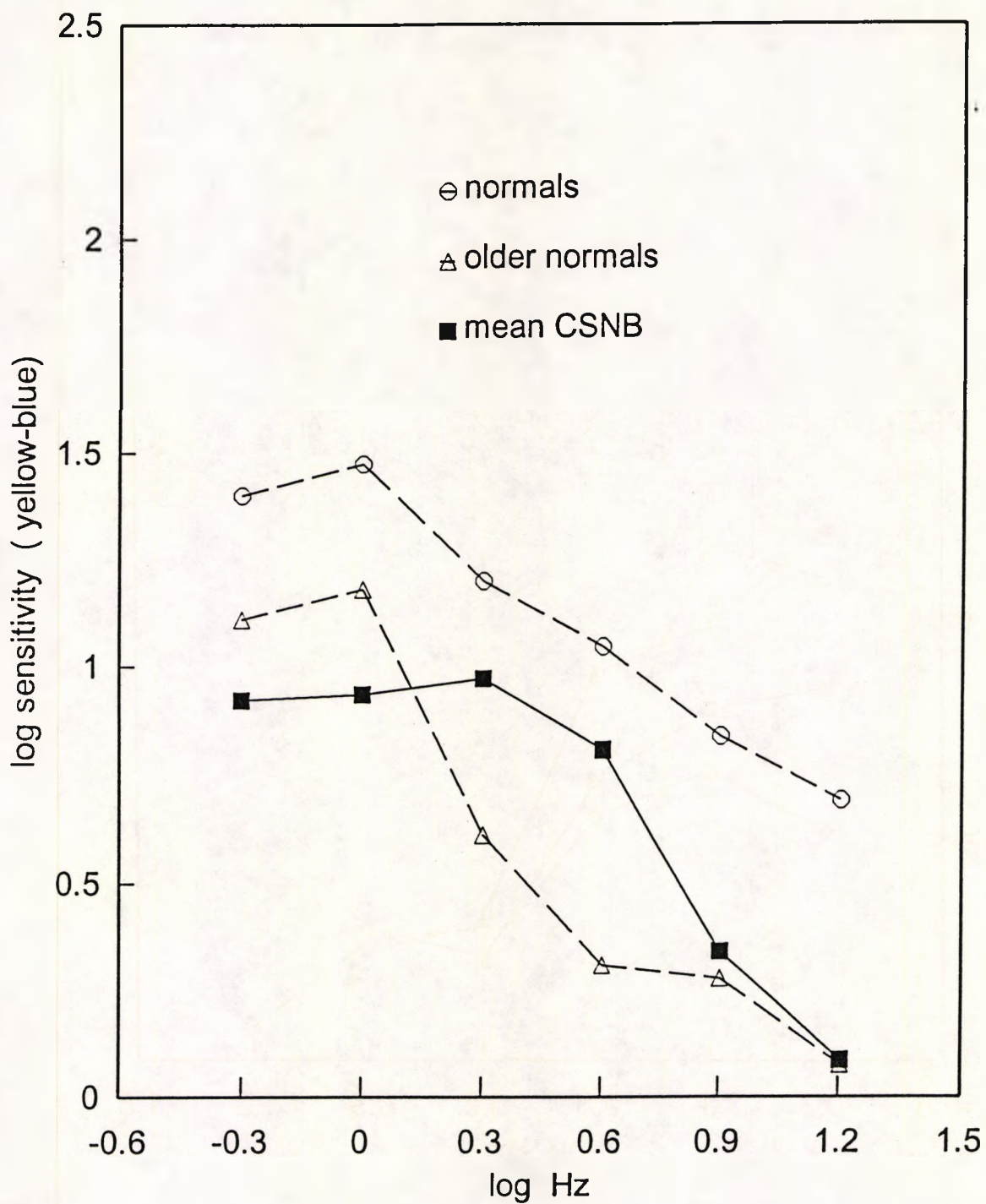


**Figure 5.6:** Blue/yellow temporal contrast sensitivity: The stimulus was equivalent to that of Figure 5.5 with the colours lying along the tritanopic colour confusion axis.

A: 3 MAR patients: Contrast sensitivity losses vary considerably. Twice the SEM of the normal mean values ranges from 0.1 LU at 16 Hz, to 0.4 LU at 4Hz 0.33 LU at 2 Hz, to 0.08 LU at 0.5 Hz



B: 5 CSNB patients: As with MAR there is considerable variability, although the losses are much less. For younger normal results, the corresponding shift in LUs is 0.08 for 0.5 Hz, 0.16 for 1 Hz, 0.32 for 2 Hz, 0.3 for 4, 0.08 for 8 and 0.05 for 16 Hz. Twice the SEM of the CSNB data produces a shift of 0.14 LU for 0.5 Hz, 0.06 for 1 Hz, 0.04 for 2 Hz, 0.16 for 4 Hz, 0.06 for 8 Hz and 0.05 LU for 16 Hz.

sensitivity loss, if present, was nearly constant across spatial frequency and no more than 0.2 log unit. In MAR 3, the average loss was 0.5 log unit and reduced at higher spatial frequencies. The mean CSNB losses to red/ green were about 0.3 log unit, and not dependent on spatial frequency. For blue/yellow gratings, MAR 2 was within the normal range, but MAR 1 and MAR 3 had losses of about 0.5 log unit, which were higher at higher spatial frequencies: they were unable to see blue/ yellow gratings of spatial frequencies  $>4$  cycles/ degree at the highest contrast we could display. CSNB patients had losses which were apparently similar to MAR. In summary, with colour-contrast gratings, the losses were much less than with achromatic, and they were not obviously spatial frequency dependent.

#### Additional tests of colour vision

MAR 1 and MAR 3 were tested with the 100- hue test: and both were within normal limits for their ages and showed no losses concentrated in any axis. Chromatic discrimination using luminance masking ( see methods) is shown in Figure 5.7 for MAR 1 and MAR 3. MAR 1 is nearly normal, but MAR 3 shows a massive tritanopia.

### DISCUSSION

Despite their good visual acuity (and in two cases good red-green vision) our MAR patients complain of greater visual disturbances than the CSNB patients with whom they have been compared. Partly they are disturbed by photopsiae, described as scintillating lights. However the main complaints are difficulties with particular tasks. One of our patients played golf, and he complained that as soon as the ball moved..... it vanished. When it was at rest he could see it! Thus without any formal psychophysical experimentation, there was a strong pointer towards M-pathway damage. Figure 5.5 shows little loss in MAR when P-cells are stimulated by Gaussians, and Figure 5.3 that the considerable loss to achromatic Gaussians (which must be mediated by M-cells at 10 Hz) is the same at high and low temporal frequencies. Additionally, in MAR both the informal detection of motion and measured achromatic motion displacements were grossly abnormal, again indicating selective M-cell losses (Schiller et al. 1990). Therefore, our results shed an interesting light on normal vision, for it follows that the low spatial-frequency range of the normal human achromatic contrast sensitivity function must reflect the activity of the M-cells ( in contrast to monkey, see below).

CSNB patients with poor visual acuity, subnormal colour vision and ERG abnormalities very like those of MAR, do not have a selective loss of low spatial

frequency achromatic vision. and therefore we have no evidence in them for any selective loss of the M pathway. Again, this indicates that there is a unusual pattern of loss in MAR, and our results cannot be explained by any quirk of the experiments.

#### Selective loss of retinal function not related to retinal locus.

At the LGN and retinal level, the proportion of magnocellular/parvocellular cells (per degree<sup>2</sup> of visual field) does not vary significantly with eccentricity from 1- 10 degrees (Silveira and Perry 1991) and is approximately 5-10%, a figure that corresponds to the foveal reconstruction of Calkins et al 1995 and the estimates of Livingstone and Hubel 1988. The MAR patients have peripheral field constriction, but ( Table 1) in the macula and paramacula where we have made measurements there is little loss of photopic threshold. Our large targets test retinal function over much more than the fovea. Thus, even if we accept that there is a reduced representation of M-cells in the region of the foveola, the detection of large chromatic Gaussians or low spatial frequency chromatic gratings where the achromatic equivalents cannot be seen, must indicate selective channel loss.

#### Cellular basis of the disturbance.

The simplest explanation of our findings is that in MAR the midget system, is relatively unaffected, while other neurones are damaged. The low spatial frequency achromatic system is grossly impaired and this implicates the M-cells. There may be some loss to blue/yellow and the second class of red/green discrimination: this may be explained if the non-spatially opponent (type II bistratified P-cells ) are affected. The rod system is also affected but the evidence from histology and the ERG implies that rod bipolars are damaged. Rod signals enter both magno and parvocellular pathways ( predominantly the former- Purpura Kaplan and Shapley 1988). Under the condition of our experiments, rod input can normally be neglected: it may be that this is the source of the photopsiae which our patients experience. The morphology, location of synapses and connectivity of retinal midget pathway differ so significantly from the other bipolar and ganglion cells that they might be spared by a disease process which affects other retinal systems. Our psychophysical experiments cannot help establish whether the damage in MAR occurs at ganglionic or preganglionic level in the non-midget pathway.



### Comparison with animal behavioural experiments.

Lesion experiments on behaving monkeys (Merigan 1989) show that elimination of P-cells results in greatly elevated thresholds to achromatic high spatial frequency targets, whereas the elimination of M-cells had no effect. Achromatic, high spatial frequency and coloured isoluminant images are generally taken to be signalled by the P system. (de Monasterio & Gouras 1975; Livingstone & Hubel 1987; Derrington & Lennie 1984; Schiller et al. 1990). All these results are consistent with our conclusion that in MAR the P-cells are relatively undamaged.

However lesion experiments in behaving monkeys indicate that for achromatic targets of low spatial frequencies and low temporal frequencies the P-system is still the most sensitive. The contrast sensitivity of individual P-cells is low - 5% Kaplan and Shapley 1986- and to account for the relatively high sensitivity (1.7%) of the entire functioning pathway (Merigan 1989) has invoked probability summation, an interpretation which has not convinced others (Shapley and Perry 1986; Kremers Lee & Kaiser 1992). Our young normals have an achromatic contrast sensitivity for low spatial frequencies that is even higher (0.4%) than Merigan's monkeys, a sensitivity that could scarcely be attributed to probability summation within the human P-cell population, again pointing to the conclusion that in normals at threshold our Gaussians must be perceived by the M-cell driven system. The discrepancy between human and lesioned monkey data may be explicable by a difference in the stimulus conditions. The monkeys maintained a steady fixation and may have been so well trained that the tremors and flicks that remained were insufficient to refresh their M-cells' larger receptive fields (Livingstone & Hubel 1987). The humans, with their unconstrained eye movements (we see them moving their eyes around) would retain the maximal sensitivity of the M pathway.

### How does immunologically induced damage cause the patients symptoms?

It seems therefore that the loss of function largely excludes the midget beta ganglion cell. This raises interesting possibilities as to the action of the antibodies. The loss of b-wave, and preservation of the receptor response in the ERG changes imply loss of rod bipolar cells (Sharpe et al. 1990; Martin & Grunert 1992), and in the mouse, a class of bipolar can be double-stained both by PKC (which identifies rod bipolars) and also, by anti-human antibodies linked to a fluorescent marker applied after incubation with MAR patient's serum. Analogous experiments on human retina are

less conclusive, but in the mouse it appears that the double label is always carried by the same cells. These findings make it less likely that the antibody in MAR could affect a number of different cell types in the retina, (although it is still possible). If the anti-melanoma antibody affects rod bipolar cells and makes the axonal presynaptic membrane very "noisy", this noise could be transmitted onward and cause the scintillations described by the patients. What pathway could connect the rod bipolar "noise" to the midget system? It has been suggested that the rod amacrine system is selective for magnocellular ganglion cells (Purpura et al. 1988; Purpura Tranchina Kaplan & Shapley 1990), consistent with our findings with achromatic targets. Other workers find that there is rod input to the bistratified ganglion cells, both the blue/yellow and the red/green, and this would explain the blue/yellow losses, and allow some loss in red/green. It is not clear if rod signals input to the midget red/green cells (Purpura et al 1990; Kolb 1991, 1994), but if so, then any rod "noise" or malfunction does not appear to affect either the colour discrimination or the high frequency spatial discrimination which this system subserves.

Finally, whatever the cause of the M-pathway loss of function, the performance by the MAR patients throws some light on the functional roles of pathways in normals. We report elsewhere (Arden Wolf & Plant 1995) another acquired condition which leads to selective damage to the colour channel.

#### 5.4 THE 'EPIDEMIC NEUROPATHY' OF CUBA, 1992 -93

During the first quarter of 1992, 39 cases of retrobulbar Optic Neuritis were diagnosed in Pinar del Rio, the tobacco growing region of Cuba. This was an unusually high number for this region and prompted the formation of a National Commission set up to define the clinical characteristics of the disease and monitor the incidence of the disease. At that time the essential elements were:

- (1) Progressive loss of vision in both eyes
- (2) Discomfort in intense light; visual improvement evident in poor lighting
- (3) Difficulties to see colours, particularly in the red/green axis
- (4) Eye fundus with mild macular pallor, mild redness of the papillomacullar bundle and peripapillary edema.
- (5) Central or cecocentral scotoma extending no more than 10 degrees
- (6) Loss of red/green colour discrimination (third Ishihara plate)

In addition these patients showed neurological disorders with a variety of manifestations: hot and cold sensations, perspiration in hands and feet accompanied by a lot of pain in their feet and legs.

Taking account of the high proportion of smokers (92.8%) together with evidence of a low urinary Vitamin B<sub>1</sub> level, the Commission concluded that the condition was a Nutritional-Toxic Optic Neuritis, similar to the previously encountered tobacco-alcohol amblyopia. Later the observation was made that it was not found in children, pregnant women, or old people, who received dietary supplementation .

By the end of 1992, there were 358 cases diagnosed cases in the same area, with 43.7% showing neurological disorders. As the disease incidence increased and spread to other areas of the country, the neurological manifestations of the peripheral type increased, and occasionally appeared as the only symptom. The frequency of the combined cases led the Commission to conclude that the disease should be considered as one condition, described as Epidemic Neuropathy, with two fundamental clinical forms: the optic and the peripheral. The epidemic curves followed a parallel pattern, but out of phase in time, where the peripheral followed the optic, both in rise and fall of the numbers diagnosed.

By March 1993, 60 diagnostic centres were set up over the whole country, and the distribution of vitamins was started in Pinar del Rio. In May a vitamin supplement (Neovitamin II) containing B-complex vitamins, vitamin A and folic acid, is distributed to the whole population. and by May there was a marked decreases in the optic form with an ongoing increase in the peripheral form. By June 1993, there were 45,822 cases in a total population of 42 million, with 56.7% belonging to the optic form. Six weeks later the epidemic had largely subsided. The condition is still thought to be due to a nutritional deficiency but a specific micronutrient has not been implicated.

#### THE OPTIC FORM OF THE DISEASE: OPTIC NEUROPATHY & / OR RETINOPATHY?

The optic form of the disease was thought to be an optic neuropathy superficially resembling those disorders associated with nutritional deficiency in alcoholics and in prisoners of war (Roman, 1994) which have been reported from the Caribbean previously (Strachan, 1897). The investigation, described in this work, was carried out over two separate visits in 1994-95, with the intention of establishing whether the optic form was solely an optic neuropathy, or whether there was also retinal damage. 24 cases in whom substantial recovery of vision had occurred following treatment were investigated. It is the results of the psychophysical investigation that are included as part of this thesis. However, since these are interpreted in conjunction with the electrophysiological results, these also are summarised. All patients were from the Instituto de Neurologia y Neurocirugia, Habana (Prof. Rosalaris Santiesteban) or the Almajeiros Hospital (Prof. Melba Marquez). The visit was organised by Dr. Gordon Plant (Hospital for Neurological Diseases, Queen Square, London).

##### 5.4.1 METHODS:

- (i) Clinical neurological examinations including visual fields were performed on all patients. We have not yet seen these.
- (ii) Pattern visual evoked responses, and pattern ERGs were obtained simultaneously using techniques which have previously been described (Arden, 1994). Black and white 30' chequerboards were used, reversing at 4 Hz. The contrast was approximately 100% and the luminance  $100 \text{ cd/m}^2$
- (iii) On the subsequent visit, Ganzfeld ERG's were studied on 9 patients who had who had 'recovered'. The stimulator used red, amber or blue light emitting diodes, the

patients were dark adapted and the pupils dilated. The flash intensities could be varied either directly or by changing the duration of the flash within the range of Bloch's Law. Rod responses and both blue and long wavelength cone responses could be separately investigated. Since this was a new technique Cuban normals were also investigated.

(iv) Psychophysical tests: Chromatic and achromatic thresholds. Stimuli were chosen to isolate either the M or P pathways according to the methods and rationale described above (Chapter 5.2). Because of limited time and difficulty of communication, the stimuli used were random optotypes and 'isoluminance' was based on the CIE values. Temporal frequency responses were not investigated. Time would not have permitted it, but the conclusions based on the work on MAR, linking the achromatic thresholds of low spatial frequencies to M-cells and the high spatial frequencies to P-cells suggested that it was not necessary. M-pathway integrity can be assessed this way.

Whilst the MAR patients were tested on a 24" NEC6FG monitor, in Cuba the images were displayed on a smaller 17" computer monitor NEC5FG. The phosphors of the different examples of NEC are not quite identical, and the CIE locations are slightly different. As with the MAR investigation, the mean luminance for all stimuli was c. 30  $\text{cd.m}^{-2}$ .

For achromatic stimuli the threshold contrast was established for sinusoidal gratings of various spatial frequencies, appearing and disappearing sinusoidally at 0.5 Hz. In order to investigate higher spatial frequencies, the patients were placed at various distances (1- 6m) from the monitor. Minimal contrast visible is limited by the characteristic of the monitor, the experience of the observers and the ambient conditions, and was accordingly more than the 0.4% found in ideal laboratory conditions, but was similar to the normal values found in other in clinical work, when standard monitors are used (Swanson et al. 1984). Additional achromatic stimuli used were letters subtending 3 degrees, appearing abruptly for a 200 ms at 1 second intervals.

All of these were used for comparison with chromatic stimuli with identical spatio-temporal content, but in which the targets were isoluminant with the background, but of a different hue, and the threshold was the minimal detectable colour contrast. This only differs from the MAR investigation in the actual choice of stimulus form and temporal profile.

#### 5.4.2 RESULTS AND CONCLUSIONS

In summary in 24 patients studied there is a reduced amplitude in the PERG of both the "P50" and "N90" component in all but 3, and there is a VER delay in all except 6. The 3 normal PERGs have normal VERs. The abnormal PERGs sometimes appear to have lost N90, but in other cases, P50 and N90 are both reduced, and the grand average does not show a selective loss of N90 (Arden, Wolf and Plant, in preparation). Clearly there is retinal damage.

In the acute stages of the condition, Ganzfeld ERGs, using standard stroboscopic illumination showed a variety of abnormalities (Plant et al. Unpublished observations.) In the work reported here, of the 9 patients who had "recovered" all patients showed an unusual minor abnormality. Although scotopic ERGs were normal, the "on" responses driven by L and M cones were enlarged, and the "off" responses to prolonged intense flashes were reduced. The flicker responses to 30 Hz flashes were also supernormal.

In nearly all patients funduscopy showed there was a loss of the optic nerve fibre layer. However, the electrophysiological results summarised above demonstrate that a retinopathy was present, in addition to the obvious loss of optic nerve fibres. The psychophysical results are interpreted with this in mind.

Some patients have normal visual acuity (as high as 1.25) and Figure 5.8 shows the average spatial contrast sensitivity function for 4 patients (filled squares) compared to 2 normals, obtained concurrently (open symbols): the dotted line give the normal result obtained by Swanson et al. (1984) who used a system similar to ours. It can be seen that there are no losses in the patients at the higher spatial frequencies, and any possible loss relative to the normals at lower spatial frequencies is less than 3dB. This is in marked contrast with the losses in chromatic sensitivity. Figure 5.9 shows these, and compares them with the achromatic loss obtained with the same targets (large letters). There may be some loss of contrast sensitivity but it is much less than for colour, especially in the tritan axis. Any departure from isoluminance would introduce luminance clues and thereby reduce the apparent colour vision losses.

Given that there is both retinal and optic nerve damage, the loss of colour vision implies damage to the parvocellular pathway. However, there is evidently no loss of achromatic contrast sensitivity to the highest spatial frequencies we employed.

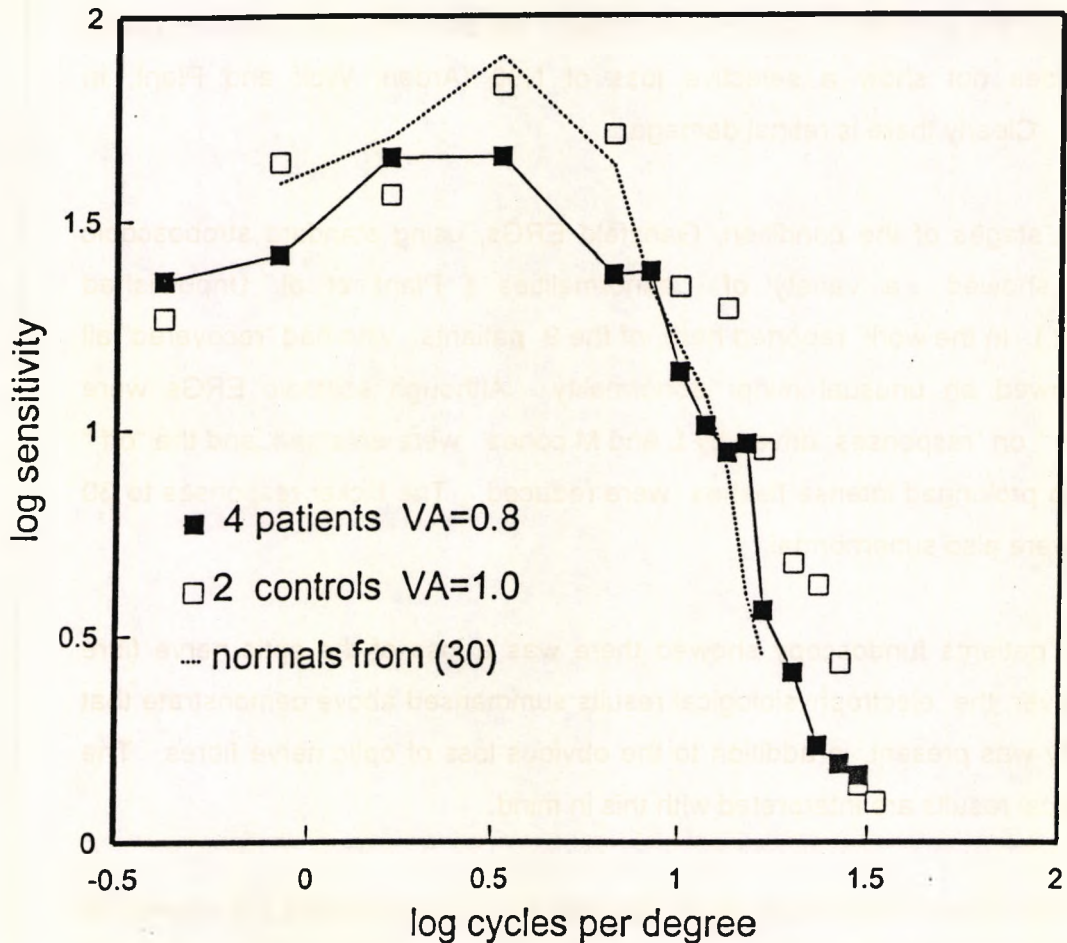


Figure 5.8 : Achromatic contrast sensitivity function in Cuban tropical "neuropathy". All results are from 4 patients in whom considerable recovery from the acute phase has already taken place, and VA is  $> 0.8$  in all of them. All have some loss of the optic nerve fibre layer on fundoscopy but the changes are mild compared with those observed in patients with more marked residual visual loss. All have abnormal ERG's. Patients are compared with 4 normals concurrently tested. Ordinate: achromatic contrast sensitivity. Dashed line: normal data from Swanson et al.,1984. Note at higher spatial frequencies, the patients have no detectable loss of contrast sensitivity. Any reduction in peak sensitivity is also small ( see text 5.4.2).

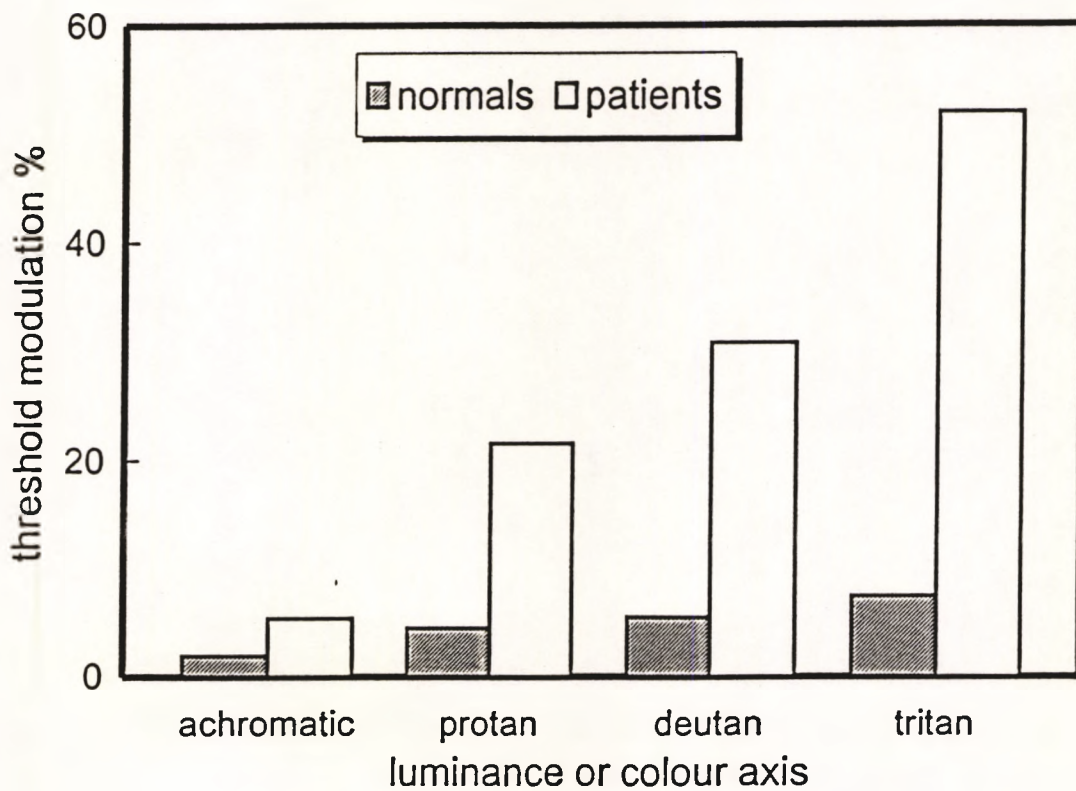


Figure 5.9: Chromatic and achromatic contrast thresholds for patients with Cuban tropical "neuropathy" compared with normals. All results are from same observers as in figure 5.8. Ordinate: luminance contrast thresholds for achromatic 3 degree targets and colour contrast thresholds for the same targets in isoluminant colour contrast. Note that the decrease of achromatic contrast sensitivity in patients is much less than the loss of colour vision and is worst for yellow-blue tritan discriminations.

These findings bear some similarity to some previous work. (i) The results of Alvarez and Kulikowski (1989) find colour losses accompanied by good achromatic vision up to 6 cycles/degree, although our results show a preservation of achromatic vision up to far higher spatial frequencies, which warrants a different explanation. (ii) The results of King-Smith, Kranda and Wood (1976) in which they cite a case where the colour losses are accompanied by normal achromatic vision. As with the Cubans, the evidence indicated that the specific colour losses must occur at the retinal opponent colour level and was interpreted as occurring at least as peripherally as the ganglion cell layer. Unfortunately the patient's acuity was not stated. Three possible explanations of our results are summarised:

1: The P cells are selectively damaged, leaving achromatic vision unaffected and the acuity and grating contrast sensitivity mediated by the M-cell system.

It is not yet conclusively established that M cells cannot mediate the detection of gratings with a spatial frequency of 30 c/ degree. The receptive field sizes of P and M cells are thought to differ only very slightly at similar retinal eccentricities, and Calkins finds that about 27% of the foveal ganglion cells are not 'midget', and insists that the 70% of midget cells act in pairs. The implication would be that the Nyquist limit for M and P vision (in the retina) is not so very different. If it is accepted that P cells are mediating grating resolution at the upper limit (under optimal conditions good observers can discriminate  $\gg$  30 c/ degree), our measurements in Cuba (in which the highest spatial frequency was 32 c/degree) are compatible with the view that in our patients M cells detected the highest spatial frequencies we used.

If this explanation is correct, there is an interesting corollary. In patients with melanoma associated retinopathy (MAR) it has been shown that there is a selective loss of M-cells (see Chapter 5.2.3.) i.e. the selectivity is the reverse of the Cuban amblyopia. In MAR there is a great loss of luminance contrast sensitivity at low spatial frequencies. Thus those results, together with the present ones, imply that M pathway cells signal achromatic thresholds for all spatial frequencies, at least under normal viewing conditions. This interpretation would require that the M-pathway has at least two subdivisions; one for the coarse spatial frequencies and one for the fine. The good acuity found in MAR would require that the 'fine' subdivision is spared and that the selective losses in the M-pathway is confined to the other subdivision.

2: Rodieck (1991) suggested that the P system consisted of 2 subdivisions; 'type I' cells concerned with acuity, and 'type II' with colour. The latter had no spatial antagonism, merely colour antagonism. (They are bistratified and ramify in two zones of the IPL. Rodieck suggests sublaminae 'a' and 'b', enabling them to receive both 'off' and 'on' signals). If this hypothesis is correct, then loss of the first category could explain the deficiency in the patients studied. However, recent work has not confirmed the earlier accounts of non-spatially organised red-green opponent cells (Dacey and Lee, 1994).

3: If retinal lateral interactions, either at the horizontal cell or amacrine cell level, are damaged in the Cuban disease (a possibility suggested to us by Lennie), then the colour opponency of the P-cells could be reduced, although the field centres, which consist of a single cone, could continue to transmit spatial information to the brain. Since the loss of surround would not affect 'sampling density', resolution would be substantially unaffected, although chromatic information would be lost at retinal level.

The mechanism of production of the photopic ERG "on" and "off" responses is not known in detail, but it is possible that the increase in the former and reduction in the latter which we have observed in this disease is a manifestation of a change in centre-surround antagonism.

Given the lack of hard evidence as to the existence of the 'type II' cells required for interpretation (2) and the controversy surrounding interpretation (1), I favour interpretation (3).

## CHAPTER 6: DISCUSSION

The thrust of this thesis is that it is possible to explore the human visual system with non-invasive techniques in greater depth than is often thought possible, using only very simple tests. Psychophysical tests were chosen with a view to isolating neural pathways; the data has been interpreted in terms of the known characteristics of individual neurons in animals and in terms of the more recent findings based on lesion experiments on operantly conditioned monkeys. This has enabled the defects in MAR and Cuban Amblyopia to be described in neurological terms, with these two unusual conditions showing that disease can be selective in targeting neurons in specific pathways. This, in turn, provides some insight into pathway functions in normals.

Rotating Stripes: With the benefit of hindsight, the preliminary experiments on the rotating stripes would have been greatly extended! I shall summarise that which can be concluded from the data, that which is unexplained, that which should have been done and was not, and that which could now be done.

As it was, the experiments undertaken were sufficient to indicate that the visual effect, namely the substructure within the band, was a direct display of two distinct temporal channels. Zone 1 was a manifestation of the low pass sustained channel and Zone 2 a non-linear band pass channel. The fact that the cut-off frequencies of the two channels differed in their dependence on luminance suggested that they correspond to physiologically distinct mechanisms. The additional qualitative characteristics of colour and contrast led to the suggestion that these distinct zones reflected the activity of the P and M-pathways and this was argued in Paper 3. Furthermore, there appeared to be selective zone loss associated with certain diseases and it was this that led to the attempt to select additional simple psychophysical tests that could be deemed to be isolating either the P- or the M-pathways.

Over the last decade, there has been a great deal of work done in establishing the spatial, temporal and chromatic properties of the P- and M-cells. Even more recently there have been lesion experiments on 'behaving monkeys' that link the single cell responses to psychophysical performance. Armed with current knowledge, I would have attempted to establish more conclusively whether or not Zones 1 and 2 are a display of P- and M-pathway activity.

The experiments on the 'stripes' described in this thesis were carried out before the theoretical analysis, described in papers 1 and 2, and did not form the basis of the analysis. With the hindsight of the analysis in which the perceived contrast across the band was shown to be a graphical display of the 'describing function' and in the case of a linear system (e.g. the camera) to be a display of the complex temporal modulation transfer function, there are other experiments that would have, and would now, be interesting to do. The first is to establish the temporal cut-off frequency at different luminances for a series of different contrasts of the stimulus stripes; this would enable the temporal frequency response (the DeLange functions) to be plotted. Because the cut-off frequency is by its very nature a threshold measurement, linearity can be assumed to operate. This could be done for both the inner and outer bands and for different spatial frequencies.

The investigation of the relation between cut-off frequency and luminance for different eccentricities would have profited by continuing reducing the luminance further. If the relationship continued to reflect that of the flicker results of Hecht and Verrijp (1933) (shown in Figure 5.8), rod responses might have appeared in the case of the wider bands involving greater eccentricity.

Given that the effect is a display of distinct psychophysical channels and possibly distinct neural pathways, the clinical potential is there, but until it is easier to establish what it is that the patient is seeing, its use is limited. A variety of stationary simulations of possible images (of the type described in Paper 3) from which the patient selects the most appropriate image - a kind of 'identikit'- is one way forward.

MAR & Cuban Amblyopia: The conclusions reached in the study of MAR and the Cuban amblyopia have depended on clinical and electrophysiological findings (and molecular biology), even though it is the psychophysics that is dealt with in this thesis. Because of the indirect nature of non-invasive work, a combined approach is clearly the strongest. It is important that these combined investigations clearly establish that there are retinal disturbances in these conditions, since this facilitates interpretation of the psychophysical results: it is unnecessary to suggest that some of the sensory disturbances are produced by, for example, damage to the visual cortex.

One message that emerged is that animal experimentation is not so conclusive so as to make human work redundant. In particular, the work on MAR patients taken in conjunction with young normals, leads to the conclusion that, with unrestrained eye

movements, it is the M-cells that set the very low thresholds for achromatic, low spatial and low temporal frequency stimuli in the normals. This is consistent with the single cell data of Kaplan and Shapley (1986) but contradicts the conclusions of Merigan (1989) and Merigan and Maunsell (1990); namely that it is the P-cells that normally set the thresholds to these stimuli. They attribute the apparent sensitivity of the P-system to probability summation. Merigan (private communication, 1995) has since agreed that the different results, and consequently the different conclusions, reflect the different experimental situations. His lesions in the P-pathway were made in the projection of peripheral retina to the LGN. This was necessary, so the visual effect would not handicap the monkey, and also because by the nature of the experiment, very precise fixation had to be maintained. For this reason, only small regions of relative scotoma were produced. This means that the size of the lesion was not sufficient to test low spatial frequencies: the preservation of fixation further reduced the sensitivity of the transient M system (Kulikowski, 1971) which in turn lead to Merigan's conclusion that the sensitivity of the M system was low for low spatial frequencies at low temporal frequencies. Probability summation of P-cell which can at most increase the sensitivity by a factor of X 3 (Kulikowski and Vidyasagar, 1987), would be insufficient to account for the high sensitivity of our young normals under the viewing conditions that prevailed and we therefore conclude that the losses in MAR are in the M-pathway.

Further reinforcement of our view lies in the results of Kulikowski et al. (1989). Not only does he (Kulikowski 1971) conclude that, with free eye movements, the transient system can mediate threshold perception of achromatic low spatial frequency targets at low temporal frequencies of presentation but, in addition, he proposes that there is a gradual transition with increasing spatial frequencies from transient M-cell activity to sustained M-cell and finally sustained P-cell participation.

The Cuban results are open to the three alternative interpretations, discussed in the previous section. Psychophysical tests setting out to investigate the chromatic responses as a function of spatial frequency, the achromatic responses as a function of temporal frequency and both as function of eccentricity and luminance, would go a long way to enabling an interpretation to be selected. Constraints on time meant that this was simply not possible. The tests that were done were carried out hurriedly under appalling conditions. Refinements had to be omitted; instructions through an interpreter were uncertain. In spite of all this, and even with there being different

interpretations possible, both the Cuban results and the MAR results do indicate that damage can be selective to specific pathways.

## REFERENCES

Alvarez, S.L. and Kulikowski, J.J. (1989). Spatial resolution limits for pattern and movement detection in patients with familial optic nerve atrophies. In *Seeing Contour and Colour*. Eds. Kulikowski, J., Dickinson, C.M. and Murray, I.J. pp401-406. Oxford Pergamon Press.

Ahnelt, P.K., Kolb, H. and Pflug, R. (1987). Identification of a subtype of cone photoreceptor, likely to be blue sensitive, in the human retina. *J. Comp. Neurol.* 255, 18-34

Alexander, K.A., Fishmann, G.A., Peachey, N.S., Marchee, A.L. and Tso, M.O.M. (1992). "On" response defects in Paraneoplastic Night Blindness With Cutaneous Malignant Melanoma. *Invest. Ophthalmol. Vis. Sci.* 33, 477-483.

Anderson, S.J. and Burr, D. (1985). Spatial and temporal selectivity of the human motion detection system. *Vision Res.* 25, 1147-1154.

Arden, G.B. (1994). An overview of the uses and abuses of electrodiagnosis in ophthalmology. *Int. J. Physiol.* 16, 113-119.

Arden, G.B., Gunduz, K. and Perry, S. (1988). Colour vision testing with a computer graphics system. *Clinical Vis. Sci.* 4, 303-320.

Arden, G.B., Wolf, J.E. and Plant, G.T. (1995). Electrophysiological and psychophysical losses in Cuban "optic neuropathy". *ARVO Abstracts . Invest. Ophthalmol. Vis. Sci.* 35 (4, suppl),3093.

Arden, G.B., Wolf, J.E. and Plant, G.T. (in preparation) Retinal Lesions in Cuban Tropical "neuropathy": an electrophysiological and psychophysical study.

Barlow, H.B. and Mollon, J.D. (1982). *The Senses*. Cambridge University Press.

Barbur, J.L., Holliday, I.E. and Ruddock, K.H. (1981). The spatial and temporal organization of motion perception units in human vision. *Acta. Psychol.* 48, 35-47.

Barbur, J.L., Harlow, A.J. and Plant, G.T. (1994). Insights into the different exploits of colour in the visual cortex. *Proceedings of the Royal Society B.*, 258, 327-324.

Baylor, D.A. (1987). Photoreceptor signals and vision: Proctor Lecture. *Invest. Ophthalmol. Vis. Sci.* 28, 34-39.

Berson, E.L. and Lessell, S. (1988). Para-neoplastic night blindness with malignant melanoma. *Am. J. Ophthalmol.* 106, 307-311.

Blakemore, C. and Campbell, F.W. (1969). On the existence of neurones in the human visual system selectively sensitive to the orientation and size of retinal images. *J.Physiol.* 203, 237-260.

Breitmeyer, B.G. and Ganz, L. (1976). Implications of sustained and transient channels for theories of visual pattern masking, saccadic suppression, and information processing. *Psychological Review*, 83, 1-36.

Brindley, G.S. (1970). *Physiology of the retina and visual pathway.* Edward Arnold Publishers Ltd., London.

Brown, J.L. (1965). Flicker and intermittent stimulation. In: *Vision and visual perception.* Ed. by C.H.Graham. John Wiley and Sons, Inc., London.

Burr, D. (1980). Motion smear. *Nature* 284, 164-165.

Calkins, D.J., Schein S.J., Tsukamoto, Y. and Sterling P. ( 1994). M and L cells in macaque retina connect to midget ganglioncells by different numbers of excitatory synapses. *Nature* 371, 70-72.

Calkins, D.J., Schein S.J., Tsukamoto, Y. and Sterling P. ( 1995). Ganglion Cell Circuits in Primate Fovea. pp 267- 274. In: *Colour Vision deficiencies XII* ed Drum B. Doc. *Ophthalmologica Proc Ser.* 57 Kluver Acad Pub. Dordrecht.

Campbell, F.W. and Robson, J.G. (1964). Application of Fourier Analysis to the modulation response of the eye. *J. Opt. Soc. Am.* 54, 581.

Campbell, F.W. and Robson, J.G. (1968). Application of Fourier Analysis to the visibility of gratings. *J. Physiol.* 197, 551-566.

Capovilla, M. Hare, W.A. and Owen, W.G. (1987). Voltage gain of signal transfer from retinal rods to bipolar cells in the tiger salamander. *J. Physiol.* 391, 125-140.

Cahal, S.R. (1972). *The structure of the retina (translation)*. Springfield, Ill, Charles C Thomas Publishers.

Chan, H. and Tyler, C.W. (1993). Spatial tuning differences between light increment and decrement patterns in fovea and periphery. *ARVO Abstracts. Invest. Ophthalmol. Vis. Sci.* 34 (4, suppl), 465.

Croner, L.J. and Kaplan, E. (1994). Receptive fields of P and M ganglion cells across the primate retina. *Vision Res.* 35, 7-24.

Crook, J.M., Lange-Malecki, B., Lee, B.B. and Valberg, A. (1988) Visual resolution of macaque retinal ganglion cells. *J. Physiol (Lond)* 396, 205-224.

Dacey, D.M. (1993). The mosaic of midget ganglion cells in the human retina. *J. Neurosci.* 13, 5334-5355.

Dacey, D.M. and Lee, B.B. (1994). The "blue-on" opponent pathway in primate retina originates from a distinct bistratified ganglion cell type. *Nature* 367, 731-735.

Davson, H. (1949). *The physiology of the eye*. Philadelphia: Blakiston Co.

De Lange, H. (1958). Research into the dynamic nature of the human fovea-cortex system with intermittent and modulated light. Attenuation characteristics with white and coloured light. *J. Opt. Soc. Amer.* 48, 777-784.

De Monasterio, F.M. and Gouras, P. (1975). Functional properties of ganglion cells of the rhesus monkey retina. *J. Physiol.*, 251, 167-195.

De Monasterio, F.M. and Gouras, P. (1975). Functional properties of the rhesus monkey retina. *J. Physiol.* 351, 167-175.

De Monasterio, F.M. (1978). Centre and surround mechanisms of opponent-color X and Y ganglion cells of retina of macaques. *J. Neurophys.* 41, 1418-1434.

Derrington, A.M. and Lennie, P. (1984). Spatial and temporal contrast sensitivities of neurones in lateral geniculate nucleus of macaque. *J. Physiol. (Lond.)*, 357, 219-240.

Dowling, J.E. (1987). *The Retina*. The Belknap Press of Harvard University Press.

Dubner, R. and Zeki S.M. (1971). Response properties and receptive fields of cells in an anatomically defined region of the superior temporal sulcus in the monkey. *Brain Res.* 35, 538-532.

Duke-Elder, W.S. (1938). *Textbook of Ophthalmology*, Vol. 1, Kimpton, London.

Falcao-Reis, F., Spileers, W., Hogg, C. and Arden, G. (1992). A new Ganzfeld electroretinographic stimulator powered by red and green light emitting diodes. *Acta Ophthalmologica*, 3, 6-49.

Falk, G. (1991). *Retinal Physiology*. Chapter 7 of *Principles and practice of Clinical Electrophysiology of Vision*. Editors: Heckenlively, J.R. and Arden, G.B. Mosby -Year Book, Inc. St. Louis. pp 69-84.

Farrell, R.J. Booth, J.M. (1975). *Design Handbook for Imagery Interpretation Equipment*, Boeing Aerospace Company, Seattle, Washington.

Glunder, H. (1987). Rotating gratings reveal the temporal transfer function of the observing system. *Journal of Modern Optics*, 34, 1365-1374.

Graham, C.H. (1965). Some basic terms and methods. In: *Vision and visual perception*. Ed. by C.H. Graham. John Wiley and Sons, Inc., London.

Green, M. (1981). Psychophysical relationships among mechanisms sensitive to pattern, motion and flicker. *Vision Res.* 21, 971-983.

Harris, M.G. (1984). The role of pattern and flicker mechanisms in determining the spatio-temporal limits of velocity perception. 1. Upper movement thresholds. *Perception*, 13, 401-407.

Hartline, H.K., and Graham, C.H. (1932). Nerve impulses from single receptors in the eye. *J.Cell.Comp. Physiol.* 1, 277-295.

Hecht, S. and Verrijp, C.D. (1933). Intermittent stimulation by light. III. The relation between intensity and critical fusion frequency for different retinal locations. *J.Gen.Physiol.* 17, 251-265.

Hecht, S. and Smith, E.L. (1936). Intermittent stimulation by light. VI. Area and the relation between critical frequency and intensity. *J. Gen.Physiol.* 19, 979-991.

Heckenlively, J. and Arden, G.B. (1991). Editors. Principles and practice of clinical electrophysiology of vision. Mosby-Year Book, Inc. St. Louis, MO.

Hirose, T. (1956). Electroretinogram in night blindness. *Acta Society of Ophthalmology, Japan*, 56, 732.

Holliday, I.E. and Ruddock, K.H. (1983). Two spatio-temporal filters in human vision. *Biol. Cybern.* 47, 173-190.

Holliday, I.E., Ruddock, K.H. and Skinner, P. (1983) Spatial filtering of retinal images by the human visual system and its consequences for visual thresholds. *SPIE Vol. 467 Image Assessment: Infrared and visible (Sira)*.

Hylkema, B.S. (1942). Examination of the visual field by determining the fusion frequency. *Acta Ophthal.* 20, 181-193.

Ikeda, M. and Boynton, R.M. (1965). Temporal summation of positive and negative flashes in the visual system. *J. Opt. Soc. Am.* 55, 1527-1534.

Ikeda, H. (1985). Transmitter action at cat retinal ganglion cells. *Prog. Ret. Res.* 4, 1-32.

Ikeda, H. and Wright, M.J. (1972). Receptive field organization of "sustained" and "transient" retinal ganglion cells.

Kaplan, E. & Shapley, R.M. (1986). The primate retina contains two types of ganglion cells, with high and low contrast sensitivity. *Proceedings of the National Academy of Science, USA.*, 83, 2755-2757.

Kellner, U., Bornfeld, N. and Forster, M.H. (1994). Severe course of cutaneous melanoma-associated retinopathy (MAR). *ARVO Abstracts. Invest. Ophthalmol. Vis. Sci.* 35 (4,suppl), 2117.

Kelly, D.H. (1961). Visual responses to time dependent stimuli. 1. Amplitude sensitivity measurements. *J.Opt. Soc. Am.* 51, 422-429.

Kelly, D.H. (1969). Flickering patterns and lateral inhibition. *J.Opt. Soc. Am. A.*, 59, 1361-1370.

Kelly, D.H. (1983). Spatiotemporal variation of chromatic and achromatic contrast thresholds. *J.Opt. Soc. Am. A.* 73, 742-750.

Kelly, D.H. and van Norren, D. (1977). Two band model of heterochromatic flicker. *J. Opt. Soc. Am.* 67, 1081.

King-Smith, P.E. and Carden, D. (1976). Luminance and opponent-color contributions to visual detection and adaptation and to temporal and spatial integration. *J.Opt. Soc. Am.*, 66, 709-717.

King Smith, P.E., Kranda, K. and Wood, I.C.J. (1976). An acquired colour defect of the opponent color-system. *Invest. Ophthalmol. Vis.Sci.* 15, 584-587.

Kim, R.Y., Retsas, S., Fitzke, F.W., Arden, G.B. and Bird, A.C. (1994). Cutaneous Melanoma-Associated Retinopathy. *Ophthalmology*, 101, 1837-1843.

Kolb, H. (1970). Organization of the outer plexiform layer of the primate retina: Electron microscopy of Golgi-impregnated cells. *Philos. Trans. R. Soc.Lond. (Biol.)* 258, 261-283.

Kolb, H. (1991). The Neural Organisation of the Human Retina. Chapter 5 of Principles and Practice of Clinical Electrophysiology of Vision. Editors: Heckenlively, J.R. and Arden, G.B., Mosby -Year Book, Inc. St. Louis. pp 25-52.

Kolb, H. (1994). The architecture of functional neural circuits in the vertebrate retina. Invest. Ophthalmol. Vis. Sci. 35, 2385-2404.

Kolb, H., Mariani, A. and Gallego, A. (1980). A second type of horizontal cell in the monkey retina. (1980). J.Comp. Neurol. 189, 31-44.

Kremers, J., Lee, B.B. and Kaiser, P.K. (1992). Sensitivity of macaque retinal ganglion cells and human observers to combined luminance and chromatic temporal modulation. J. Opt. Soc. Am. (A ), 9, 1477-1485.

Kremers, J., Lee, B.B. and Yeh, T. (1995). Receptive field dimensions of monkey retinal ganglion cells In Colour Vision deficiencies XII. ed Drum B.pgs 399-408. Doc. Ophthalmologica Proc. Ser. 57 Kluver Acad Pub. Dordrecht

Kuffler S.W. (1973). The single cell approach in the visual system and the study of receptive fields. Invest. Ophthalmol. 12, 794-813.

Kulikowski, J.J. and Tolhurst, D.J. (1973). Psychophysical evidence for sustained and transient detectors in human vision. J. Physiol. (Lond.) 232, 149-162.

Kulikowski, J.J. and Vidyasagar, T.R. (1987). Contrast thresholds of single/multi unit responses and field potentials in the striate cortex of cat and macaque. Invest. Ophthal. Vis. Sci. (Suppl) 28, 125.

Kulikowski, J.J. (1989). "The role of P and M systems" in Seeing Contour and Colour. Eds. Kulikowski, J.J., Dickinson C.M. and Murray, I.J. 232-237.

Kulikowski, J.J. (1971). Effect of eye movements on the contrast sensitivity of spatio-temporal patterns. Vision Res. 11, 261-273.

Landis, C. (1954). Determinants of the critical fusion threshold. Physiol. Rev. 34, 259-286.

Lee, B.B. (1991). On the relation between cellular sensitivity and psychophysical detection. From Pigments to Perception: Advances in Understanding Visual Processes. Ed. Valberg, A. and Lee, B.B., 105-115.

Lee, B.B. (1995) Receptive Field Structure in the Primate Retina. Vision Res, in press.

Lee, B.B., Martin, P.R and Valberg A. (1988 ) The physiological basis of heterochromatic flicker photometry demonstrated in the ganglion cells of the macaque retina. J.Physiol. Lond. 404 , 323-347.

Lee, B.B., Martin, P.R and Valberg A. (1989a ) Sensitivity of macaque retinal ganglion cells to chromatic and luminance flicker. J. Physiol. Lond. 414 , 223-243.

Lee, B.B., Martin, P.R and Valberg A. (1989b) Amplitude and phase of responses of macaque retinal ganglion cells to flickering stimuli. J. Physiol. Lond. 414 , 245-263.

Lee, B.B., Pokorny, J., Smith, V.C., Martin, P.R., and Valberg, A. (1990). Luminance and chromatic modulation sensitivity of macaque ganglion cells and human observers. J. Opt. Soc. Am. (A) 7 (12), 2223-2236.

Le Gros Clark, W.E. and Penman, G.G. (1934) The projection of the retina in the lateral geniculate body. Proc. Roy. Soc. (London) 114, 291-313.

Lennie, P. (1992). The mechanics of colour opponency. Perception, 21-suppl. 2, p9

Lennie, P., Krauskopf, J., Sclar, G. (1990). Chromatic mechanisms in striate cortex of macaque. J. Neurosci. 10, 649-669.

Linberg, K.A., Fisher, S.K., & Kolb, H.. (1987). Are there three types of horizontal cell in the human retina? Invest. Ophthalmol. Vis. Sci. 28, 262.

Livingstone, M.S. and Hubel, D.H. (1987). Psychophysical evidence for separate channels for the perception of form, colour, movement, and depth. J.Neurosci. 7, 3416-3468.

Livingstone, M.S. and Hubel, D.H. (1988). Do the relative mapping densities of the magnocellular and parvocellular systems vary with eccentricity? *J. Neurosci.*, 8, 4334-4339.

Macmillan, N.A. and Creelman, C.D. (1991). *Detection theory: a Users Guide*. Cambridge University Press.

Magoun, H and Ranson, S. (1935). The afferent path of the light reflex. The central path of the light reflex. *Arch. Ophthalmol.* 13, 862-874.

Malpeli, J.G., Schiller, P.H., Colby, C.L. (1981). Response properties of single cells in monkey striate cortex during reversible inactivation of individual lateral geniculate laminae. *J. Neurophysiol.* 46, 1102-1119.

Mandler and Makous (1984). A three channel model of temporal frequency perception. *Vis. Res.* 24, 1181-1187.

Mandler (1984). Temporal frequency discrimination above threshold. *Vis. Res.* 24, 1873-1880.

Marc, R.E. and Sperling, H.G. Chromatic organization of primate cones. *Science* 196, 454-456.

Martin, P.R. and Grunert, U. (1992). Spatial density and immunoreactivity of bipolar cells in the macaque monkey retina. *J. Comp. Neurol.* 323, 269-287.

Merigan, W.H. (1989) Chromatic and achromatic vision of macaques: role of the P pathway. *J. Neurosci.* 776-783.

Merigan, W.H. and Katz, L.M. (1990). Spatial resolution across the macaque retina. *Vision Res.* 30, 985-991.

Merigan, W.H. and Maunsell, J.H.R. (1990). Macaque vision after magnocellular lateral geniculate lesions. *Visual Neurosci.* 5, 347-352.

Merigan, W.H. and Maunsell, J.H.R. (1993). How parallel are the primate visual pathways? *Annu. Rev. Neurosci.* 16, 369-402.

Merigan, W.H. (1995). Personal communication.

Milam, A.H., Saari, J.C., Jacobson, S.G., Lobinski, W.P., Feun, L.G, and Alexander, K.R. (1993). Autoantibodies against retinal bipolar cells in cutaneous melanoma-associated retinopathy. *Invest. Ophthalmol. Vis. Sci.* 34, 91-100.

Milam, A.H. and Saari, J.C. (1994). Autoantibodies against retinal rod bipolar cells in melanoma-associated retinopathy. *ARVO Abstracts. Invest. Ophthalmol. Vis. Sci.* 35(4, suppl), 2116.

Minckler, D.S. (1980). The organization of nerve fibre bundles in the primate optic nerve head. *Arch. Ophthalmol.* 98, 1630-1636.

Miyake, Y. (1989). X-linked congenital stationary night blindness. *AMA Archives of Ophthalmology* 107, 635-636.

Mollon, J. (1989) "Tho' she kneel'd in that place where they grew..." *J. Exp. Biol.* 146, 21-38.

Moulden, B., Renshaw, J. and Mather, G. (1984). Two channels for flicker in the human visual system. *Perception* 13, 387-400.

Mullen, K.T. (1985). The contrast sensitivity of human colour vision to red-green and blue-yellow chromatic gratings. *J. Physiol.* 359, 381-400.

Murray, I., MacCana, F. and Kulikowski, J.J. (1983). Contribution of two movement detecting mechanisms to central and peripheral vision. *Vision Res.* 23, 151-159.

Nelson, R. (1977). Cat cones have rod input: A comparison of the response properties of cones and horizontal cell bodies in the retina of the cat. *J. Comp. Neurol.* 172, 109-136.

Nelson, R., Famiglietti, E.V. and Kolb, H. (1978). Intracellular staining reveals different levels of stratification for on-center and off-center in the cat retina. *J. Neurophysiol.* 4, 472-483.

Noble, K.G., Carr, R.E. and Siegel, I.M. (1990). Autosomal dominant congenital stationary night blindness and normal fundus with an electronegative electroretinogram. *Am. J. Ophthalmol.*, 109, 44-48.

Øesterberg, G.A. (1935). Topography of the layer of rods and cones in the human retina. *Acta. Ophthalmol. Suppl.* V1.

Perry, V.H., Oehler, R., and Cowey, A. (1984). Retinal ganglion cells that project to the dorsal lateral geniculate nucleus in the macaque monkey. *Neuroscience* 12, 1101-1123.

Perry, V.H. and Silveira, L.C.L. (1988). Functional lamination in the ganglion cell layer of the macaque's retina. *Neurosci.* 25, 217-224.

Polyak, S.L. (1941). *The Retina*. Chicago. University of Chicago Press.

Polyak, S.L. (1957). *The Vertebrate Visual System*. Chicago. University of Chicago Press .

Plant et al. (Unpublished observations)

Purpura, K., Kaplan, E. and Shapley, R.M. (1988). Background light and the contrast gain of primate P and M retinal ganglion cells. *Proceedings of the National Academy of Sciences.USA.* 85, 4534-4537.

Purpura, K., Tranchina, V., Kaplan, E. and Shapley, R.M. (1990). Light adaptation in the primate retina: Analysis of changes in gain and dynamics of monkey retinal ganglion cells. *Visual Neuroscience* 4, 75-93.

Reid, R.C. and Shapley, R.M. (1992). Spatial structure of cone inputs to receptive fields in primate geniculate nucleus. *Nature* 356, 716-718.

Riggs, L.A. (1954). Electroretinography in cases of night blindness. *Am. J. Ophthalmology* 38, 70-78.

Ripps, H., Carr, R.E., Siegel, I.M. and Greenstein, V.C. (1984). Functional abnormalities in vincristine-induced night blindness. *Invest. Ophthalmol. Vis. Sci.* 25, 787-794.

Robson, J.G. (1966). Spatial and temporal contrast-sensitivity functions of the visual system. *J. Opt. Soc. Am.* 56, 1141-1142.

Rodieck, R.W. (1991). Which cells code for colour? From Pigments to Perception: Advances in Understanding Visual Processes. Editors: Valberg, A. and Lee, B.B., 83-93.

Roman, G.C. (1994). An epidemic in Cuba of optic neuropathy, sensineural deafness, peripheral sensory neuropathy and dorsolateral myeloneuropathy. *J. Neurol. Sci.* 127, 11-28.

Ruddock, K.H. (1977). The organization of human vision for pattern detection and recognition. *Rep. Prog. Phys.* 40, 503-563.

Ruskell, G. (1988). Neurology of visual perception. Chapter 1 of *Optometry*. Editors: Edwards, K. and Llewellyn, R., Butterworths.

Schiller, P.H. (1882). Central connections on the retinal ON- and OFF- pathways. *Nature (London)* 297, 580-583.

Schiller, P.H. (1984). The connections of the retinal ON- and OFF- pathways on the lateral geniculate nucleus of the monkey. *Vision Res.* 24, 923-932.

Schiller, P.H. and Malpeli, J.G. (1978). Functional specificity of lateral geniculate nucleus laminae of the rhesus monkey. *J. Neurophysiol.* 41, 788-797.

Schiller, P.H., Sandell, J.H. and Maunsell, J.H.R. (1986). Functions of the ON- and OFF- channels of the visual system. *Nature (London)* 322, 824-825.

Schiller, P.H., Logothetis, N.K. and Elliot, R.C. (1990). Functions of the colour-opponent and broad-band channels of the visual system. *Nature* 343, 68-70.

Sekiguchi, N. and Williams, D.R. (1993). Efficiency for detecting isoluminant and isochromatic interference fringes *J. Opt. Soc. Amer. A.* 10, 2118-2133.

Sestokas, A.K., Lehmkuhle, S. and Kratz, K.E. (1987). Visual latency of ganglion X- and Y-cells: a comparison with geniculate X- and Y-cells. *Vision Res.* 27, 1399-1408.

Shapley, R. (1991). Neural mechanisms of contrast sensitivity. *Vision and Visual Dysfunction*. Vol. 10, Ed. J.Cronly-Dillon. Macmillan Press.

Shapley, R. and Perry, V.H. (1986). Cat and monkey retinal ganglion cells and their visual functional roles. *Trends Neurosci.* 40, 229-235.

Sharp, C.R. (1974). The contrast sensitivity of the peripheral field to drifting sinusoidal gratings. *Vision Res.* 14, 905-906.

Sharpe, D.A., Arden, G.B., Kemp, C.M. and Bird, A.C. (1990). Electrophysiological psychophysical and densitometric studies in congenital stationary night blindness. *Clinical Vis. Sci.* 5, 217-230.

Silveira, L.C.L. and Perry V.H. (1991). The topography of magnocellular projecting ganglion cells ( M-ganglion cells ) in the primate retina . *Neuroscience* 40, 217-237

Singer, W. and Bedworth, N. (1973). Inhibitory interaction between X and Y units in the cat lateral geniculate nucleus. *Brain Res.* 49, 291-307.

Smith, R.A. (1971). Studies of temporal frequency adaptation in visual contrast sensitivity. *J Physiol., Lond.* 216, 531-552.

Stone J. and Dreher, B. (1973). Projection of X and Y cells of the cat's lateral geniculate nucleus to areas 17 and 18 of the visual cortex. *J. Neurophysiol.* 36, 551-567.

Strachan, H. On a form of multiple peripheral neuritis prevalent in the West Indies. (1897). *Practitioner* 59, 417-484.

Swanson, W.H., Wilson, H.R. and Geise, C.G. (1984). Contrast matching data predicted from contrast increment thresholds. *Vision Res.* 24, 63-75.

Thompson, P. (1983). Discrimination of moving gratings at and above detection thresholds. *Vision Res.* 23, 1533-1538.

Tolhurst, D.J. (1975). Sustained and transient channels in human vision. *Vision Res.* 15, 1151-1155.

Tsukamoto, Y., Masarachi, P., Schein, S.J. and Sterling, P. (1992) Gap junctions between the pedicles of macaque foveal cones. *Vision Res.* 32, 1809-1815.

Tyrnel, R.A., and Owens, A. (1988). a rapid technique to assess the resting states of the eyes and other threshold phenomena: MOBS. *Behaviour research methods, instruments and computers.* 20 (2): 137-141.

Ungerleider, L.G., and Mishkin, M. Two cortical visual systems. In *The analysis of visual behaviour.* Ed. D.J. Ingle, R.J.W. Mansfield, M.S. Goodale. pp549-86. Cambridge, Mass. MIT Press.

Van Nes, F.L. and Bouman, M.A. (1967). Spatial modulation transfer in the human eye. *J. Opt. Soc. Am.* 57, 401-406.

Victor, J.D. (1987). The dynamics of the cat retinal X-cell centre. *J. Physiol.* 386, 219-246.

Walls, G.L. (1942). *The vertebrate eye.* Bloomfield Hills, Michigan.

Walraven, J., Enroth-Cugell, C., Hood, D.C., Macleod, D.I.A., and Schnapf, J.L. (1990). The control of visual sensitivity; in 'Visual Perception'; Edited: Spillmann, L. and Werner, J.S.

Wässle, H. Boycott, B.B. and Rohrenbeck, J. (1989). Horizontal cells in the monkey retina: cone connections and dendritic retina. *Eur. J. Neurosci.*, 1, 421-435.

Watson, A.B. and Robson, J.G. (1981). Discrimination at threshold: labelled detectors in human vision. *Vis. Res.* 21, 1115-1122.

Watanabe, M. and Rodieck, R.W. (1989). Parasol and midget ganglion cells of the primate retina. *J. Comp. Neurol.*, 289, 434-454.

Weisel, T.N. and Hubel, D.H. (1966). Spatial and chromatic interactions in the lateral geniculate body of the rhesus monkey. *J. Neurophysiol.* 29, 1115-1156.

Wolf, J.E. (1987). Rotating stripes and the impulse response of the eye: I. Uniform illumination. *Spatial Vision* 2, 199-211.

Wolf, J.E. (1987). Rotating stripes and the impulse response of the eye: II. Stroboscopic illumination. *Spatial Vision* 2, 213-222.

Wolf, J.E. and Lusty, N.G. (1994). Rotating Stripes provide a simultaneous display of sustained and transient channels. *Spatial Vision* 8, 369-379.

Zeki, S.M. (1980). The representation of colours in the cerebral cortex. *Nature* 284, 412-417.

Zrenner, E. (1983). Neurophysiological aspects of color vision in primates. Springer-Verlag, Berlin.